Developing Sphingosine-1-Phosphate Transporter (Spns2) Inhibitors for the Treatment of Multiple Sclerosis

Christopher W. Shrader

Dissertation submitted to the faculty of the Virginia Polytechnic Institute and State University in partial fulfillment of the requirements for the degree of

Doctor of Philosophy

In

Chemistry

Webster L. Santos, Chair
Andrew N. Lowell
John B. Matson
Emily Mevers

2/26/2024
Blacksburg, VA

Keywords: Sphingosine-1-phosphate • S1P • Spns2 • lymphopenia • transporter inhibitor • autoimmune disease • multiple sclerosis

Abstract

Sphingosine-1-phosphate (S1P) is a ubiquitous signaling molecule. S1P is formed from sphingosine *via* phosphorylation by one of its two kinases (SphK1 and SphK2). Once produced, it can be exported out of the cell by Spinster homologue 2 (Spns2) or major facilitator domain containing 2B (mfsd2b) where it acts as a ligand for G-protein coupled receptors $S1P_{1\text{-}5}$. S1P has important, ubiquitous extracellular functions in the body including cellular survival, proliferation, and migration. Indeed, lymphocyte trafficking is reliant on the gradient of S1P found where S1P levels are high in blood and low in tissue. This makes the S1P pathway an attractive target for a potential immunosuppressant and anti-inflammatory agent. Disruption of the S1P gradient through genetic knockout and small molecule based Spns2 inhibition have both been shown to provide potential treatment in renal fibrosis. Thus, there is an urgent need for developing Spns2 inhibitors to explore their therapeutic value.

Work in this dissertation discloses the design, synthesis, and activities of several highly potent Spns2 inhibitors. Several structures were investigated and allowed for the discovery and development of benzimidazole derivative **4.13h**. This structure is comprised of a 3-cyclopropylphenoxy tail, a benzimidazole core, and a piperazine head group. *In vitro* assays demonstrated the compound has an IC_{50} = 27 ± 6 nM, making it the most potent Spns2 inhibitor to date. Intraperitoneal (IP) and per oral (PO) administration of **4.13h** reduced circulating lymphocyte counts by 49% and 34% respectively, recapitulating the lymphopenia observed with Spns2 knockout mice. Pharmacokinetic studies revealed that **4.13h** has a C_{max} = 480 nM and a $t_{1/2}$ = 8.33 h in mice. Taken together, these results suggest that **4.13h** presents a novel Spns2 inhibitor that can serve as a chemical tool for exploring

Spns2 related biology and as a potential immunosuppressive agent for the treatment of diseases such as multiple sclerosis or renal fibrosis.

General Audience Abstract

Autoimmune diseases are caused when a person's immune system attacks its own healthy cells. In a person with multiple sclerosis, their immune system becomes sensitized to the myelin sheath that covers their neurons in the central nervous system. This results in the degradation of the myelin sheath and irreversible degradation of the nerve cell axons. This damage leads to the development of several neurological impairments, such as pain, fatigue, mobility problems, and numbness. While there is no cure for multiple sclerosis, disease-modifying therapies are typically taken by patients to suppress their immune system and slow disease progression.

Sphingsoine-1-phosphate (S1P) is a lipid that is important for the trafficking of lymphocytes into a person's central nervous system. This trafficking is largely due to the natural gradient of S1P which is high levels in blood but low in tissues. Lymphocytes will follow this gradient from areas of low S1P concentration (lymphatic tissue) to areas with higher S1P concentrations. Modulation of S1P levels is the mechanism of action for several FDA approved drugs as they target primarily S1P1 receptors to achieve lower levels of circulating lymphocytes. However, targeting this receptor also results in cardiovascular side effects such as first-dose bradycardia. The transporter for S1P, spinster homolog 2 (Spns2), which is upstream of the S1P receptors, is another viable target that our lab has recently been targeting. Spns2 inhibition decreases extracellular S1P levels and result in reduced lymphocytes in mice models. In this dissertation, several inhibitors were developed and assessed for their *in vitro* and *in vivo* ability to inhibit Spns2.

Acknowledgements

To begin, I would like to thank my advisor, Dr. Webster Santos, for all the direction and guidance he has given me over the past five years. Coming into graduate school without lab experience, he helped me to properly get started with research and was very patient with teaching me. This allowed me to flourish as a chemist during my graduate career. He always had the time to talk to me about any issues I was having and provided me the necessary training to grow into an independent thinker and chemist. I would also like to thank my committee members: Dr. Andrew Lowell, Dr. John Matson, and Dr. Emily Mevers for their constructive feedback during my milestones in graduate school. This feedback helped me to improve my scientific writing skills.

I would like to thank my collaborators at the University of Virginia: Dr. Kevin Lynch, Dr. Yugesh Kharel, and Dr. Tao Huang. Starting this project when it was young, it proved to be a difficult task. We quickly and accurately received all *in vitro* and *in vivo* data, even through multiple assay design iterations. Without these great collaborators, the success of the Spns2 project would not be what it is today.

I also need to thank my friends and colleagues including Dr. Christopher Sibley, Dr. Andrew Bage, Dr. Joseph Salamoun, Dr. Ariel Burgio, Dr. Justin Grams, Dr. Daniel Foster, Dr. Jacob Murray, Dr. Christopher Garcia, Dr. Swetha Jos, Kyle Dunnavant, Mary Foutz, Nick Buchbinder, Emily Krinos, Mario Hernandez, Christine Tan, and Abigail Agner. I especially want to thank Dr. Ariel Burgio who allowed me to collaborate on the benzoxazole paper which helped me with scaffold development in lab and Mary Foutz for all the board game nights.

Lastly, I would like to thank my family for their support. My parents, Kristi and Wayne Shrader, have been huge supporters in my times and always helped me when I needed it. I need to thank my wife Courtney Wells. Coming with me on my journey to Blacksburg as my girlfriend and becoming my wife during graduate school is not an easy task. However, she was always there to support me in the most challenging of situations. At the end of my graduate school career, our son, Julian, was born. I look forward to beginning this next phenomenal chapter in our life together. Thank you for everything.

Table of Contents

List of Figures

List of Tables

List of Schemes

Chapter 1: S1P Modulation Through Spns2 Inhibition for Autoimmune Diseases

1.1 Contributions

Dr. Ashley Peralta synthesized compound **4**, the initial hit when screening for Spns2 inhibitors. Dr. Russell Fritzemeier synthesized lead compound **SLF1081851** and Dr. Ariel Burgio synthesized **SLB1122168**. All biological data was collected at the University of Virginia by Dr. Yugesh Kharel, Dr. Tao Huang, and Dr. Kevin Lynch.

1.2 Abstract

Sphinsosine-1-phosphate (S1P) is part of a ubiquitous class of chemotactic lipid cellular signalers that are responsible for several functions including cell proliferation and anti-inflammation. S1P can be transported out of the cell into the extracellular space by one of its two transporters, Mfsd2b or Spns2. Once in the extracellular space, S1P can interact with its receptors, S1P1-5. S1P1 agonism is important for T-cell egress out of the lymph nodes. Modulation of these receptors to result in lymphopenia is well known and a mechanism of action for five FDA-approved drugs for the treatment of multiple sclerosis (MS) and ulcerative colitis. Inhibition of S1P1 also leads to on-target cardiovascular effects including hypotension and bradycardia. S1P modulation through targeting another node of the pathway may be targeted to provide therapeutic benefit while avoiding these effects, which has allowed for growing interest in novel inhibitors of Spns2 to elucidate their therapeutic potential.

1.3 Biosynthesis of Sphingosine-1-phosphate

Sphingolipids are a class of systemic lipids and have important roles in signal transduction, cell recognition, immune response, cell proliferation, and cell apoptosis.[1]

Sphingolipids can be broken down into four individual components: an alkyl chain typically composed of 18-20 carbon atoms, a polar head group containing either an amine or amide, a secondary alcohol, and a terminal alcohol or ether linker.[2] Generation of sphingosine-1-phosphate (S1P) begins in the endoplasmic reticulum (ER) with *de novo* synthesis of ceramide (**1**) from l-serine and palmitoyl-CoA through serine palmitoyl-CoA transferase.[3] Alternatively, ceramide can be generated from sphingomyelin through sphingomyelinase.[3] Once generated, ceramide can be hydrolyzed into sphingosine (**2**) by ceramidase. Sphingosine (**2)** can then go forward to be phosphorylated by the two isoforms of sphingosine kinase: SphK1 and SphK2.[4] S1P can also be irreversibly degraded into phosphoethanolamine and 2-hexadecanal *via* S1P lyase (Figure 1.1).

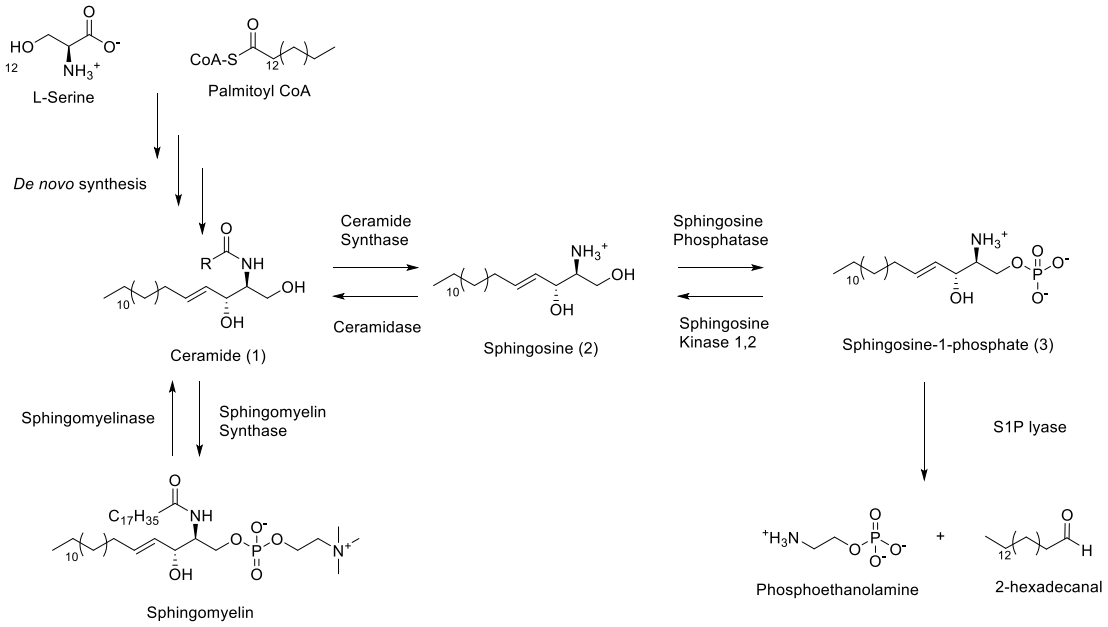

Figure 1.1. Depiction of the biological S1P synthesis pathway.

1.4 The Function of Intra- and Extracellular S1P

S1P can be found intra- and extracellularly. Intracellularly, S1P acts in the nucleus, mitochondria, and the ER and has been correlated with both proliferative and apoptotic effects.[5] SphK2 located in the nucleus produces S1P that serves to inhibit histone deacetylase 1 and 2 (HDAC1/2).[6] This inhibition leads to transcription and expression of the P21 protein, which is associated with cell cycle arrest causing cell death.[6] However, S1P is located in the nucleus and increases stabilization of human telomerase reverse transcriptase (hTERT) by promoting phosphorylation.[7] This interaction and stabilization with hTERT increases the activity of hTERT and promotes cell proliferation.[7] S1P produced in the ER by SphK2 has been suggested to up-regulate ceramide synthase 2 activity, resulting in the production of ceramide, leading to apoptosis.[8] Mitochondrial S1P interacts with Bcl-2 homologous antagonist killer (BAK) protein production.[9] The increase in the production of BAK results in increased mitochondrial membrane permeabilization, which allows the pro-apoptotic messenger cytochrome c to be released in the cytosol.[9] S1P also can be shuttled out of the cell *via* spinster homolog 2 (Spns2), with the exception of erythrocytes, which utilize major facilitator superfamily domain containing 2B (mfsd2b). Once out of the cell, S1P has a high affinity for its G-protein coupled receptors (GPCR) S1P1-5. The interaction with these receptors results in a cascade signaling effect that leads to cell survival and proliferation.[10] These receptors are highly expressed in tissues, especially S1P1-3, with S1P1 being the most ubiquitous of the GPCRs.[10] The different receptors can be found with varying localization that results in differing cellular functionalization. S1P1-3 tend to be found ubiquitously, while $S1P_4$ is localized to lymphatic tissue and S1P5 is in endothelial cells within the blood brain barrier (BBB).[11]

S1P1 is heavily involved in regulation of the immune system and vascular development during embryogenesis. While each receptor has localized function, they are all associated with cell survival and proliferation. S1P1 plays a key role in lymphocyte trafficking. S1P has a natural gradient that is high concentration in blood and lymph (1 - 2 μM) compared to surrounding tissue (200 - 500 nM).[12] Lymphocyte trafficking from the lymph nodes to circulating lymph is thought to be mediated by this gradient.[13] Mice studies have been used to suggest this correlation where deletion of S1P1 in hematopoietic stem cells led to the marked decrease of circulating T cells in peripheral lymph, resulting in T cells not being transported out of the thymus.[12, 14, 15] The importance of S1P and its receptors in regard to the lymphatic system has been studied extensively for the development of small molecule S1P1 agonists for inflammatory and autoimmune diseases.[16-19]

1.5 Multiple Sclerosis

Multiple sclerosis (MS) is an inflammatory disease that leads to demyelination of the axons in the central nervous system.[20] Distinctive features of this disease involve axonal damage in the brain and spinal cord accompanied with plaques and lesions that cause scarring. Chronic inflammation leads to demyelination of the fatty sheath that covers nerve axons, which serves to protect the axons as well as increase the rate of action potentials.[21] These action potentials are nerve impulses that result from depolarization of the membrane potential and are trans-neuronal cell signals. Having sections of myelin covering the axons is essential for the action potentials to propagate properly down the central nervous system (CNS) and mediate signals from one nerve cell to another. Demyelination occurs because of T-cell, in particular $CD4^+$ and $CD8^+$, mediated autoimmune attacks. In MS, cerebral endothelial cells have abnormalities that allow T-cells to cross the blood brain barrier

(BBB) due to compromised vascular integrity and attack the CNS.[22, 23] Upon entry into the cerebrospinal fluid (CSF), lymphocytes can attack the myelin sheath resulting in degradation and exposure of axons, thereby reducing action potentials. Action potentials are responsible for controlling things such as motor function, speech, vision, and other primary functions of the CNS; degradation of which can cause these controls to be impaired or fail completely.[22] Additionally, this loss of motor control is accompanied with pain, fatigue, and other physical ailments such as tremors and spinal cord weakness.

1.6 S1P Receptor Modulators for Treatment of MS

S1P exists in a concentration gradient high in the blood compared to tissues.[12] The levels of S1P in blood and plasma are in micromolar concentrations, while the levels in tissue are found in nanomolar concentrations.[24] The S1P gradient is known to be a regulator of immune system traffic, specifically that of T-cell lymphocytes.[25] Lymphocytes follow this gradient in a chemotactic response. Some notable FDA-approved drugs that modulate the sphingosine pathway are fingolimod (Gilenya®, FTY720, Novartis)[19, 26], siponimod (Mayzent®, BAF312, Novartis)[16, 27], ozanimod (Zeposia®, RPC1063, Celgene)[28, 29], and etrasimod (Pfizer, APD-334, Velsipity) (Figure 1.2).[30, 31] Fingolimod is a prodrug that becomes phosphorylated *in vivo* by SphK2 and acts as a functional agonist on S1P1,3,4,5 where it causes receptor internalization and degradation.[18] Loss of these receptors blocks the egress of lymphocytes from the blood to secondary lymphatic tissue leading to lymphopenia.[29] The immunosuppressive property of S1P modulators slows the progression of MS in patients and results in symptomatic relief. Siponimod and ozanimod are S1P1,5 agonists, etrasimod targets S1P1,4,5, and ponesimod is exclusive to S1P1.[29] All of these

induce lymphopenia and also cause first-dose bradycardia and depressed atrioventricular conduction, an unavoidable on-target effect of S1P1 inhibition.[18, 29, 32]

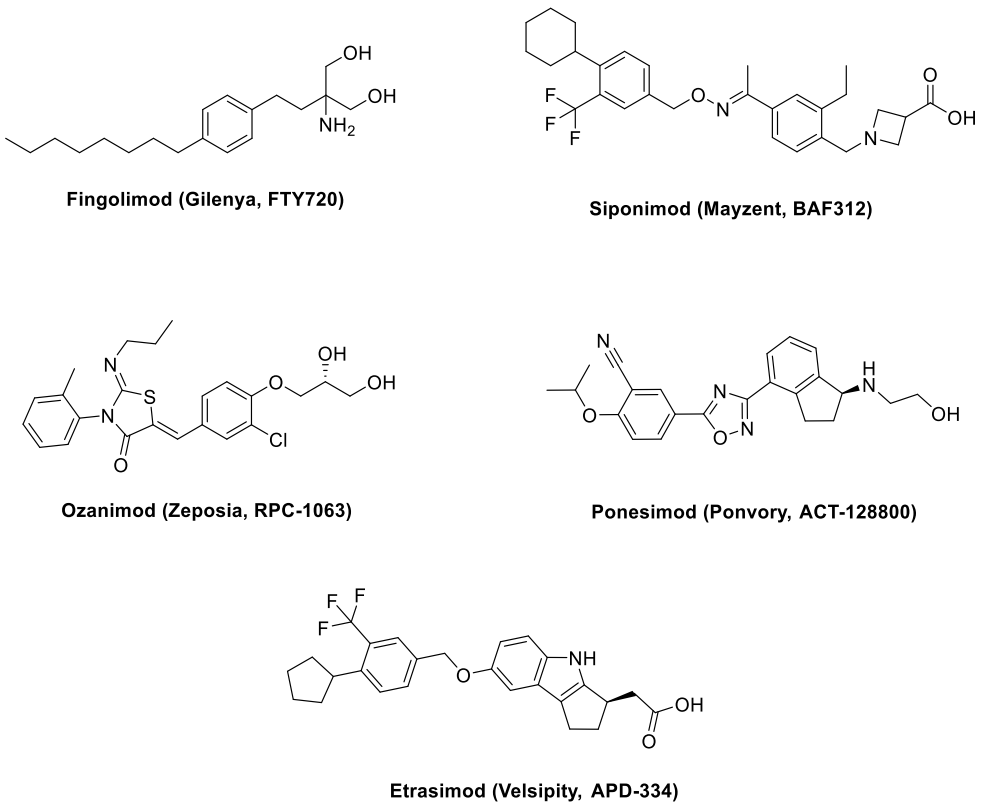

Figure 1.2. FDA approved drugs that target the sphingosine pathway.

1.7 S1P Correlation to MS

In patients with MS, the concentration of S1P in the CSF is significantly higher (2.2 ± 2.7 nM, $p < 0.01$) than that of a control group (0.69 ± 1.1 nM).[33] Knowing this increase is present, it is suggested that increased levels of S1P in the CSF are associated with the inflammation and influx of lymphocytes in the CNS that is observed in MS patients. It is established that lymphocytes have a chemotactic response to the steep gradient of S1P in the blood, so having higher levels than usual in the CNS should cause them to traffic into the CNS where they are not typically found.[10]

1.8 Spns2 and Potential Immunosuppressant Therapeutic Use

Targeting the S1P pathway through the inhibition of Spns2 could allow for the avoidance of cardiovascular issues seen with current S1P modulators while potentially providing the same therapeutic benefit. The advantage of targeting this pathway has been proven through the inhibition of other nodes in the S1P pathway, such as Spns2 and each of S1P's kinases.[34, 35] Spns2 is necessary for maintaining levels of lymph S1P, as plasma levels are controlled through Mfsd2b.[35] Germline knockout of the *Spns2* gene results in approximately 80% reduction of lymph S1P, while there is a non-significant reduction in blood and plasma S1P.[35, 36] Spns2 deletion statistically reduces circulating T- and B-cells.[36] With this in formation, Spns2 inhibition is expected to result in lymphopenia similar to S1P receptor modulators. The advantage would be avoiding the undesirable on-target effects caused by S1P receptor modulation. Spns2 deletion has demonstrated protective effects in mice experimental autoimmune encephalomyelitis (EAE), a model for MS.[35] Spns2 inhibition also reduces levels of pro-fibrotic cytokines in human cell models of renal fibrosis.[37-38] Our laboratory has also exhibited an Spns2 inhibitor that is protective in kidney fibrosis models while fingolimod failed to do so.[37]

1.9 Structure and Mechanism of Transport for Spns2

Recent research has shed light on the mechanism of Spns2-mediated S1P export. Spns2 acts as an ATP-independent transporter for S1P. Specifically, Spns2 acts through an alternating-access mechanism as a facilitated-diffusion uniporter using cryo-electron microscopy.[39, 40] The alternating-access model has S1P bind intracellularly to its transporter Spns2. Once bound on the inside-facing conformation, a conformational change occurs which shifts the opening of the protein to be facing the extracellular space. Once

outward-facing, S1P can be released into the extracellular space.[41] **SLF1081851** was also subjected to molecular docking studies in which it was shown to bind inside of Spns2, preventing it from conforming into its outward-facing state, preventing the release of S1P (Figure 1.3).[39]

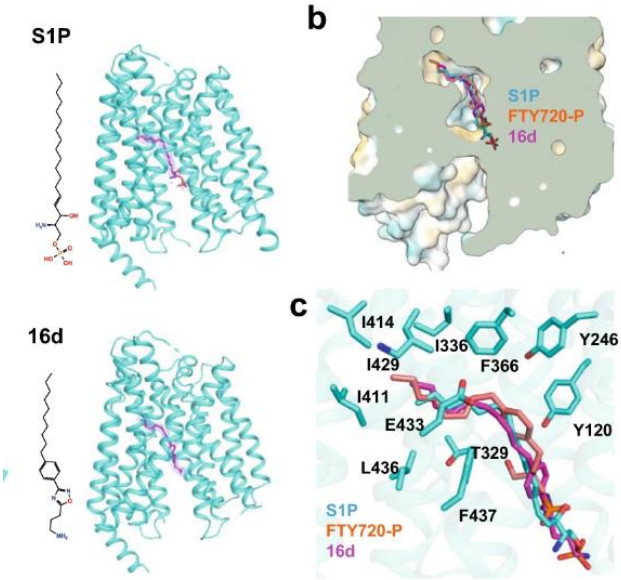

Figure 1.3. Modeling studies of **SLF1081851** (16d) inside of Spns2. It is predicted to bind in the same location as S1P and **FTY720**, locking the transporter from conforming. Figure adapted from reference.[40]

1.10 First- and second-generation Spns2 Inhibitors

Initially, the Santos lab screened a large known library of SphK inhibitors for activity against Spns2 in a *Saccharomyces cerevisiae* assay.[42-47] Screening revealed compound **4** that had inhibitory activity against Spns2 (Figure 1.4).[42] Similar to endogenous S1P, this compound is comprised of a long straight alkyl chain, a phenyl and 1,2,4-oxadiazole core, and a polar guanidinium head group. These regions were divided into three distinct regions to be explored through structure-activity relationship studies.

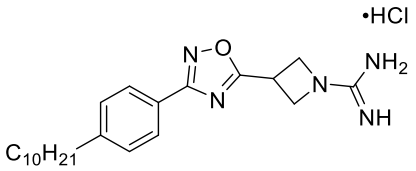

4

Figure 1.4. Initial hit from SphK2 screening for Spns2 inhibitors.

Looking at endogenous S1P, phosphate head groups were initially incorporated into structures. However, phosphate groups proved to be non-beneficial, so focus was shifted toward positively charged moieties such as guanidine and amines. However, previous work from our lab has shown that guanidines have poor oral bioavailability due to their pKa causing complete protonation in physiological pH.[46, 48-51] The structure-activity relationship (SAR) study that proceeded this work allowed for the discovery of **SLF1081851**, the first reported Spns2 inhibitor.[42] **SLF1081851** comprises of a decyl tail, a phenyl ring, oxadiazole, and propylamine head group (Figure 1.5). **SLF1081851** displayed a 67% inhibition of Spns2 in HeLa cells at 2 μM concentration and a dose-response assay was used to determine an IC_{50} = 1.93 ± 0.04 μM. Additional assays were performed using published protocol to investigate whether **SLF1081851** inhibited SphK1 and SphK2 in which it showed no activity (SphK1 IC_{50} ≥ 30 μM; SphK2 IC_{50} ≈ 30 μM) (Figure 1.5).[46] SAR studies around the tail length, varying heterocyclic replacements of the oxadiazole ring, and head groups showed this compound to be the most potent.

When administered *in vivo*, **SLF1081851** displayed modest lymphopenia in mice after a single 20 mg/kg intraperitoneal (IP) injection. Unfortunately, **SLF1081851** displayed a narrow therapeutic window, as toxicity was observed at 30 mg/kg dose.

Toxicity and low potency necessitated further study into compounds with increased potency and better performing pharmacokinetic properties.

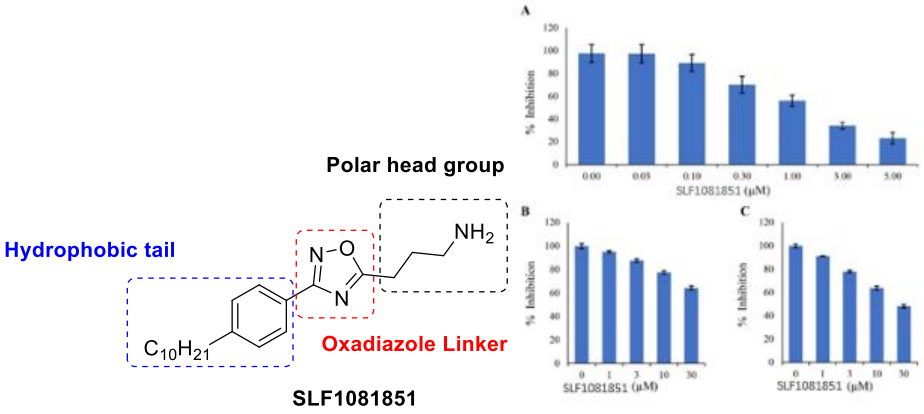

Figure 1.5. *In vitro* studies of SLF1081851. (A) Dose-dependent assessment against Spns2, (B) Inhibition of mSphK2, (C) Inhibition of mSphK1. All assays performed in duplicate. Figure is adapted from reference with modifications.[42]

When investigating the core of **SLF1081851**, it was hypothesized that a fusion of the phenyl ring and 1,2,4-oxadiazole core to a 5,6-bicyclic ring system could occur to increase conformational rigidity and polarity of the molecule. Ring fusion led to the benzoxazole series, which identified **SLB1122168** as a highly potent inhibitor of Spns2 (Figure 1.6).[52] Bearing a pyrrolidine head group, this highly activity inhibitor displayed a 77 ± 4% inhibition of Spns2 at 300 nM concentration. A dose-response assay revealed this compound had an IC_{50} = 94 ± 6 nM.

When administered to mice, **SLB1122168** resulted in significant reduction of lymphocytes after a single 10 mg/kg IP injection after testing blood levels at 4- and 16-hours post-dose.[52] **SLB1122168** also displayed ideal pharmacokinetic properties with a

half-life of 8 ± 0.2 hours and a C_{max} of 4 μM in rats (Figure 1.7). Rats also displayed a 55% reduction in lymphocytes after 10 mg/kg IP injection.

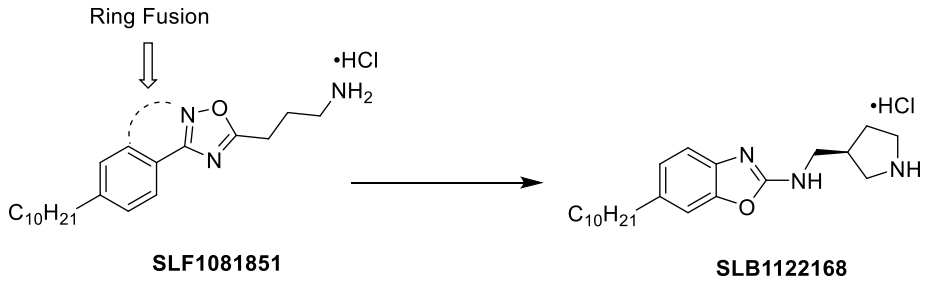

Figure 1.6. SAR approach for discovery of 2-aminobenzoxazole structure.[52]

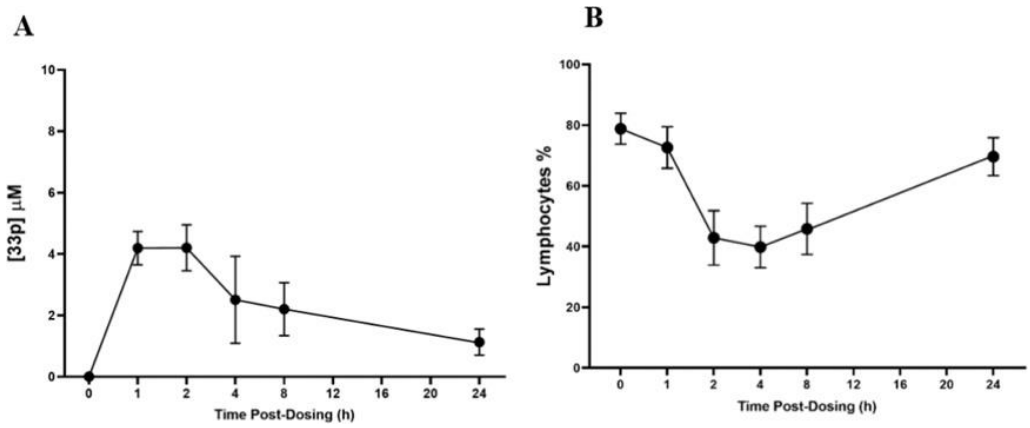

Figure 1.7. Pharmacodynamic/pharmacokinetic profiling analysis of **SLB1122168**. Male rats (Sprague Dawley strain, 4 weeks old, n=6) were injected (IP) with a single 10 mg/kg dose. (A) **SLB1122168** levels in blood (B) Circulating lymphocytes percentage after **SLB1122168** administration.

Unfortunately, **SLB1122168** suffers from poor oral bioavailability and did not cause lymphopenia in mice or rats per oral (PO). This is hypothesized to be due to the high cLogP (6.82) and large number of rotatable bonds that **SLB1122168** has, which violate Lipinski's

Rule of 5.[53] It is hypothesized that reducing these values should help to improve oral bioavailability.

1.11 Conclusion

S1P is a ubiquitous signaling molecule that has a pathway with multiple nodes for manipulation for the treatment of autoimmune diseases such as multiple sclerosis, renal fibrosis, and ulcerative colitis. Modulation of S1P activity through inhibition of S1P1-5 is proven to be beneficial through several FDA approved drugs. Unfortunately, unwanted on-target side effects are observed with these drugs. Immunosuppressive effects obtained through other nodes in the S1P pathway may avoid these on-target effects. Spns2, a transporter of S1P, is beneficial for MS in mice knockout studies, as they display lower clinical scores in EAE models.[36] Our group has discovered two generations of Spns2 inhibitors, revealing lead compounds **SLF1081851** and **SLB1122168**. While both compounds display inhibitory activity against Spns2 *in vitro* and lymphopenia *in vivo*, they both unfortunately suffer with unwanted pharmacokinetics such as poor oral bioavailability and low-dose toxicity. Thus, Spns2 inhibitors could be valuable as therapeutics for autoimmune diseases while improving the pharmacokinetic properties of these compounds.

1.12 References

1. Hannun, Y. A.; Obeid, L. M., Principles of bioactive lipid signalling: lessons from sphingolipids. *Nat Rev Mol Cell Biol* **2008,** *9* (2), 139-150.

2. Larsen, P. J.; Tennagels, N., On ceramides, other sphingolipids and impaired glucose homeostasis. *Mol. Metab.* **2014,** *3* (3), 252-260.

3. Cantalupo, A.; Di Lorenzo, A., S1P Signaling and De Novo Biosynthesis in Blood Pressure Homeostasis. *J Pharmacol Exp Ther* **2016,** *358* (2), 359-370.

4. Santos, W. L.; Lynch, K. R., Drugging sphingosine kinases. *ACS Chem. Biol.* **2015,** *10* (1), 225-233.

5. Maceyka, M.; Harikumar, K. B.; Milstien, S.; Spiegel, S., Sphingosine-1-phosphate signaling and its role in disease. *Trends Cell Biol.* **2012,** *22* (1), 50-60.

6. Hait, N. C.; Allegood, J.; Maceyka, M.; Strub, G. M.; Harikumar, K. B.; Singh, S. K.; Luo, C.; Marmorstein, R.; Kordula, T.; Milstien, S.; Spiegel, S., Regulation of histone acetylation in the nucleus by sphingosine-1-phosphate. *Science* **2009,** *325* (5945), 1254-1257.

7. Panneer Selvam, S.; De Palma, R. M.; Oaks, J. J.; Oleinik, N.; Peterson, Y. K.; Stahelin, R. V.; Skordalakes, E.; Ponnusamy, S.; Garrett-Mayer, E.; Smith, C. D.; Ogretmen, B., Binding of the sphingolipid S1P to hTERT stabilizes telomerase at the nuclear periphery by allosterically mimicking protein phosphorylation. *Sci Signal* **2015,** *8* (381), ra58.

8. Laviad, E. L.; Albee, L.; Pankova-Kholmyansky, I.; Epstein, S.; Park, H.; Merrill, A. H., Jr.; Futerman, A. H., Characterization of ceramide synthase 2: tissue distribution, substrate specificity, and inhibition by sphingosine 1-phosphate. *J. Biol. Chem.* **2008,** *283* (9), 5677-5684.

9. Chipuk, J. E.; McStay, G. P.; Bharti, A.; Kuwana, T.; Clarke, C. J.; Siskind, L. J.; Obeid, L. M.; Green, D. R., Sphingolipid metabolism cooperates with BAK and BAX to promote the mitochondrial pathway of apoptosis. *Cell* **2012,** *148* (5), 988-1000.

10. Goetzl, E. J.; Wang, W.; McGiffert, C.; Huang, M. C.; Graler, M. H., Sphingosine 1-phosphate and its G protein-coupled receptors constitute a multifunctional immunoregulatory system. *J. Cell. Biochem.* **2004,** *92* (6), 1104-1114.

11. Hobson, A. D.; Harris, C. M.; van der Kam, E. L.; Turner, S. C.; Abibi, A.; Aguirre, A. L.; Bousquet, P.; Kebede, T.; Konopacki, D. B.; Gintant, G.; Kim, Y.; Larson, K.; Maull, J. W.; Moore, N. S.; Shi, D.; Shrestha, A.; Tang, X.; Zhang, P.; Sarris, K. K., Discovery of A-971432, An Orally Bioavailable Selective Sphingosine-1-Phosphate Receptor 5 (S1P5) Agonist for the Potential Treatment of Neurodegenerative Disorders. *J. Med. Chem.* **2015,** *58* (23), 9154-9170.

12. Hla, T.; Venkataraman, K.; Michaud, J., The vascular S1P gradient-cellular sources and biological significance. *Biochim Biophys Acta* **2008,** *1781* (9), 477-482.

13. Schwab, S. R.; Pereira, J. P.; Matloubian, M.; Xu, Y.; Huang, Y.; Cyster, J. G., Lymphocyte Sequestration Through S1P Lyase Inhibition and Disruption of S1P Gradients. *Science* **2005,** *309* (5741), 1735-1739.

14. Proia, R. L.; Hla, T., Emerging biology of sphingosine-1-phosphate: its role in pathogenesis and therapy. *J. Clin. Invest.* **2015,** *125* (4), 1379-1387.

15. Nijnik, A.; Clare, S.; Hale, C.; Chen, J.; Raisen, C.; Mottram, L.; Lucas, M.; Estabel, J.; Ryder, E.; Adissu, H.; Sanger Mouse Genetics, P.; Adams, N. C.; Ramirez-Solis, R.; White, J. K.; Steel, K. P.; Dougan, G.; Hancock, R. E., The role of sphingosine-1-phosphate transporter Spns2 in immune system function. *J. Immunol.* **2012,** *189* (1), 102-111.

16. Scott, L. J., Siponimod: A Review in Secondary Progressive Multiple Sclerosis. *CNS Drugs* **2020,** *34* (11), 1191-1200.

17. Dyckman, A. J., Modulators of Sphingosine-1-phosphate Pathway Biology: Recent Advances of Sphingosine-1-phosphate Receptor 1 (S1P(1)) Agonists and Future Perspectives. *J. Med. Chem.* **2017,** *60* (13), 5267-5289.

18. Park, S. J.; Im, D. S., Sphingosine 1-Phosphate Receptor Modulators and Drug Discovery. *Biomol. Ther. (Seoul)* **2017,** *25* (1), 80-90.

19. Baumruker, T.; Billich, A.; Brinkmann, V., FTY720, an immunomodulatory sphingolipid mimetic: translation of a novel mechanism into clinical benefit in multiple sclerosis. *Expert Opin. Investig. Drugs* **2007,** *16* (3), 283-289.

20. Lublin, F. D.; Reingold, S. C.; Cohen, J. A.; Cutter, G. R.; Sorensen, P. S.; Thompson, A. J.; Wolinsky, J. S.; Balcer, L. J.; Banwell, B.; Barkhof, F.; Bebo, B., Jr.; Calabresi, P. A.; Clanet, M.; Comi, G.; Fox, R. J.; Freedman, M. S.; Goodman, A. D.; Inglese, M.; Kappos, L.; Kieseier, B. C.; Lincoln, J. A.; Lubetzki, C.; Miller, A. E.; Montalban, X.; O'Connor, P. W.; Petkau, J.; Pozzilli, C.; Rudick, R. A.; Sormani, M. P.; Stuve, O.; Waubant, E.; Polman, C. H., Defining the clinical course of multiple sclerosis: the 2013 revisions. *Neurology* **2014,** *83* (3), 278-286.

21. Bean, B. P., The action potential in mammalian central neurons. *Nat Rev Neurosci* **2007,** *8* (6), 451-465.

22. Compston, A.; Coles, A., Multiple sclerosis. *Lancet* **2008,** *372* (9648), 1502-1517.

23. Minagar, A.; Jy, W.; Jimenez, J. J.; Alexander, J. S., Multiple sclerosis as a vascular disease. *Neurol. Res.* **2006,** *28* (3), 230-235.

24. Kharel, Y.; Huang, T.; Salamon, A.; Harris, T. E.; Santos, W. L.; Lynch, K. R., Mechanism of sphingosine 1-phosphate clearance from blood. *Biochem. J.* **2020,** *477* (5), 925-935.

25. Chi, H., Sphingosine-1-phosphate and immune regulation: trafficking and beyond. *Trends Pharmacol. Sci.* **2011,** *32* (1), 16-24.

26. Berdyshev, E. V.; Gorshkova, I.; Skobeleva, A.; Bittman, R.; Lu, X.; Dudek, S. M.; Mirzapoiazova, T.; Garcia, J. G.; Natarajan, V., FTY720 inhibits ceramide synthases and up-regulates dihydrosphingosine 1-phosphate formation in human lung endothelial cells. *J. Biol. Chem.* **2009,** *284* (9), 5467-5477.

27. Behrangi, N.; Fischbach, F.; Kipp, M., Mechanism of Siponimod: Anti-Inflammatory and Neuroprotective Mode of Action. *Cells* **2019,** *8* (1), 24.

28. Cohan, S.; Lucassen, E.; Smoot, K.; Brink, J.; Chen, C., Sphingosine-1-Phosphate: Its Pharmacological Regulation and the Treatment of Multiple Sclerosis: A Review Article. *Biomedicines* **2020,** *8* (7), 227.

29. Roy, R.; Alotaibi, A. A.; Freedman, M. S., Sphingosine 1-Phosphate Receptor Modulators for Multiple Sclerosis. *CNS Drugs* **2021,** *35* (4), 385-402.

30. Sandborn, W. J.; Vermeire, S.; Peyrin-Biroulet, L.; Dubinsky, M. C.; Panes, J.; Yarur, A.; Ritter, T.; Baert, F.; Schreiber, S.; Sloan, S.; Cataldi, F.; Shan, K.; Rabbat, C. J.; Chiorean, M.; Wolf, D. C.; Sands, B. E.; D'Haens, G.; Danese, S.; Goetsch, M.; Feagan, B. G., Etrasimod as induction and maintenance therapy for ulcerative colitis (ELEVATE): two randomised, double-blind, placebo-controlled, phase 3 studies. *Lancet* **2023,** *401* (10383), 1159-1171.

31. Buzard, D. J.; Kim, S. H.; Lopez, L.; Kawasaki, A.; Zhu, X.; Moody, J.; Thoresen, L.; Calderon, I.; Ullman, B.; Han, S.; Lehmann, J.; Gharbaoui, T.; Sengupta, D.; Calvano, L.; Montalban, A. G.; Ma, Y. A.; Sage, C.; Gao, Y.; Semple, G.; Edwards, J.; Barden, J.; Morgan, M.; Chen, W.; Usmani, K.; Chen, C.; Sadeque, A.; Christopher, R. J.; Thatte, J.; Fu, L.; Solomon, M.; Mills, D.; Whelan, K.; Al-Shamma, H.; Gatlin, J.; Le, M.; Gaidarov, I.; Anthony, T.; Unett, D. J.; Blackburn, A.; Rueter, J.; Stirn, S.; Behan, D. P.; Jones, R.

M., Discovery of APD334: Design of a Clinical Stage Functional Antagonist of the Sphingosine-1-phosphate-1 Receptor. *ACS Med. Chem. Lett.* **2014,** *5* (12), 1313-1317.

32. Sanna, M. G.; Liao, J.; Jo, E.; Alfonso, C.; Ahn, M. Y.; Peterson, M. S.; Webb, B.; Lefebvre, S.; Chun, J.; Gray, N.; Rosen, H., Sphingosine 1-phosphate (S1P) receptor subtypes S1P1 and S1P3, respectively, regulate lymphocyte recirculation and heart rate. *J. Biol. Chem.* **2004,** *279* (14), 13839-13848.

33. Kulakowska, A.; Zendzian-Piotrowska, M.; Baranowski, M.; Kononczuk, T.; Drozdowski, W.; Gorski, J.; Bucki, R., Intrathecal increase of sphingosine 1-phosphate at early stage multiple sclerosis. *Neurosci. Lett.* **2010,** *477* (3), 149-152.

34. Okuniewska, M.; Fang, V.; Baeyens, A.; Raghavan, V.; Lee, J. Y.; Littman, D. R.; Schwab, S. R., SPNS2 enables T cell egress from lymph nodes during an immune response. *Cell Rep.* **2021,** *36* (2), 109368.

35. Hasan, Z.; Nguyen, T. Q.; Lam, B. W. S.; Wong, J. H. X.; Wong, C. C. Y.; Tan, C. K. H.; Yu, J.; Thiam, C. H.; Zhang, Y.; Angeli, V.; Nguyen, L. N., Postnatal deletion of Spns2 prevents neuroinflammation without compromising blood vascular functions. *Cell Mol Life Sci* **2022,** *79* (11), 541.

36. Donoviel, M. S.; Hait, N. C.; Ramachandran, S.; Maceyka, M.; Takabe, K.; Milstien, S.; Oravecz, T.; Spiegel, S., Spinster 2, a sphingosine-1-phosphate transporter, plays a critical role in inflammatory and autoimmune diseases. *FASEB J.* **2015,** *29* (12), 5018-5028.

37. Tanaka, S.; Zheng, S.; Kharel, Y.; Fritzemeier, R. G.; Huang, T.; Foster, D.; Poudel, N.; Goggins, E.; Yamaoka, Y.; Rudnicka, K. P.; Lipsey, J. E.; Radel, H. V.; Ryuh, S. M.; Inoue, T.; Yao, J.; Rosin, D. L.; Schwab, S. R.; Santos, W. L.; Lynch, K. R.; Okusa, M. D.,

Sphingosine 1-phosphate signaling in perivascular cells enhances inflammation and fibrosis in the kidney. *Sci. Transl. Med.* **2022,** *14* (658), eabj2681.

38. Zhang, X.; Ritter, J. K.; Li, N., Sphingosine-1-phosphate pathway in renal fibrosis. *Am J Physiol Renal Physiol* **2018,** *315* (4), F752-F756.

39. Chen, H.; Ahmed, S.; Zhao, H.; Elghobashi-Meinhardt, N.; Dai, Y.; Kim, J. H.; McDonald, J. G.; Li, X.; Lee, C. H., Structural and functional insights into Spns2-mediated transport of sphingosine-1-phosphate. *Cell* **2023,** *186* (12), 2644-2655 e2616.

40. Duan, Y.; Leong, N. C. P.; Zhao, J.; Zhang, Y.; Nguyen, D. T.; Ha, H. T. T.; Wang, N.; Xia, R.; Xu, Z.; Ma, Z.; Qian, Y.; Yin, H.; Zhu, X.; Zhang, A.; Guo, C.; Xia, Y.; Nguyen, L. N.; He, Y., Structural basis of Sphingosine-1-phosphate transport via human SPNS2. *Cell Res.* **2023**.

41. Quistgaard, E. M.; Low, C.; Guettou, F.; Nordlund, P., Understanding transport by the major facilitator superfamily (MFS): structures pave the way. *Nat Rev Mol Cell Biol* **2016,** *17* (2), 123-132.

42. Fritzemeier, R.; Foster, D.; Peralta, A.; Payette, M.; Kharel, Y.; Huang, T.; Lynch, K. R.; Santos, W. L., Discovery of In Vivo Active Sphingosine-1-phosphate Transporter (Spns2) Inhibitors. *J. Med. Chem.* **2022,** *65* (11), 7656-7681.

43. Sibley, C. D.; Morris, E. A.; Kharel, Y.; Brown, A. M.; Huang, T.; Bevan, D. R.; Lynch, K. R.; Santos, W. L., Discovery of a Small Side Cavity in Sphingosine Kinase 2 that Enhances Inhibitor Potency and Selectivity. *J. Med. Chem.* **2020,** *63* (3), 1178-1198.

44. Mathews, T. P.; Kennedy, A. J.; Kharel, Y.; Kennedy, P. C.; Nicoara, O.; Sunkara, M.; Morris, A. J.; Wamhoff, B. R.; Lynch, K. R.; Macdonald, T. L., Discovery, biological

evaluation, and structure-activity relationship of amidine based sphingosine kinase inhibitors. *J. Med. Chem.* **2010,** *53* (7), 2766-2778.

45. Kennedy, A. J.; Mathews, T. P.; Kharel, Y.; Field, S. D.; Moyer, M. L.; East, J. E.; Houck, J. D.; Lynch, K. R.; Macdonald, T. L., Development of amidine-based sphingosine kinase 1 nanomolar inhibitors and reduction of sphingosine 1-phosphate in human leukemia cells. *J. Med. Chem.* **2011,** *54* (10), 3524-3548.

46. Patwardhan, N. N.; Morris, E. A.; Kharel, Y.; Raje, M. R.; Gao, M.; Tomsig, J. L.; Lynch, K. R.; Santos, W. L., Structure-activity relationship studies and in vivo activity of guanidine-based sphingosine kinase inhibitors: discovery of SphK1- and SphK2-selective inhibitors. *J. Med. Chem.* **2015,** *58* (4), 1879-1899.

47. Congdon, M. D.; Kharel, Y.; Brown, A. M.; Lewis, S. N.; Bevan, D. R.; Lynch, K. R.; Santos, W. L., Structure-Activity Relationship Studies and Molecular Modeling of Naphthalene-Based Sphingosine Kinase 2 Inhibitors. *ACS Med. Chem. Lett.* **2016,** *7* (3), 229-234.

48. Hsu, P. H.; Chiu, D. C.; Wu, K. L.; Lee, P. S.; Jan, J. T.; Cheng, Y. E.; Tsai, K. C.; Cheng, T. J.; Fang, J. M., Acylguanidine derivatives of zanamivir and oseltamivir: Potential orally available prodrugs against influenza viruses. *Eur J Med Chem* **2018,** *154*, 314-323.

49. Saczewski, F.; Balewski, L., Biological activities of guanidine compounds. *Expert Opin. Ther. Pat.* **2009,** *19* (10), 1417-1448.

50. Sun, J.; Dahan, A.; Amidon, G. L., Enhancing the intestinal absorption of molecules containing the polar guanidino functionality: a double-targeted prodrug approach. *J. Med. Chem.* **2010,** *53* (2), 624-632.

51. Caine, B. A.; Dardonville, C.; Popelier, P. L. A., Prediction of Aqueous pK (a) Values for Guanidine-Containing Compounds Using Ab Initio Gas-Phase Equilibrium Bond Lengths. *ACS Omega* **2018,** *3* (4), 3835-3850.

52. Burgio, A. L.; Shrader, C. W.; Kharel, Y.; Huang, T.; Salamoun, J. M.; Lynch, K. R.; Santos, W. L., 2-Aminobenzoxazole Derivatives as Potent Inhibitors of the Sphingosine-1-Phosphate Transporter Spinster Homolog 2 (Spns2). *J. Med. Chem.* **2023,** *66* (8), 5873-5891.

53. Lipinski, C. A.; Lombardo, F.; Dominy, B. W.; Feeney, P. J., Experimental and computational approaches to estimate solubility and permeability in drug discovery and development settings. *Adv. Drug Del. Rev.* **1997,** *23* (1-3), 3-25.

Chapter 2: Imidazole-Based Sphingosine-1-phosphate Transporter Spns2 Inhibitors

2.1 Contributions

This chapter is an adaptation of "Imidazole-Based Sphingosine-1-phosphate Transporter Spns2 Inhibitors" written by the author, Daniel Foster, Yugesh Kharel, Tao Huang, Kevin Lynch, and Webster Santos that is published (*Bioorg. Med. Chem. Lett*., **2023**, *96*, 129519). Dr. Russell Fritzemeier synthesized compound SLF1081851, the lead compound represented for the first-generation Spns2 inhibitor. Dr. Daniel Foster synthesized and characterized compounds **2.7a-g**. All other work in this chapter was prepared and synthesized by Christopher Shrader. The biological data was carried out by Dr. Tao Huang, Dr. Yugesh Kharel, and Dr. Kevin Lynch at the University of Virginia. Dr. Webster Santos provided guidance and oversight throughout this project.

2.2 Abstract

Sphingosine-1-phosphate (S1P) is a chemotactic lipid that influences immune cell positioning. S1P concentration gradients are necessary for proper egress of lymphocytes from the thymus and secondary lymphoid tissues. This trafficking is interdicted by S1P receptor modulators, and it is expected that S1P transporter (Spns2) inhibitors, by reshaping S1P concentration gradients, will do the same. We previously reported **SLF1081851** as a prototype Spns2 inhibitor, which provided a scaffold to investigate the importance of the oxadiazole core and the terminal amine. In this report, we disclose a structure-activity relationship study by incorporating imidazole as both a linker and surrogate for a positive charge in **SLF1081851**. *In vitro* inhibition of Spns2-dependent S1P transport in HeLa cells identified **2.7b** as an inhibitor with an IC_{50} of 1.4 ± 0.3 μM. The SAR studies reported herein indicate that imidazolium can be a substitute for the terminal

amine in **SLF1081851** and that Spns2 inhibition is highly dependent on the lipid alkyl tail length.

2.3 Introduction

Sphingosine-1-phosphate (S1P) is part of a class of bioactive sphingolipids responsible for many functions in humans. S1P plays a pivotal role in maintaining endothelial barrier integrity and immune cell regulation among many others. S1P is intracellularly generated by the phosphorylation of sphingosine (Sph) catalyzed by either isoform of sphingosine kinase (SphK1, SphK2).[1] Once phosphorylated, S1P can be dephosphorylated by a lipid phosphate phosphatase (e.g. LPP3), irreversibly degraded by S1P lyase, or be transported into the extracellular space by either Spinster homolog 2 (Spns2) or major facilitator superfamily domain containing 2B (Mfsd2b).[1] Extracellular S1P acts as a ligand to G-protein coupled receptors (in mammals, S1P1-5). In particular, binding to S1P1 results in receptor internalization and thereby blocks lymphocyte recognition of S1P leading to reduced egress from lymph nodes to efferent lymph.[2-3] In fact, this functional antagonism is thought to be the primary mechanism of action of clinically approved drugs for remitting relapsing multiple sclerosis and ulcerative colitis.[4-5, 6] Fingolimod (FTY720) was the first drug approved with this mechanism of action, acting as a prodrug that requires phosphorylation to its active form **FTY720-P**.[6] **FTY720-P** can then bind to S1P1,3-5, disrupt the S1P gradient causing lymphopenia and resulting in slower progression of relapsing remitting multiple sclerosis.[4] Currently, four S1P receptor modulating drugs (Fingolimod, Siponimod, Ozanimod, Ponesimod) have been approved by the FDA and a fifth (Etrasimod) is the subject of a New Drug Application (Figure 2.1).[7-9] Drugs in this class are known as S1P receptor modulators (SRMs). SRMs have adverse

on-target cardiovascular effects, including first-dose bradycardia due to delayed atrioventricular conduction.[10] Because the S1P transporter, Spns2, lies upstream of S1P receptors in the signaling cascade,

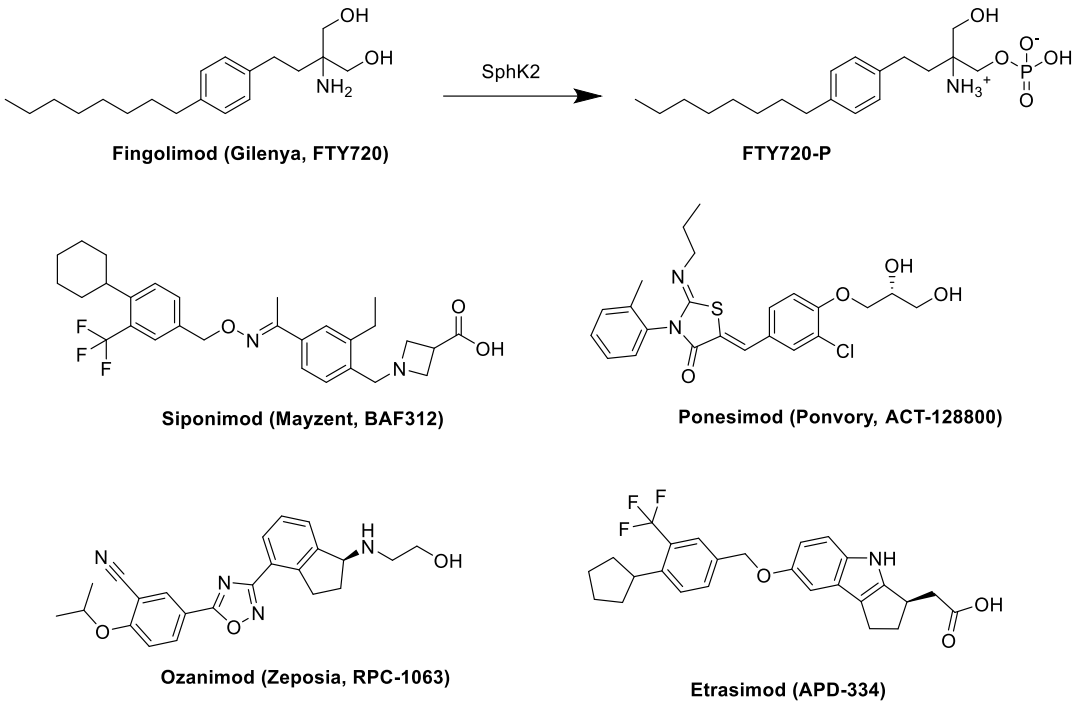

Figure 2.1. S1P receptor modulating drugs: Fingolimod[6] (Gilenya®) undergoes phosphorylation *in vivo* by SphK2 to the active FTY720-P; Siponimod[7-8] (Mayzent®); Ponesimod[9] (Ponvory®); Ozanimod[9] (Zeposia®); Etrasimod[11].

Spns2 inhibitors might circumvent this issue while maintaining the same therapeutic benefit. Indeed, Spns2 is expressed by endothelial cells, which provide lymph S1P [12-15] A second S1P transporter, Mfsd2b, is expressed by red blood cells and is responsible for S1P present in plasma.[16] Results from studies using mouse strains rendered Spns2 deficient via genetic manipulation implicate this transporter in the formation and maintenance of the blood-brain barrier,[17] vascular integrity, and lymphocyte trafficking.[14] Germline ablation of the Spns2 gene results in severe lymphopenia and when mice were subjected to the

experimental autoimmune encephalomyelitis (EAE) model, the severity of MS clinical scores improved.[14] Furthermore, mice deficient in Spns2 are protected in two renal fibrosis models including ischemia reperfusion injury and folic acid induced toxicity.[18]

Our laboratories recently reported the first inhibitor of Spns2, **SLF1081851**, which has an IC_{50} = 1.93 ± 0.04 μM in an S1P release assay (Figure 2.2).[19] When administered *in vivo*, **SLF1081851** induced lymphopenia[19] (a hallmark of Spns2 inhibition) and exhibited protective properties in kidney injury models.[18] Structure-activity relationship investigations on the linker region of **SLF1081851** generated **SLB1122168** wherein the phenyl and oxadiazole ring were fused.[20] In continuation of our studies, we investigated several isoteres[21] of the 1,2,4-oxadizole ring to improve both potency and pharmacokinetic properties of **SLF1081851**.

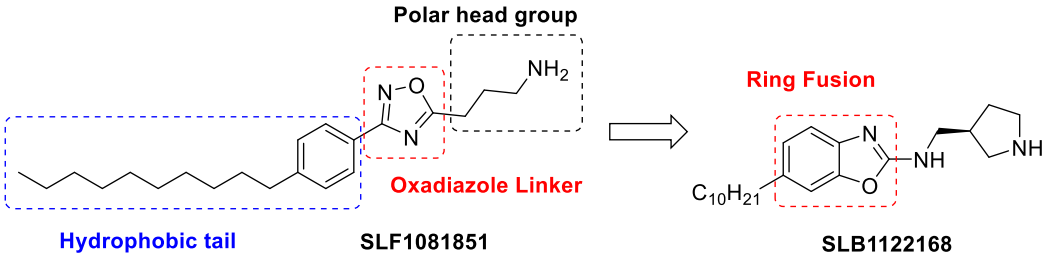

Figure 2.2. The reported Spns2 inhibitors **SLF1081851** and **SLB1122168**.

For example, an imidazole ring changes the polarity of the linker while affording a hydrogen bond donor. In addition, the imidazole ring could provide additional anchor points for functionalization that could improve binding affinity. Further, we envisioned the replacement of the terminal amine to an imidazole or imidazolium could retain potency.

2.4 Results and Discussion

We divided compound **SLF1081851** into three distinct sections: a hydrophobic tail, an oxadiazole linker, and a polar, cationic head group, *e.g.*, ammonium (Figure 2.2).[19] Initial studies with **SLF1081851** where the linker is replaced with imidazole led to **SLF1091935**, which is a good starting point.[19] Further elaboration of this scaffold is described in Schemes 2.1-2.2. The synthesis began with a two-step, one-pot hydroboration of 1-decene followed by Suzuki-Miyaura cross-coupling to generate 4-decylacetophenone **2.2**. Bromination using *N*-bromosuccinimide (NBS) afforded alpha bromoketone **2.3**, which was reacted with *N*-Boc-gamma-aminobutyric acid (GABA) to yield **2.4**. Dehydration of **2.4** using excess ammonium acetate in refluxing toluene formed the *N*-Boc-protected imidazole **2.5**. Elaboration of the imidazole N-H with a series of alkyl halides provided the desired intermediates **2.6a-e**. Compound **2.6e** was converted to primary amide **2.6f** using ammonia in methanol. Finally, HCl-promoted Boc deprotection of **2.6** afforded the final compounds **2.7a-f** as hydrochloride salts. Next, we synthesized derivatives that incorporate oxadiazole as the linker and with imidazolium salt as a surrogate for the terminal positive charge in **SLF1081851** as depicted in Scheme 2.2. Nucleophilic aromatic substitution of 4-fluorobenzonitrile with 1H-imidazole provided **2.9**, which was converted to amidoxime **2.10** with hydroxylamine hydrochloride and triethylamine (TEA) in refluxing ethanol. HCTU-mediated coupling of **2.10** with various alkyl carboxylic acids and Hünig's base at 100 °C provided the 1,2,4-oxadiazoles **2.11a-e**. Methylation of **2.11a-e** in MeCN at 70 °C with MeI afforded final compounds **2.12a-e**.

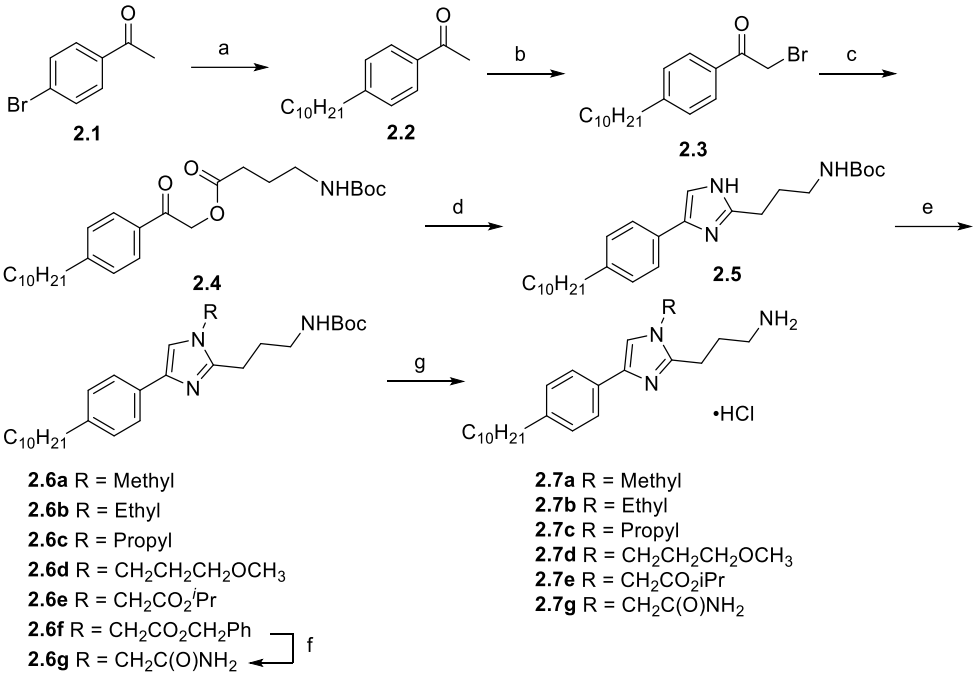

Scheme 2.1. (a) (i)1-decene (1.2 equiv), 9-BBN (1.2 equiv), THF, 66 °C, 1 h; (ii) 4-bromoacetophenone (1.0 equiv), Pd(dppf)Cl_2•CH_2Cl_2 (0.05 equiv), KOH (aq) (3.0 equiv), THF, 66 °C, 4 h, 79%; (b) NBS (1.0 equiv), p-TsOH (1.6 equiv), MeCN, 82 °C, 2 h, 82%; (c) *N*-Boc-GABA (1.1 equiv), K_2CO_3 (3.0 equiv), MeCN, rt, 16 h, 91%; (d) ammonium acetate (20 equiv), toluene, 110 °C, 5 h, 85%; (e) NaH (1.1 equiv), THF, 0 °C, 0.5 h followed by alkylhalide (1.1 equiv), THF, rt, 4 h, 29-76%; (f) 7 N NH_3, MeOH, 60 °C, 24 h, 68%. (g) 4 M HCl/dioxane, CH_2Cl_2, rt, 2 h, 35-76%.

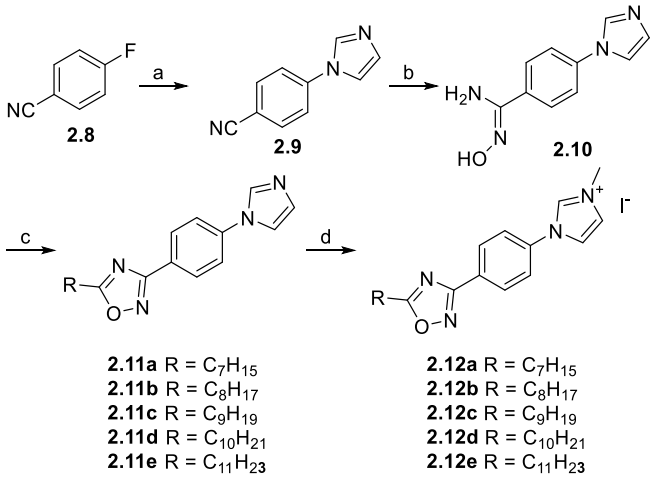

Scheme 2.2. (a) 1*H*-imidazole, NaH, DMF, 0 °C, 10 min followed by 4-fluorobenzonitrile, DMF, 100 °C, 5 h, 66%; (b) NH_2OH·HCl, EtOH, TEA, 80 °C, 16 h, 91%; (c) alkyl carboxylic acid, DIEA, HCTU, DMF, 100 °C, 16 h, 36-58%; (d) MeI, MeCN, 70 °C, 3 h, 30-52%.

With putative Spns2 inhibitors in hand, the compounds were tested for Spns2 inhibition using an S1P release assay in HeLa cells.[22] As shown in Table 2.1, introduction of methyl and ethyl substituents on the imidazole ring in **2.7a** and **2.7b** indicated 51% inhibition at 2 μM, suggesting the imidazole proton is not vital for activity and small alkyl groups can be accommodated in the binding pocket. Longer substituent length with incorporation of a propyl moiety in **2.7c** or an ether in **2.7d** for hydrogen bonding showed a significant decrease in activity at 11% inhibition. Introduction of an isopropylester **2.7e** or primary amide **2.7g** to probe H-bond interactions and sterics displayed decreased activity.

Next, we investigated the Spns2 inhibitory effects of terminal imidazole (**2.11a**-**e**) and imidazolium salts (**2.12a**-**e**) at 3 μM. As shown in Table 2.2, various tail lengths ranging from heptyl to undecyl showed moderate activity for both scaffolds (entries 1-10). In general, the imidazolium salts performed as better inhibitors when compared to the neutral imidazole analogs. In addition, as the tail length increases from heptyl (**2.12a**) to nonyl (**2.12c**), a corresponding increase in potency is observed. As the alkyl length further increased to undecyl, a precipitous drop in S1P transport activity ensued. This activity is consistent with our previous work, where the nonyl and decyl tails were the ideal length for optimum activity.[19] Overall, these results suggest that the positive charge in imidazolium compound **2.12c** can be a surrogate for the positive charge in **SLF1081851**. Our results in Tables 2.1 and 2.2 suggest that methyl and ethyl groups on imidazole **2.7a**-**b** are the most potent among the series tested.

Table 2.1. Spns2 inhibitory activity of various imidazole derivatives.[a]

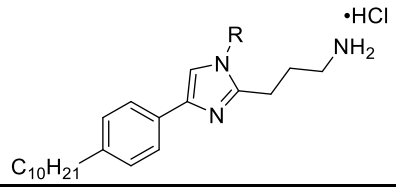

Entry	Cmpd	R	% Inh
1	**2.7a**		51 ± 3
2	**2.7b**		51 ± 1
3	**2.7c**	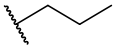	7 ± 3
4	**2.7d**	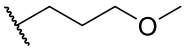	11 ± 2
5	**2.7e**	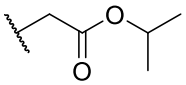	27 ± 0
6	**2.7g**	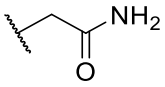	10 ± 2
7	**SLF1081851**		67 ± 1

[a]All compounds tested at 2 μM. Spns2 inhibition is shown as relative extracellular S1P levels in comparison to levels in control with no inhibitor present. Cellular media extracted and S1P levels quantified via LC/MS. Assays performed in duplicate.

Thus, we performed a dose-response study as shown in Figure 2.3. Increasing inhibitor concentration from 0.3 μM to 10 μM resulted in a corresponding decrease in S1P transport as quantified by LC/MS. The methyl (**2.7a**) and ethyl (**2.7b**) analogs were found to have IC_{50} = 2.82 ± 0.6 μM and IC_{50} = 1.4 ± 0.3 μM, respectively (Figure 2.3). Indeed, ethyl imidazole **2.7b** improved S1P transport inhibition when compared to the parent scaffold of **SLF1081851** (IC_{50} = 1.93 μM).

Table 2.2. Spns2 inhibitory activity with different tail lengths.[a]

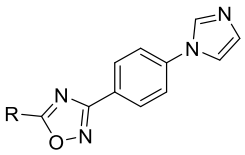

2.11a-e

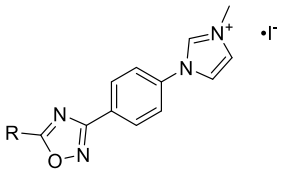

2.12a-e

Cmpd	R	% Inh	Cmpd	R	% Inh
2.11a	C_7H_{15}	12 ± 8	**2.12a**	C_7H_{15}	0
2.11b	C_8H_{17}	22 ± 1	**2.12b**	C_8H_{17}	26 ± 9
2.11c	C_9H_{19}	28 ± 12	**2.12c**	C_9H_{19}	47 ± 0
2.11d	$C_{10}H_{21}$	33 ± 5	**2.12d**	$C_{10}H_{21}$	41 ± 11
2.11e	$C_{11}H_{23}$	25 ± 9	**2.12e**	$C_{11}H_{23}$	3 ± 2

[a]All compounds tested at 3 µM. Spns2 inhibition is shown as relative extracellular S1P levels in comparison to levels in control with no inhibitor present. Cellular media extracted and S1P levels quantified via LC/MS. Assays performed in duplicate.

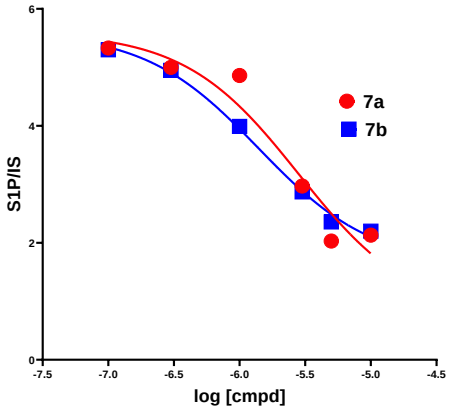

Figure 2.3. Dose response curve for **2.7a** and **2.7b** in HeLa cells. IC_{50} determined to be 2.82 ± 0.6 µM and 1.4 ± 0.3 µM, respectively.

2.5 Conclusion

In conclusion, we performed a structure-activity profiling on **SLF1081851** with a focus on imidazole as both a linker and terminal surrogate for a positive charge. An attractive feature of this moiety is the ability to decorate the 1H-imidazole with various

groups to probe both steric and electronic effects. Our studies suggest that small hydrophobic groups such as methyl and ethyl can be accommodated affording a slightly improved compound **2.7b**. Further, we found that a terminal positive charge in imidazolium salts can substitute for the cationic nitrogen in **SLF1081851** and the S1P transport inhibitory activity is dependent on the alkyl tail length, which is consistent with our previous report. Overall, our studies can be used in further understanding the consequence of inhibiting S1P transport via Spns2. These investigations will be reported in due course.

2.6 Future Directions

The results from the SAR study around the internal imidazole based structures show promising activity for this heterocycle. Analysis of the substitution on the imidazole ring suggests that there could be a strong hydrogen bond interaction driving Spns2 interaction. As the size of the functional group gets larger on the imidazole, activity goes down. This generates interest in a fusion of the two internal rings to form a benzimidazole. Benzimidazoles are a privileged scaffold seen in many FDA approved structures.[23-27] Fusion of the rings would allow for the ammonium head group to remain present and this important hydrogen bonding interaction to help drive activity in our inhibitors. This would also allow for increased hydrophilicity and decreased rotatable bonds.

2.7 References

1. Cartier, A.; Hla, T., Sphingosine 1-phosphate: Lipid signaling in pathology and therapy. *Science* **2019,** *366* (6463).

2. Goetzl, E. J.; Wang, W.; McGiffert, C.; Huang, M. C.; Graler, M. H., Sphingosine 1-phosphate and its G protein-coupled receptors constitute a multifunctional immunoregulatory system. *J. Cell. Biochem.* **2004,** *92* (6), 1104-1114.

3. Hannun, Y. A.; Obeid, L. M., Principles of bioactive lipid signalling: lessons from sphingolipids. *Nat Rev Mol Cell Biol* **2008,** *9* (2), 139-150.

4. Chi, H., Sphingosine-1-phosphate and immune regulation: trafficking and beyond. *Trends Pharmacol. Sci.* **2011,** *32* (1), 16-24.

5. Dyckman, A. J., Modulators of Sphingosine-1-phosphate Pathway Biology: Recent Advances of Sphingosine-1-phosphate Receptor 1 (S1P(1)) Agonists and Future Perspectives. *J. Med. Chem.* **2017,** *60* (13), 5267-5289.

6. Baumruker, T.; Billich, A.; Brinkmann, V., FTY720, an immunomodulatory sphingolipid mimetic: translation of a novel mechanism into clinical benefit in multiple sclerosis. *Expert Opin. Investig. Drugs* **2007,** *16* (3), 283-289.

7. Behrangi, N.; Fischbach, F.; Kipp, M., Mechanism of Siponimod: Anti-Inflammatory and Neuroprotective Mode of Action. *Cells* **2019,** *8* (1), 24.

8. Roy, R.; Alotaibi, A. A.; Freedman, M. S., Sphingosine 1-Phosphate Receptor Modulators for Multiple Sclerosis. *CNS Drugs* **2021,** *35* (4), 385-402.

9. Cohan, S.; Lucassen, E.; Smoot, K.; Brink, J.; Chen, C., Sphingosine-1-Phosphate: Its Pharmacological Regulation and the Treatment of Multiple Sclerosis: A Review Article. *Biomedicines* **2020,** *8* (7), 227.

10. Camm, J.; Hla, T.; Bakshi, R.; Brinkmann, V., Cardiac and vascular effects of fingolimod: mechanistic basis and clinical implications. *Am. Heart J.* **2014,** *168* (5), 632-644.

11. Sandborn, W. J.; Vermeire, S.; Peyrin-Biroulet, L.; Dubinsky, M. C.; Panes, J.; Yarur, A.; Ritter, T.; Baert, F.; Schreiber, S.; Sloan, S.; Cataldi, F.; Shan, K.; Rabbat, C. J.; Chiorean, M.; Wolf, D. C.; Sands, B. E.; D'Haens, G.; Danese, S.; Goetsch, M.; Feagan,

B. G., Etrasimod as induction and maintenance therapy for ulcerative colitis (ELEVATE): two randomised, double-blind, placebo-controlled, phase 3 studies. *Lancet* **2023,** *401* (10383), 1159-1171.

12. Pham, T. H.; Baluk, P.; Xu, Y.; Grigorova, I.; Bankovich, A. J.; Pappu, R.; Coughlin, S. R.; McDonald, D. M.; Schwab, S. R.; Cyster, J. G., Lymphatic endothelial cell sphingosine kinase activity is required for lymphocyte egress and lymphatic patterning. *J. Exp. Med.* **2010,** *207* (1), 17-27.

13. Nagahashi, M.; Kim, E. Y.; Yamada, A.; Ramachandran, S.; Allegood, J. C.; Hait, N. C.; Maceyka, M.; Milstien, S.; Takabe, K.; Spiegel, S., Spns2, a transporter of phosphorylated sphingoid bases, regulates their blood and lymph levels, and the lymphatic network. *FASEB J.* **2013,** *27* (3), 1001-1011.

14. Okuniewska, M.; Fang, V.; Baeyens, A.; Raghavan, V.; Lee, J. Y.; Littman, D. R.; Schwab, S. R., SPNS2 enables T cell egress from lymph nodes during an immune response. *Cell Rep.* **2021,** *36* (2), 109368.

15. Fukuhara, S.; Simmons, S.; Kawamura, S.; Inoue, A.; Orba, Y.; Tokudome, T.; Sunden, Y.; Arai, Y.; Moriwaki, K.; Ishida, J.; Uemura, A.; Kiyonari, H.; Abe, T.; Fukamizu, A.; Hirashima, M.; Sawa, H.; Aoki, J.; Ishii, M.; Mochizuki, N., The sphingosine-1-phosphate transporter Spns2 expressed on endothelial cells regulates lymphocyte trafficking in mice. *J. Clin. Invest.* **2012,** *122* (4), 1416-1426.

16. Vu, T. M.; Ishizu, A. N.; Foo, J. C.; Toh, X. R.; Zhang, F.; Whee, D. M.; Torta, F.; Cazenave-Gassiot, A.; Matsumura, T.; Kim, S.; Toh, S. E. S.; Suda, T.; Silver, D. L.; Wenk, M. R.; Nguyen, L. N., Mfsd2b is essential for the sphingosine-1-phosphate export in erythrocytes and platelets. *Nature* **2017,** *550* (7677), 524-528.

17. Wang, Z.; Zheng, Y.; Wang, F.; Zhong, J.; Zhao, T.; Xie, Q.; Zhu, T.; Ma, F.; Tang, Q.; Zhou, B.; Zhu, J., Mfsd2a and Spns2 are essential for sphingosine-1-phosphate transport in the formation and maintenance of the blood-brain barrier. *Sci Adv* **2020,** *6* (22), eaay8627.

18. Tanaka, S.; Zheng, S.; Kharel, Y.; Fritzemeier, R. G.; Huang, T.; Foster, D.; Poudel, N.; Goggins, E.; Yamaoka, Y.; Rudnicka, K. P.; Lipsey, J. E.; Radel, H. V.; Ryuh, S. M.; Inoue, T.; Yao, J.; Rosin, D. L.; Schwab, S. R.; Santos, W. L.; Lynch, K. R.; Okusa, M. D., Sphingosine 1-phosphate signaling in perivascular cells enhances inflammation and fibrosis in the kidney. *Sci. Transl. Med.* **2022,** *14* (658), eabj2681.

19. Fritzemeier, R.; Foster, D.; Peralta, A.; Payette, M.; Kharel, Y.; Huang, T.; Lynch, K. R.; Santos, W. L., Discovery of In Vivo Active Sphingosine-1-phosphate Transporter (Spns2) Inhibitors. *J. Med. Chem.* **2022,** *65* (11), 7656-7681.

20. Burgio, A. L.; Shrader, C. W.; Kharel, Y.; Huang, T.; Salamoun, J. M.; Lynch, K. R.; Santos, W. L., 2-Aminobenzoxazole Derivatives as Potent Inhibitors of the Sphingosine-1-Phosphate Transporter Spinster Homolog 2 (Spns2). *J. Med. Chem.* **2023,** *66* (8), 5873-5891.

21. Kumari, S.; Carmona, A. V.; Tiwari, A. K.; Trippier, P. C., Amide Bond Bioisosteres: Strategies, Synthesis, and Successes. *J. Med. Chem.* **2020,** *63* (21), 12290-12358.

22. Kharel, Y.; Huang, T.; Santos, W. L.; Lynch, K. R., Assay of Sphingosine 1-phosphate Transporter Spinster Homolog 2 (Spns2) Inhibitors. *SLAS Discov* **2023,** *28* (6), 284-287.

23. Alpan, A. S.; Zencir, S.; Zupko, I.; Coban, G.; Rethy, B.; Gunes, H. S.; Topcu, Z., Biological activity of bis-benzimidazole derivatives on DNA topoisomerase I and HeLa, MCF7 and A431 cells. *J Enzyme Inhib Med Chem* **2009,** *24* (3), 844-849.

24. Tong, Y.; Bouska, J. J.; Ellis, P. A.; Johnson, E. F.; Leverson, J.; Liu, X.; Marcotte, P. A.; Olson, A. M.; Osterling, D. J.; Przytulinska, M.; Rodriguez, L. E.; Shi, Y.; Soni, N.; Stavropoulos, J.; Thomas, S.; Donawho, C. K.; Frost, D. J.; Luo, Y.; Giranda, V. L.; Penning, T. D., Synthesis and evaluation of a new generation of orally efficacious benzimidazole-based poly(ADP-ribose) polymerase-1 (PARP-1) inhibitors as anticancer agents. *J. Med. Chem.* **2009,** *52* (21), 6803-6813.

25. Keri, R. S.; Hiremathad, A.; Budagumpi, S.; Nagaraja, B. M., Comprehensive Review in Current Developments of Benzimidazole-Based Medicinal Chemistry. *Chem Biol Drug Des* **2015,** *86* (1), 19-65.

26. Faheem, M.; Rathaur, A.; Pandey, A.; Singh, V. K.; Tiwari, A. K., A Review on the Modern Synthetic Approach of Benzimidazole Candidate. *Chemistryselect* **2020,** *5* (13), 3981-3994.

27. Law, C. S. W.; Yeong, K. Y., Benzimidazoles in Drug Discovery: A Patent Review. *Chemmedchem* **2021,** *16* (12), 1861-1877.

Chapter 3: Structure-Activity Relationship Studies of Linker and Head Region of Spns2 Inhibitors

3.1 Contributions

Dr. Russell Fritzemeier synthesized lead compound **SLF1081851**, and Dr. Daniel Foster synthesized compound **SLF80821178**. All other compounds in this chapter were synthesized and characterized by Christopher Shrader. Work was completed under the guidance of Dr. Webster Santos. All biological data was characterized at the University of Virginia by Dr. Tao Huang, Dr. Yugesh Kharel, and Dr. Kevin Lynch.

3.2 Abstract

Previous work from our lab had identified **SLF80821178**, a second-generation inhibitor based upon **SLF1081851**, as *in vivo* active Spns2 inhibitor. Administration of **SLF80821178** to mice induced lymphopenia after intraperitoneal (IP) administration. While effective in mice, **SLF80821178** had poor oral bioavailability and short drug exposure due to metabolic liabilities in the compound. In this report, the design, synthesis, and activity of a variety of scaffolds of Spns2 inhibitors is disclosed. These compounds comprise of multiple scaffolds used to explore the binding pocket of S1P inside of its transporter Spns2. The compounds consist of phenyl-oxadiazole systems, heterocyclic amides, and phenylureas. The campaign allowed us to confirm the importance of a nonpolar tail and a polar head group. We were also able to probe the three-dimensional space of the binding pocket with fused ring systems. The results of this study around phenylureas were successful in developing a low nanomolar IC_{50} inhibitor of Spns2 with prolonged activity *in vivo.* Of particular note was analog (*R*)-**3.16k,** which had similar activity to **SLF80821178** (IC_{50} = 53 ± 4 nM). With an IC_{50} = 128 ± 9 nM, this compound

also induced lymphopenia in mice after IP dose of 10 mg/kg. Our modifications to **SLF80821178** helped to reduce metabolic liabilities and allow for longer-lasting reduction of circulating lymphocytes.

3.3 Introduction

While **SLF1081851** provided a scaffold for first-generation Spns2 inhibitors, it has low potency, a low therapeutic window, and poor oral bioavailability, which necessitates a new generation of inhibitors (Figure 3.1).[1]

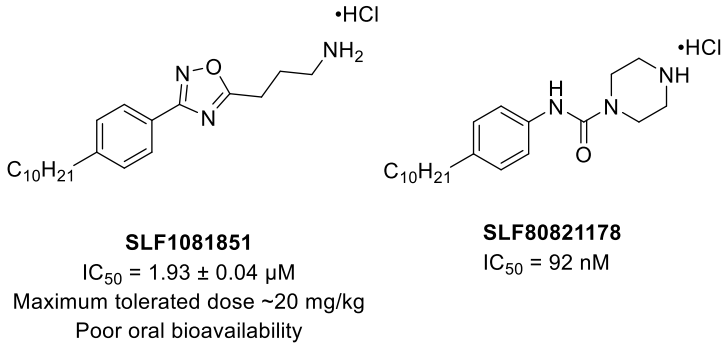

Figure 3.1. First generation Spns2 inhibitor **SLF1081851** and lead Spns2 inhibitor **SLF80821178**.[1]

The internal core comprising of the phenyl ring and 1,2,4-oxadiazole were investigated as well as the head region of the molecule. Previous reports have shown that replacement of the oxadiazole ring with other heterocycles such as imidazole, oxazole, and pyrazoles did not improve inhibitory activity.[1, 2] However, no reports have been made on the translocation of the rings. Relocating the rings to reverse their order could enhance interactions inside the protein binding pocket not seen in **SLF1081851**. Our lab also recently discovered **SLF80821178**, a highly potent inhibitor of Spns2 (Figure 3.1). **SLF80821178** consists of a decyl tail and a phenylurea with a piperazine head group. It

incorporates a urea into the head group to replace the oxadiazole ring and a piperazine warhead in the pharmacophore. Amides act as bioisosteres for 1,2,4-oxadiazole rings and have a high prevalence in drugs.[3, 4] Replacement of the oxadiazole ring could also provide metabolic stability, as metabolizing enzymes catalyze ring opening through cleavage of the N-O bond.[5-7] While **SLF80821178** has very potent activity *in vitro* (IC_{50} = 53 ± 4 nM), it exhibits issues such as poor oral bioavailability and metabolic liabilities. For example, the piperazine ring is commonly hydroxylated by cytochrome P450 during metabolism.[8] When administered IP, **SLF80821178** exhibited lymphopenia in mice after 4 hours. However, **SLF80821178** was not effective under oral administration in mice as well as it suffers from a short half-life of 4 hours. Lymphopenia post 4-hours *in vivo* is not observed in mice with this compound, unfortunately. It was first postulated that replacement of the phenyl ring with a heterocycle could help improve the oral bioavailability and pharmacokinetic properties of **SLF80821178** through increased polarity and electronic interactions.[9, 10]

We hypothesized that replacement of the internal phenyl ring could be beneficial to our inhibitors (Figure 3). Replacement of the phenyl ring with a heterocycle could improve metabolic stability by preventing oxidation.[11-13] Increased hydrophilicity could also improve oral bioavailability, as cLogP values would decrease to better match ideal drug-like properties described by Lipinski.[14, 15] Azoles were also targeted as they can potentially improve *in vivo* metabolic properties.[16, 17] Another approach to improve the pharmacokinetic properties of **SLF80821178** was a structure-activity relationship (SAR) study around the head group. The studies included derivatives such as carbamates, benzamides, and various amines in the urea scaffold.[17] To maintain a similar overall heavy-atom length, an undecyl tail was chosen for this series.

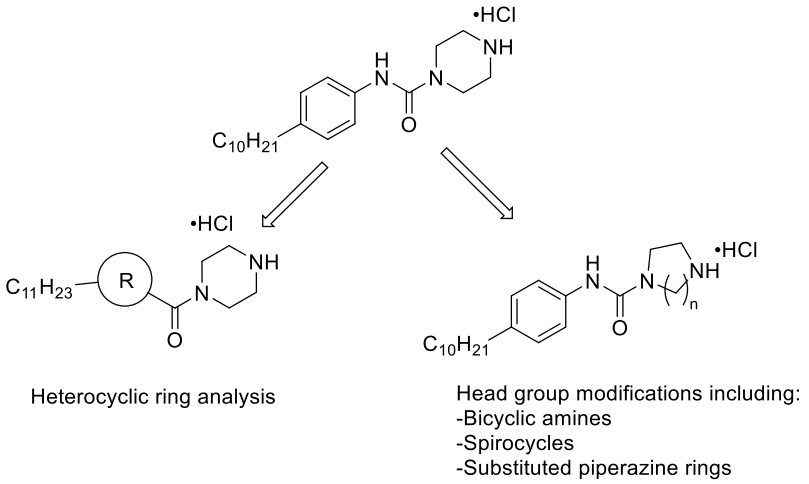

Figure 3.2. General structures of the scaffolds explored in the study campaign around **SLF80821178**.

However, bicyclic, spiro, and substituted piperazine rings were not investigated in the SAR study around **SLF80821178** (Figure 3.2). These compounds would add steric bulk through fused rings to better understand the three-dimensional space of the binding pocket. These head groups would also function to reduce potential metabolic liabilities of the inhibitors. By reducing the possible metabolic liabilities of our structures and increasing hydrophilicity, our goal was to achieve increased oral bioavailability and slow down metabolism of our structures.

3.4 Chemical Synthesis

Synthesis of the reversed-core scaffold began with reaction between commercially available 4-iodobenzonitrile and hydroxylamine hydrochloride to afford the amidoxime **3.2** in 91% yield.[18, 19] HCTU-mediated coupling and cyclization with undecanoic acid was used to generate the 1,2,4-oxadiazole ring intermediate **3.3** in 70% yield.[20] From this common intermediate, a two-step, one-pot hydroboration followed by Suzuki-Miyaura

cross-coupling was performed with *N*-Boc-allylamine and *N*-Boc-vinylamine to give **3.4a** and **3.4b** in 64% and 89% yield, respectively.[21] Finally, an HCl-mediated Boc deprotection was performed to afford final compounds **3.5a** and **3.5b** with 85% and 80% yields as hydrochloride salts.

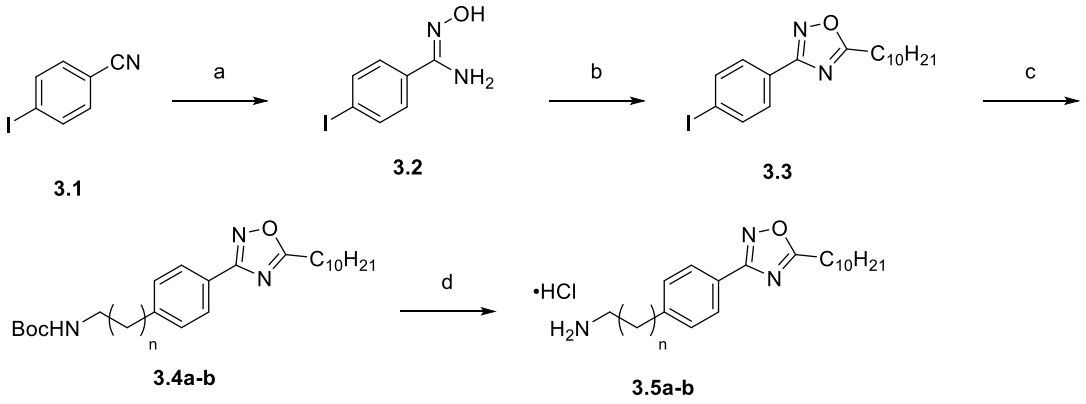

Scheme 3.1. (a) hydroxylamine hydrochloride (2.2 equiv.), triethylamine (3.0 equiv.), EtOH, 80 °C, 16 h, 91%; (b) Undecanoic acid (1.2 equiv.), HCTU (1.2 equiv.), diisopropylethylamine (1.8 equiv.), DMF, 100 °C, 16 h, 70%; (c) (i) 1-decene (2.0 equiv.), 9-BBN (2.1 equiv.), 70 °C, 1 h. (ii) Aryl iodide (1.0 equiv.), $PdCl_2(dppf)\cdot CH_2Cl_2$ (0.05 equiv.), 3 M aq. KOH (3.0 equiv.), THF, 70 °C, 16 h, 64-89%; (d) 4 M HCl in dioxane (10.0 equiv.), DCM, 20 °C, 16 h, 80-85%.

The heterocyclic core inhibitors were synthesized beginning with commercially available heterocyclic carboxylic acids. These were subjected to HCTU-mediated coupling of *N*-Boc-piperazine to form the amide head group compounds **3.6a-c** in 40-67% yield. The undecyl tail was then installed with a substitution using 1-bromoundecane to afford **3.7a-c** in 36-66% yield. Finally, HCl-mediated Boc deprotection was performed using 4 M HCl in dioxane to afford final products **3.8a-c** as hydrochloride salts in 81-87% yield. Synthesis of **3.13** began with formation of the terminal hydroxylamine **3.10** with 1-tridecanenitrile and hydroxylamine hydrochloride in 62% yield. Ring closure with ethyl 2-

chloro-2-oxoacetate and pyridine afforded the ethyl ester 1,2,4-oxadiazole ring **3.11** in 90% yield. Substitution of the ethyl ether using *N*-Boc-piperazine in refluxing ethanol was performed to generate **3.12** in 90% yield. Finally, HCl-assisted Boc deprotection afforded final product **3.13** in 97% yield as a hydrochloride salt.

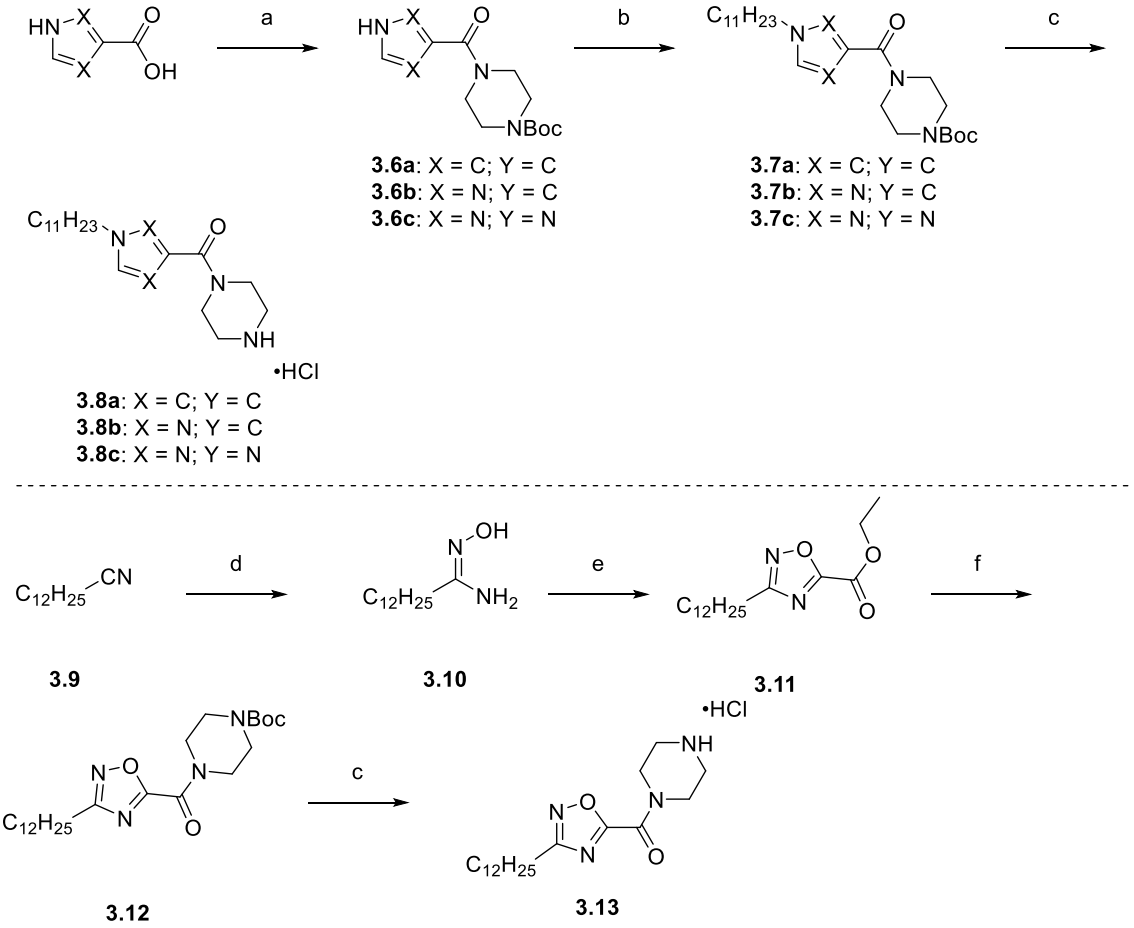

Scheme 3.2. (a) *N*-Boc-piperazine (1.1 equiv.), HCTU (1.1 equiv.), diisopropylethylamine (2.0 equiv.), DCM, 20 °C, 2 h, 40-67%; (b) 1-bromoundecane (1.5 equiv.), potassium carbonate (3.0 equiv.), DMF, 20 °C, 3 h, 36-66%; (c) 4 M HCl in dioxane (10.0 equiv.), DCM, 20 °C, 16 h, 81-97%; (d) hydroxylamine hydrochloride (3.0 equiv.), triethylamine (3.0 equiv.), ethanol, reflux, 16 h, 62%; (e) ethyl 2-chloro-2-oxoacetate (1.5 equiv.), pyridine (3.0 equiv.), dichloroethane, reflux, 2 h, 90%; (f) *N*-Boc-piperazine (2.0 equiv.), triethylamine (3.0 equiv.), ethanol, 20 °C, 3 h, 90%.

Working to improve the bioavailability and metabolic profile of **SLF80821178**, the head group of the molecule was modified with polar amines. Synthesis of these derivatives

began with commercially available 4-decylaniline. Two-step, one-pot generation of the isocyanate *in situ* was performed using triphosgene and triethylamine followed by addition of appropriate *N*-Boc protected amines were added to form the phenylurea compounds **3.15a-n** in 32-88% yield. The resulting intermediate was treated with hydrochloric acid to afford **3.16a-n** as a hydrochloride salt in 71-95% yield.

3.5 HeLa cell-based *in vitro* evaluation

HeLa cells were transfected with pcDNA3.1 plasmids, which encode mouse Spns2 and incubated in sphingosine-containing media. S1P catabolic pathways were halted by the addition of 4-deoxypyridoxine (1 mM), Na_3VO_4 (0.2 mM), and NaF (2 mM). The inhibitors were introduced to the media and the cells were incubated for 18 hours at 37 ºC. Following incubation, media was collected, an internal standard was added (5 μL of 0.5 μM d_7-S1P in methanol) and 150 μL of 100% trichloroacetic acid were added. After mixing, the tubes were chilled on ice for 45-60 minutes. The precipitate was collected *via* centrifugation and washed with water. The pellets were then recentrifuged and 300 μL methanol was introduced to the final pellet and mixed vigorously. Afterward, 160 μL of supernatant fluid was added to an HPLC vial and levels of S1P and d_7-S1P were quantified by LC-MS/MS. Inhibition is reported as a percent decrease in S1P release relative to the vehicle where no inhibitor was introduced.

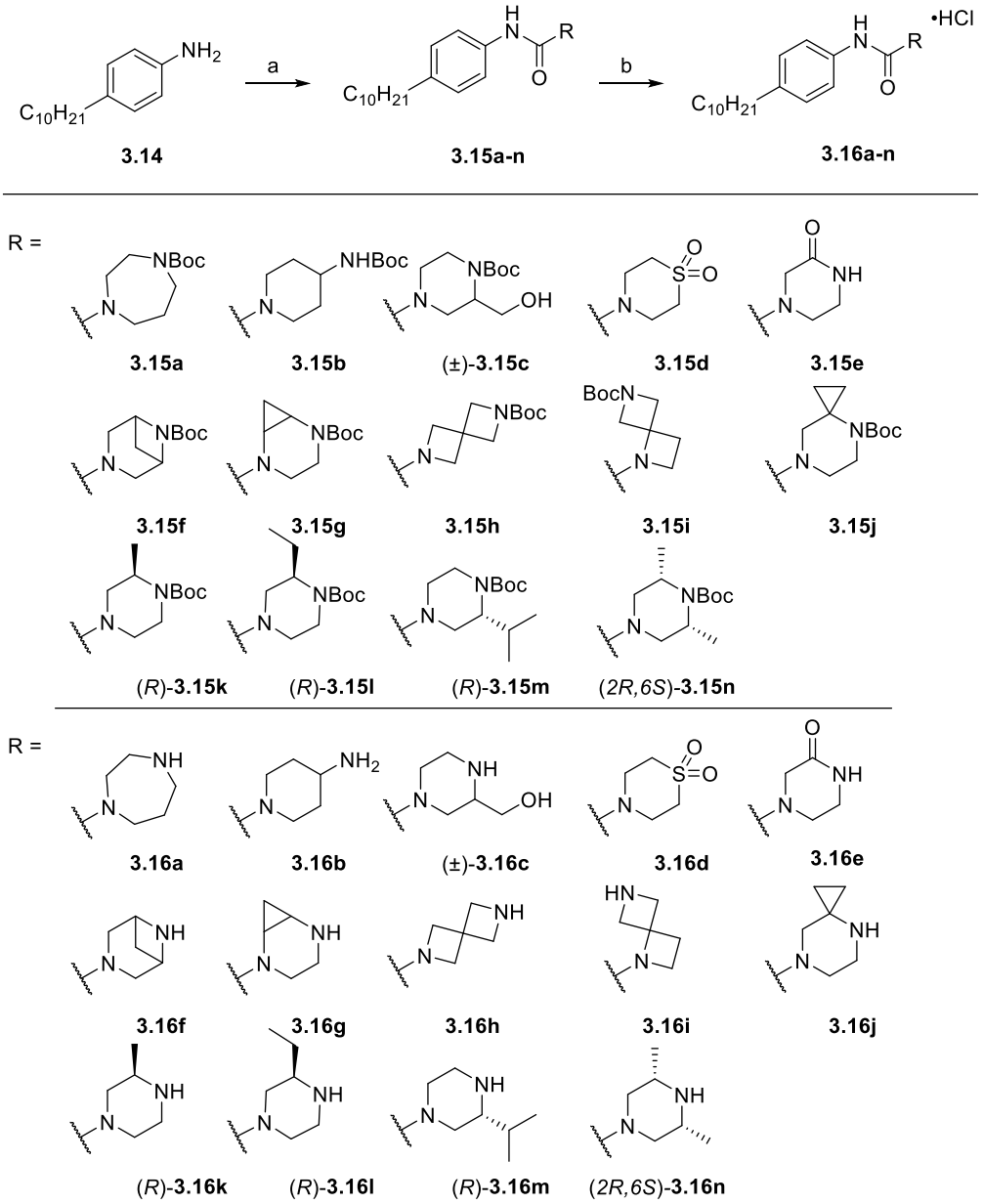

Scheme 3.3. (a) Triphosgene (0.5 equiv.), triethylamine (2.3 equiv.), *N*-Boc-amine (1.5 equiv.), DCM, 20 °C, 3 h, 32-88%; (b) 4 M HCl in dioxane (10.0 equiv.), DCM, 20 °C, 2 h, 71-95%.

3.6 *In Vitro* Evaluation of Inhibitors

Unfortunately, the reversed-core structures **3.5a** and **3.5b** displayed no activity when tested in HeLa cells at 1 μM concentration for Spns2 activity. Complete abolishment

of activity helped to better understand the binding interactions inside the Spns2 transporter. It was postulated that flipping the core of the molecule added too much polarity into the tail region of the inhibitors. As a result, the focus was shifted away from this scaffold and toward modification of **SLF80821178**.

Modification of the phenyl ring to a heterocycle was deemed attractive. It has been well established that phenyl rings pose metabolic issues as well as increase the hydrophobic properties of a drug. Replacement to a heterocycle with varying numbers of heteroatoms was hypothesized to improve the pharmacokinetic/pharmacodynamic profile.[22-24] To maintain a comparable total atom length, an undecyl tail was installed to replace the decyl tail. Pyrrole compound **3.8a** was found to have 48 ± 4% inhibition at 1 μM concentration. Increasing the heteroatom count to pyrazole **3.8b** and 1,2,4-triazole ring **3.8c** abolished all Spns2 inhibitory activity. Interestingly, replacement to a 1,2,4-oxadiazole ring with **3.13** increased S1P export by 80 ± 26% at 1 μM concentration (Table 3.1).

Focus was then shifted away from the core of the molecule and toward modification of the head group. Initially, modification of the piperazine headgroup to other bioisosteres was investigated.[25, 26] 1,4-diazepane was initially tested with **3.16a** to determine if increased ring size would show benefit from increased steric bulk in the binding pocket.[26, 27] This showed a comparable activity of 60 ± 5% inhibition at 300 nM. Next, modification of the number and type of hydrogen-bond donors and acceptors were tested to evaluate their impact. Replacement of the piperazine to a 1,4-aminopiperidine with **3.16b** exhibited 21 ± 4% inhibition. The lack of improvement to activity led toward investigation of additional hydrogen bonding functional groups while retaining the piperazine ring or related isosteres. For example, introduction of a primary alcohol group in the 2 position of

the head group with **(±)-3.16c** was probed to not only test additional hydrogen bonding potential but to also mimic endogenous sphingosine as well as FTY720.[28, 29] Unfortunately, this analog completely abolished activity. Conversion from the piperazine ring to the thiomorpholine 1,1-dioxide heterocyclic ring **3.16d** to increase hydrophilicity and polar interactions in the binding pocket was not advantageous as no statistically significant reduction in S1P transport was observed. In addition, **3.16e** was synthesized to determine the importance of the secondary ammonium group in **SLF80821178**. Since an amide will be neutral at physiological pH, the positive charge of the ammonium head group was found to be necessary as **3.16e** possessed no ability to inhibit Spns2.[30] Thus, focus was shifted away from increasing head group polarity and toward identifying bioisosteres of the piperazine ring.

Bicyclic, spiro, and substituted piperazines were deemed viable targets as rigid isosteres for piperazine.[31-36] To start, diazabicyclo head groups were synthesized. These fused ring systems would allow for probing of the binding pocket with rigid, three-dimensional systems.[33, 37] **3.16f-g** were synthesized to test diazabicycloheptane rings. 3,6-diazabicyclo[3.1.1]heptane **3.16f** and 2,5-diazabicyclo[4.1.0]heptane **3.16g** showed 0% and 7 ± 5% inhibition, respectively. As these possessed little to no activity, work was shifted toward azaspirocycles. Azaspirocycles increase the distance between the two nitrogen atoms in the head group while not increasing the steric bulk.[38] Piperazine has a distance of 2.86 Å from each nitrogen compared to the 1,6-diazasprio[3.3]heptane ring in **3.16h** which is 3.94 Å apart.[34] This increased distance could improve binding interactions inside Spns2 to increase affinity for the transporter. 1,6- and 2,6-diazasprio[3.3]heptane rings were chosen as mimetics for piperazine. 1,6- (**3.16h**) and 2,6 (**3.16i**), unfortunately,

were both inactive S1P transporter inhibitors in HeLa cells. However, 4,7-diazapsiro[2.5]octane showed modest activity with compound **3.16j** at 34 ± 15% inhibition. Oxidation by cytochrome P450 to 2-oxopiperazine is a metabolic liability.[8, 11, 12]

With modest activity in substitution on the 2-positon of the piperazine ring, this necessitated further exploration of structural analogs. With limited availability in materials and tight tolerances on functional groups observed in this series, derivatives were limited to alkyl substitution. The 2-positon of the piperazine ring was decorated with (*R*)-methyl, (*R*)-ethyl, and (*R*)-isopropyl groups. Methyl-substituted (*R*)-**3.16k** showed fantastic activity of 74 ± 6% inhibition at 300 nM concentration. Unfortunately, larger groups were not tolerated. Ethyl [(*R*)-**3.16l**] and isopropyl [(*R*)-**3.16m**] groups were detrimental at 13 ± 3% and 16 ± 1%, respectively. (*2R,6S*)-**3.16n** with the (*2S,6R*)-dimethylpiperazine head group was not tolerated with 0% inhibition. A concentration-dependent study was performed with (*R*)-**3.16k** due to its excellent inhibitory activity. As shown in Figure 3.3, a sigmoidal dose-response curve was generated with an increasing concentration of (*R*)-**3.16k**. (*R*)-**3.16k** possessed an IC_{50} value of 128 ± 9 nM. This IC_{50} value is similar in potency to **SLF80821178** (IC_{50} = 53 ± 4 nM), which necessitated the need for *in vivo* studies.

During this SAR study, the linker and head region were investigated for S1P inhibitory activity and increased oral bioavailability compared to **SLF80821178**. This work indicates that replacement of the phenyl ring with a heterocycle is not preferred. Maintaining the six-membered secondary amine in the head group is preferred compared to bicyclic amines and spirocycles. Addition of an (*R*)-2-methylpiperazine ring ((*R*)-3.16k) to the phenylurea scaffold provided us with excellent inhibitory activity *in vitro*.

Additionally, (*R*)-3.16k induced lymphopenia in mice after 16 h when administered IP. As such, additional work will focus on modification on the tail region of **SLF80821178**.

Table 3.1. Impact of heterocyclic replacement of aryl ring on Spns2 inhibition.[a]

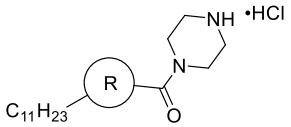

Cmpd	R	% Inh	Cmpd	R	% Inh
3.8a	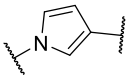	48 ± 4	**3.8c**	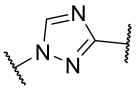	NS
3.8b	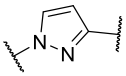	NS	**3.13**	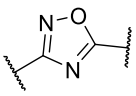	-80 ± 26

[a]Inhibitory data for heterocyclic amide derivatives in HeLa cells. Spns2 inhibition is reported as the percent decrease in S1P transport out of cell compared to control with no inhibitor present. All compounds tested at 1 µM concentration. Post-incubation, cell media was extracted and S1P concentrations were measured by LC-MS/MS. Assays were performed in triplicate. NS, no significant difference relative to control.

3.7 *In vivo* Assay

Compound **3.16k** (10 mg/kg) or an equal volume of vehicle (36.1% PEG400/9.1% ethanol/4.6% Solutol/50% H_2O) was administered by IP injection or oral gavage into mice (C57BL/6j strain). After 6-16 hours, blood samples were collected, and lymphocyte counts were analyzed from 20 µL of mice blood using Heska HT5 Element blood analyzer. All animal protocols were approved prior to experimentation by the University of Virginia School of Medicine's Animal Care and Use Committee.

Table 3.2. Impact of functional group on Spns2 inhibition.[a]

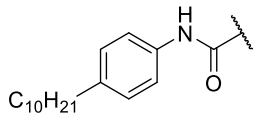

Cmpd	R	% Inh	Cmpd	R	% Inh
3.16a	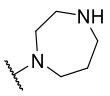	60 ± 5	**3.16h**[b]	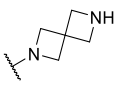	ns
3.16b	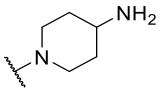	21 ± 4	**3.16i**[b]		ns
(±)-**3.16c**	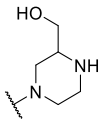	ns	**3.16j**		34 ± 15
3.16d[c]	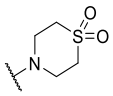	ns	(*R*)-**3.16k**		74 ± 6
3.16e[c]	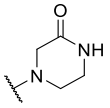	ns	(*R*)-**3.16l**	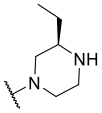	13 ± 3
3.16f	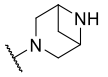	ns	(*R*)-**3.16m**	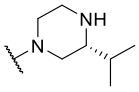	16 ± 1
3.16g	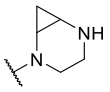	7 ± 5	(*2R,6S*)-**3.16n**	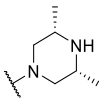	ns

[a]Inhibitory data for phenylurea derivatives in HeLa cells. Spns2 inhibition is reported as the percent decrease in S1P transport out of cell compared to the control with no inhibitor present. All compounds tested at 300 nM concentration. Post-incubation, cell media was extracted and S1P concentrations were measured by LC-MS/MS. Assays were performed in triplicate and all compounds are hydrochloride salts unless otherwise noted. NS, no significant difference relative to control. [b]**3.16i** is a trifluoroacetate salt. [c]**3.16d-e** are neutral compounds.

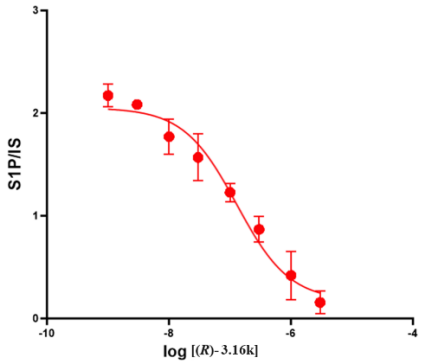

Figure 3.3. Dose-response assessment of (*R*)-**3.16k** in HeLa cells.

3.8 Biological Data

With *in vitro* activity being similar to **SLF80821178**, *in vivo* data was investigated using (*R*)-**3.16k** in cohorts of mice to determine circulating lymphocyte counts. Administration to mice of (*R*)-**3.16k** drove statistically significant lymphopenia in mice after 16 hours, a phenotype of Spns2 inhibition, which suggests that metabolism on the piperazine at the 2 position is likely occurring on **SLF80821178**, as it lacked activity at 16 hours post-dose (dose: 10 mg/kg) (Figure 3.4). With this data in hand, oral administration into mice was performed. Unfortunately, when administered orally in mice (dose: 20 mg/kg) after 4 hours, there was no statistically significant reduction in circulating lymphocytes (Figure 3.4). While the compound improved properties with IP administration, it is hypothesized that substitution on the piperazine ring increased the lipophilicity of the compound to inhibit absorption in the gastrointestinal tract.

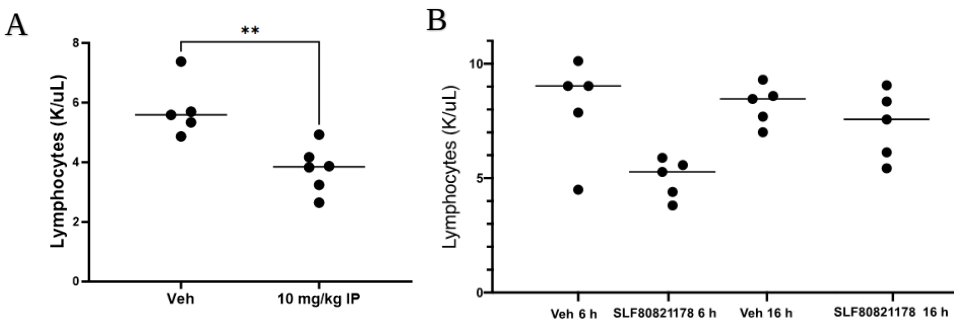

Figure 3.4. Biological evaluation of (*R*)-**3.16k** in female (C57BL/6j strain) mice. (a) Mice were injected with (*R*)-**3.16k** intraperiotoneally (10 mg/kg dose) or vehicle. Blood was then drawn after 16 hours post-dose. (b) Mice were injected with **SLF80821178** and blood was drawn after 6 h and 16 h post-dose. Circulating lymphocytes levels were measured. T test: ** ≤ 0.01.

3.9 Conclusions

This report entails several novel classes of Spns2 inhibitors. They comprise of phenyl-oxadiazole, heterocyclic analogues of benzamides, and phenylureas scaffolds that have significant *in vitro* activity against Spns2-mediated S1P transport. This SAR study shows a strong bias for endocyclic six-membered secondary amine head groups. It helps to prove the importance of a non-polar tail region and polar head group, as the oxadiazole core was found to be unnecessary and increased polarity was found to be not tolerated in the head region. Modification of the piperazine head group with the phenylureas with alkyl substitution in the 2-position was found to work best with comparable data to **SLF80821178**. *In vivo* data demonstrated a decrease in circulating lymphocytes with a single 20 mg/kg IP injection in mice after 16 hours. Future work will be aimed at continuing the SAR study around **SLF80821178** with investigations in the tail region of the compound as well as incorporating these head structures into different scaffolds.

3.10 References

1. Fritzemeier, R.; Foster, D.; Peralta, A.; Payette, M.; Kharel, Y.; Huang, T.; Lynch, K. R.; Santos, W. L., Discovery of In Vivo Active Sphingosine-1-phosphate Transporter (Spns2) Inhibitors. *J. Med. Chem.* **2022,** *65* (11), 7656-7681.

2. Shrader, C. W.; Foster, D.; Kharel, Y.; Huang, T.; Lynch, K. R.; Santos, W. L., Imidazole-based sphingosine-1-phosphate transporter Spns2 inhibitors. *Bioorg Med Chem Lett* **2023,** *96*, 129516.

3. Kumari, S.; Carmona, A. V.; Tiwari, A. K.; Trippier, P. C., Amide Bond Bioisosteres: Strategies, Synthesis, and Successes. *J. Med. Chem.* **2020,** *63* (21), 12290-12358.

4. Camci, M.; Karali, N., Bioisosterism: 1,2,4-Oxadiazole Rings. *Chemmedchem* **2023,** *18* (9), e202200638.

5. Dalvie, D. K.; Kalgutkar, A. S.; Khojasteh-Bakht, S. C.; Obach, R. S.; O'Donnell, J. P., Biotransformation reactions of five-membered aromatic heterocyclic rings. *Chem. Res. Toxicol.* **2002,** *15* (3), 269-299.

6. Maciolek, C. M.; Ma, B.; Menzel, K.; Laliberte, S.; Bateman, K.; Krolikowski, P.; Gibson, C. R., Novel cytochrome P450-mediated ring opening of the 1,3,4-oxadiazole in setileuton, a 5-lipoxygenase inhibitor. *Drug Metab. Dispos.* **2011,** *39* (5), 763-770.

7. Lan, S. J.; Weliky, I.; Schreiber, E. C., Metabolic studies with trans-5-amino-3-(2-(5-nitro-2-furyl)vinyl)-1,2,4-(5- 14 C)oxadiazole (SQ 18,506). 1. Reductive cleavage of the 1,2,4-oxadiazole ring. *Xenobiotica* **1973,** *3* (2), 97-102.

8. Alsubi, T. A.; Attwa, M. W.; Darwish, H. W.; Abuelizz, H. A.; Kadi, A. A., Piperazine ring toxicity in three novel anti-breast cancer drugs: an in silico and in vitro

metabolic bioactivation approach using olaparib as a case study. *Naunyn Schmiedebergs Arch Pharmacol* **2023,** *396* (7), 1435-1450.

9. Jampilek, J., Heterocycles in Medicinal Chemistry. *Molecules* **2019,** *24* (21).

10. Fruhauf, A.; Behringer, M.; Meyer-Almes, F. J., Significance of Five-Membered Heterocycles in Human Histone Deacetylase Inhibitors. *Molecules* **2023,** *28* (15).

11. El-Haj, B. M.; Ahmed, S. B. M.; Garawi, M. A.; Ali, H. S., Linking Aromatic Hydroxy Metabolic Functionalization of Drug Molecules to Structure and Pharmacologic Activity. *Molecules* **2018,** *23* (9).

12. Lazzara, P. R.; Moore, T. W., Scaffold-hopping as a strategy to address metabolic liabilities of aromatic compounds. *RSC Med Chem* **2020,** *11* (1), 18-29.

13. Ritchie, T. J.; Macdonald, S. J. F., Heterocyclic replacements for benzene: Maximising ADME benefits by considering individual ring isomers. *Eur J Med Chem* **2016,** *124*, 1057-1068.

14. Lipinski, C. A.; Lombardo, F.; Dominy, B. W.; Feeney, P. J., Experimental and computational approaches to estimate solubility and permeability in drug discovery and development settings. *Adv. Drug Del. Rev.* **1997,** *23* (1-3), 3-25.

15. Lazerwith, S. E.; Bahador, G.; Canales, E.; Cheng, G.; Chong, L.; Clarke, M. O.; Doerffler, E.; Eisenberg, E. J.; Hayes, J.; Lu, B.; Liu, Q.; Matles, M.; Mertzman, M.; Mitchell, M. L.; Morganelli, P.; Murray, B. P.; Robinson, M.; Strickley, R. G.; Tessler, M.; Tirunagari, N.; Wang, J.; Wang, Y.; Zhang, J. R.; Zheng, X.; Zhong, W.; Watkins, W. J., Optimization of Pharmacokinetics through Manipulation of Physicochemical Properties in a Series of HCV Inhibitors. *ACS Med. Chem. Lett.* **2011,** *2* (10), 715-719.

16. Godamudunage, M. P.; Grech, A. M.; Scott, E. E., Comparison of Antifungal Azole Interactions with Adult Cytochrome P450 3A4 versus Neonatal Cytochrome P450 3A7. *Drug Metab Dispos* **2018,** *46* (9), 1329-1337.

17. Ghosh, A. K.; Brindisi, M., Urea Derivatives in Modern Drug Discovery and Medicinal Chemistry. *J. Med. Chem.* **2020,** *63* (6), 2751-2788.

18. Sahyoun, T.; Arrault, A.; Schneider, R., Amidoximes and Oximes: Synthesis, Structure, and Their Key Role as NO Donors. *Molecules* **2019,** *24* (13).

19. Jeong, H. J.; Park, Y. D.; Park, H. Y.; Jeong, I. Y.; Jeong, T. S.; Lee, W. S., Potent inhibitors of lipoprotein-associated phospholipase A(2): benzaldehyde O-heterocycle-4-carbonyloxime. *Bioorg Med Chem Lett* **2006,** *16* (21), 5576-5579.

20. Sibley, C. D.; Morris, E. A.; Kharel, Y.; Brown, A. M.; Huang, T.; Bevan, D. R.; Lynch, K. R.; Santos, W. L., Discovery of a Small Side Cavity in Sphingosine Kinase 2 that Enhances Inhibitor Potency and Selectivity. *J. Med. Chem.* **2020,** *63* (3), 1178-1198.

21. Collier, P. N.; Campbell, A. D.; Patel, I.; Raynham, T. M.; Taylor, R. J., Enantiomerically pure alpha-amino acid synthesis via hydroboration-suzuki cross-coupling. *J. Org. Chem.* **2002,** *67* (6), 1802-1815.

22. Martins, P.; Jesus, J.; Santos, S.; Raposo, L. R.; Roma-Rodrigues, C.; Baptista, P. V.; Fernandes, A. R., Heterocyclic Anticancer Compounds: Recent Advances and the Paradigm Shift towards the Use of Nanomedicine's Tool Box. *Molecules* **2015,** *20* (9), 16852-16891.

23. Kabir, E.; Uzzaman, M., A review on biological and medicinal impact of heterocyclic compounds. *Results in Chemistry* **2022,** *4*, 100606.

24. Vitaku, E.; Smith, D. T.; Njardarson, J. T., Analysis of the structural diversity, substitution patterns, and frequency of nitrogen heterocycles among U.S. FDA approved pharmaceuticals. *J. Med. Chem.* **2014,** *57* (24), 10257-10274.

25. Xu, K.; Hsieh, C. J.; Lee, J. Y.; Riad, A.; Izzo, N. J.; Look, G.; Catalano, S.; Mach, R. H., Exploration of Diazaspiro Cores as Piperazine Bioisosteres in the Development of sigma2 Receptor Ligands. *Int. J. Mol. Sci.* **2022,** *23* (15).

26. Meanwell, N. A.; Loiseleur, O., Applications of Isosteres of Piperazine in the Design of Biologically Active Compounds: Part 1. *J Agric Food Chem* **2022,** *70* (36), 10942-10971.

27. Meanwell, N. A., Synopsis of some recent tactical application of bioisosteres in drug design. *J. Med. Chem.* **2011,** *54* (8), 2529-2591.

28. Baumruker, T.; Billich, A.; Brinkmann, V., FTY720, an immunomodulatory sphingolipid mimetic: translation of a novel mechanism into clinical benefit in multiple sclerosis. *Expert Opin. Investig. Drugs* **2007,** *16* (3), 283-289.

29. Chi, H., Sphingosine-1-phosphate and immune regulation: trafficking and beyond. *Trends Pharmacol. Sci.* **2011,** *32* (1), 16-24.

30. Simplicio, A. L.; Clancy, J. M.; Gilmer, J. F., Prodrugs for amines. *Molecules* **2008,** *13* (3), 519-547.

31. Hiesinger, K.; Dar'in, D.; Proschak, E.; Krasavin, M., Spirocyclic Scaffolds in Medicinal Chemistry. *J. Med. Chem.* **2021,** *64* (1), 150-183.

32. Moshnenko, N.; Kazantsev, A.; Chupakhin, E.; Bakulina, O.; Dar'in, D., Synthetic Routes to Approved Drugs Containing a Spirocycle. *Molecules* **2023,** *28* (10).

33. Lovering, F.; Bikker, J.; Humblet, C., Escape from flatland: increasing saturation as an approach to improving clinical success. *J. Med. Chem.* **2009,** *52* (21), 6752-6756.

34. Burkhard, J.; Carreira, E. M., 2,6-Diazaspiro[3.3]heptanes: synthesis and application in Pd-catalyzed aryl amination reactions. *Org. Lett.* **2008,** *10* (16), 3525-3526.

35. Burkhard, J. A.; Guerot, C.; Knust, H.; Rogers-Evans, M.; Carreira, E. M., Synthesis and structural analysis of a new class of azaspiro[3.3]heptanes as building blocks for medicinal chemistry. *Org. Lett.* **2010,** *12* (9), 1944-1947.

36. Burkhard, J. A.; Wagner, B.; Fischer, H.; Schuler, F.; Muller, K.; Carreira, E. M., Synthesis of azaspirocycles and their evaluation in drug discovery. *Angew Chem Int Ed Engl* **2010,** *49* (20), 3524-3527.

37. Gao, D.; Penno, C.; Wunsch, B., Rigid Scaffolds: Synthesis of 2,6-Bridged Piperazines with Functional Groups in all three Bridges. *ChemistryOpen* **2020,** *9* (8), 874-889.

38. Degorce, S. L.; Bodnarchuk, M. S.; Scott, J. S., Lowering Lipophilicity by Adding Carbon: AzaSpiroHeptanes, a logD Lowering Twist. *ACS Med. Chem. Lett.* **2019,** *10* (8), 1198-1204.

Chapter 4: Development Of a Highly Active Benzimidazole Scaffold With *In Vivo* Activity Toward Spns2 Inhibition

4.1 Contributions

The compounds in this chapter were mainly synthesized and analyzed by Christopher Shrader. Christine Tan synthesized **4.7a**, **4.7j**, and **4.7k**, Mario Hernandez synthesized **4.13a** and **4.13b**, and Abigail Agner synthesized **4.13e** and **4.13f.** Dr. Russell Fritzemeier synthesized **SLF1081851,** and Dr. Ariel Burgio synthesized **SLB1122168**, the two lead compounds mentioned in this chapter. Tail modification ideas were inspired by Kyle Dunnavant's work. The work was completed under guidance from Dr. Webster L. Santos. All presented biological data was performed and collected by Dr. Kevin Lynch, Dr. Yugesh Kharel, and Dr. Tao Huang at the University of Virginia.

4.2 Abstract

The sphingosine-1-phosphate (S1P) receptor S1P1 is a well-established target in FDA approved drugs for the treatment of multiple sclerosis and ulcerative colitis. Targeting this receptor blocks the egress of T-lymphocytes as the S1P is important in the positioning of immune cells. Unfortunately, all S1P receptor modulators lead to unwanted cardiovascular side-effects, specifically first-dose bradycardia. To circumvent this shortcoming, inducing lymphopenia by targeting the S1P pathway upstream from the receptors could provide therapeutic benefit while avoiding unwanted side-effects. A genetic knockout of the S1P pathway at its transporter Spinster homolog 2 (Spns2) produces a lymphopenic phenotype; therefore, Spns2 inhibitors are expected to recapitulate this phenotype but are currently underdeveloped. Spns2 has a need for a high potency, orally bioavailable inhibitor. **SLF1081851** and **SLB1122168** represent 1st and 2nd

generation inhibitors disclosed by the Santos lab. However, these suffer from poor oral bioavailability. This necessitates further investigation into Spns2 inhibitors that possess better pharmacokinetic properties for oral administration. Studies around these two inhibitors allowed us to discover the 2-amidobenzimidazole series. A structure-activity relationship study was performed on the head and tail regions of this scaffold. Various polar head groups were tested for their activity to inhibit S1P transporter. Our studies revealed a strong preference for secondary amines such as pyrrolidine and piperazine. Investigation of the tail region was performed by homologation from octyl to decyl length. The results indicate a preference for a 9 heavy-atom length with the nonyl tail. The most successful inhibitors were developed from incorporating phenyl ethers at the terminal region of the tail. The addition of a meta-cyclopropyl ring to the phenoxy ether tail (**4.13h**) showed excellent inhibitory activity at 85% reduction at 300 nM concentration. In a dose-response manner, **4.13h** potently inhibited S1P transport with an IC_{50} = 27 ± 6 nM. To determine *in vivo* efficacy, **4.13h** was administered intraperitoneally (IP) and orally to mice, which afforded a dose-dependent reduction of circulating lymphocytes, a phenotype observed with Spns2 inhibition. The discovery of **4.13h** provides a valuable tool for exploration of both the therapeutic value of targeting Spns2 as well as the physiological results of S1P modulation through its transporter.

4.3 Introduction

Recently, the Santos lab has disclosed the discovery of two generations of Spns2 inhibitors.[1, 2] The first generation of inhibitors reported compound **SLF1081851**, which inhibited Spns2 in an *in vitro* HeLa-cell based S1P release assay (IC_{50} = 1.93 ± 0.04 μM) (Figure 4.1).[1, 3] Administration of **SLF1081851** in mice *via* intraperitoneal (IP) injection

resulted in dose-dependent lymphopenia as well as exhibiting protective properties in a mouse kidney model of renal fibrosis.[1, 4] **SLF1081851** provided a scaffold on which to improve the PK/PD properties of the inhibitors, given its relatively poor potency and low therapeutic window (maximum tolerated dose ~30mg/kg).[5] Structure-activity relationship (SAR) studies on the fusion of the phenyl and oxadiazole rings in **SLF1081851** and various head groups led to the discovery of **SLB1122168** (Figure 4.1).[2] Bearing a fused heterocycle core and secondary amine head group, **SLB1122168** exhibited *in vitro* Spns2 inhibition with an IC_{50} = 94 ± 6 nM. *In vivo* assays resulted in lymphopenia in mice and rats post IP injection.[2] **SLB1122168** also showed a favorable half-life of 8 h in rats, where direct correlation of drug levels with lymphopenia as a pharmacodynamic marker was observed.[2, 6]

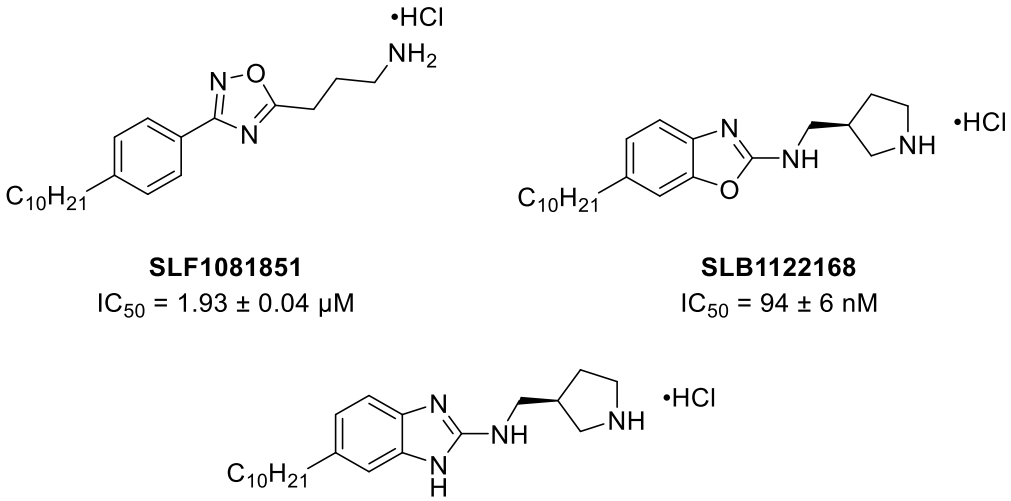

Figure 4.1. First generation Spns2 inhibitor **SLF1081851**, second generation Spns2 inhibitor **SLB1122168**, and first benzimidazole **38p** reported by the Santos lab.[1-2]

However, **SLB1122168** suffers from poor oral bioavailability as no lymphopenia is observed when administered to mice orally. Our studies focused on maintaining or improving Spns2 inhibitory activity while gaining oral bioavailability *in vivo*. We began our studies by investigating the 5,6-bicyclic core of **SLB1122168**.[7] Unfortunately, **SLB1122168** has a cLogP of 6.8 and 12 rotatable bonds, which violates the ideal drug-like properties laid out by Lipinski and Veber (Figure 4.2).[8-10]

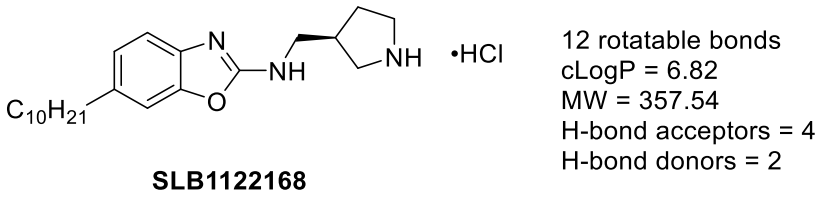

Figure 4.2. Assessment of the drug-like properties of **SLB11226168** as laid out by Lipinski and Veber.[8-9]

We envisioned that a compound with similar *in vitro* activity, a cLogP below 5, and rotatable bonds under 10 to fit Lipinski's Rule of 5 and Veber's Rule would result in a compound with attractive oral bioavailability.[11] The SAR study performed around **SLB1122168** identified **38p**, a compound containing a 2-aminobenzimidazole (Figure 4.1).[2] While **38p** had lower inhibitory activity at 34 ± 1% compared to **SLB1122168**'s activity of 87 ± 7% at 1 μM, this compound provided a promising hit from for further development. Benzimidazole are an important privileged scaffold[12] found in FDA approved drugs and have biological applications such in cancer,[13-15] autoimmune diseases,[16-18] and neurological disorders.[19-21] Looking at how we could improve the PK/PD profile of **SLF1081851** and **SLB1122168**, we hypothesized that increasing hydrophilicity through introduction of additional hydrogen bonding potential could be beneficial. Molecular docking studies of **SLB1122168** in the binding pocket of Spns2 have revealed

a Trp440 residue in the binding location of this inhibitor (Figure 4.3).[22] The amide carbonyl in the 2-position of our scaffold could provide strong hydrogen binding interactions with this residue to increase potency. Therefore, an SAR study around the head and tail region of our 2-amidobenzimidazoles was performed to evaluate its potential as an inhibitor.

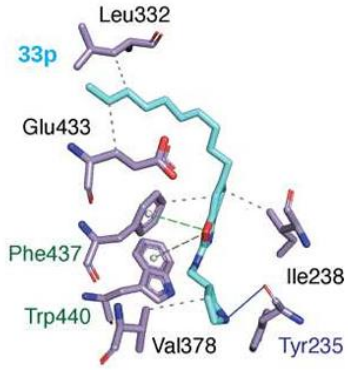

Figure 4.3. Molecular docking studies of **SLB1122168** show key binding interactions in Spns2. Figure is adapted from reference.[22]

4.4 Chemical Synthesis

Modification of the benzimidazole headgroup synthesis is described in Scheme 4.1. Reaction of 4-bromo-1,2-phenyldiamine with di-tert-butyl dicarbonate provided the di-Boc-protected phenyldiamine **4.2** in 77% yield.[23] A one-pot hydroboration of 1-decene followed by Suzuki-Miyaura cross-coupling was performed to install the decyl tail affording **4.3** in 90% yield. Boc deprotection using 4 M hydrogen chloride in dioxane afforded the HCl salt intermediate **4.4** in 88% yield. Cyclization with methyl 2,2,2-trichloroacetimidate in glacial acetic acid generated common intermediate **4.5** in 73% yield.[24, 25] Diversification of **4.5** was possible by reaction using various *N*-Boc-amines to afford **4.6a-m** in 30-68% yield.[26, 27] Finally, Boc deprotection using 4 M hydrogen chloride in dioxane afforded final compounds **4.7a-m** as the hydrogen chloride salts in 70-95% yield.

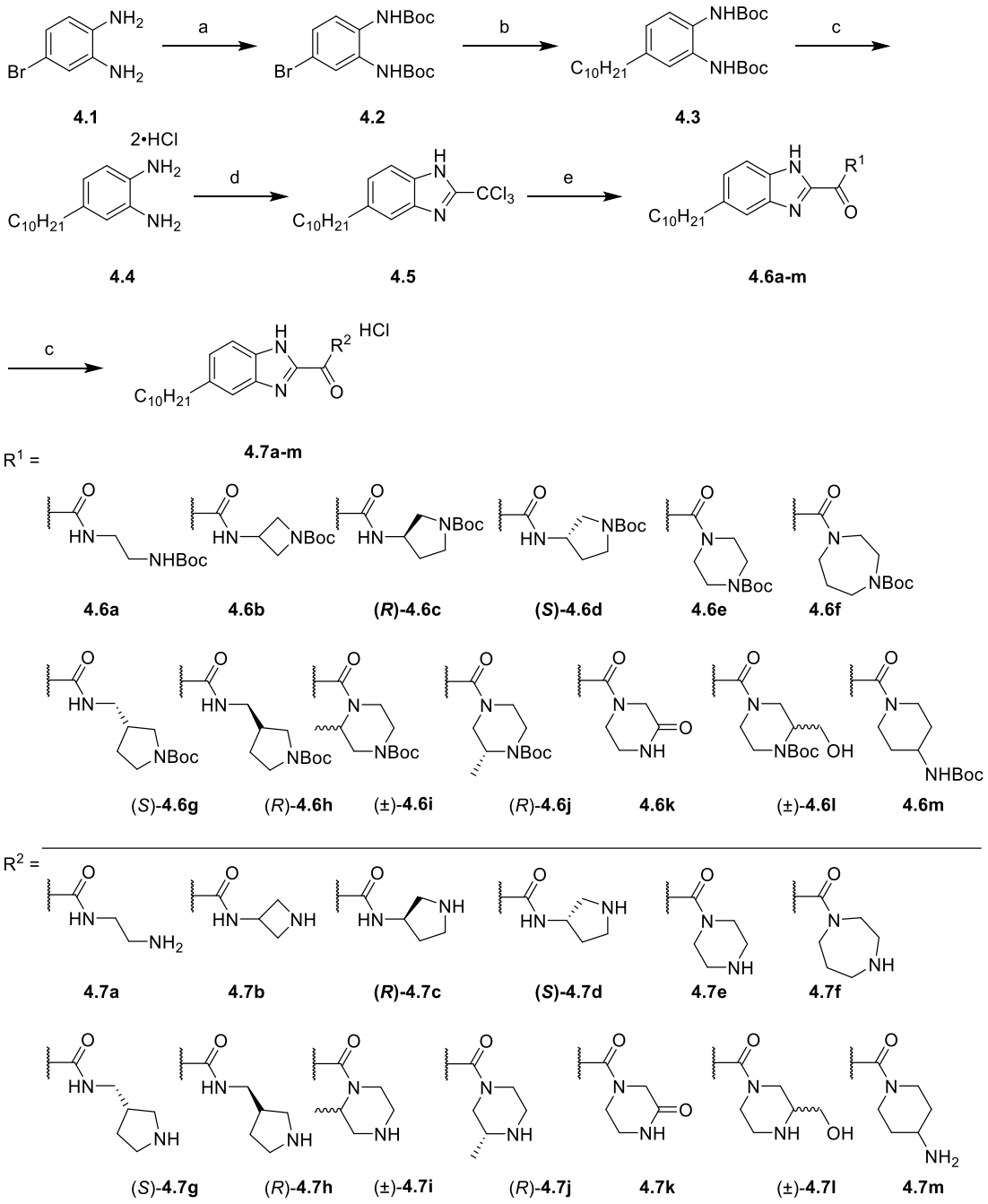

Scheme 4.1. (a) Di-*tert*-butyl dicarbonate (4.0 equiv.), 2.5 M aq. NaOH (5.0 equiv.), DCM, 20 °C, 16 h, 77%; (b) (i) 1-decene (1.2 equiv.), 9-BBN (1.5 equiv.), THF, 70 °C, 1 h. (ii) Aryl bromide (1.0 equiv.), $PdCl_2(dppf)\cdot CH_2Cl_2$ (0.05 equiv.), 3 M aq. KOH (3.0 equiv.), THF, 70 °C, 16 h, 90%; (c) 4 M HCl in dioxane (10.0 equiv.), DCM, 20 °C, 1 h, 70-95%; (d) Methyl 2,2,2-trichloroacetimidate (1.1 equiv.), AcOH, 0 °C to 20 °C, 3 h, 73%; (e) *N*-Boc-amine (1.2 equiv.), $NaHCO_3$ (10.0 equiv.), 1:2 water:THF, 50 °C, 2 h, 30-68%.

Tail modifications were performed following Scheme 4.2. Cyclization of 4-bromo-1,2-phenyldiamine with methyl 2,2,2-trichloroacetimidate in acetic acid afforded intermediate **4.8** in 92% yield. Reaction with *N*-Boc-piperazine in aqueous THF allowed for generation of amide **4.9** in 84% yield. To improve the reaction yield for the cross-coupling step, the benzimidazole N-H was protected using 2-(trimethylsilyl)ethoxymethyl chloride (SEM-Cl) and sodium hydride to afford **4.10** in quantitative yield.[28] Then, a one-pot hydroboration of various alkenes was performed followed by Suzuki-Miyaura cross-coupling to afford intermediates **4.11a-l** in 61-86% yield. The SEM group was then removed using tetrabutylammonium fluoride (TBAF) in refluxing THF to afford product **4.12a-l** in 38-93% yield.[29, 30] Boc deprotection in 4 M hydrochloric acid in dioxane afforded the final compounds **4.13a-l** in 85-95% yield as hydrogen chloride salts. Alkene tails for cross-coupling were synthesized through substitution of the appropriate 1-bromoalkene using the substituted phenols **4.14a-j** to afford alkene ether tails **4.15a-j** in 25-72% yield (Scheme 4.3).

4.5 *In Vitro* Analysis of Inhibitors

Inhibitors were screened at 300 nM concentration in the previously described mouse Spns2 HeLa cell based S1P release assay (*vide supra*, Chapter 3). To begin, we kept the decyl tail consistent as this had the best activity in previous reports.[1, 2] Various alkyl and cycloalkyl amine head groups were tested for their activities as shown in Table 4.1. To begin, **4.7a** was synthesized as a mimic of **SLF1081851** and showed low activity at 23 ± 9% compared to **SLF1081851's** 30 ± 7% at 300 nM. Thus, we switched to secondary amines as they showed improved activity in our previous reports.[2] The effect of ring size was explored first.

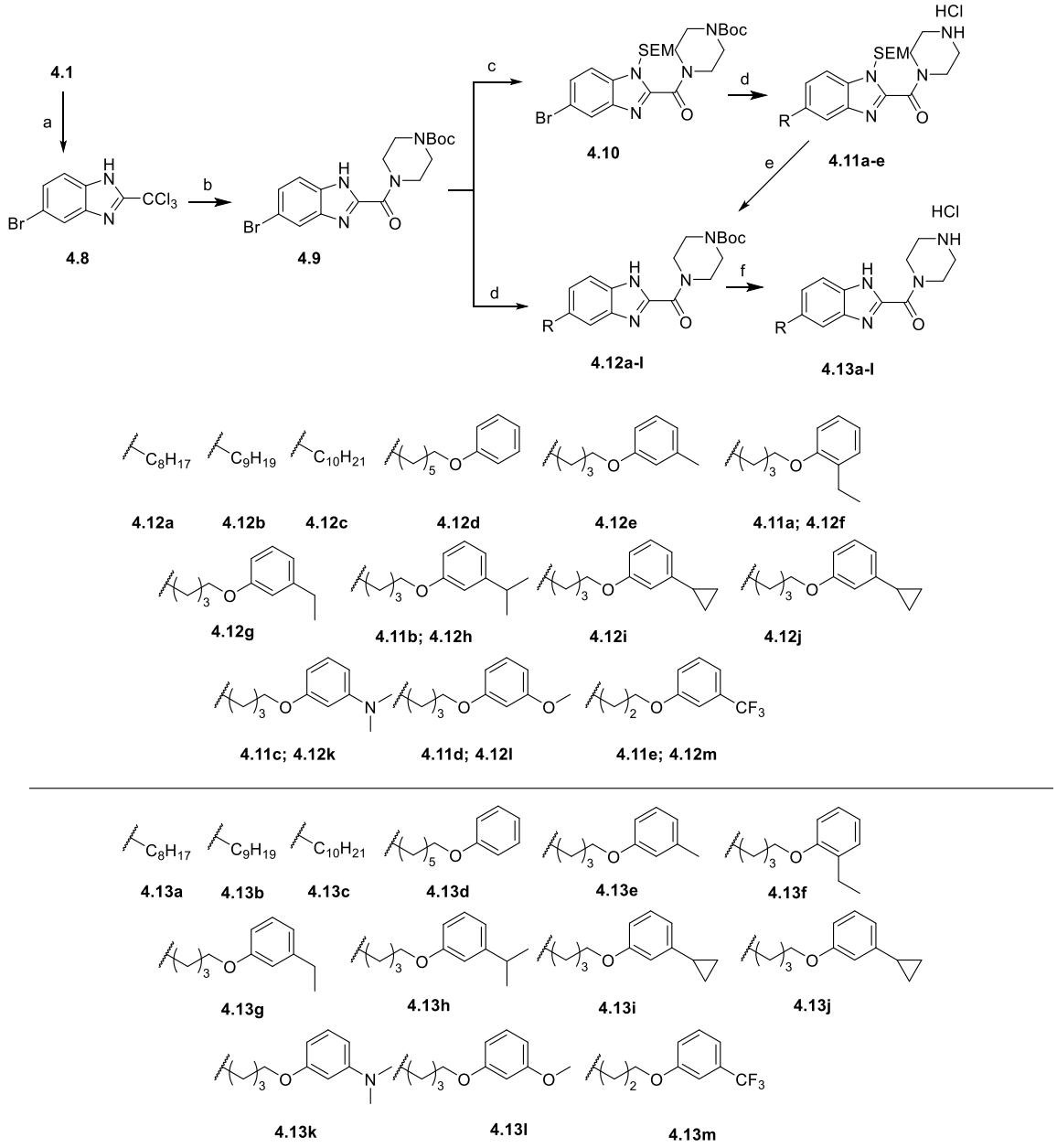

Scheme 4.2. (a) Methyl 2,2,2-trichloroacetimidate (1.1 equiv.), AcOH, 0 °C to 20 °C, 3 h, 92%; (b) *N*-Boc-piperazine (1.2 equiv.), $NaHCO_3$ (10.0 equiv.), 1:2 water:THF, 50 °C, 2 h, 84%; (c) NaH (1,1 equiv.), SEM-Cl (1.1 equiv.), THF, 0 °C to 20 °C, 2 h, 98% (d) (i) Alkene (2.0 equiv.), 9-BBN (2.3 equiv.), THF, 70 °C, 1 h. (ii) Aryl bromide (1.0 equiv.), $PdCl_2(dppf)\cdot CH_2Cl_2$ (0.15 equiv.), 3 M aq. K_2CO_3 (3.0 equiv.), THF, 70 °C, 16 h, 61-86%; (e) TBAF (3.0 equiv.), THF, 70 °C, 3 h, 38-93% (f) 4 M HCl in dioxane (10.0 equiv.), DCM, 20 °C, 1 h, 85-95%.

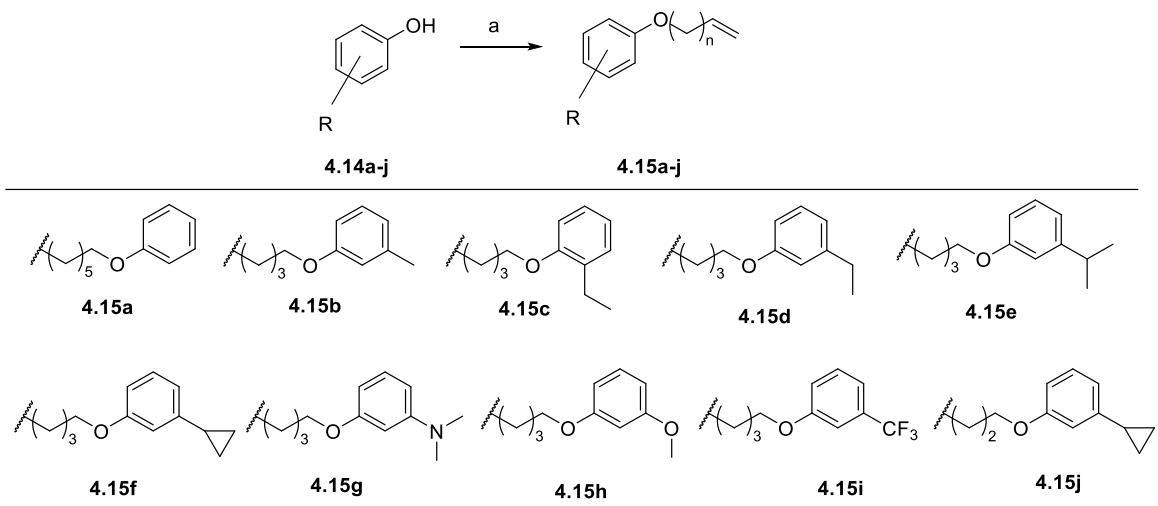

Scheme 4.3. (a) K_2CO_3 (2.0 equiv.), 1-bromoalkene (1.2 equiv.), MeCN, reflux, 16 h, 25-72%.

Azetidine (**4.7b**), pyrrolidines (**4.7c**-**d**), pyrrolidine (**4.7e**), piperazine (**4.7f**), and 1,4-diazapane (**4.7f**) were evaluated. Azetidine (**4.7b**) had low activity with 12 ± 19% inhibition and 1,4-diazepane (**4.7f**) showed no inhibition. However, there was a clear preference for the five- and six-membered ring size. Piperazine (**4.7e**) had very potent activity at 67 ± 3% inhibitory activity. **4.7c** and **4.7d** showed good activity with 60 ± 3% and 44 ± 2%, respectively. Similar to previous reports with pyrrolidine rings on the benzoxazole scaffold, there was a clear preference for the (*S*)-isomer.[2] To add flexibility in the head group, an additional methylene linker was added between the amide and pyrrolidine ring in **4.7g-h**, which reduced activity to 10 ± 3% and 15 ± 1%, respectively. Adding steric bulk with the substituted piperazine rings **4.7i-j** showed decreased activity with the (*R*)-methyl substitution (**4.7j**) being slightly tolerated with a 45 ± 2% inhibition. Removal of the positive charge by replacement of the secondary amine with an endocyclic amide with **4.7k** showed the ammonium was important as activity was abolished to 0% inhibition. Additional hydrogen bonding potential with **4.7l** bearing an alcohol group

showed 9 ± 3% inhibition and extending the terminal ammonium to a primary amine with the 4-aminopiperidine **4.7m** abolished all activity.

With compound **4.7e** being the best of the series, investigation of the tail using the piperazine head group was performed as shown in Table 4.2. Initially, a homologation study was performed to determine ideal tail length of alkyl chains. Octyl (**4.13a**), nonyl (**4.13b**), and decyl (**4.13c**) tails were synthesized and these had inhibition activity of 86 ± 0%, 86 ± 0%, and 67 ± 3%, respectively. Homologation studies on the tail concluded a slight preference for octyl and nonyl length. Optimization of **4.13c** to better match Lipinski's Rules was performed. Specifically, reducing the number of rotatable bonds and cLogP. We designed tails that reduced these values while maintaining the lipophilicity observed in the tail region. This led to the discovery of the phenoxy tail series, which reduced cLogP values from 5.87 (**4.7e**) to 4.59 (**4.13c**). Initially, unsubstituted phenoxy (**4.13c**) was synthesized and this had 49 ± 1% inhibition. Thus, expanded on substitution on the phenyl ring. *meta*-Substitution has been shown to have the best activity for phenylurea Spns2 inhibitors, so we began our studies with the *m*-methyl phenoxy tail **4.13d**. Seeing activity at 39 ± 3%, we extended this one methylene unit longer to the ethyl group (**4.13f**) and it showed 50 ± 3%. Increasing size to the larger isopropyl group (**4.13g**) showed comparable activity to ethyl with 50 ± 3% inhibition. Next, we cyclized the isopropyl group to a cyclopropyl ring (**4.13h**), and it showed excellent activity at 85 ± 1% inhibition. With this being the best inhibitor synthesized, **4.13i** was synthesized to test one atom length shorter to determine if it followed the pattern of straight-chain alkyl tails. Unfortunately, this was not tolerated as activity diminished to 25 ± 4% inhibition observed. Other functional groups were tested for electronics effects with *N*,*N*-dimethyl (**4.13j**),

methoxy (**4.13k**), and trifluoromethyl (**4.13l**). None of these outperformed our best inhibitor with this series, **4.13h**.

Table 4.1. Assessment of head groups on benzimidazoles for Spns2 inhibition.[a]

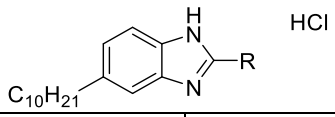

Cmpd	R	% Inh	Cmpd	R	% Inh
SLF1081851		30 ± 7	(S)-**4.7g**	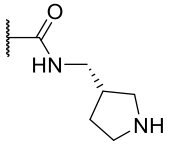	10 ± 3
4.7a	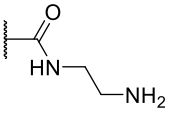	23 ± 9	(*R*)-**4.7h**	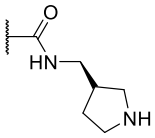	15 ± 1
4.7b[b]	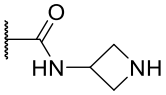	12 ± 19	(±)-**4.7i**	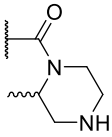	31 ± 2
(*R*)-**4.7c**	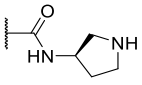	44 ± 2	(*R*)-**4.7j**	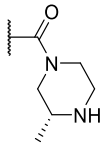	45 ± 2
(*S*)-**4.7d**	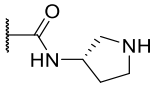	60 ± 3	**4.7k**[c]	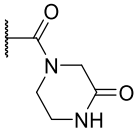	0
4.7e	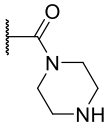	67 ± 3	(±)-**4.7l**	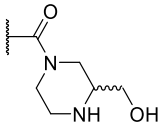	9 ± 3
4.7f	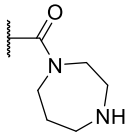	0	**4.7m**	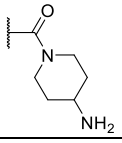	0

[a]Inhibitory data for benzimidazoles with diversified polar head groups in HeLa cells. Spns2 inhibition is reported as the percent decrease in S1P transport out of cell compared to the control with no inhibitor present. Compounds were tested at 300 nM concentration. Post-incubation, cell media was extracted and S1P concentrations were measured by LC-MS/MS. Assays were performed in triplicate. [b]**4.7b** is a trifluoroacetate salt. [c]**4.7k** is a neutral compound.

A concentration-dependent study was performed with the two most potent inhibitors, **4.13b** and **4.13h**. As shown in Figure 4.4, a sigmoidal dose-response curve was generated as concentrations of the two inhibitors were increased. IC_{50} values for **4.13b** and **4.13h** were found to be 21 ± 12 nM and 27 ± 6 nM respectively.

4.6 Biological Data

Compounds for this portion of the SAR were tested in the previously described *in vivo* assay (*vide supra*, Chapter 3). **4.13b** and **4.13h** displayed high *in vitro* efficacy, which made them ideal candidates for further investigation *in vivo*. Administration of a single 10 mg/kg IP injection after 4 hours for both **4.13b** (Figure 4.5) and **4.13h** (Figure 4.6) showed statistically significant reductions in circulating lymphocytes. Decreased circulating lymphocyte levels are a phenotype of Spns2 inhibition.[31-33]

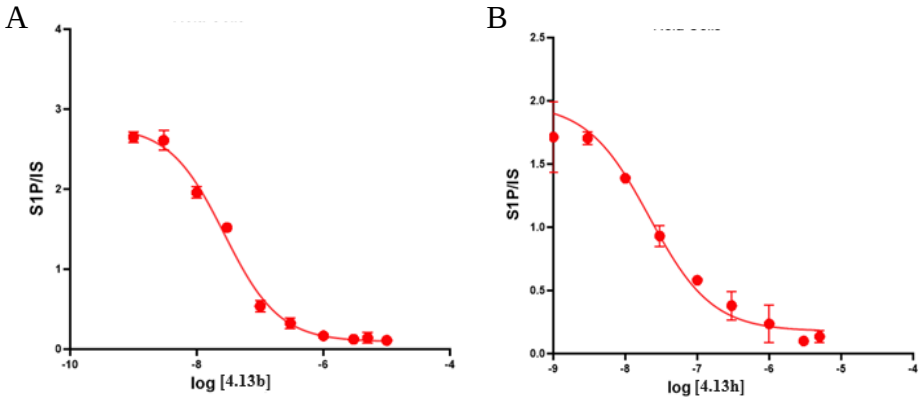

Figure 4.4. Dose-response assessment of **4.13b** (A) and **4.13h** (B) in HeLa cells demonstrated that **4.13b** and **4.13h** possessed IC_{50} values of 21 ± 12 and 27 ± 6 nM respectively.

Unfortunately, when administered PO, **4.13b** performed poorly with no observable lymphopenia. However, at 20 mg/kg PO after 4 hours, **4.13h** showed 34% lymphopenia and no effect on blood and plasma S1P levels was observed (Figure 4.6). While some studies suggest that complete knockout of the *Spns2* gene drives modest plasma S1P concentration decreases, often report no change.[33-35] To determine the safety and

tolerability of **4.13h**, a 14-day chronic dosing study was performed. At 20 mg/kg, no observable sign of toxicity such as changes in fur, eyes, recurrence of secretions, changes in gait, posture, and response to handling were observed.

Table 4.2. Assessment of tail replacement on benzimidazoles for Spns2 inhibitory activity.[a]

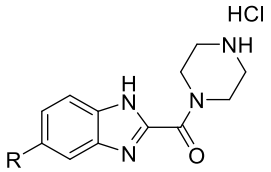

Cmpd	R	% Inh	Cmpd	R	% Inh
4.13a	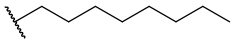	86 ± 0	**4.13g**	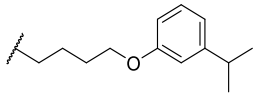	51 ± 0
4.13b	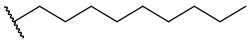	86 ± 0	**4.13h**	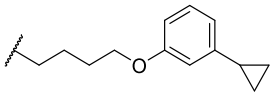	85 ± 1
4.7e	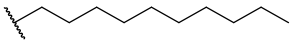	67 ± 3	**4.13i**	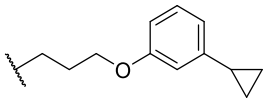	25 ± 4
4.13c	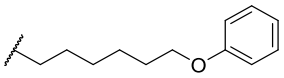	49 ± 1	**4.13j**	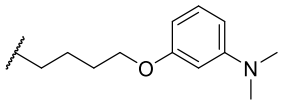	30 ± 4
4.13d	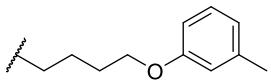	39 ± 3	**4.13k**	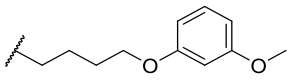	20 ± 5
4.13e	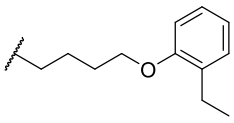	50 ± 3	**4.13l**	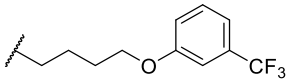	42 ± 2
4.13f	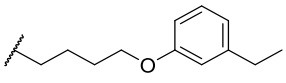	33 ± 8			

[a]Spns2 inhibition is reported as the percent decrease in S1P transport out of cell compared to the control with no inhibitor present. Compounds were tested at 300 nM concentration. Post-incubation, cell media was extracted and S1P concentrations were measured by LC-MS/MS. Assays were performed in triplicate.

A B

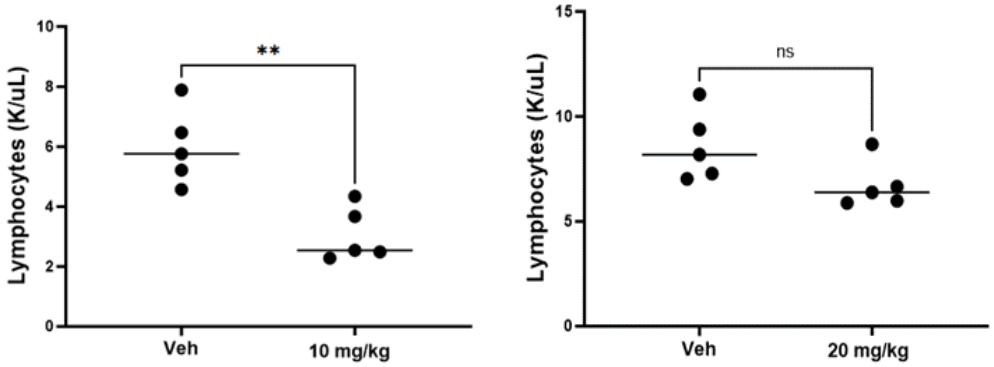

Figure 4.5. Biological evaluation of **4.13b** in female (C57BL/6j strain) mice. (A) Mice were injected with **4.13b** administered intraperiotoneally (10 mg/kg dose) or vehicle. Blood was then drawn after 4 hours post-dose and circulating lymphocytes levels were measured. (B) Mice were adminstered **4.13b** per oral or vehicle and blood was drawn 4 hours post-dose. Circulating lymphocytes levels were measured. T test: ** ≤ 0.01.

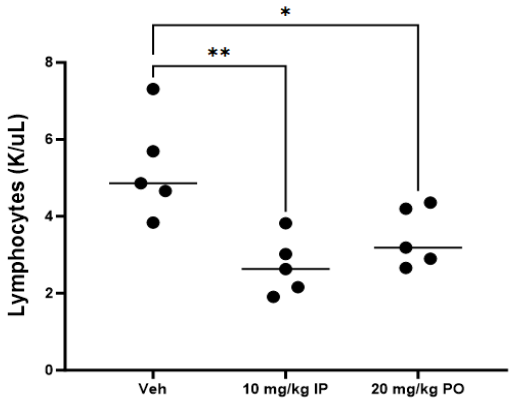

Figure 4.6. Biological evaluation of **4.13h** in female (C57BL/6j strain) mice. Mice were injected with **4.13h** administered IP (10 mg/kg), PO (20 mg/kg), or vehicle. Blood was then drawn after 4 hours post-dose and circulating lymphocytes were measured. T test: * ≤ 0.05; ** ≤ 0.01.

Preliminary pharmacokinetic studies were conducted and **4.13h** was shown to have maximum serum concentration levels in 2 hours (C_{max} = 480 nM) in mice. It was also determined to have a metabolic half-life of 8.33 hours in mice (Figure 4.7). Further biological assessments for **4.13h** are currently being performed.

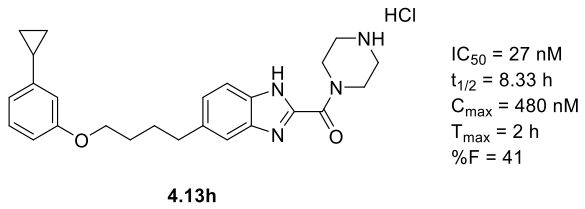

Figure 4.7. Pharmacokinetic profile of **4.13h** in mice.

4.7 Conclusions:

In this report, several novel structures of Spns2 inhibitors were disclosed. The SAR campaign around the 2-amidobenzimidazole scaffold showed a strong preference for pyrrolidine and piperazine rings in the head region. Modifications to the piperazine ring were shown to be poorly tolerated as well as larger rings and primary amines not preferred. The tail homologation study showed a strong preference for the nonyl length tail. Butyl-phenoxy tails were shown to be highly active and with the *meta*-substituted cyclopropyl ring being best. **4.13h** was found to be the best compound of this series showing excellent *in vitro* and *in vivo* activity. Pharmacokinetic properties were studied and suggestive of a highly bioavailable compound that significantly reduced lymphocyte count. Further testing on **4.13h** for disease-model studies will be evaluated. Future work will be aimed at continuation of the SAR study around **4.13h** investigating the tail further as well as substitution off the benzimidazole N-H.

4.8 Future Directions:

The SAR study around **4.13h** is of great interest given its success *in vivo.* Additional work on derivatives of this compound must be developed. Of particular interest is further exploration of the tail region (Figure 4.8). Previous work has shown a sensitive tolerance for the functional groups in this region. However, adding more rigidity to the tail to

minimize rotatable bonds is favorable. This should help to reduce any metabolic liabilities in the compound, as this would lead to less oxidation sites.[36] Ring systems as well as conformationally locked double bonds in the tail would help to lock the inhibitor into a structure that promotes binding in the protein.[37] Another location of interest for future work would be additional functionalization on the internal benzimidazole ring. Many modifications could be assessed with the benzimidazole ring, such as additional functionality ortho and meta to the tail. Additionally, imidazopyridine rings should be tested as this would lower the cLogP value even further to promote oral bioavailability.[38-39]

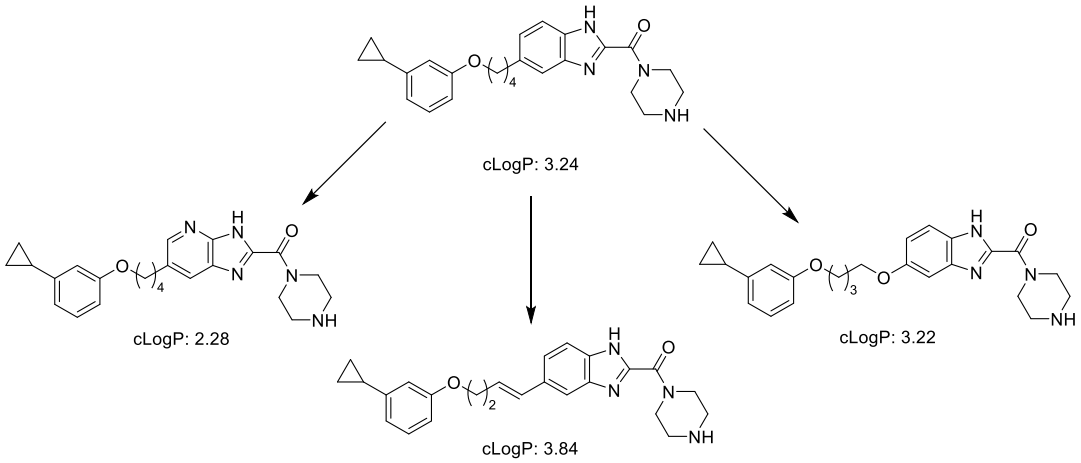

Figure 4.8. Potential modifications of the tail and core of **4.13h**.

4.9 References

1. Fritzemeier, R.; Foster, D.; Peralta, A.; Payette, M.; Kharel, Y.; Huang, T.; Lynch, K. R.; Santos, W. L., Discovery of In Vivo Active Sphingosine-1-phosphate Transporter (Spns2) Inhibitors. *J. Med. Chem.* **2022,** *65* (11), 7656-7681.

2. Burgio, A. L.; Shrader, C. W.; Kharel, Y.; Huang, T.; Salamoun, J. M.; Lynch, K. R.; Santos, W. L., 2-Aminobenzoxazole Derivatives as Potent Inhibitors of the Sphingosine-1-Phosphate Transporter Spinster Homolog 2 (Spns2). *J. Med. Chem.* **2023,** *66* (8), 5873-5891.

3. Kharel, Y.; Huang, T.; Santos, W. L.; Lynch, K. R., Assay of Sphingosine 1-phosphate Transporter Spinster Homolog 2 (Spns2) Inhibitors. *SLAS Discov* **2023,** *28* (6), 284-287.

4. Tanaka, S.; Zheng, S.; Kharel, Y.; Fritzemeier, R. G.; Huang, T.; Foster, D.; Poudel, N.; Goggins, E.; Yamaoka, Y.; Rudnicka, K. P.; Lipsey, J. E.; Radel, H. V.; Ryuh, S. M.; Inoue, T.; Yao, J.; Rosin, D. L.; Schwab, S. R.; Santos, W. L.; Lynch, K. R.; Okusa, M. D., Sphingosine 1-phosphate signaling in perivascular cells enhances inflammation and fibrosis in the kidney. *Sci. Transl. Med.* **2022,** *14* (658), eabj2681.

5. Goldstein, M. J.; Peters, M.; Weber, B. L.; Davis, C. B., Optimizing the Therapeutic Window of Targeted Drugs in Oncology: Potency-Guided First-in-Human Studies. *Clin. Transl. Sci.* **2021,** *14* (2), 536-543.

6. Bachmann, K.; Pardoe, D.; White, D., Scaling basic toxicokinetic parameters from rat to man. *Environ. Health Perspect.* **1996,** *104* (4), 400-407.

7. Zou, Y.; Zhang, Y.; Liu, X.; Song, H.; Cai, Q.; Wang, S.; Yi, C.; Chen, J., Research Progress of Benzothiazole and Benzoxazole Derivatives in the Discovery of Agricultural Chemicals. *Int. J. Mol. Sci.* **2023,** *24* (13).

8. Lipinski, C. A.; Lombardo, F.; Dominy, B. W.; Feeney, P. J., Experimental and computational approaches to estimate solubility and permeability in drug discovery and development settings. *Adv. Drug Del. Rev.* **1997,** *23* (1-3), 3-25.

9. Veber, D. F.; Johnson, S. R.; Cheng, H. Y.; Smith, B. R.; Ward, K. W.; Kopple, K. D., Molecular properties that influence the oral bioavailability of drug candidates. *J. Med. Chem.* **2002,** *45* (12), 2615-2623.

10. Bickerton, G. R.; Paolini, G. V.; Besnard, J.; Muresan, S.; Hopkins, A. L., Quantifying the chemical beauty of drugs. *Nat. Chem.* **2012,** *4* (2), 90-98.

11. Andrews, C. W.; Bennett, L.; Yu, L. X., Predicting human oral bioavailability of a compound: development of a novel quantitative structure-bioavailability relationship. *Pharm. Res.* **2000,** *17* (6), 639-644.

12. Guo, Y.; Hou, X.; Fang, H., Recent Applications of Benzimidazole as a Privileged Scaffold in Drug Discovery. *Mini Rev. Med. Chem.* **2021,** *21* (11), 1367-1379.

13. Faheem, M.; Rathaur, A.; Pandey, A.; Singh, V. K.; Tiwari, A. K., A Review on the Modern Synthetic Approach of Benzimidazole Candidate. *Chemistryselect* **2020,** *5* (13), 3981-3994.

14. Alpan, A. S.; Zencir, S.; Zupko, I.; Coban, G.; Rethy, B.; Gunes, H. S.; Topcu, Z., Biological activity of bis-benzimidazole derivatives on DNA topoisomerase I and HeLa, MCF7 and A431 cells. *J Enzyme Inhib Med Chem* **2009,** *24* (3), 844-849.

15. Tong, Y.; Bouska, J. J.; Ellis, P. A.; Johnson, E. F.; Leverson, J.; Liu, X.; Marcotte, P. A.; Olson, A. M.; Osterling, D. J.; Przytulinska, M.; Rodriguez, L. E.; Shi, Y.; Soni, N.; Stavropoulos, J.; Thomas, S.; Donawho, C. K.; Frost, D. J.; Luo, Y.; Giranda, V. L.; Penning, T. D., Synthesis and evaluation of a new generation of orally efficacious benzimidazole-based poly(ADP-ribose) polymerase-1 (PARP-1) inhibitors as anticancer agents. *J. Med. Chem.* **2009,** *52* (21), 6803-6813.

16. Sondhi, S. M.; Singh, N.; Kumar, A.; Lozach, O.; Meijer, L., Synthesis, anti-inflammatory, analgesic and kinase (CDK-1, CDK-5 and GSK-3) inhibition activity evaluation of benzimidazole/benzoxazole derivatives and some Schiff's bases. *Bioorg Med Chem* **2006,** *14* (11), 3758-3765.

17. Keri, R. S.; Hiremathad, A.; Budagumpi, S.; Nagaraja, B. M., Comprehensive Review in Current Developments of Benzimidazole-Based Medicinal Chemistry. *Chem Biol Drug Des* **2015,** *86* (1), 19-65.

18. Eskandari, M.; Asgharzadeh, F.; Askarnia-Faal, M. M.; Naimi, H.; Avan, A.; Ahadi, M.; Vossoughinia, H.; Gharib, M.; Soleimani, A.; Naghibzadeh, N.; Ferns, G.; Ryzhikov, M.; Khazaei, M.; Hassanian, S. M., Mebendazole, an anti-helminth drug, suppresses inflammation, oxidative stress and injury in a mouse model of ulcerative colitis. *Sci. Rep.* **2022,** *12* (1), 10249.

19. Law, C. S. W.; Yeong, K. Y., Benzimidazoles in Drug Discovery: A Patent Review. *Chemmedchem* **2021,** *16* (12), 1861-1877.

20. Mahurkar, N. D.; Gawhale, N. D.; Lokhande, M. N.; Uke, S. J.; Kodape, M. M., Benzimidazole: A versatile scaffold for drug discovery and beyond - A comprehensive review of synthetic approaches and recent advancements in medicinal chemistry. *Results in Chemistry* **2023,** *6*, 101139.

21. Siddiqui, N.; Andalip; Bawa, S.; Ali, R.; Afzal, O.; Akhtar, M. J.; Azad, B.; Kumar, R., Antidepressant potential of nitrogen-containing heterocyclic moieties: An updated review. *J. Pharm. Bioallied Sci.* **2011,** *3* (2), 194-212.

22. Sauer, D.; Li, H.; Pike, A.; Chang, Y.-N.; Prakaash, D.; Gelová, Z.; Stanka, J.; Moreau, C.; Scott, H.; Wunder, F.; Wolf, G.; Scacioc, A.; McKinley, G.; Batoulis, H.;

Mukhopadhyay, S.; Garofoli, A.; Pinto-Fernández, A.; Kessler, B.; Burgess-Brown, N.; Superti-Furga, G., Transport and inhibition of the sphingosine-1-phosphate exporter SPNS2. *PREPRINT (Version 1) available at Research Square [https://doi.org/10.21203/rs.3.rs-3616536/v1]* **2023**.

23. Khotavivattana, T.; Calderwood, S.; Verhoog, S.; Pfeifer, L.; Preshlock, S.; Vasdev, N.; Collier, T. L.; Gouverneur, V., Synthesis and Reactivity of (18)F-Labeled alpha,alpha-Difluoro-alpha-(aryloxy)acetic Acids. *Org. Lett.* **2017,** *19* (3), 568-571.

24. Holan, G.; Samuel, E. L.; Ennis, B. C.; Hinde, R. W., 2-Trihalogenomethylbenzazoles. Part I. Formation. *Journal of the Chemical Society C: Organic* **1967,** (0), 20-25.

25. Zhang, L.; Chen, X.; Liu, J.; Zhu, Q.; Leng, Y.; Luo, X.; Jiang, H.; Liu, H., Discovery of novel dual-action antidiabetic agents that inhibit glycogen phosphorylase and activate glucokinase. *Eur J Med Chem* **2012,** *58*, 624-639.

26. Holan, G.; Samuel, E. L., 2-trihalogenomethylbenzazoles. II. Reactions of 2-trihalogenomethylbenzimidazoles with ammonia and amines. *J. Chem. Soc. Perkin 1* **1967,** *1* (0), 25-29.

27. Venable, J. D.; Cai, H.; Chai, W.; Dvorak, C. A.; Grice, C. A.; Jablonowski, J. A.; Shah, C. R.; Kwok, A. K.; Ly, K. S.; Pio, B.; Wei, J.; Desai, P. J.; Jiang, W.; Nguyen, S.; Ling, P.; Wilson, S. J.; Dunford, P. J.; Thurmond, R. L.; Lovenberg, T. W.; Karlsson, L.; Carruthers, N. I.; Edwards, J. P., Preparation and biological evaluation of indole, benzimidazole, and thienopyrrole piperazine carboxamides: potent human histamine h(4) antagonists. *J. Med. Chem.* **2005,** *48* (26), 8289-8298.

28. Lin, R.; Chiu, G.; Yu, Y.; Connolly, P. J.; Li, S.; Lu, Y.; Adams, M.; Fuentes-Pesquera, A. R.; Emanuel, S. L.; Greenberger, L. M., Design, synthesis, and evaluation of 3,4-disubstituted pyrazole analogues as anti-tumor CDK inhibitors. *Bioorg Med Chem Lett* **2007,** *17* (16), 4557-4561.

29. Govek, S. P.; Overman, L. E., Total synthesis of asperazine. *J. Am. Chem. Soc.* **2001,** *123* (38), 9468-9469.

30. Chandra, T.; Broderick, W. E.; Broderick, J. B., An efficient deprotection of N-trimethylsilylethoxymethyl (SEM) groups from dinucleosides and dinucleotides. *Nucleosides Nucleotides Nucleic Acids* **2010,** *29* (2), 132-143.

31. Okuniewska, M.; Fang, V.; Baeyens, A.; Raghavan, V.; Lee, J. Y.; Littman, D. R.; Schwab, S. R., SPNS2 enables T cell egress from lymph nodes during an immune response. *Cell Rep.* **2021,** *36* (2), 109368.

32. Hisano, Y.; Kobayashi, N.; Yamaguchi, A.; Nishi, T., Mouse SPNS2 functions as a sphingosine-1-phosphate transporter in vascular endothelial cells. *PLoS ONE* **2012,** *7* (6), e38941.

33. Spiegel, S.; Maczis, M. A.; Maceyka, M.; Milstien, S., New insights into functions of the sphingosine-1-phosphate transporter SPNS2. *J. Lipid Res.* **2019,** *60* (3), 484-489.

34. Mendoza, A.; Bréart, B.; Ramos-Perez, Willy D.; Pitt, Lauren A.; Gobert, M.; Sunkara, M.; Lafaille, Juan J.; Morris, Andrew J.; Schwab, Susan R., The Transporter Spns2 Is Required for Secretion of Lymph but Not Plasma Sphingosine-1-Phosphate. *Cell Reports* **2012,** *2* (5), 1104-1110.

35. Donoviel, M. S.; Hait, N. C.; Ramachandran, S.; Maceyka, M.; Takabe, K.; Milstien, S.; Oravecz, T.; Spiegel, S., Spinster 2, a sphingosine-1-phosphate transporter,

plays a critical role in inflammatory and autoimmune diseases. *FASEB J.* **2015,** *29* (12), 5018-5028.

36. Meunier, B.; de Visser, S. P.; Shaik, S., Mechanism of oxidation reactions catalyzed by cytochrome p450 enzymes. *Chem Rev* **2004,** *104* (9), 3947-3980.

37. Brameld, K. A.; Kuhn, B.; Reuter, D. C.; Stahl, M., Small molecule conformational preferences derived from crystal structure data. A medicinal chemistry focused analysis. *J Chem Inf Model* **2008,** *48* (1), 1-24.

38. Leeson, P. D.; Springthorpe, B., The influence of drug-like concepts on decision-making in medicinal chemistry. *Nat Rev Drug Discov* **2007,** *6* (11), 881-890.

39. Kerru, N.; Gummidi, L.; Maddila, S.; Gangu, K. K.; Jonnalagadda, S. B., A Review on Recent Advances in Nitrogen-Containing Molecules and Their Biological Applications. *Molecules* **2020,** *25* (8).

Chapter 5: Experimental and Supporting Information

5.1 General Materials and Synthetic Procedures

Unless otherwise specified, reactions were performed using Schlenk technique under Argon or Nitrogen atmosphere. All glassware was oven-dried overnight or flame-dried. Chemicals were obtained from commercial sources and used without further purification unless otherwise noted. Acetonitrile and DMF were dried using an Innovative Technology Pure SolvMD solvent purification system prior to use. TLC analysis was performed using Silicycle aluminum backed silica gel F-254 plates. Column chromatography was performed using SiliaFlash P60 40-63 μm, 60 Å. NMR spectroscopic experiments were performed using an Agilent U4-DD2 400-MR 400 MHz, Varian Inova 400 MHz, Bruker Avance II 500 MHz, or Bruker Avance III 600 MHz spectrometer. Chemical shifts are reported in δ ppm and ^{1}H and ^{13}C NMR and referenced using residual protonated solvent (Chloroform, methanol, or DMSO) or an internal standard (TMS). Data are reported as follows: chemical shift, multiplicity (s = singlet, d = doublet, t = triplet, q = quartet, dd = doublet of doublets, dt = doublet of triplets, m = multiplet), coupling constants (Hz), and integration. ESI mass spectra were obtained using an Agilent 6220 TOF LC-MS or Waters Synapt-G2S Q-TOF LCMS. Purity assessments were performed by Waters ultraperformance liquid chromatography (UPLC) analysis. UPLC conditions: Solvent A: Water (0.1%TFA); solvent B: acetonitrile (0.1% TFA); column: Acquity BEH C18 1.7 μm 2.1 × 50mm; method: isocratic 60% A, 40% B from 0 to 3.50 min then linear gradient from 40 to 95% B by 5 min, return to 40% B by 6min, then hold for 2min at 60% A, 40% B; UV wavelength = 280 nm; flow rate: 0.613 mL/min. All compounds tested in biological assays

were assessed to have ≥95% purity by high-performance liquid chromatography (HPLC), unless otherwise noted.

***In vitro* Spns2 assay.** Written procedure provided by collaborator Dr. Kevin Lynch at the University of Virginia Department of Pharmacology.

HeLa cells were transfected with a pcDNA3.1 plasmid encoding mouse Spns2 or mouse Spns2Arg200Ser (transport dead mutant). Transfected cell pools were selected by inclusion of geneticin (G418) in the cell media. Wild type, but not R200S, Spns2 expressing cells were found to release S1P into the culture media in excess of non-transfected cultures. To assay test articles, HeLa cells were plated onto 12-well plates and grown to near confluence. Release assay medium (1.5mL; RPMI 1640 with 0.2% fatty acid free BSA) was added to each well. The release medium was supplemented with 4-deoxypyridoxine (to 1 mM), NaF (2 mM) and Na_3VO_4 (0.2 mM) to retard degradation of S1P by S1P lyase and S1P phosphatases. Putative inhibitors were introduced into duplicate wells (at 2 μM) and plates were placed in a tissue culture incubator for 18-20 hours. Following this incubation, media was collected, internal standard (5 μL of 0.5 μM d_7-S1P in methanol) and 150 μL of 100% trichloroacetic acid were added and the mixture held on ice for 30-60 minutes. The precipitated material was collected by centrifugation, the pellets washed with water, recentrifuged and the final pellet mixed vigorously after adding 0.3 mL methanol. After further centrifugation, 0.15 mL of the supernatant fluid was added to LC vials and S1P and d_7-S1P were quantified by MS/MS.

***In vivo* Animal Studies**

Inhibitors (10 or 20 mg/kg) or an equal volume of vehicle (36.1% PEG400/9.1% ethanol/4.6% Solutol/50% H_2O) was administered by intraperitoneal injection or oral

gavage into mice (C57BL/6j strain). After 6-16 hours, blood samples were collected and lymphocyte counts were analyzed from 20 µL of mice blood using Heska HT5 Element blood analyzer. All animal protocols were approved prior to experimentation by the University of Virginia School of Medicine's Animal Care and Use Committee.

5.2 Procedures and Characterization for Chapter 2

General Procedure 2.1: Nucleophilic aromatic substitution: To a flame-dried round-bottom flask containing a stir bar was added 1H-imidazole (1.5 equiv., 422 mg, 6.19 mmol) and DMF (0.4 M). The mixture was then purged with Ar and cooled to 0 °C with an ice bath. Sodium hydride (1.5 equiv., 248 mg, 6.19 mmol, 60% dispersion in mineral oil) was added, and the reaction was allowed to stir for 10 minutes. Once hydrogen gas evolution had ceased, 4-fluorobenzonitrile (1.0 equiv., 500 mg, 4.13 mmol) was added and the reaction was heated to 100 °C for 5 hours with reaction progress monitored by TLC. Once complete, the reaction was allowed to cool to room temperature and methanol was added to quench any remaining sodium hydride. The reaction mixture was concentrated *in vacuo* and purified *via* silica gel chromatography to afford the desired product.

General Procedure 2.2: Amidoxime synthesis: To a flame-dried round-bottom flask containing a solution of 200 proof ethanol (0.3 M) and substituted benzonitrile (1.0 equiv., 651 mg, 3.85 mmol), was added hydroxylamine hydrochloride (2.2 equiv., 588 mg, 8.47 mmol) followed by TEA (3.0 equiv., 1.17 g, 11.5 mmol). The reaction was heated under reflux for 16 hours with reaction progress monitored by TLC. Once complete, the reaction was allowed to cool to room temperature and concentrated *in vacuo*. Addition of ethyl acetate formed a white precipitate that was filtered off. The precipitate was washed with water three times to afford the desired product.

General Procedure 2.3: 1,2,4 oxadiazole ring synthesis: To a solution of benzamidoxime (1.0 equiv., 80 mg, 0.40 mmol) in DMF (0.3 M) under argon, was added undecanoic acid (1.2 equiv., 88 mg, 0.47 mmol), diisopropylethylamine (1.8 equiv., 92 mg, 0.71 mmol), and HCTU (1.2 equiv., 200 mg, 0.47 mmol). The reaction was heated to 105 °C for 16 hours and reaction progress was monitored by TLC. Once complete, the reaction was allowed to cool to room temperature and the resulting solution was partitioned between ethyl acetate and aqueous lithium bromide solution. The aqueous layer was washed three times with additional ethyl acetate and the combined organic layers were dried over Na_2SO_4, filtered, and concentrated *in vacuo*. The reaction mixture was purified *via* silica gel chromatography to afford the desired product.

General Procedure 2.4: Methylation: To a solution of 3-(4-(-1H-imidazol-1-yl)phenyl)-5-decyl-1,2,4-oxadiazole (1.0 equiv., 33 mg, 94 µmol) in acetonitrile (0.05 M), was added iodomethane (1.0 equiv., 13 mg, 94 µmol). The reaction was heated to 70 °C for 3 hours with reaction progress monitored by TLC. Once complete, the reaction was allowed to cool to room temperature and concentrated *in vacuo*. Diethyl ether was added to the resulting concentrate, forming a precipitate that was collected and subjected to trituration by an appropriate solvent system to afford the desired product as an iodide salt.

General Procedure 2.5: Imidazole alkylation: To an oven-dried round-bottom flask containing a stir bar was added NaH (1.1 equiv. 60% dispersion in mineral oil) and THF (0.1 M). The mixture was then purged with argon and cooled to 0 °C in an ice bath. The appropriate aryl imidazole (1.0 equiv.) was added, and the mixture was allowed to stir for 30 minutes. Either an alkyl halide (1.1 equiv.) or an *N*-Boc-bromoalkylamine (3.0 equiv.) was slowly added to the flask. The reaction was allowed to slowly warm to room

temperature overnight. Following completion as monitored by TLC, the reaction mixture was concentrated *in vacuo* and purified with ethyl acetate and hexanes *via* silica gel chromatography to afford the desired products.

General Procedure 2.6: Boc Deprotection: To a 6-dram vial containing an *N*-Boc-protected amine (1.0 equiv.) was added CH_2Cl_2 (0.2 M), followed by HCl (10 equiv, 4 M in dioxane). The resulting mixture was allowed to stir until complete consumption of starting material was observed *via* TLC (1-4 hours). The reaction mixture was concentrated *in vacuo* and the residue was rinsed with diethyl ether until a precipitate formed. The precipitate was subjected to trituration with an appropriate solvent system to afford pure product as the hydrochloride salt.

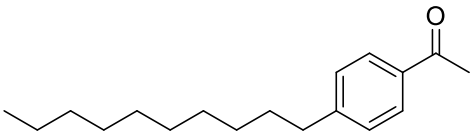

1-(4-Decylphenyl)ethan-1-one (2.2): To a pressure-sealed tube containing 1-decene (1.2 equiv., 2537 mg, 18.09 mmol) was added THF and 9-BBN (1.2 equiv., 0.5 M, 2207 mg, 18.09 mmol) dropwise under inert atmosphere. The resulting mixture was stirred at 70 °C for 1 hour, followed by the addition of 4-bromoacetophenone (1.0 equiv., 3000 mg, 15.07 mmol), aqueous KOH (3.0 equiv., 3.0 M, 2537 mg, 45.21 mmol), and $Pd(dppf)Cl_2 \cdot CH_2Cl_2$ (0.01 equiv., 110.1 mg, 150.7 µmol). The resulting mixture was stirred at 70 °C for 16 hours, and reaction progress was monitored by TLC. The crude mixture was loaded onto celite, concentrated *in vacuo*, and purified *via* silica gel chromatography (5% ethyl acetate/hexanes) to give 1-(4-decylphenyl)ethan-1-one (79%, 3.083 g) as a white solid. ^{1}H NMR (400 MHz, $CDCl_3$) δ 7.88 (d, *J* = 8.3 Hz, 2H), 7.26 (d, *J* = 8.3 Hz, 2H), 2.66 (t, *J* = 7.7 Hz, 2H), 2.58 (s, 3H), 1.62 (p, *J* = 8.8 Hz, 2H), 1.38 – 1.20 (m, 14H), 0.88 (t, *J* = 6.7 Hz, 3H). ^{13}C NMR (101

MHz, $CDCl_3$) δ 198.0, 149.0, 135.1, 128.7, 128.6, 36.1, 32.0, 31.3, 29.7, 29.7, 29.6, 29.5, 29.4, 26.7, 22.8, 14.3. HRMS: (ESI) [2M+H]+ calc. for $C_{36}H_{57}O_2$, 521.4353, observed, 521.4331.

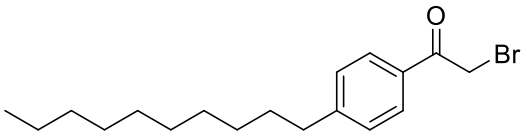

2-Bromo-1-(4-decylphenyl)ethan-1-one (2.3): To a round-bottom flask containing a solution of 1-(4-Decylphenyl)ethan-1-one (1.0 equiv., 3084 mg, 11.84 mmol) in MeCN (0.3 M) was added NBS (1.0 equiv., 2108 mg, 11.84 mmol) and p-toluenesulfonic acid monohydrate (1.6 equiv., 3491 mg, 18.36 mmol) and the reaction mixture was heated to reflux for 2 hours. The flask was then removed from the heating source and allowed to stir at room temperature for an additional 18 hours. The crude reaction mixture was concentrated *in vacuo*, dissolved in CH_2Cl_2, and partitioned with brine. The organic layer was further rinsed three times with brine, dried over sodium sulfate, filtered, loaded onto celite, and purified *via* silica gel chromatography (5% ethyl acetate/hexanes) to give 2-bromo-1-(4-decylphenyl)ethan-1-one (82%, 3.28 g) as a light pink solid. ^{1}H NMR (400 MHz, $CDCl_3$) δ 7.90 (d, *J* = 8.3 Hz, 2H), 7.29 (d, *J* = 8.2 Hz, 2H), 4.43 (s, 2H), 2.67 (t, *J* = 7.7 Hz, 2H), 1.63 (p, *J* = 8.0 Hz, 2H), 1.29 (d, *J* = 23.7 Hz, 14H), 0.88 (t, *J* = 6.7 Hz, 3H). ^{13}C NMR (101 MHz, $CDCl_3$) δ 191.1, 150.1, 131.8, 129.2, 129.0, 36.2, 32.0, 31.1, 31.1, 29.7, 29.7, 29.6, 29.4, 29.4, 22.8, 14.2. HRMS: (ESI) [2M+Na]+ calc. for $C_{36}H_{54}Br_2NaO_2$, 701.2362, observed, 701.2361.

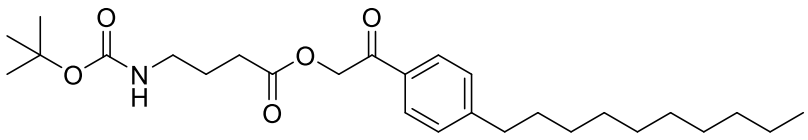

2-(4-Decylphenyl)-2-oxoethyl 4-((*tert*-butoxycarbonyl)amino)butanoate (2.4): 2-Bromo-1-(4-

decylphenyl)ethan-1-one (1.0 equiv., 2646 mg, 7.798 mmol), *N*-Boc-GABA (1.1 equiv., 1743 mg, 8.578 mmol), and K_2CO_3 (3.0 equiv., 3233 mg, 23.39 mmol) were added to a round-bottom flask. The flask was purged with argon and MeCN (0.2 M) was added. The mixture was allowed to stir overnight at room temperature. The crude mixture was loaded onto celite, concentrated *in vacuo*, and purified *via* column chromatography (30% ethyl acetate/hexanes) to give 2-(4-decylphenyl)-2-oxoethyl 4-((*tert*-butoxycarbonyl)amino)butanoate (89%, 3217 mg) as an off-white solid. ^{1}H NMR (400 MHz, $CDCl_3$) δ 7.82 (d, *J* = 8.4 Hz, 2H), 7.28 (d, *J* = 8.1 Hz, 2H), 5.34 (s, 2H), 4.82 (t, *J* = 6.1 Hz, 1H), 3.23 (q, *J* = 6.7 Hz, 2H), 2.66 (t, *J* = 7.7 Hz, 2H), 2.54 (t, *J* = 7.2 Hz, 2H), 1.91 (p, *J* = 7.1 Hz, 2H), 1.62 (p, *J* = 7.6 Hz, 2H), 1.44 (s, 9H), 1.38 – 1.18 (m, 14H), 0.86 (t, *J* = 6.8 Hz, 3H). ^{13}C NMR (101 MHz, $CDCl_3$) δ 191.9, 172.8, 156.1, 150.0, 131.9, 129.0, 128.0, 79.2, 66.0, 39.8, 36.2, 32.0, 31.3, 31.1, 29.7, 29.6, 29.5, 29.4, 29.3, 28.5, 25.4, 22.8, 14.2. HRMS: (ESI) [M+Na]+ calc. for $C_{27}H_{43}NNaO_5$, 484.3033, observed, 484.3032.

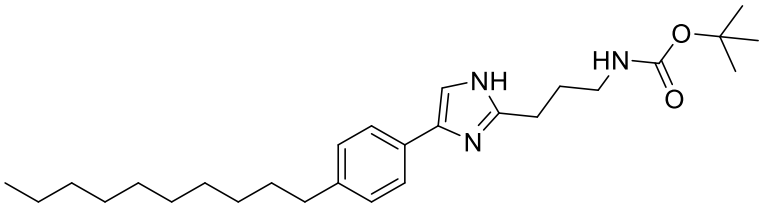

***tert*-butyl (3-(4-(4-decylphenyl)-1H-imidazol-2-yl)propyl)carbamate (2.5):** To a round-bottom flask attached to a condenser was added alpha acyl ketone **3.30** (1.0 equiv., 3217 mg, 8.037 mmol) and ammonium acetate (20.0 equiv., 12.39 g, 160.7 mmol). Toluene (0.3 M) was then added and the mixture heated under reflux for 5 hours. The mixture was subsequently concentrated *in vacuo* and diluted with ethyl acetate. The organic layer was rinsed three times with a saturated aqueous $NaHCO_3$ solution. The washed organic layer was dried over sodium sulfate, concentrated *in vacuo*, and purified *via* column

chromatography (100% ethyl acetate) to give *tert*-butyl (3-(4-(4-decylphenyl)-1H-imidazol-2-yl)propyl)carbamate as a white solid (73%, 2.610 g). ^{1}H NMR (400 MHz, $CDCl_3$) δ 11.32 (s, 1H), 7.58 (s, 2H), 7.46 (d, *J* = 8.5 Hz, 2H), 7.25 (d, *J* = 8.9 Hz, 1H), 5.02 (s, 1H), 3.22 (q, *J* = 6.2 Hz, 2H), 2.83 – 2.75 (m, 2H), 1.85 – 1.75 (m, 2H), 1.48 (s, 9H). ^{13}C NMR (101 MHz, $CDCl_3$) δ 157.9, 148.7, 131.8, 126.3, 120.0, 111.8, 80.3, 38.7, 29.7, 28.5, 24.7. HRMS: (ESI) [M+H]+ calc. for $C_{27}H_{44}N_3O_2$, 442.3428, observed, 442.3433.

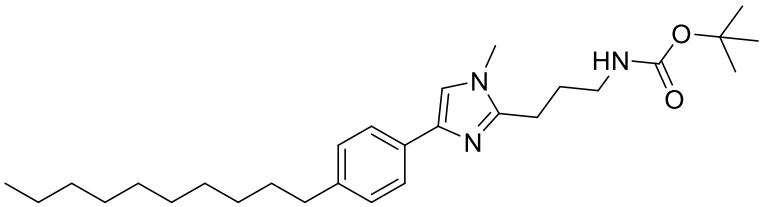

***tert*-butyl (3-(4-(4-decylphenyl)-1-methyl-1H-imidazol-2-yl)propyl)carbamate (2.6a):** Synthesized according to General Procedure 2.5 with methyl iodide. Purified *via* column chromatography (100% ethyl acetate). White solid (63%, 65 mg). ^{1}H NMR (400 MHz, d_4-MeOD) δ 7.57 (d, *J* = 8.3 Hz, 2H), 7.22 (s, 1H), 7.14 (d, *J* = 8.4 Hz, 2H), 3.63 (s, 3H), 3.12 (t, *J* = 6.7 Hz, 2H), 2.75 (t, *J* = 7.6 Hz, 2H), 2.58 (t, *J* = 7.6 Hz, 2H), 1.85 (p, *J* = 7.6 Hz, 2H), 1.59 (p, *J* = 7.3 Hz, 2H), 1.44 (s, 9H), 1.36 – 1.22 (m, 14H), 0.88 (t, *J* = 7.0 Hz, 3H). ^{13}C NMR (101 MHz, d_4-MeOD) δ 158.5, 149.8, 142.4, 140.8, 132.8, 129.5, 125.8, 117.9, 79.9, 40.8, 36.6, 33.1, 33.1, 32.7, 30.7, 30.7, 30.6, 30.5, 30.3, 29.4, 28.8, 24.7, 23.7, 14.5. HRMS: (ESI) [M+H]+ calc. for $C_{28}H_{46}N_3O_2$, 456.3585, observed, 456.3592.

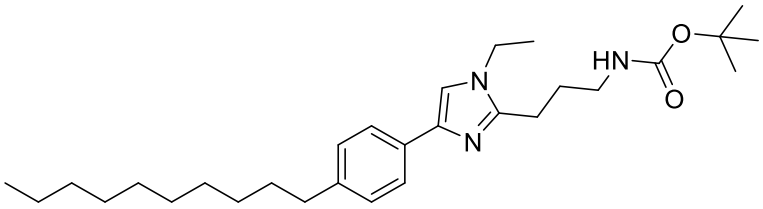

***tert*-butyl (3-(4-(4-decylphenyl)-1-ethyl-1H-imidazol-2-yl)propyl)carbamate (2.6b):** Synthesized

according to General Procedure 2.5 with ethyl iodide. Purified *via* column chromatography (80-100% ethyl acetate/hexanes). Yellow oil (75%, 80 mg). ^{1}H NMR (400 MHz, $CDCl_3$) δ 7.63 (d, *J* = 8.0 Hz, 2H), 7.14 (d, *J* = 7.9 Hz, 2H), 7.06 (s, 1H), 5.87 (t, *J* = 5.0 Hz, 1H), 3.88 (q, *J* = 7.3 Hz, 2H), 3.24 (q, *J* = 6.1 Hz, 2H), 2.76 (t, *J* = 7.1 Hz, 2H), 2.58 (t, *J* = 7.7 Hz, 2H), 1.97 (p, *J* = 6.7 Hz, 2H), 1.59 (p, *J* = 7.5 Hz, 2H), 1.47 – 1.37 (m, 12H), 1.35 – 1.17 (m, 14H), 0.87 (t, *J* = 6.7 Hz, 3H). HRMS: (ESI) [M+H]+ calc. for $C_{29}H_{48}N_3O_2$, 470.3741, observed, 470.3741.

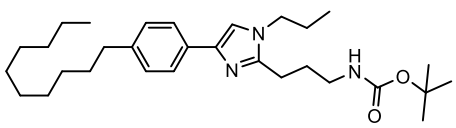

tert-butyl (3-(4-(4-decylphenyl)-1-propyl-1H-imidazol-2-yl)propyl)carbamate (2.6c): Synthesized according to General Procedure 2.5 with propyl iodide. Purified via column chromatography (50% ethyl acetate/hexanes). Light yellow oil (80%, 88 mg). ^{1}H NMR (400 MHz, $CDCl_3$) δ 7.64 (d, *J* = 8.1 Hz, 2H), 7.14 (d, *J* = 7.9 Hz, 2H), 7.04 (s, 1H), 5.90 (t, *J* = 5.9 Hz, 1H), 3.79 (t, *J* = 7.2 Hz, 2H), 3.25 (q, *J* = 6.1 Hz, 2H), 2.75 (t, *J* = 7.1 Hz, 2H), 2.58 (t, *J* = 7.7 Hz, 2H), 1.98 (p, *J* = 6.8 Hz, 2H), 1.78 (h, *J* = 7.4 Hz, 2H), 1.60 (p, *J* = 7.3 Hz, 2H), 1.44 (s, 9H), 1.37 – 1.18 (m, 14H), 0.95 (t, *J* = 7.4 Hz, 3H), 0.87 (t, *J* = 6.8 Hz, 3H). ^{13}C NMR (101 MHz, $CDCl_3$) δ 156.36, 147.75, 141.24, 140.09, 131.84, 128.65, 124.70, 114.50, 78.88, 47.65, 40.68, 35.79, 32.01, 31.62, 29.73, 29.71, 29.65, 29.45, 29.37, 28.59, 27.69, 24.82, 24.37, 22.80, 14.23, 11.31. HRMS: (ESI) [M+H]+ calc. for $C_{30}H_{50}N_3O_2$, 484.3898, observed, 484.3895.

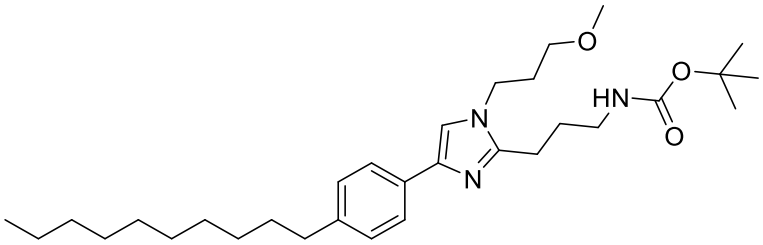

***tert*-butyl (3-(4-(4-decylphenyl)-1-(3-methoxypropyl)-1H-imidazol-2-yl)propyl)carbamate (2.6d):**

Synthesized according to General Procedure 2.5 with 1-bromo-3-methoxypropane. Purified *via* column chromatography (30-60% ethyl acetate/hexanes). Yellow oil (58%, 68 mg). ^{1}H NMR (400 MHz, $CDCl_3$) δ 7.64 (d, *J* = 8.2 Hz, 2H), 7.14 (d, *J* = 8.2 Hz, 2H), 7.04 (s, 1H), 5.91 (t, *J* = 5.5 Hz, 1H), 3.95 (t, *J* = 6.9 Hz, 2H), 3.34 – 3.30 (m, 5H), 3.25 (q, *J* = 6.0 Hz, 2H), 2.76 (t, *J* = 7.1 Hz, 2H), 2.58 (t, *J* = 7.7 Hz, 2H), 1.98 (h, *J* = 5.5 Hz, 4H), 1.59 (p, *J* = 7.6 Hz, 2H), 1.44 (s, 9H), 1.35 – 1.19 (m, 14H), 0.87 (t, *J* = 6.8 Hz, 3H). ^{13}C NMR (101 MHz, $CDCl_3$) δ 156.4, 148.0, 141.3, 140.3, 131.8, 128.7, 124.7, 114.5, 78.9, 68.5, 58.8, 42.6, 40.7, 35.8, 32.0, 31.6, 31.0, 29.7, 29.7, 29.6, 29.4, 29.4, 28.6, 27.6, 24.6, 22.8, 14.2. HRMS: (ESI) [M+H]+ calc. for $C_{31}H_{52}N_3O_3$, 514.4003, observed, 514.4000.

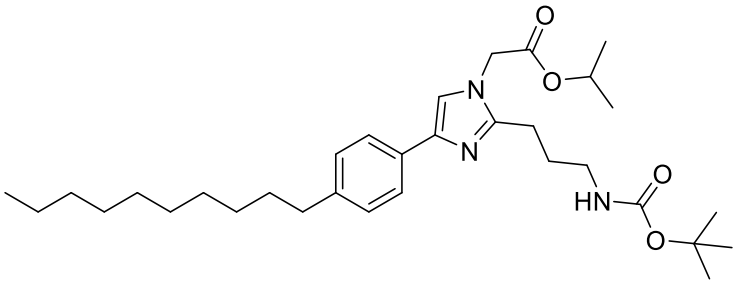

***iso*propyl-2-(2-(3-((*tert*-butoxycarbonyl)amino)propyl)-4-(4-decylphenyl)-1H-imidazol-1- yl)acetate (2.6e):**

Synthesized according to General Procedure 2.5 with *iso*propyl 2-bromoacetate. Purified *via* column chromatography (40-50% ethyl acetate/hexanes). Light yellow oil (76%, 139 mg). ^{1}H NMR (400 MHz, $CDCl_3$) δ 7.64 (d, *J* = 8.2 Hz, 2H), 7.14 (d, *J* = 8.2 Hz, 2H),

7.04 (s, 1H), 5.77 (t, *J* = 5.7 Hz, 1H), 5.08 (hept, *J* = 6.3 Hz, 1H), 4.55 (s, 2H), 3.23 (q, *J* = 5.9 Hz, 2H), 2.69 (t, *J* = 7.1 Hz, 2H), 2.57 (t, *J* = 7.9 Hz, 2H), 1.98 (p, *J* = 7.1 Hz, 2H), 1.58 (p, *J* = 7.5 Hz, 2H), 1.44 (s, 9H), 1.35 – 1.21 (m, 20H), 0.86 (t, *J* = 7.0 Hz, 3H). ^{13}C NMR (101 MHz, $CDCl_3$) δ 167.2, 156.3, 148.3, 141.5, 140.5, 131.6, 128.6, 124.9, 115.5, 78.9, 70.2, 47.7, 40.4, 35.8, 32.0, 31.6, 29.7, 29.7, 29.6, 29.4, 29.4, 28.6, 27.4, 24.5, 22.8, 21.8, 14.2. HRMS: (ESI) [M+H]+ calc. for $C_{32}H_{52}N_3O_4$, 542.3952, observed, 542.3952.

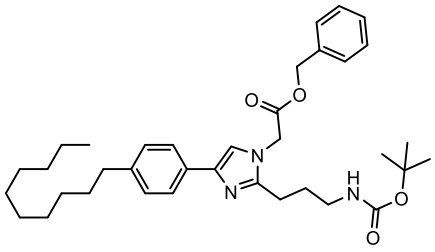

benzyl 2-(2-(3-((tert-butoxycarbonyl)amino)propyl)-4-(4-decylphenyl)-1H-imidazol-1-yl)acetate (2.6f): Purified *via* column chromatography (40-45% ethyl acetate/hexanes). Clear oil (29%, 96 mg). ^{1}H NMR (400 MHz, $CDCl_3$) δ 7.64 (d, *J* = 8.2 Hz, 2H), 7.42 – 7.29 (m, 5H), 7.15 (d, *J* = 8.2 Hz, 2H), 7.05 (s, 1H), 5.69 (t, *J* = 5.4 Hz, 1H), 5.21 (s, 2H), 4.64 (s, 2H), 3.20 (q, *J* = 5.8 Hz, 2H), 2.67 (t, *J* = 7.1 Hz, 2H), 2.60 (t, *J* = 7.3 Hz, 2H), 1.93 (p, *J* = 7.1 Hz, 2H), 1.60 (p, *J* = 7.6 Hz, 2H), 1.45 (s, 9H), 1.36 – 1.20 (m, 14H), 0.88 (t, *J* = 6.8 Hz, 3H). ^{13}C NMR (101 MHz, $CDCl_3$) δ 167.50, 156.33, 148.42, 141.56, 140.67, 134.87, 131.48, 128.92, 128.86, 128.70, 128.66, 124.91, 115.55, 78.93, 67.86, 47.48, 40.41, 35.81, 32.01, 31.60, 29.74, 29.73, 29.65, 29.45, 29.38, 28.60, 27.37, 24.49, 22.80, 14.23. HRMS: (ESI) [M+H]+ calc. for $C_{36}H_{52}N_3O_4$, 590.3952, observed, 590.3950.

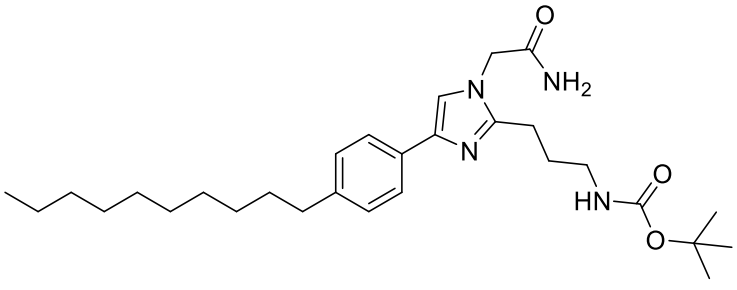

***tert*-butyl (3-(1-(2-amino-2-oxoethyl)-4-(4-decylphenyl)-1H-imidazol-2-yl)propyl)carbamate (2.6g):** Benzyl 2-(2-(3-((tert-butoxycarbonyl)amino)propyl)-4-(4-decylphenyl)-1H-imidazol-1-yl)acetate (1.0 equiv.) was dissolved in methanol and added to a pressure vial containing a stir bar. To the solution was added ammonia (20.0 equiv, 7 N in methanol) and the pressure vial was sealed and purged with argon. The mixture was heated to 70 ºC for 72 hours or until TLC showed the complete consumption of starting material. The reaction mixture was concentrated *in* vacuo and triturated with diethyl ether and hexanes, dried, and used without further purification. White solid (68%, 55 mg). ^{1}H NMR (400 MHz, d$_4$-MeOD) δ 7.59 (d, *J* = 8.3 Hz, 2H), 7.26 (s, 1H), 7.15 (d, *J* = 8.0 Hz, 2H), 4.71 (s, 2H), 3.13 (t, *J* = 6.7 Hz, 2H), 2.72 (t, *J* = 7.7 Hz, 2H), 2.59 (t, *J* = 7.6 Hz, 2H), 1.88 (p, *J* = 7.0 Hz, 2H), 1.60 (p, *J* = 7.1 Hz, 2H), 1.43 (s, 9H), 1.37 – 1.25 (m, 14H), 0.89 (t, *J* = 6.7 Hz, 3H). ^{13}C NMR (101 MHz, d$_4$-MeOD) δ 171.7, 158.5, 150.3, 142.6, 141.0, 132.7, 129.6, 125.9, 117.8, 79.9, 49.0, 40.8, 36.6, 33.1, 32.7, 30.7, 30.7, 30.6, 30.5, 30.4, 29.4, 28.8, 24.7, 23.7, 14.5. HRMS: (ESI) [M+H]+ calc. for $C_{29}H_{47}N_4O_3$, 499.3643, observed, 499.3647.

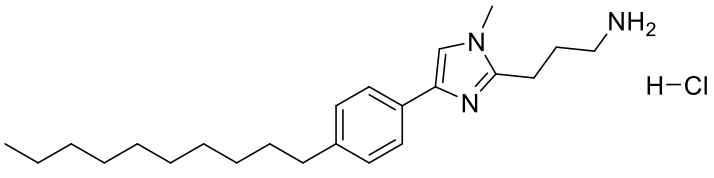

3-(4-(4-Decylphenyl)-1-methyl-1H-imidazol-2-yl)propan-1-amine hydrochloride (2.7a): Synthesized according to General Procedure 2.6. Purified *via* trituration with diethyl ether and ethyl acetate. White

solid (75%, 42 mg). ^{1}H NMR (400 MHz, d$_4$-MeOD) δ 7.80 (s, 1H), 7.67 (d, *J* = 8.3 Hz, 2H), 7.33 (d, *J* = 8.2 Hz, 2H), 3.93 (s, 3H), 3.22 (t, *J* = 7.9 Hz, 2H), 3.13 (t, *J* = 7.7 Hz, 2H), 2.66 (t, *J* = 7.6 Hz, 2H), 2.20 (p, *J* = 7.9 Hz, 2H), 1.64 (p, *J* = 6.8 Hz, 2H), 1.38 – 1.21 (m, 14H), 0.89 (t, *J* = 6.8 Hz, 3H). ^{13}C NMR (101 MHz, d$_4$-MeOD) δ 147.6, 146.2, 134.0, 130.5, 126.6, 125.1, 119.9, 39.7, 36.6, 35.1, 33.0, 32.5, 30.7, 30.7, 30.6, 30.4, 30.3, 26.0, 23.7, 22.7, 14.4. HRMS: (ESI) [M+H]+ calc. for $C_{23}H_{38}N_3$, 356.3060, observed, 356.3057.

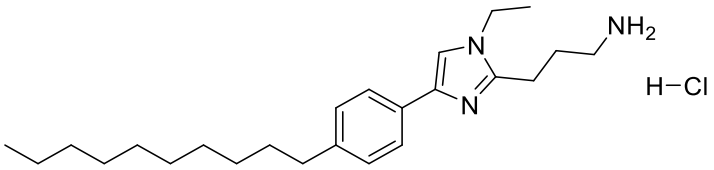

3-(4-(4-decylphenyl)-1-ethyl-1H-imidazol-2-yl)propan-1-amine hydrochloride (2.7b): Synthesized according to General Procedure 2.6. Purified *via* trituration with ethyl acetate and diethyl ether. White solid (56%, 35 mg). ^{1}H NMR (400 MHz, d$_4$-MeOD) δ 7.59 (d, *J* = 8.2 Hz, 2H), 7.44 (s, 1H), 7.19 (d, *J* = 8.0 Hz, 2H), 4.06 (q, *J* = 7.3 Hz, 2H), 3.09 (t, *J* = 7.1 Hz, 2H), 2.95 (t, *J* = 7.3 Hz, 2H), 2.61 (t, *J* = 7.6 Hz, 2H), 2.12 (p, *J* = 7.2 Hz, 2H), 1.62 (p, *J* = 7.0 Hz, 2H), 1.45 (t, *J* = 7.3 Hz, 3H), 1.37 – 1.22 (m, 14H), 0.89 (t, *J* = 6.7 Hz, 3H). ^{13}C NMR (101 MHz, d$_4$-MeOD) δ 147.8, 143.1, 140.2, 131.8, 129.8, 125.9, 116.4, 42.2, 40.2, 36.6, 33.1, 32.7, 30.7, 30.7, 30.6, 30.5, 30.3, 26.5, 24.5, 23.7, 16.4, 14.4. HRMS: (ESI) [M+H]+ calc. for $C_{24}H_{40}N_3$, 370.3217, observed, 370.3207.

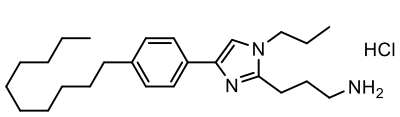

3-(4-(4-decylphenyl)-1-propyl-1H-imidazol-2-yl)propan-1-amine hydrochloride (2.7c): Purified via trituration with ethyl acetate and diethyl ether. White solid (60%, 46 mg). ^{1}H NMR (400 MHz, cd$_3$od) δ 7.58 (d, *J* = 8.3 Hz, 2H), 7.36 (s, 1H), 7.17 (d, *J* = 8.4 Hz, 2H), 3.95 (t, *J* =

7.2 Hz, 2H), 3.09 (t, *J* = 7.0 Hz, 2H), 2.91 (t, *J* = 7.2 Hz, 2H), 2.60 (t, *J* = 7.6 Hz, 2H), 2.11 (p, *J* = 7.1 Hz, 2H), 1.84 (h, *J* = 7.4 Hz, 2H), 1.61 (p, *J* = 7.4 Hz, 2H), 1.37 – 1.20 (m, 14H), 0.98 (t, *J* = 7.4 Hz, 3H), 0.89 (t, *J* = 6.8 Hz, 3H). ^{13}C NMR (101 MHz, cd_3od) δ 148.26, 142.70, 140.83, 132.60, 129.67, 125.77, 116.85, 48.64, 40.33, 36.61, 33.06, 32.68, 30.72, 30.70, 30.59, 30.44, 30.29, 26.55, 25.21, 24.88, 23.72, 14.44, 11.33. HRMS: (ESI) [M+H]+ calc. for $C_{25}H_{42}N_3$, 384.3373, observed, 384.3371.

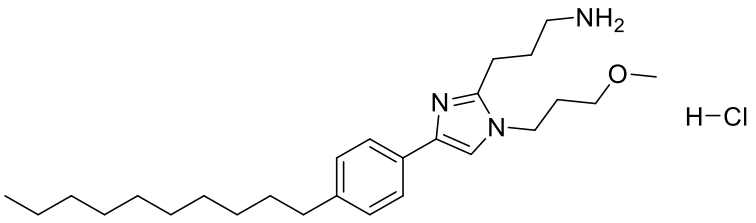

3-(4-(4-decylphenyl)-1-(3-methoxypropyl)-1H-imidazol-2-yl)propan-1-amine hydrochloride (2.7d):

Synthesized according to General Procedure 2.6. Purified *via* column chromatography (10-15% methanol/CH_2Cl_2). Off-white solid (76%, 45 mg). ^{1}H NMR (400 MHz, d_4-MeOD) δ 7.91 (s, 1H), 7.71 (d, *J* = 7.8 Hz, 2H), 7.32 (d, *J* = 7.7 Hz, 2H), 4.34 (t, *J* = 6.8 Hz, 2H), 3.49 (t, *J* = 5.4 Hz, 2H), 3.34 (s, 3H), 3.25 (t, *J* = 7.9 Hz, 2H), 3.15 (t, *J* = 7.4 Hz, 2H), 2.65 (t, *J* = 7.6 Hz, 2H), 2.29 – 2.14 (m, 4H), 1.62 (p, *J* = 7.2 Hz, 2H), 1.37 – 1.21 (m, 14H), 0.88 (t, *J* = 6.6 Hz, 3H). ^{13}C NMR (101 MHz, d_4-MeOD) δ 147.4, 146.1, 134.4, 130.4, 126.6, 125.1, 118.5, 69.7, 59.0, 46.3, 39.8, 36.6, 33.0, 32.4, 30.8, 30.7, 30.7, 30.5, 30.4, 30.2, 26.5, 23.7, 22.7, 14.4. HRMS: (ESI) [M+H]+ calc. for $C_{26}H_{44}N_3O$, 414.3479, observed, 414.3477.

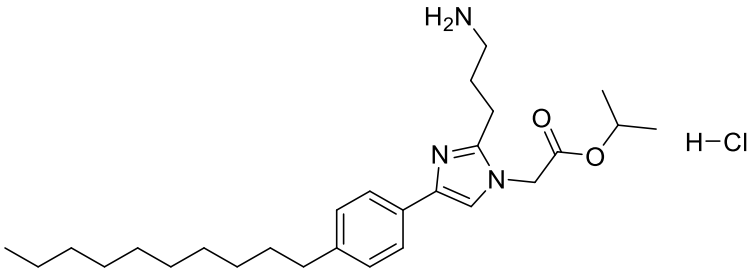

***iso*propyl 2-(2-(3-aminopropyl)-4-(4-decylphenyl)-1H-imidazol-1-yl)acetate hydrochloride (2.7e):** Synthesized according to General Procedure 2.6. Purified *via* column chromatography (10% methanol/CH_2Cl_2). Yellow solid (35%, 43 mg). ^{1}H NMR (400 MHz, d_4-MeOD) δ 7.58 (d, *J* = 8.1 Hz, 2H), 7.33 (s, 1H), 7.17 (d, *J* = 8.0 Hz, 2H), 5.09 (hept, *J* = 6.3 Hz, 1H), 4.92 – 4.85 (m, 2H), 3.07 (t, *J* = 7.0 Hz, 2H), 2.84 (t, *J* = 7.0 Hz, 2H), 2.60 (t, *J* = 7.6 Hz, 2H), 2.11 (p, *J* = 7.0 Hz, 2H), 1.62 (p, *J* = 7.4 Hz, 2H), 1.43 – 1.20 (m, 20H), 0.89 (t, *J* = 6.7 Hz, 3H). ^{13}C NMR (101 MHz, d_4-MeOD) δ 169.3, 149.3, 142.8, 141.0, 132.5, 129.7, 125.8, 118.0, 71.3, 48.4, 40.3, 36.6, 33.1, 32.7, 30.7, 30.7, 30.6, 30.5, 30.3, 26.3, 24.7, 23.7, 22.0, 14.5. ^{1}H NMR shows overlap of α-carbon protons with water signal. HRMS: (ESI) [M+H]+ calc. for $C_{27}H_{44}N_3O_2$, 442.3428, observed, 442.3423.

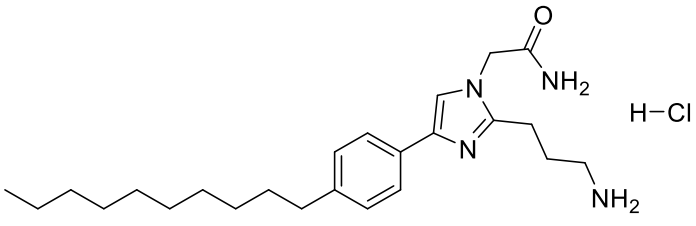

2-(2-(3-aminopropyl)-4-(4-decylphenyl)-1H-imidazol-1-yl)acetamide hydrochloride (2.7g): Synthesized according to General Procedure 2.6. Purified *via* trituration with ethyl acetate and diethyl ether. White solid (74%, 29 mg). ^{1}H NMR (400 MHz, d_4-MeOD) δ 7.80 (s, 1H), 7.66 (d, *J* = 7.9 Hz, 2H), 7.35 (d, *J* = 8.0 Hz, 2H), 5.12 (s, 2H), 3.17 (t, *J* = 7.9 Hz, 2H), 3.10 (t, *J* = 7.7 Hz, 2H), 2.67 (t, *J* = 7.6 Hz, 2H), 2.21 (p, *J* = 7.8 Hz, 2H), 1.64 (p, *J* = 7.4 Hz, 2H),

1.44 – 1.22 (m, 14H), 0.89 (t, *J* = 6.6 Hz, 3H). ^{13}C NMR (101 MHz, d_4-MeOD) δ 169.1, 148.9, 146.4, 134.4, 130.5, 126.7, 125.0, 119.8, 50.5, 39.7, 36.6, 33.1, 32.5, 30.7, 30.7, 30.6, 30.4, 30.3, 26.3, 23.7, 22.9, 14.4. HRMS: (ESI) [M+H]+ calc. for $C_{24}H_{39}N_4O$, 399.3118, observed, 399.3114.

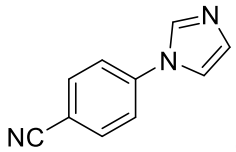

4-(-1H-imidazol-1-yl)benzonitrile (2.9): Synthesized according to General Procedure 2.1. 455 mg, 65%, white solid. ^{1}H NMR (400 MHz, $CDCl_3$) δ 8.02 – 7.94 (m, 1H), 7.85 – 7.79 (m, 2H), 7.62 – 7.51 (m, 2H), 7.38 (t, *J* = 1.4 Hz, 1H), 7.30 – 7.21 (m, 1H). ^{13}C NMR (101 MHz, $CDCl_3$) δ 140.4, 135.2, 134.0, 131.4, 121.2, 117.8, 117.5, 110.8. HRMS: (ESI) $[M+H]^+$ calc. for $C_{10}H_8N_3^+$ 170.0713, observed, 170.0720.

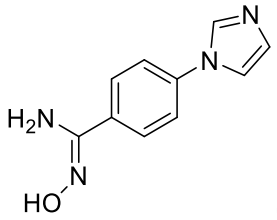

(Z)-N'-hydroxy-4-(-1H-imidazol-1-yl)benzimidamide (2.10): Synthesized according to General Procedure 2.2. 561 mg, 72%, white solid. ^{1}H NMR (500 MHz, d_6-DMSO) δ 9.85 (s, 1H), 9.75 (s, 1H), 8.34 (t, *J* = 1.2 Hz, 1H), 7.83 – 7.78 (m, 3H), 7.71 – 7.66 (m, 2H), 7.14 – 7.13 (m, 1H), 5.96 (s, 2H). ^{13}C NMR (126 MHz, d_6-DMSO) δ 150.1, 137.1, 135.5, 131.5, 129.8, 126.8, 119.7, 117.9. HRMS: (ESI) $[M+H]^+$ calc. for $C_{10}H_{11}N_4O^+$ 203.0927, observed, 203.0932.

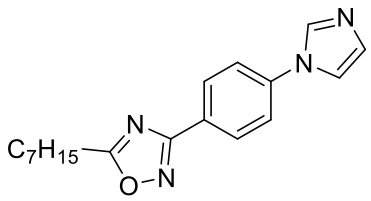

3-(4-(-1H-imidazol-1-yl)phenyl)-5-heptyl-1,2,4-oxadiazole (2.11a): Synthesized according to General Procedure 2.3. 89 mg, 58%,

yellow solid. ^{1}H NMR (500 MHz, d$_4$-MeOD) δ 8.26 (s, 1H), 8.17 – 8.13 (m, 2H), 7.74 – 7.68 (m, 2H), 7.66 (s, 1H), 7.18 (s, 1H), 2.95 (t, *J* = 7.6 Hz, 2H), 1.84 (p, *J* = 7.5 Hz, 2H), 1.45 – 1.26 (m, 9H), 0.91 – 0.87 (m, 3H). ^{13}C NMR (126 MHz, d$_4$-MeOD) δ 180.8, 167.1, 139.1, 135.5, 129.2, 128.6, 125.9, 120.9, 118.0, 31.4, 28.7, 28.5, 26.2, 25.9, 22.3, 13.0. HRMS: (ESI) $[M+H]^+$ calc. for $C_{18}H_{23}N_4O^+$ 311.1866, observed, 311.1874.

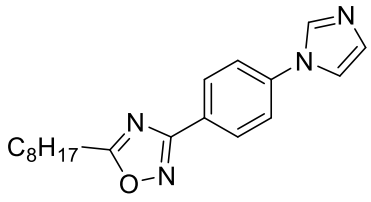

3-(4-(-1H-imidazol-1-yl)phenyl)-5-octyl-1,2,4-oxadiazole

(2.11b): Synthesized according to General Procedure 2.3. 73 mg, 44%, yellow solid. ^{1}H NMR (500 MHz, d$_4$-MeOD) δ 8.28 (s, 1H), 8.22 – 8.17 (m, 2H), 7.77 – 7.73 (m, 2H), 7.69 (s, 1H), 7.20 (s, 1H), 2.99 (t, *J* = 7.5 Hz, 2H), 1.87 (p, *J* = 7.5 Hz, 2H), 1.48 – 1.25 (m, 13H), 0.92 – 0.87 (m, 4H). ^{13}C NMR (126 MHz, d$_4$-MeOD) δ 182.2, 168.5, 140.5, 136.9, 130.5, 130.0, 127.3, 122.3, 119.5, 32.9, 30.2, 30.2, 30.0, 27.6, 27.2, 23.7, 14.4. HRMS: (ESI) $[M+H]^+$ calc. for $C_{19}H_{25}N_4O^+$ 325.2023, observed, 325.2027.

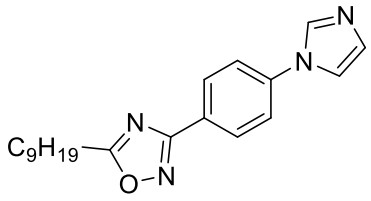

3-(4-(-1H-imidazol-1-yl)phenyl)-5-nonyl-1,2,4-oxadiazole

(2.11c): Synthesized according to General Procedure 2.3. 67 mg, 40%, yellow solid. ^{1}H NMR (400 MHz, d$_4$-MeOD) δ 8.28 (s, 1H), 8.23 – 8.17 (m, 2H), 7.78 – 7.73 (m, 2H), 7.70 – 7.68 (m, 1H), 7.20 (s, 1H), 2.99 (t, *J* = 7.5 Hz, 2H), 1.88 (p, *J* = 7.5 Hz, 2H), 1.48 – 1.23 (m, 14H), 0.93 – 0.85 (m, 3H). ^{13}C NMR (101 MHz, d$_4$-MeOD) δ 182.3, 168.5, 140.5, 136.9, 130.6, 130.1, 127.3, 122.4, 119.5, 33.0, 30.5, 30.3, 30.2, 30.0, 27.6, 27.2, 23.7, 14.4. HRMS: (ESI) $[M+H]^+$ calc. for $C_{20}H_{27}N_4O^+$ 339.2179, observed, 339.2203.

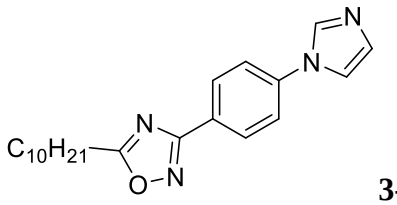

3-(4-(-1H-imidazol-1-yl)phenyl)-5-decyl-1,2,4-oxadiazole (2.11d): Synthesized according to General Procedure 2.3. 73 mg, 52%, off white solid. ^{1}H NMR (400 MHz, $CDCl_3$) δ 8.25 – 8.17 (m, 2H), 7.95 (s, 1H), 7.56 – 7.48 (m, 2H), 7.36 (s, 1H), 7.25 (s, 1H), 2.96 (t, *J* = 7.6 Hz, 2H), 1.88 (p, *J* = 7.6 Hz, 2H), 1.44 – 1.23 (m, 15H), 0.92 – 0.84 (m, 3H). ^{13}C NMR (101 MHz, $CDCl_3$) δ 180.4, 167.3, 139.3, 135.4, 130.9, 129.1, 126.1, 121.3, 117.8, 31.8, 29.5, 29.4, 29.3, 29.1, 29.0, 26.6, 22.6, 14.1. HRMS: (ESI) $[M+H]^+$ calc. for $C_21H_{29}N_4O^+$ 353.2336, observed, 353.2349.

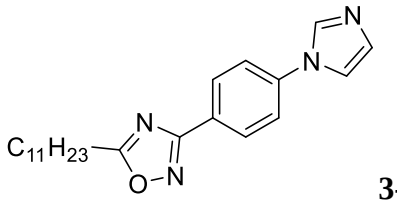

3-(4-(-1H-imidazol-1-yl)phenyl)-5-undecyl-1,2,4-oxadiazole (2.11e): Synthesized according to General Procedure 2.3. 65 mg, 36%, yellow solid. ^{1}H NMR (500 MHz, d_4-MeOD) δ 8.28 (s, 1H), 8.19 (tt, *J* = 6.1, 3.0 Hz, 2H), 7.74 (tt, *J* = 7.7, 3.1 Hz, 2H), 7.69 (s, 1H), 7.20 (s, 1H), 3.33 (s, 1H), 3.03 – 2.93 (m, 2H), 1.93 – 1.82 (m, 2H), 1.48 – 1.21 (m, 17H), 0.93 – 0.84 (m, 3H).^{13}C NMR (126 MHz, d_4-MeOD) δ 180.8, 167.1, 139.1, 135.5, 129.3, 128.7, 125.9, 120.9, 118.0, 31.7, 29.3, 29.3, 29.1, 29.1, 28.8, 28.6, 26.2, 25.9, 22.3, 13.1. HRMS: (ESI) $[M+H]^+$ calc. for $C_{22}H_{31}N_4O^+$ 367.2492, observed, 367.2500.

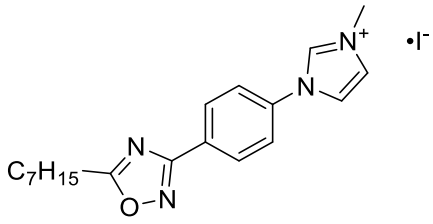

1-(4-(5-heptyl-1,2,4-oxadiazol-3-yl)phenyl)-3-methyl-1H-imidazol-3-ium iodide (2.12a): Synthesized according to General Procedure 2.4. 12 mg, 41%, brown solid. ^{1}H NMR (400 MHz, $CDCl_3$) δ 9.80 (s, 1H), 8.26 – 8.21 (m, 2H), 7.84 – 7.79 (m, 2H), 7.72 – 7.69 (m, 1H), 7.63 – 7.60 (m, 1H), 4.16 (s, 3H), 2.94 (t, *J* = 7.6 Hz, 2H), 1.87 (p, *J* = 7.6 Hz, 2H), 1.49 – 1.24 (m, 8H), 0.91 – 0.86 (m, 3H). ^{13}C NMR (151 MHz, $CDCl_3$) δ 180.9, 166.8, 136.2, 135.6, 129.7, 129.3, 124.9, 122.7, 121.0, 37.5, 31.9, 29.2, 29.2, 26.8, 26.7, 22.8, 14.2. HRMS: (ESI) $[M+H]^+$ calc. for $C_{19}H_{25}N_4O^+$ 325.2023, observed, 325.2029.

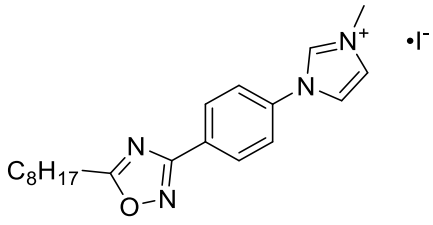

1-(4-(5-octyl-1,2,4-oxadiazol-3-yl)phenyl)-3-methyl-1H-imidazol-3-ium iodide (2.12b): Synthesized according to General Procedure 2.4. 12 mg, 52%, brown solid. ^{1}H NMR (400 MHz, $CDCl_3$) δ 9.60 (s, 1H), 8.25 – 8.18 (m, 2H), 7.81 – 7.73 (m, 2H), 7.68 – 7.64 (m, 1H), 7.58 – 7.52 (m, 1H), 4.15 – 4.08 (m, 3H), 2.92 (t, *J* = 7.6 Hz, 2H), 1.84 (p, *J* = 7.6 Hz, 2H), 1.46 – 1.20 (m, 10H), 0.90 – 0.82 (m, 3H). ^{13}C NMR (151 MHz, $CDCl_3$) δ 180.9, 166.8, 136.3, 136.1, 129.8, 129.4, 124.8, 122.7, 120.6, 37.9, 32.0, 29.7, 29.5, 29.5, 29.2, 29.2, 26.8, 26.7, 22.8, 14.3. HRMS: (ESI) $[M+H]^+$ calc. for $C_{20}H_{27}N_4O^+$ 339.2179, observed, 339.2175.

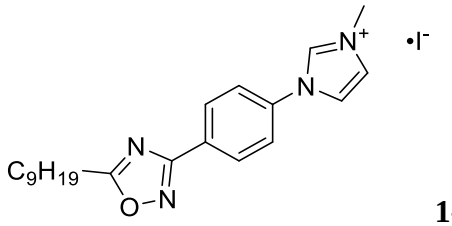

1-(4-(5-nonyl-1,2,4-oxadiazol-3-yl)phenyl)-3-methyl-1H-imidazol-3-ium iodide (2.12c): Synthesized according to General Procedure 2.4. 10 mg, 41%, white solid. ^{1}H NMR (500 MHz, $CDCl_3$) δ 10.38 (s, 1H), 8.27 – 8.21 (m, 2H), 7.96 – 7.90 (m, 2H), 7.82 (t, *J* = 1.9 Hz, 1H), 7.77 (t, *J* = 1.8 Hz, 1H), 4.26 (s, 3H), 2.95 (t, *J* = 7.7 Hz, 2H), 1.87 (p, *J* = 7.6 Hz, 2H), 1.49 – 1.21 (m, 13H), 0.91 – 0.85 (m, 3H). ^{13}C NMR (126 MHz, $CDCl_3$) δ 180.8, 166.7, 136.1, 135.8, 129.6, 129.1, 125.0, 122.6, 120.7, 37.7, 31.8, 29.4, 29.2, 29.1, 29.1, 26.6, 26.6, 22.7, 14.1. HRMS: (ESI) $[M+H]^+$ calc. for $C_21H_{29}N_4O^+$ 353.2336, observed, 353.2343.

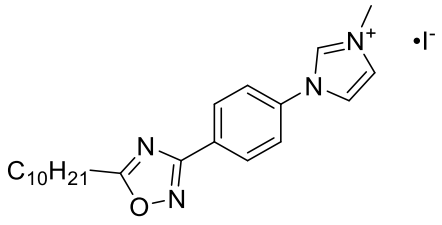

1-(4-(5-decyl-1,2,4-oxadiazol-3-yl)phenyl)-3-methyl-1H-imidazol-3-ium iodide (2.12d): Synthesized according to General Procedure 2.4. 41 mg, 89%, yellow solid. ^{1}H NMR (400 MHz, d_4-MeOD) δ 8.33 – 8.28 (m, 2H), 8.15 (d, *J* = 2.1 Hz, 1H), 7.90 – 7.85 (m, 2H), 7.81 (d, *J* = 2.1 Hz, 1H), 4.05 (s, 3H), 3.00 (t, *J* = 7.5 Hz, 2H), 1.87 (p, *J* = 7.5 Hz, 2H), 1.47 – 1.21 (m, 15H), 0.92 – 0.83 (m, 3H). ^{13}C NMR (126 MHz, $CDCl_3$) δ 180.8, 166.7, 136.2, 136.0, 129.6, 129.3, 124.7, 122.6, 120.5, 37.8, 31.9, 29.5, 29.4, 29.3, 29.1, 29.1, 26.6, 26.6, 22.7, 14.1. HRMS: (ESI) $[M+H]^+$ calc. for $C_{22}H_{31}N_4O^+$ 367.2492, observed, 367.2496.

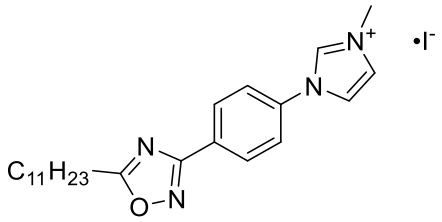

1-(4-(5-undecyl-1,2,4-oxadiazol-3-yl)phenyl)-3-methyl-1H-imidazol-3-ium iodide (2.12e): Synthesized according to General Procedure 2.4. 7 mg, 30%, yellow solid. ^{1}H NMR (500 MHz, $CDCl_3$) δ 10.49 (d, *J* = 1.7 Hz, 1H), 8.26 – 8.18 (m, 2H), 7.97 – 7.89 (m, 2H), 7.81 (dt, *J* = 14.2, 1.9 Hz, 2H), 2.92 (t, *J* = 7.6 Hz, 2H), 1.84 (p, *J* = 7.6 Hz, 2H), 1.45 – 1.35 (m, 2H), 1.37 – 1.19 (m, 15H), 0.88 – 0.82 (m, 3H). ^{13}C NMR (126 MHz, $CDCl_3$) δ 180.7, 166.7, 136.0, 135.9, 129.5, 129.1, 125.0, 122.6, 120.7, 37.8, 31.9, 29.6, 29.4, 29.3, 29.1, 29.1, 26.6, 26.6, 22.7, 14.1. HRMS: (ESI) $[M+H]^+$ calc. for $C_{23}H_{33}N_4O^+$ 381.2649, observed, 381.2648.

5.3 Procedures and Characterization for Chapter 3

General Procedure 4.1: Amidoxime Synthesis To a round-bottom flask with stir bar containing a solution of 200 proof ethanol (0.2 M) and substituted benzonitrile (1.0 equiv.) was added hydroxylamine hydrochloride (2.2 equiv.) followed by TEA (3.0 equiv.). The reaction was heated under reflux for 16 hours with reaction progress monitored by TLC. Once complete, the reaction was allowed to cool to room temperature and concentrated *in vacuo*. Addition of ethyl acetate formed a white precipitate that was filtered off. The resulting mixture was then purified by silica gel chromatography with an appropriate ethyl acetate/hexanes solvent system to afford the pure product.

General Procedure 4.2: HCTU-Assisted 1,2,4-Oxadiazole Ring Closure To a round bottom flask with stir bar containing benzamidoxime (1.0 equiv.) in DMF (0.3 M) under argon, was added undecanoic acid (1.2 equiv.), diisopropylethylamine (1.8 equiv.), and HCTU (1.2 equiv.). The reaction was heated to 105 °C for 16 hours and reaction progress was monitored by TLC. Once complete, the reaction was allowed to cool to room temperature and the resulting solution was partitioned between ethyl acetate and aqueous lithium bromide solution. The aqueous layer was washed three times with additional ethyl acetate and the combined organic layers were dried over Na_2SO_4, filtered, and concentrated *in vacuo*. The reaction mixture was purified *via* silica gel chromatography to afford the desired product.

General Procedure 4.3: One-Pot Hydroboration-Suzuki-Miyaura Cross-Coupling To a flame-dried pressure vial with stir bar under argon was added alkene (2.0 equiv.) followed by 9-BBN (2.1 equiv., 0.5 M in THF). The reaction was allowed to stir under reflux for 60 minutes. After, the reaction mixture was allowed to cool to room

temperature. Aryl halide (1.0 equiv.) was added, followed by $PdCl_2(dppf)\cdot CH_2Cl_2$ (0.05 equiv.), followed by dropwise addition of a 3 M $KOH_{(aq)}$ solution(3.0 equiv.). This was then heated back up to reflux and allowed to for an additional 2-16 hours at which reaction progress was tracked by consumption of the aryl halide *via* TLC. The mixture was cooled, filtered over celite, and concentrated under reduced pressure to afford the crude product. The resulting mixture was the purified by silica gel chromatography with an appropriate ethyl acetate/hexanes solvent system to afford the pure product.

General Procedure 4.4: HCl-Assisted Boc Deprotection: To a 6-dram vial containing an *N*-Boc-protected amine (1.0 equiv.) was added CH_2Cl_2 (0.2 M), followed by HCl (10 equiv, 4 M in dioxane). The resulting mixture was allowed to stir until complete consumption of starting material was observed *via* TLC (1-4 hours). The reaction mixture was concentrated *in vacuo* and the residue was rinsed with diethyl ether until a precipitate formed. The precipitate was subjected to trituration with an appropriate solvent system to afford pure product as the hydrochloride salt.

General Procedure 4.5: HCTU-Assisted Amide Coupling To a solution of appropriate carboxylic acid (1.0 equiv.) in DCM (0.2 M) under argon, was added *N*-Boc-piperazine (1.1 equiv.), diisopropylethylamine (2.0 equiv.), and HCTU (1.1 equiv.). The reaction was allowed to stir at room temperature for 2 hours and reaction progress was monitored by TLC. Once complete, the reaction was concentrated *in vacuo*. The reaction mixture was purified *via* silica gel chromatography to afford the desired product.

General Procedure 4.6: Substitution of 1-Bromoundecane. To a solution of heterocyclic amide (1.0 equiv.) in DMF (0.2 M) was added 1-bromoundecane (1.5 equiv.) followed by potassium carbonate (3.0 equiv.). This was allowed to stir at room temperature

for 3 hours or until complete. Once complete, the reaction was partitioned between ethyl acetate and aqueous lithium bromide solution. The aqueous layer was washed three times with additional ethyl acetate and the combined organic layers were dried over Na_2SO_4, filtered, and concentrated *in vacuo*. The reaction mixture was purified *via* silica gel chromatography to afford the desired product.

General Procedure 4.7: Urea Coupling To a flame dried vial containing a stir bar under argon was added triphosgene (0.5 equiv) followed by anhydrous dichloromethane (0.2 M) and a appropriate aniline (1.0 equiv) in dichloromethane (2 mL) was added dropwise. This mixture was stirred for 30 min at room temperature and then treated with triethylamine (2.3 equiv) in dichloromethane (0.2 M). After 30 min, *N*-Boc-protected amine (1.5 equiv) was added. The reaction mixture was stirred for 16 hours at room temperature, evaporated to dryness, treated with water (10 mL) and extracted with DCM (3 × 20 mL). The organic phase was dried over anhydrous sodium sulphate, filtered, and purified *via* silica chromatography.

General Procedure 4.8: TFA Boc Deprotection To a solution of *N*-Boc-amine in DCM (0.2 M) was added TFA (10.0 equiv.). The resulting mixture was stirred at room temperature for 16 hours or until complete. The reaction mixture was then triturated with diethyl ether to afford pure product.

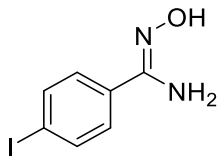

(Z)-N'-hydroxy-4-iodobenzimidamide (3.2): Synthesized according to General Procedure 4.1. Purified via column chromatography (30% ethyl

acetate/hexanes). White solid (91%, 519 mg). ^{1}H NMR (400 MHz, cdcl$_3$) δ 7.76 – 7.72 (m, 2H), 7.39 – 7.35 (m, 2H), 4.82 (s, 2H). ^{13}C NMR (126 MHz, DMSO) δ 150.2, 136.9, 132.9, 127.5, 95.3. ^{13}C NMR (126 MHz, DMSO) δ 150.2, 136.9, 132.9, 127.5, 95.3.

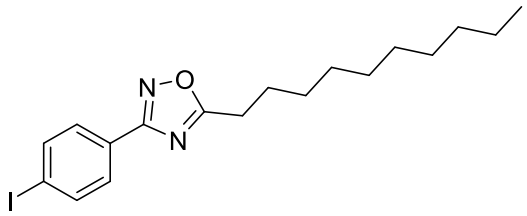

5-decyl-3-(4-iodophenyl)-1,2,4-oxadiazole (3.3): Synthesized according to General Procedure 4.2. Purified via column chromatography (10% ethyl acetate/hexanes). White solid (70%, 2.19 g). ^{1}H NMR (400 MHz, cdcl$_3$) δ 7.85 – 7.77 (m, 4H), 2.97 – 2.89 (m, 2H), 1.86 (p, *J* = 7.5 Hz, 2H), 1.46 – 1.22 (m, 14H), 0.91 – 0.82 (m, 3H). ^{13}C NMR (101 MHz, cdcl$_3$) δ 180.3, 167.7, 138.5, 138.0, 133.1, 128.9, 126.5, 97.7, 31.9, 29.5, 29.4, 29.3, 29.1, 29.0, 26.6, 22.7, 14.1. HRMS: (ESI) $[M+H]^+$ calc. for $C_{18}H_{26}IN_2O^+$ 413.1084, observed, 413.1061.

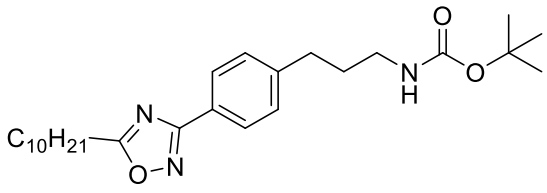

tert-butyl (3-(4-(5-decyl-1,2,4-oxadiazol-3-yl)phenyl)propyl)carbamate (3.4a): Synthesized according to General Procedure 4.3. Purified via column chromatography (10% ethyl acetate/hexanes). Yellow oil (89%, 144 mg). ^{1}H NMR (400 MHz, cdcl$_3$) δ 7.97 (dd, *J* = 8.3, 1.4 Hz, 2H), 7.29 – 7.25 (m, 2H), 2.92 (td, *J* = 7.6, 1.4 Hz, 2H), 2.69 (t, *J* = 7.8 Hz, 2H), 1.90 – 1.78 (m, 6H), 1.44 (s, 9H), 1.36 – 1.22 (m, 14H), 0.90 – 0.84 (m, 3H). ^{13}C NMR (101 MHz, cdcl$_3$) δ 180.1, 168.3, 156.1, 145.1, 129.0, 127.7, 124.9, 32.2, 32.0, 31.7, 29.6, 29.5, 29.4, 29.2, 29.2, 28.5, 26.8, 26.8,

26.4, 22.8, 22.2, 14.2. HRMS: (ESI) $[M+H]^+$ calc. for $C_{26}H_{42}N_3O_3^+$ 444.3221, observed, 444.3205.

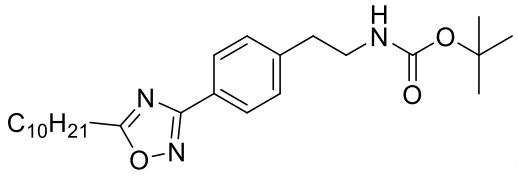

tert-butyl (4-(5-decyl-1,2,4-oxadiazol-3-yl)phenethyl)carbamate (3.4b): Synthesized according to General Procedure 4.3. Purified via column chromatography (10% ethyl acetate/hexanes). Yellow solid (64%, 101 mg). ^{1}H NMR (400 MHz, cdcl$_3$) δ 8.00 (d, *J* = 7.8 Hz, 2H), 7.30 (d, *J* = 7.8 Hz, 2H), 3.40 (q, *J* = 6.6 Hz, 2H), 2.96 – 2.81 (m, 4H), 1.85 (h, *J* = 6.6 Hz, 3H), 1.43 (s, 9H), 1.28 (d, *J* = 13.2 Hz, 14H), 0.87 (t, *J* = 6.7 Hz, 3H). ^{13}C NMR (101 MHz, cdcl$_3$) δ 180.0, 168.1, 155.8, 142.3, 129.3, 127.6, 125.2, 32.1, 31.8, 29.5, 29.4, 29.2, 29.1, 29.0, 28.4, 26.6, 26.6, 26.2, 22.6, 22.0, 14.1. HRMS: (ESI) $[M+H]^+$ calc. for $C_{25}H_{40}N_3O_3^+$ 430.3064, observed, 430.3048.

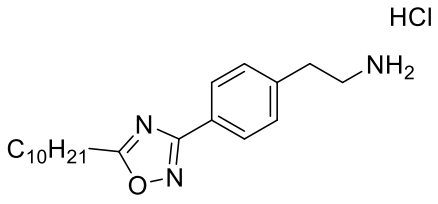

2-(4-(5-decyl-1,2,4-oxadiazol-3-yl)phenyl)ethan-1-amine hydrochloride (3.5a): Synthesized according to General Procedure 4.4. Purified *via* trituration with diethyl ether. White solid (80%, 41 mg). ^{1}H NMR (400 MHz, cd$_3$od) δ 8.07 – 8.02 (m, 2H), 7.48 – 7.43 (m, 2H), 3.26 – 3.20 (m, 2H), 3.05 (dd, *J* = 8.9, 6.6 Hz, 2H), 2.99 (d, *J* = 7.5 Hz, 2H), 1.86 (d, *J* = 7.4 Hz, 2H), 1.44 – 1.29 (m, 14H), 0.92 – 0.86 (m, 3H). ^{13}C NMR (101 MHz, cd$_3$od) δ 182.1, 169.1, 141.5, 130.5, 128.9, 127.2, 41.6, 34.4, 33.1, 30.6, 30.5, 30.4, 30.2, 30.0, 27.6, 27.2, 23.7, 14.4. HRMS: (ESI) $[M+H]^+$ calc. for $C_{20}H_{32}N_3O^+$ 330.2540, observed, 330.2540.

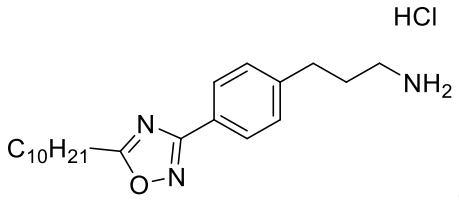

3-(4-(5-decyl-1,2,4-oxadiazol-3-yl)phenyl)propan-1-amine hydrochloride (3.5b): Synthesized according to General Procedure 4.4. Purified *via* trituration with diethyl ether. White solid (85%, 51 mg). ^{1}H NMR (500 MHz, MeOD) δ 8.02 – 7.97 (m, 2H), 7.42 – 7.38 (m, 2H), 2.97 (td, *J* = 7.7, 3.1 Hz, 4H), 2.80 (t, *J* = 7.8 Hz, 2H), 2.06 – 1.97 (m, 2H), 1.86 (p, *J* = 7.5 Hz, 2H), 1.43 – 1.25 (m, 14H), 0.92 – 0.87 (m, 3H). ^{13}C NMR (126 MHz, MeOD) δ 182.0, 169.2, 145.5, 130.1, 128.6, 126.3, 40.2, 33.4, 33.1, 30.6, 30.5, 30.4, 30.2, 30.1, 30.0, 27.6, 27.2, 23.7, 14.5. HRMS: (ESI) $[M+H]^+$ calc. for $C_{21}H_{34}N_3O^+$ 344.2696, observed, 344.2696.

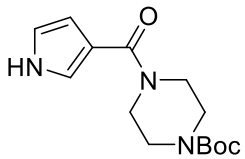

tert-butyl 4-(1H-pyrrole-3-carbonyl)piperazine-1-carboxylate (3.6a): Synthesized according to General Procedure 3.5. Purified via column chromatography (% ethyl acetate/hexanes). Brown solid (67%, 169 mg). ^{1}H NMR (500 MHz, DMSO) δ 11.20 (s, 1H), 7.11 (dt, *J* = 3.2, 1.7 Hz, 1H), 6.77 (q, *J* = 2.5 Hz, 1H), 6.25 (td, *J* = 2.6, 1.6 Hz, 1H), 3.58 (t, *J* = 5.4 Hz, 4H), 3.30 (s, 4H), 1.41 (s, 9H). ^{13}C NMR (126 MHz, $CDCl_3$) δ 171.9, 159.7, 126.7, 123.7, 121.8, 113.9, 85.3, 33.1. HRMS: (ESI) $[M+H]^+$ calc. for $C_{14}H_{22}N_3O_3^+$, 280.1656, observed, 280.1639.

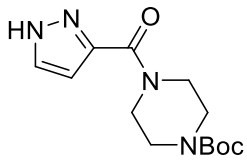

tert-butyl 4-(1H-pyrazole-3-carbonyl)piperazine-1-carboxylate (3.6b): Synthesized according to General Procedure 3.5. Purified via column

chromatography (70-100% ethyl acetate/hexanes). White solid (40%, 150 mg). ^{1}H NMR (500 MHz, $CDCl_3$) δ 8.27 (s, 1H), 7.76 (s, 1H), 6.58 (d, *J* = 2.3 Hz, 1H), 3.96 – 3.80 (m, 2H), 3.40 – 3.33 (m, 4H), 3.14 – 3.07 (m, 2H). ^{13}C NMR (126 MHz, $CDCl_3$) δ 165.0, 154.2, 107.5, 79.5, 53.9, 28.2, 18.2, 16.8, 12.7. HRMS: (ESI) $[M+H]^+$ calc. for $C_{13}H_{21}N_4O_3^+$ 281.1608, observed, 281.1591.

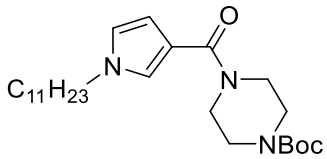

tert-butyl 4-(1-undecyl-1H-pyrrole-3-carbonyl)piperazine-1-carboxylate (3.7a): Synthesized according to General Procedure 4.7. Purified via column chromatography (70-100% ethyl acetate/hexanes). Yellow solid (66%, 41 mg). ^{1}H NMR (400 MHz, cdcl$_3$) δ 7.05 – 7.02 (m, 1H), 6.60 – 6.56 (m, 1H), 6.27 – 6.24 (m, 1H), 3.88 – 3.81 (m, 2H), 3.74 – 3.69 (m, 4H), 3.48 – 3.43 (m, 4H), 1.76 (p, *J* = 7.0 Hz, 2H), 1.48 (d, *J* = 1.1 Hz, 9H), 1.27 (d, *J* = 12.0 Hz, 17H), 0.91 – 0.85 (m, 3H). ^{13}C NMR (101 MHz, cdcl$_3$) δ 166.8, 154.8, 124.1, 120.7, 118.0, 108.9, 80.2, 50.1, 44.2, 32.0, 31.3, 29.7, 29.6, 29.5, 29.4, 29.2, 28.5, 26.8, 22.8, 14.2. HRMS: (ESI) $[M+H]^+$ calc. for $C_{25}H_{44}N_3O_3^+$, 434.3377, observed, 434.3351.

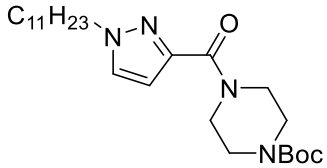

tert-butyl 4-(1-undecyl-1H-pyrazole-3-carbonyl)piperazine-1-carboxylate (3.7b): Synthesized according to General Procedure 4.7. Purified via column chromatography (50% ethyl acetate/hexanes). White solid (38%, 47 mg). ^{1}H NMR (400 MHz, cdcl$_3$) δ 7.35 (d, *J* = 2.3 Hz, 1H), 6.67 (d, *J* = 2.3 Hz, 1H), 4.10 (t, *J* = 7.2 Hz, 2H), 4.04 – 3.98 (m, 2H), 3.78 – 3.70 (m, 2H), 3.50 – 3.45 (m, 4H), 1.87 – 1.79 (m, 3H), 1.46 (s, 9H), 1.28 – 1.22 (m, 16H), 0.89 – 0.84 (m, 3H). ^{13}C NMR (126 MHz,

$CDCl_3$) δ 167.1, 154.8, 137.9, 133.9, 128.7, 98.6, 79.5, 66.0, 49.6, 49.3, 45.4, 45.1, 42.6, 39.2, 38.3, 29.5, 28.9, 28.6, 15.4. HRMS: (ESI) $[M+H]^+$ calc. for $C_{19}H_{35}N_4O^+$, 435.3330, observed, 435.3305.

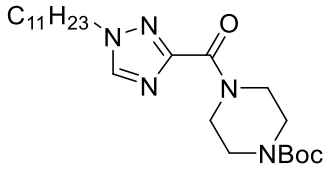

tert-butyl 4-(1-undecyl-1H-1,2,4-triazole-3-carbonyl)piperazine-1-carboxylate (3.7c): Synthesized according to General Procedure 4.7. Purified via column chromatography (50-80% ethyl acetate/hexanes). White solid (36%, 55 mg). ^{1}H NMR (500 MHz, $CDCl_3$) δ 7.87 (s, 1H), 4.37 (t, *J* = 7.3 Hz, 2H), 3.86 – 3.82 (m, 2H), 3.76 – 3.71 (m, 2H), 3.54 – 3.47 (m, 4H), 1.88 – 1.82 (m, 2H), 1.46 (s, 9H), 1.31 – 1.19 (m, 18H), 0.85 (t, *J* = 6.9 Hz, 3H). ^{13}C NMR (126 MHz, $CDCl_3$) δ 158.2, 154.6, 149.6, 146.7, 80.6, 50.5, 47.1, 42.5, 32.0, 30.2, 29.7, 29.6, 29.6, 29.4, 29.2, 28.5, 26.6, 22.8, 14.2. HRMS: (ESI) $[M+H]^+$ calc. for $C_{23}H_{42}N_5O_3^+$, 436.3282, observed, 436.3262.

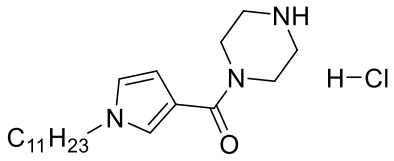

piperazin-1-yl(1-undecyl-1H-pyrrol-3-yl)methanone hydrochloride (3.8a): Synthesized according to General Procedure 4.4. Purified *via* trituration with diethyl ether. Brown solid (80%, 32 mg). ^{1}H NMR (400 MHz, cd_3od) δ 7.20 (t, *J* = 2.0 Hz, 1H), 6.77 (dd, *J* = 2.9, 2.1 Hz, 1H), 6.34 (dd, *J* = 2.9, 1.8 Hz, 1H), 4.03 – 3.96 (m, 4H), 3.94 (t, *J* = 7.1 Hz, 3H), 3.32 – 3.24 (m, 6H), 1.77 (p, *J* = 7.1 Hz, 2H), 1.38 – 1.22 (m, 20H), 0.90 (t, *J* = 6.6 Hz, 4H). ^{13}C NMR (151 MHz, MeOD) δ 169.2, 125.8, 122.8, 117.2, 110.1, 50.8, 44.6, 43.2, 33.1, 32.5, 30.7, 30.7, 30.7, 30.5, 30.3, 27.7, 23.7, 14.4. HRMS: (ESI) $[M+H]^+$ calc. for $C_{20}H_{36}N_3O^+$, 334.2853, observed, 334.2856.

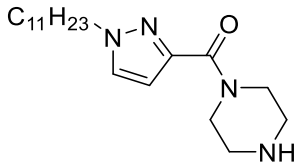

piperazin-1-yl(1-undecyl-1H-pyrazol-3-yl)methanone hydrochloride (3.8b): Synthesized according to General Procedure 4.4. Purified *via* trituration with diethyl ether. White solid (81%, 31 mg). ^{1}H NMR (500 MHz, MeOD) δ 7.70 (d, *J* = 2.4 Hz, 1H), 6.69 (d, *J* = 2.3 Hz, 1H), 4.39 (s, 2H), 4.19 (t, *J* = 7.0 Hz, 2H), 3.99 (s, 2H), 3.34 – 3.31 (m, 4H), 1.86 (p, *J* = 7.1 Hz, 2H), 1.34 – 1.25 (m, 16H), 0.89 (t, *J* = 6.9 Hz, 3H). ^{13}C NMR (126 MHz, MeOD) δ 164.7, 146.4, 132.2, 109.7, 53.5, 44.9, 40.5, 33.1, 31.4, 30.7, 30.7, 30.6, 30.5, 30.2, 27.6, 23.7, 14.4. HRMS: (ESI) $[M+H]^+$ calc. for $C_{19}H_{35}N_4O^+$, 335.2805, observed, 335.2815.

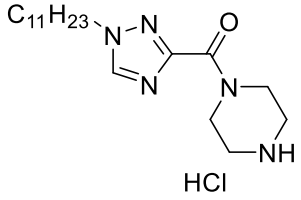

piperazin-1-yl(1-undecyl-1H-1,2,4-triazol-3-yl)methanone hydrochloride (3.8c): Synthesized according to General Procedure 4.4. Purified *via* trituration with diethyl ether. White solid (87%, 41 mg). ^{1}H NMR (400 MHz, MeOD) δ 8.05 (s, 1H), 4.42 – 4.35 (m, 2H), 4.16 – 4.08 (m, 2H), 4.07 – 4.00 (m, 2H), 3.41 – 3.32 (m, 5H), 1.89 (p, *J* = 7.0 Hz, 2H), 1.36 – 1.27 (m, 19H), 0.90 (t, *J* = 6.3 Hz, 3H). ^{13}C NMR (126 MHz, MeOD) δ 159.2, 150.5, 147.4, 51.5, 45.0, 44.7, 44.3, 40.2, 33.1, 30.9, 30.7, 30.7, 30.6, 30.5, 30.2, 27.5, 23.7, 14.4. HRMS: (ESI) $[M+H]^+$ calc. for $C_{18}H_{34}N_5O^+$, 336.2758, observed, 336.2750.

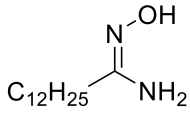

(Z)-N'-hydroxytridecanimidamide (3.10): Synthesized according to General Procedure . Purified via column chromatography (50% ethyl acetate/hexanes). White solid (62%, 145 mg). ^{1}H NMR (500 MHz, DMSO) δ 8.66 (s, 1H), 5.27 (s, 2H), 1.95 – 1.89 (m, 2H), 1.45 (t, *J* = 7.5 Hz, 2H), 1.25 – 1.22 (m, 18H), 0.88 – 0.84 (m, 3H). ^{13}C NMR (126 MHz, DMSO) δ 152.8, 31.3, 30.8, 29.1, 29.1, 28.9, 28.8, 28.7, 28.2, 28.1, 26.4, 22.1, 14.0. HRMS: (ESI) $[M+H]^+$ calc. for $C_{13}H_{29}N_2O^+$, 229.2274, observed, 229.2263.

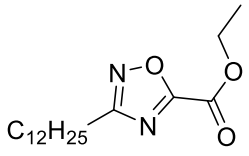

ethyl 3-dodecyl-1,2,4-oxadiazole-5-carboxylate (3.11): Synthesized according to General Procedure . Purified via column chromatography (50-70% ethyl acetate/hexanes). solid (90%, 140 mg). ^{1}H NMR (400 MHz, cdcl$_3$) δ 4.52 (q, *J* = 7.1 Hz, 2H), 2.85 – 2.77 (m, 2H), 1.78 (p, *J* = 7.5 Hz, 2H), 1.45 (t, *J* = 7.2 Hz, 3H), 1.37 – 1.22 (m, 18H), 0.87 (t, *J* = 6.8 Hz, 3H). ^{13}C NMR (151 MHz, $CDCl_3$) δ 171.9, 166.2, 154.2, 63.8, 31.9, 29.6, 29.5, 29.4, 29.3, 29.1, 29.0, 28.7, 28.6, 26.0, 25.4, 22.6, 14.1. HRMS: (ESI) $[M+H]^+$ calc. for $C_{17}H_{31}N_2O_3^+$, 311.2329, observed, 311.2319.

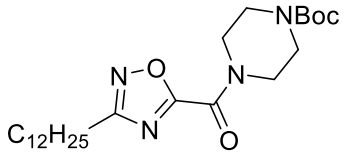

tert-butyl 4-(3-dodecyl-1,2,4-oxadiazole-5-carbonyl)piperazine-1-carboxylate (3.12): Synthesized according to General Procedure . Purified via column chromatography (50% ethyl acetate/hexanes). White solid (76%, 55 mg). ^{1}H NMR (500 MHz, $CDCl_3$) δ 3.81 – 3.73 (m, 4H), 3.57 – 3.50 (m, 4H), 2.79 (t, *J* = 7.6 Hz, 2H), 1.76 (p, *J* = 7.6 Hz, 2H), 1.48 (s, 9H), 1.38 – 1.23 (m, 18H), 0.87 (t, *J* = 6.9

Hz, 3H). ^{13}C NMR (126 MHz, $CDCl_3$) δ 170.8, 168.3, 154.8, 154.5, 80.8, 46.8, 42.8, 32.1, 29.8, 29.8, 29.7, 29.6, 29.5, 29.3, 29.2, 28.5, 27.0, 26.1, 22.8, 14.3. HRMS: (ESI) $[M+H]^+$ calc. for $C_{24}H_{43}N_4O_4^+$, 451.3279, observed, 451.3264.

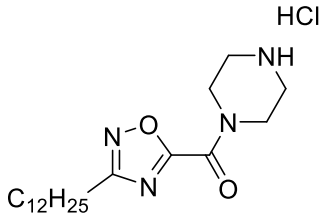

(3-dodecyl-1,2,4-oxadiazol-5-yl)(piperazin-1-yl)methanone hydrochloride (3.13): Synthesized according to General Procedure 4.4. Purified *via* trituration with diethyl ether. White solid (87%, 46 mg). ^{1}H NMR (600 MHz, MeOD) δ 4.29 – 4.23 (m, 2H), 4.07 – 4.02 (m, 2H), 3.41 – 3.35 (m, 4H), 4.1 Hz, 4H), 2.82 (t, *J* = 7.5 Hz, 2H), 1.77 (p, *J* = 7.5 Hz, 2H), 1.42 – 1.26 (m, 18H), 0.90 (t, *J* = 7.0 Hz, 3H). ^{13}C NMR (151 MHz, MeOD) δ 170.7, 167.6, 154.3, 43.4, 43.1, 42.7, 39.1, 31.7, 29.4, 29.4, 29.3, 29.2, 29.1, 28.9, 28.7, 26.5, 25.3, 22.4, 13.1. HRMS: (ESI) $[M+H]^+$ calc. for $C_{19}H_{35}N_4O_2^+$, 351.2755, observed, 351.2750.

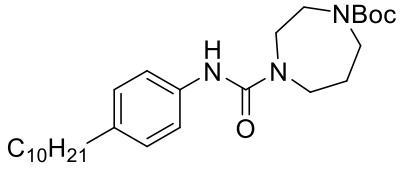

tert-butyl 4-((4-decylphenyl)carbamoyl)-1,4-diazepane-1-carboxylate (3.15a): Synthesized according to General Procedure 4.7. Purified via column chromatography (50% ethyl acetate/hexanes). Brown oil (15%, 30 mg). ^{1}H NMR (500 MHz, $CDCl_3$) δ 7.25 (d, *J* = 7.7 Hz, 2H), 7.13 – 7.04 (m, 2H), 6.41 – 6.24 (m, 1H), 3.62 – 3.45 (m, 6H), 3.40 (t, *J* = 6.2 Hz, 1H), 2.54 (t, *J* = 7.7 Hz, 2H), 2.02 – 1.93 (m, 1H), 1.94 – 1.82 (m, 2H), 1.76 – 1.64 (m, 1H), 1.49 – 1.40 (m, 9H), 1.33 – 1.20 (m, 15H), 0.88 (t, *J* = 6.8 Hz, 3H). ^{13}C NMR (126 MHz, $CDCl_3$) δ 155.5, 155.0*, 155.0, 154.9*, 138.0, 137.7, 136.5*, 136.4*, 128.8, 128.7, 120.2, 120.1, 80.0, 48.8, 48.3, 47.9,

47.1, 46.1, 46.0, 45.9, 35.3, 31.9, 31.6, 29.6, 29.6, 29.5, 29.3, 29.3, 28.4, 22.7, 14.1. Material isolated as an approximately 1:1 ratio of rotamers. HRMS: (ESI) $[M+H]^+$ calc. for $C_{27}H_{46}N_3O_3^+$ 460.3534, observed, 460.3521.

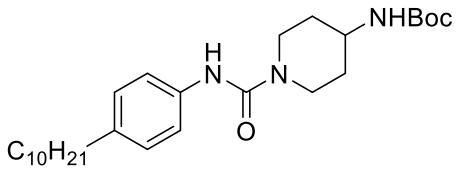

tert-butyl (1-((4-decylphenyl)carbamoyl)piperidin-4-yl)carbamate (3.15b): Synthesized according to General Procedure 4.7. Purified via column chromatography (30-50% ethyl acetate/hexanes). Clear oil (26%, 56 mg). ^{1}H NMR (500 MHz, $CDCl_3$) δ 7.22 (d, *J* = 8.0 Hz, 2H), 7.07 (d, *J* = 8.1 Hz, 2H), 6.44 (s, 1H), 4.50 (s, 1H), 3.98 (d, *J* = 13.5 Hz, 2H), 3.63 (s, 1H), 2.96 (t, *J* = 12.6 Hz, 2H), 2.53 (t, *J* = 7.8 Hz, 2H), 1.97 (d, *J* = 12.5 Hz, 2H), 1.60 – 1.53 (m, 2H), 1.45 (s, 8H), 1.32 – 1.18 (m, 15H), 0.87 (t, *J* = 6.8 Hz, 3H). ^{13}C NMR (126 MHz, $CDCl_3$) δ 155.2, 138.0, 136.7, 128.9, 120.3, 79.7, 47.9, 43.4, 35.4, 32.4, 32.0, 31.7, 29.7, 29.6, 29.5, 29.4, 28.5, 22.8, 14.2. HRMS: (ESI) $[M+H]^+$ calc. for $C_{27}H_{46}N_3O_3^+$, 460.3534, observed, 460.3530.

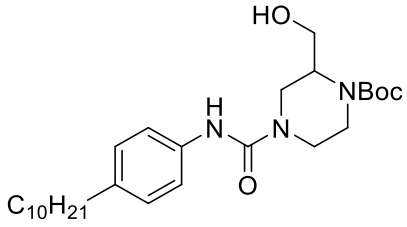

tert-butyl 4-((4-decylphenyl)carbamoyl)-2-(hydroxymethyl)piperazine-1-carboxylate (3.15c): Synthesized according to General Procedure 4.7. Purified via column chromatography (50-70% ethyl acetate/hexanes). Yellow oil (35%, 72 mg). ^{1}H NMR (500 MHz, $CDCl_3$) δ 7.23 – 7.19 (m, 2H), 7.10 – 7.04 (m, 2H), 4.29 – 3.71 (m, 5H), 3.68 – 3.52 (m, 2H), 3.15 – 2.86 (m, 3H), 2.52 (t, *J* = 7.7 Hz, 2H), 1.59 – 1.52 (m, 2H), 1.46 (s, 9H), 1.31 – 1.23 (m, 14H), 0.87 (t, *J* = 6.9 Hz, 3H). ^{13}C NMR (126 MHz, $CDCl_3$) δ 155.9, 155.0, 154.0, 137.9, 136.5, 128.8, 120.1, 80.7,

57.8, 51.5, 43.5, 39.0, 35.3, 31.9, 31.6, 29.6, 29.5, 29.3, 29.3, 28.4, 28.3, 22.7, 14.1. HRMS: (ESI) $[M+H]^+$ calc. for $C_{27}H_{46}N_3O_4^+$, 476.3483, observed, 476.3104.

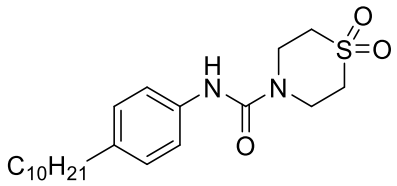

N-(4-decylphenyl)thiomorpholine-4-carboxamide 1,1-dioxide (3.15d): Synthesized according to General Procedure 4.7. Purified via column chromatography (35-55% ethyl acetate/hexanes). White solid (69%, 215 mg). ^{1}H NMR (500 MHz, $CDCl_3$) δ 7.23 – 7.17 (m, 2H), 7.15 – 7.08 (m, 2H), 6.76 (s, 1H), 3.95 – 3.87 (m, 4H), 3.06 – 2.98 (m, 4H), 2.56 (t, *J* = 7.7 Hz, 2H), 1.57 (p, *J* = 7.1 Hz, 2H), 1.27 (d, *J* = 16.6 Hz, 14H), 0.88 (t, *J* = 6.8 Hz, 3H). ^{13}C NMR (126 MHz, $CDCl_3$) δ 154.8, 139.3, 135.6, 129.1, 121.1, 51.9, 43.4, 35.4, 32.0, 31.7, 29.7, 29.7, 29.6, 29.5, 29.4, 22.8, 14.3. HRMS: (ESI) $[M+H]^+$ calc. for $C_{21}H_{35}N_2O_3S^+$ 395.2363, observed, 395.2369.

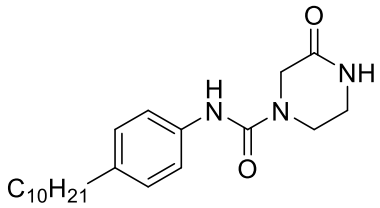

N-(4-decylphenyl)-3-oxopiperazine-1-carboxamide (3.15e): Synthesized according to General Procedure 4.7. Purified via column chromatography (40-80% ethyl acetate/hexanes). White solid (88%, 136 mg). ^{1}H NMR (400 MHz, DMSO) δ 8.46 (s, 1H), 8.07 (s, 1H), 7.35 (d, *J* = 8.0 Hz, 2H), 7.03 (d, *J* = 8.1 Hz, 2H), 4.00 (s, 2H), 3.63 – 3.56 (m, 2H), 3.24 – 3.18 (m, 2H), 2.49 – 2.45 (m, 2H), 1.55 – 1.47 (m, 2H), 1.29 – 1.19 (m, 14H), 0.89 – 0.81 (m, 3H). ^{13}C NMR (151 MHz, DMSO) δ 167.1, 155.0, 138.2, 136.4, 128.5, 120.4, 48.1, 40.8, 40.5, 35.0, 31.8, 31.6, 29.5, 29.5, 29.4, 29.2, 29.1, 22.6, 14.4. HRMS: (ESI) $[M+H]^+$ calc. for $C_{21}H_{34}N_3O_2^+$ 360.2646, observed, 360.2651.

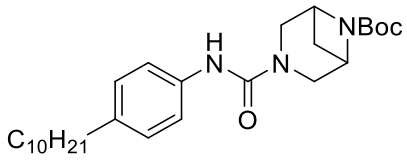

N-(4-decylphenyl)-3,6-diazabicyclo[3.1.1]heptane-3-carboxamide hydrochloride (3.15f): Synthesized according to General Procedure 4.7. Purified via column chromatography (30-50% ethyl acetate/hexanes). Clear oil (34%, 125 mg). ^{1}H NMR (500 MHz, $CDCl_3$) δ 7.31 – 7.27 (m, 2H), 7.08 – 7.04 (m, 2H), 6.61 (s, 1H), 4.18 – 3.90 (m, 4H), 3.41 (s, 2H), 2.58 – 2.47 (m, 3H), 1.58 – 1.52 (m, 2H), 1.41 (s, 8H), 1.36 (d, *J* = 8.8 Hz, 1H), 1.32 – 1.20 (m, 15H), 0.88 – 0.84 (m, 3H). ^{13}C NMR (126 MHz, $CDCl_3$) δ 156.5, 155.8, 137.8, 136.5, 128.7, 120.3, 80.7, 58.5, 57.4, 45.0, 44.3, 35.3, 31.9, 31.6, 29.6, 29.6, 29.4, 29.3, 28.5, 28.3, 22.7, 14.2. HRMS: (ESI) $[M+H]^+$ calc. for $C_{27}H_{44}N_3O_3^+$, 458.3377, observed, 458.3367.

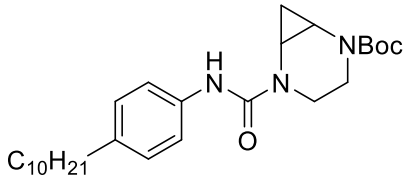

tert-butyl 5-((4-decylphenyl)carbamoyl)-2,5-diazabicyclo[4.1.0]heptane-2-carboxylate (3.15g): Synthesized according to General Procedure 4.7. Purified via column chromatography (30-50% ethyl acetate/hexanes). Clear oil (52%, 112 mg). ^{1}H NMR (500 MHz, $CDCl_3$) δ 7.34 – 7.30 (m, 2H), 7.12 – 7.08 (m, 2H), 6.93 – 6.84 (m, 1H), 4.15 – 4.03 (m, 1H), 3.45 (q, *J* = 9.1 Hz, 1H), 3.33 – 3.12 (m, 2H), 3.07 – 2.84 (m, 2H), 2.59 – 2.51 (m, 2H), 1.61 – 1.55 (m, 2H), 1.49 (s, 9H), 1.31 – 1.23 (m, 14H), 0.87 (t, *J* = 6.9 Hz, 3H), 0.69 – 0.62 (m, 1H). ^{13}C NMR (126 MHz, $CDCl_3$) δ 156.0, 155.1, 138.0, 136.2, 128.8, 119.9, 80.6, 80.3, 42.9, 41.7, 39.8, 39.5, 35.3, 31.9, 31.6, 29.6, 29.6, 29.5, 29.3, 29.3, 28.4, 27.4, 22.7, 14.8, 14.6, 14.1. HRMS: (ESI) $[M+H]^+$ calc. for $C_{27}H_{44}N_3O_3^+$ 458.3377, observed, 458.3364.

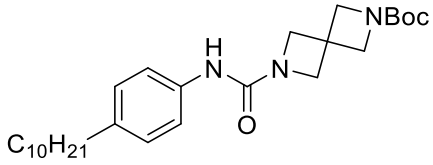

tert-butyl 6-((4-decylphenyl)carbamoyl)-2,6-diazaspiro[3.3]heptane-2-carboxylate (3.15h): Synthesized according to General Procedure 4.7. Purified via column chromatography (30-50% ethyl acetate/hexanes). White solid (27%, 59 mg). ^{1}H NMR (500 MHz, $CDCl_3$) δ 7.29 – 7.23 (m, 2H), 7.09 – 7.05 (m, 2H), 6.38 (s, 1H), 4.04 (d, *J* = 33.4 Hz, 8H), 2.53 (t, *J* = 7.7 Hz, 2H), 1.60 – 1.52 (m, 2H), 1.44 (s, 9H), 1.33 – 1.22 (m, 14H), 0.88 (t, *J* = 6.8 Hz, 3H). ^{13}C NMR (126 MHz, $CDCl_3$) δ 156.7, 156.0, 138.1, 136.0, 128.8, 120.0, 80.0, 59.6, 35.4, 32.1, 32.0, 31.7, 29.7, 29.6, 29.4, 29.4, 28.4, 22.8, 14.2. HRMS: (ESI) $[M+H]^+$ calc. for $C_{27}H_{44}N_3O_3^+$, 458.3377, observed, 458.3373.

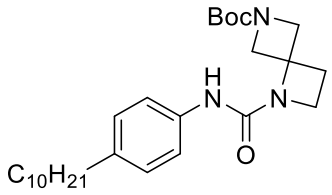

tert-butyl 1-((4-decylphenyl)carbamoyl)-1,6-diazaspiro[3.3]heptane-6-carboxylate (3.15i): Synthesized according to General Procedure 4.7. Purified via column chromatography (30-50% ethyl acetate/hexanes). Clear oil (22%, 53 mg). ^{1}H NMR (500 MHz, $CDCl_3$) δ 7.32 – 7.27 (m, 2H), 7.10 – 7.06 (m, 2H), 4.56 (d, *J* = 9.5 Hz, 2H), 3.99 (d, *J* = 9.6 Hz, 2H), 3.89 (t, *J* = 7.2 Hz, 2H), 2.55 – 2.51 (m, 2H), 2.41 (t, *J* = 7.2 Hz, 2H), 1.59 – 1.52 (m, 2H), 1.31 – 1.22 (m, 15H), 0.87 (t, *J* = 6.9 Hz, 3H). ^{13}C NMR (126 MHz, $CDCl_3$) δ 156.5, 154.2, 137.9, 136.0, 128.9, 119.6, 80.1, 63.1, 60.5, 45.2, 35.4, 32.0, 31.7, 29.7, 29.7, 29.6, 29.4, 29.3, 28.4, 28.0, 22.8, 14.2. HRMS: (ESI) $[M+H]^+$ calc. for $C_{27}H_{44}N_3O_3^+$, 458.3377, observed, 458.3383.

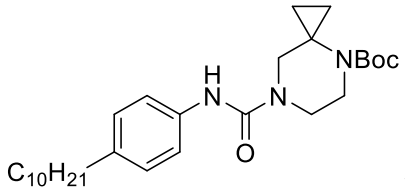

tert-butyl 7-((4-decylphenyl)carbamoyl)-4,7-diazaspiro[2.5]octane-4-carboxylate (3.15j): Synthesized following General Procedure 4.7. Purified via column chromatography (35-55% ethyl acetate/hexanes). Clear oil (24%, 48 mg) ^{1}H NMR (500 MHz, $CDCl_3$) δ 7.21 (d, *J* = 8.2 Hz, 2H), 7.07 (d, *J* = 8.1 Hz, 2H), 6.42 (s, +1H), 3.60 – 3.55 (m, 2H), 3.48 – 3.43 (m, 2H), 2.53 (t, *J* = 7.7 Hz, 2H), 1.60 – 1.53 (m, 2H), 1.47 (s, 9H), 1.30 – 1.22 (m, 14H), 1.02 – 0.97 (m, 2H), 0.88 (t, *J* = 6.8 Hz, 3H), 0.85 – 0.82 (m, 2H). ^{13}C NMR (126 MHz, $CDCl_3$) δ 155.6, 155.5, 138.0, 136.4, 128.7, 120.3, 80.3, 50.3, 45.7, 43.4, 37.9, 35.3, 31.9, 31.6, 29.6, 29.6, 29.5, 29.3, 29.3, 28.4, 22.7, 14.1, 13.8. HRMS: (ESI) $[M+H]^+$ calc. for $C_{28}H_{46}N_3O_3^+$ 472.3534, observed, 472.3521.

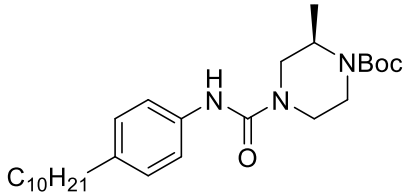

tert-butyl (R)-4-((4-decylphenyl)carbamoyl)-2-methylpiperazine-1-carboxylate (3.15k): Synthesized according to General Procedure 4.7. Purified via column chromatography (20-50% ethyl acetate/hexanes). Clear oil (54%, 56mg). ^{1}H NMR (400 MHz, $cdcl_3$) δ 7.26 – 7.22 (m, 2H), 7.11 – 7.07 (m, 2H), 6.36 (s, 1H), 4.26 (s, 1H), 3.88 (t, *J* = 13.3 Hz, 2H), 3.74 – 3.67 (m, 1H), 3.31 – 3.23 (m, 1H), 3.23 – 3.14 (m, 1H), 3.09 – 2.99 (m, 1H), 2.58 – 2.50 (m, 2H), 1.60 – 1.52 (m, 2H), 1.48 (s, 9H), 1.33 – 1.22 (m, 15H), 1.20 (d, *J* = 6.7 Hz, 3H), 0.90 – 0.84 (m, 3H). ^{13}C NMR (126 MHz, $CDCl_3$) δ 155.5, 154.6, 138.1, 136.3, 128.8, 120.3, 80.1, 47.6, 43.9, 38.3, 35.3, 31.9, 31.6, 29.6, 29.6, 29.6, 29.5, 29.3, 29.3, 28.4, 22.7, 15.9, 14.1. HRMS: (ESI) $[M+H]^+$ calc. for $C_{27}H_{46}N_3O_3^+$ 460.3534, observed, 460.3538

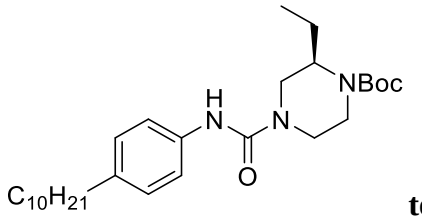

tert-butyl (R)-4-((4-decylphenyl)carbamoyl)-2-ethylpiperazine-1-carboxylate (3.15l): Synthesized according to General Procedure 4.7. Purified via column chromatography (30-50% ethyl acetate/hexanes). Clear oil (54%, 175 mg). ^{1}H NMR (500 MHz, $CDCl_3$) δ 7.23 – 7.18 (m, 2H), 7.02 (d, *J* = 8.2 Hz, 2H), 6.96 (s, 1H), 4.02 – 3.74 (m, 4H), 3.04 – 2.90 (m, 2H), 2.85 (t, *J* = 12.2 Hz, 1H), 2.50 (t, *J* = 7.7 Hz, 2H), 1.64 – 1.51 (m, 3H), 1.44 (s, 9H), 1.30 – 1.21 (m, 14H), 0.85 (dt, *J* = 10.1, 7.0 Hz, 6H). ^{13}C NMR (126 MHz, $CDCl_3$) δ 155.8, 154.9, 137.8, 136.6, 128.6, 120.6, 80.0, 70.6, 65.8, 60.4, 45.9, 43.8, 35.3, 31.9, 31.6, 29.6, 29.5, 29.3, 29.3, 28.4, 22.7, 22.5, 14.1, 10.5. HRMS: (ESI) $[M+H]^+$ calc. for $C_{28}H_{48}N_3O_3^+$, 474.3690, observed, 474.3682.

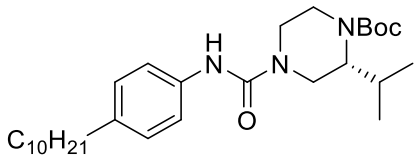

tert-butyl (R)-4-((4-decylphenyl)carbamoyl)-2-isopropylpiperazine-1-carboxylate (3.15m): Synthesized according to General Procedure 4.7. Purified via column chromatography (30-50% ethyl acetate/hexanes). Clear oil (76%, 176 mg). ^{1}H NMR (500 MHz, $CDCl_3$) δ 7.24 – 7.20 (m, 2H), 7.10 – 7.06 (m, 2H), 6.33 (s, 1H), 4.17 – 4.03 (m, 2H), 3.99 – 3.74 (m, 2H), 3.07 – 2.92 (m, 3H), 2.57 – 2.50 (m, 2H), 1.59 – 1.53 (m, 2H), 1.47 (s, 9H), 1.31 – 1.24 (m, 14H), 1.02 (d, *J* = 6.6 Hz, 3H), 0.90 – 0.85 (m, 6H). ^{13}C NMR (126 MHz, $CDCl_3$) δ 155.4, 155.0, 138.2, 136.4, 128.9, 120.4, 80.2, 71.0, 35.4, 32.2, 32.0, 31.7, 29.8, 29.7, 29.6, 29.5, 29.4, 28.5, 26.3, 22.8, 22.1, 20.4, 14.3. HRMS: (ESI) $[M+H]^+$ calc. for $C_{29}H_{50}N_3O_3^+$, 488.3847, observed, 488.3843.

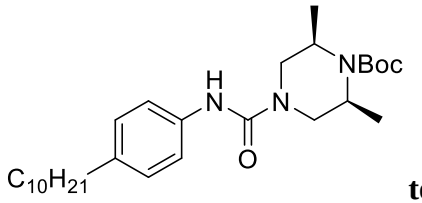

tert-butyl (2R,6S)-4-((4-decylphenyl)carbamoyl)-2,6-dimethylpiperazine-1-carboxylate (3.15n): Synthesized according to General Procedure 4.7. Purified via column chromatography (30-50% ethyl acetate/hexanes). White solid (40%, 91 mg). ^{1}H NMR (400 MHz, cdcl$_3$) δ 7.26 (d, *J* = 7.7 Hz, 2H), 7.10 (d, *J* = 8.0 Hz, 2H), 6.40 (s, 1H), 4.22 (q, *J* = 6.7 Hz, 2H), 3.84 (d, *J* = 13.1 Hz, 2H), 3.15 (dd, *J* = 13.2, 4.6 Hz, 2H), 2.54 (t, *J* = 7.7 Hz, 2H), 1.57 (t, *J* = 7.4 Hz, 2H), 1.48 (s, 10H), 1.34 – 1.20 (m, 20H), 0.88 (t, *J* = 6.7 Hz, 3H). HRMS: (ESI) [M+H]$^+$ calc. for $C_{28}H_{48}N_3O_3^+$, 474.3690, observed, 474.3692.

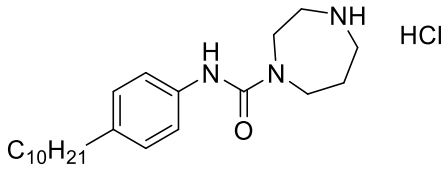

N-(4-decylphenyl)-1,4-diazepane-1-carboxamide hydrochloride (3.16a): Synthesized according to General Procedure 4.4. Purified *via* trituration with diethyl ether. Light brown solid (74%, 19 mg). ^{1}H NMR (600 MHz, MeOD) δ 7.31 – 7.25 (m, 2H), 7.12 – 7.09 (m, 2H), 3.86 – 3.81 (m, 2H), 3.69 (t, *J* = 6.1 Hz, 2H), 3.37 – 3.33 (m, 4H), 2.59 – 2.54 (m, 2H), 2.17 (p, *J* = 6.0 Hz, 2H), 1.63 – 1.55 (m, 2H), 1.34 – 1.26 (m, 14H), 0.93 – 0.87 (m, 3H). ^{13}C NMR (151 MHz, MeOD) δ 156.6, 138.1, 136.6, 128.1, 121.7, 46.6, 45.3, 44.8, 42.1, 34.9, 31.7, 31.4, 29.4, 29.3, 29.2, 29.1, 28.9, 25.6, 22.3, 13.1. HRMS: (ESI) [M+H]$^+$ calc. for $C_{22}H_{38}N_3O^+$ 360.3009, observed, 360.3018.

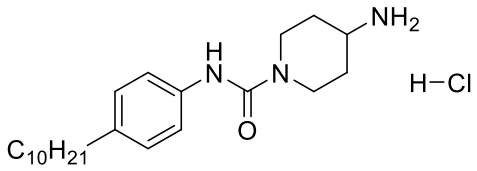

4-amino-N-(4-decylphenyl)piperidine-1-carboxamide hydrochloride (3.16b): Synthesized according to General Procedure 4.4. Purified *via* trituration with diethyl ether. Brown solid (70%, 17 mg). ^{1}H NMR (500 MHz, MeOD) δ 7.26 – 7.21 (m, 2H), 7.11 – 7.06 (m, 2H), 4.26 (dp, *J* = 14.2, 2.3 Hz, 2H), 3.37 (td, *J* = 11.5, 5.6 Hz, 1H), 2.98 (ddd, *J* = 14.3, 12.1, 2.4 Hz, 2H), 2.56 (t, *J* = 7.6 Hz, 2H), 2.08 – 2.02 (m, 2H), 1.63 – 1.52 (m, 4H), 1.37 – 1.27 (m, 14H), 0.90 (t, *J* = 6.9 Hz, 3H). ^{13}C NMR (126 MHz, MeOD) δ 157.9, 139.2, 138.2, 129.5, 122.5, 49.8, 43.6, 36.3, 33.1, 32.8, 31.1, 30.8, 30.7, 30.6, 30.5, 30.3, 23.7, 14.4. HRMS: (ESI) $[M+H]^+$ calc. for $C_{22}H_{38}N_3O^+$, 360.3009, observed, 360.3015.

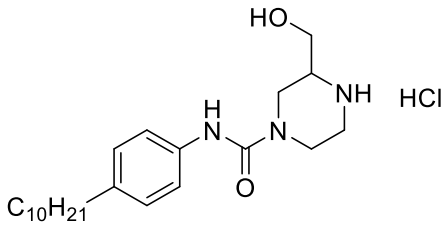

N-(4-decylphenyl)-3-(hydroxymethyl)piperazine-1-carboxamide hydrochloride (3.16c): Synthesized according to General Procedure 4.4. Purified *via* trituration with diethyl ether. White solid (88%, 16 mg). ^{1}H NMR (500 MHz, MeOD) δ 7.28 – 7.23 (m, 2H), 7.13 – 7.08 (m, 2H), 4.25 (dtd, *J* = 14.5, 3.7, 1.9 Hz, 2H), 3.84 (dd, *J* = 11.9, 4.0 Hz, 1H), 3.70 (dd, *J* = 11.9, 6.1 Hz, 1H), 3.41 (dt, *J* = 12.7, 2.8 Hz, 1H), 3.38 – 3.35 (m, 1H), 3.30 – 3.26 (m, 1H), 3.23 – 3.15 (m, 2H), 2.58 – 2.52 (m, 2H), 1.59 (q, *J* = 7.3 Hz, 2H), 1.30 (d, *J* = 16.4 Hz, 14H), 0.90 (t, *J* = 7.0 Hz, 3H). ^{13}C NMR (126 MHz, MeOD) δ 157.6, 139.5, 137.9, 129.6, 122.4, 60.3, 57.6, 44.5, 44.1, 42.2, 36.3, 33.1, 32.8, 30.7, 30.7, 30.6, 30.5, 30.3, 23.7, 14.4. HRMS: (ESI) $[M+H]^+$ calc. for $C_{22}H_{38}N_3O_2^+$, 376.2959, observed, 376.2948.

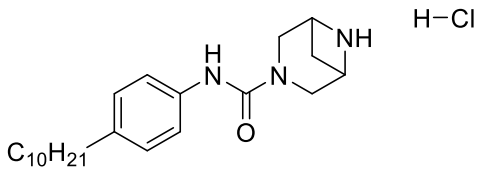

N-(4-decylphenyl)-3,6-diazabicyclo[3.1.1]heptane-3-carboxamide hydrochloride (3.16f): Synthesized according to General Procedure 4.4. Purified *via* trituration with diethyl ether. Light brown solid (50%, 54 mg). ^{1}H NMR (500 MHz, MeOD) δ 7.35 – 7.31 (m, 2H), 7.14 – 7.10 (m, 2H), 4.48 (d, *J* = 6.5 Hz, 2H), 4.07 – 3.98 (m, 4H), 3.04 (dt, *J* = 10.6, 6.5 Hz, 1H), 2.62 – 2.53 (m, 2H), 1.93 (d, *J* = 10.6 Hz, 1H), 1.65 – 1.55 (m, 2H), 1.34 – 1.27 (m, 14H), 0.90 (t, *J* = 6.9 Hz, 3H). ^{13}C NMR (126 MHz, MeOD) δ 156.8, 138.3, 136.4, 128.2, 121.7, 58.3, 45.8, 34.9, 31.7, 31.4, 29.4, 29.3, 29.2, 29.1, 28.9, 28.3, 22.4, 13.1. HRMS: (ESI) $[M+H]^+$ calc. for $C_{22}H_{36}N_3O^+$, 358.2853, observed, 358.2850.

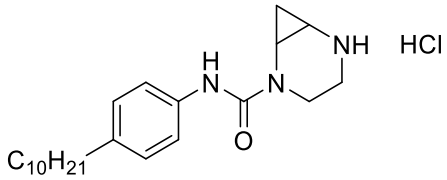

N-(4-decylphenyl)-2,5-diazabicyclo[4.1.0]heptane-2-carboxamide hydrochloride (3.16g): Synthesized according to General Procedure 4.4. Purified *via* trituration with diethyl ether. White solid (77%, 20 mg). ^{1}H NMR (600 MHz, MeOD) δ 7.38 – 7.32 (m, 2H), 7.16 – 7.12 (m, 2H), 4.19 – 4.13 (m, 1H), 3.42 – 3.38 (m, 1H), 3.28 – 3.24 (m, 2H), 3.13 – 3.05 (m, 2H), 2.59 (t, *J* = 7.6 Hz, 2H), 1.61 (h, *J* = 6.9 Hz, 2H), 1.47 (q, *J* = 7.5 Hz, 1H), 1.36 – 1.25 (m, 16H), 0.95 – 0.89 (m, 3H). ^{13}C NMR (151 MHz, MeOD) δ 156.5, 138.4, 136.2, 128.2, 121.8, 40.8, 36.0, 34.9, 31.7, 31.4, 29.4, 29.3, 29.2, 29.1, 28.9, 28.6, 25.9, 22.3, 13.1, 10.5. HRMS: (ESI) $[M+H]^+$ calc. for $C_{22}H_{36}N_3O^+$ 358.2853, observed, 358.2846.

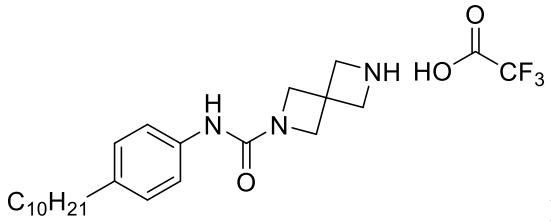

N-(4-decylphenyl)-2,6-diazaspiro[3.3]heptane-2-carboxamide 2,2,2-trifluoroacetate (3.16h): Synthesized according to General Procedure 4.8. Purified *via* trituration with diethyl ether. White solid (97%, 25 mg). ^{1}H NMR (500 MHz, MeOD) δ 7.28 (d, *J* = 8.1 Hz, 2H), 7.07 (d, *J* = 8.2 Hz, 2H), 4.24 (d, *J* = 17.3 Hz, 8H), 2.54 (t, *J* = 7.6 Hz, 2H), 1.62 – 1.53 (m, 2H), 1.29 (d, *J* = 13.6 Hz, 15H), 0.89 (t, *J* = 6.8 Hz, 3H). ^{13}C NMR (126 MHz, MeOD) δ 159.3, 139.0, 137.8, 129.6, 121.6, 60.1, 56.6, 36.6, 36.3, 33.1, 32.8, 30.7, 30.7, 30.6, 30.5, 30.3, 23.7, 14.4. HRMS: (ESI) $[M+H]^+$ calc. for $C_{22}H_{36}N_3O^+$, 358.2853, observed, 358.2864.

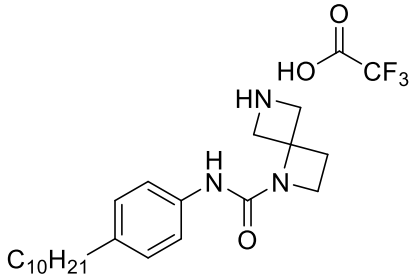

N-(4-decylphenyl)-1,6-diazaspiro[3.3]heptane-1-carboxamide 2,2,2-trifluoroacetate (3.16i): Synthesized according to General Procedure 4.8. Purified *via* trituration with diethyl ether. Yellow oil (97%, 25 mg). ^{1}H NMR (400 MHz, cd$_3$od) δ 7.37 – 7.32 (m, 2H), 7.13 – 7.08 (m, 2H), 4.71 (d, *J* = 12.6 Hz, 2H), 4.29 – 4.19 (m, 2H), 3.99 (t, *J* = 7.2 Hz, 2H), 2.60 – 2.50 (m, 4H), 1.65 – 1.54 (m, 2H), 1.36 – 1.27 (m, 14H), 0.94 – 0.86 (m, 3H). ^{13}C NMR (126 MHz, MeOD) δ 157.4, 139.3, 137.4, 129.6, 122.0, 66.4, 58.2, 47.5, 36.3, 33.1, 32.8, 30.7, 30.7, 30.6, 30.5, 30.3, 28.0, 23.7, 14.4. HRMS: (ESI) $[M+H]^+$ calc. for $C_{22}H_{36}N_3O^+$, 358.2853, observed, 358.2874.

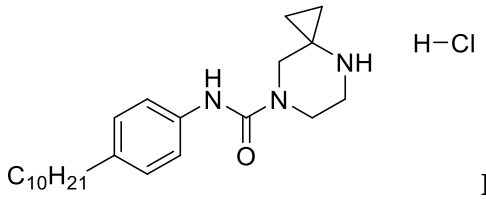

N-(4-decylphenyl)-4,7-diazaspiro[2.5]octane-7-carboxamide hydrochloride (3.16j): Synthesized according to General Procedure 4.4. Purified *via* trituration with diethyl ether. White solid (83%, 33 mg). ^{1}H NMR (500 MHz, MeOD) δ 7.28 – 7.23 (m, 2H), 7.12 – 7.08 (m, 2H), 3.87 (t, *J* = 5.2 Hz, 2H), 3.70 (s, 2H), 3.39 (t, *J* = 5.3 Hz, 2H), 2.56 (t, *J* = 7.6 Hz, 2H), 1.63 – 1.54 (m, 2H), 1.34 – 1.26 (m, 14H), 1.15 – 1.10 (m, 2H), 1.10 – 1.05 (m, 2H), 0.92 – 0.87 (m, 3H). ^{13}C NMR (126 MHz, MeOD) δ 157.7, 139.5, 137.9, 129.6, 122.5, 68.1, 44.8, 42.3, 39.2, 36.3, 33.1, 32.8, 30.7, 30.7, 30.6, 30.5, 30.3, 23.7, 14.4, 10.2. HRMS: (ESI) $[M+H]^+$ calc. for $C_{23}H_{38}N_3O^+$ 372.3009, observed, 372.3013.

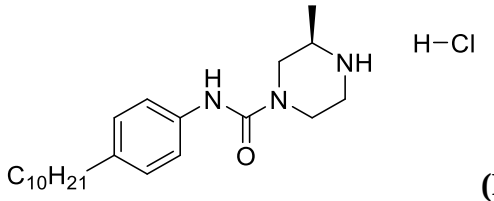

(R)-N-(4-decylphenyl)-3-methylpiperazine-1-carboxamide hydrochloride (3.16k): Synthesized according to General Procedure 4.4. Purified *via* trituration with diethyl ether. Light brown solid (84%, 36 mg). ^{1}H NMR (400 MHz, cd_3od) δ 7.28 – 7.24 (m, 2H), 7.12 – 7.08 (m, 2H), 4.30 – 4.23 (m, 2H), 3.46 – 3.40 (m, 1H), 3.40 – 3.34 (m, 1H), 3.29 – 3.23 (m, 1H), 3.20 – 3.11 (m, 1H), 3.04 (dd, *J* = 14.5, 10.6 Hz, 1H), 2.60 – 2.52 (m, 2H), 1.63 – 1.54 (m, 2H), 1.37 (d, *J* = 6.6 Hz, 3H), 1.34 – 1.26 (m, 14H), 0.94 – 0.85 (m, 3H). ^{13}C NMR (151 MHz, MeOD) δ 157.4, 139.4, 137.9, 129.6, 122.4, 52.5, 48.4, 44.3, 41.9, 36.3, 33.1, 32.8, 30.7, 30.7, 30.6, 30.4, 30.3, 23.7, 16.0, 14.4. HRMS: (ESI) $[M+H]^+$ calc. for $C_{22}H_{38}N_3O^+$ 360.3009, observed, 360.3006.

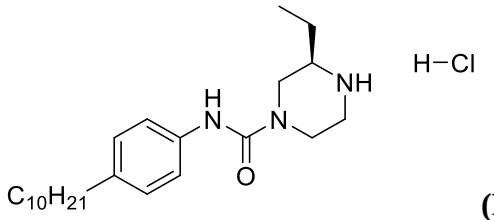

(R)-N-(4-decylphenyl)-3-ethylpiperazine-1-carboxamide hydrochloride (3.16l): Synthesized according to General Procedure 4.4. Purified *via* trituration with diethyl ether. Light brown solid (78%, 118 mg). ^{1}H NMR (500 MHz, MeOD) δ 7.31 – 7.27 (m, 2H), 7.11 – 7.08 (m, 2H), 4.37 – 4.31 (m, 1H), 4.29 – 4.23 (m, 1H), 3.43 – 3.36 (m, 1H), 3.36 – 3.28 (m, 1H), 3.21 – 3.10 (m, 2H), 3.10 – 3.01 (m, 1H), 2.58 – 2.51 (m, 2H), 1.80 – 1.67 (m, *J* = 7.2, 6.8 Hz, 2H), 1.62 – 1.54 (m, 2H), 1.36 – 1.21 (m, 15H), 1.08 (t, *J* = 7.5 Hz, 3H), 0.90 (t, *J* = 6.9 Hz, 3H). ^{13}C NMR (126 MHz, MeOD) δ 157.5, 139.3, 138.0, 129.6, 122.5, 57.7, 46.7, 44.4, 42.1, 36.3, 33.1, 32.8, 30.7, 30.7, 30.6, 30.5, 30.3, 24.7, 23.7, 14.5, 9.9. HRMS: (ESI) $[M+H]^+$ calc. for $C_{23}H_{40}N_3O^+$ 374.3166, observed, 374.3163.

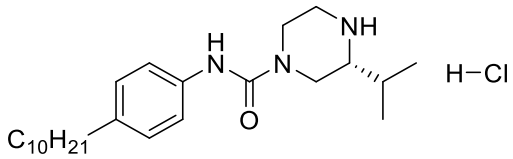

(R)-N-(4-decylphenyl)-3-isopropylpiperazine-1-carboxamide hydrochloride (3.16m): Synthesized according to General Procedure 4.4. Purified *via* trituration with diethyl ether. White solid (55%, 71 mg). ^{1}H NMR (500 MHz, MeOD) δ 7.29 – 7.24 (m, 2H), 7.12 – 7.07 (m, 2H), 4.43 – 4.38 (m, 1H), 4.29 (ddt, *J* = 14.2, 3.8, 2.1 Hz, 1H), 3.43 (dt, *J* = 12.5, 2.5 Hz, 1H), 3.27 (dt, *J* = 12.0, 2.7 Hz, 1H), 3.22 – 3.14 (m, 1H), 3.09 – 3.00 (m, 2H), 2.56 (t, *J* = 7.6 Hz, 2H), 1.98 (h, *J* = 6.8 Hz, 1H), 1.59 (q, *J* = 7.2 Hz, 2H), 1.34 – 1.25 (m, 14H), 1.12 (dd, *J* = 9.8, 6.9 Hz, 6H), 0.90 (t, *J* = 7.0 Hz, 3H). ^{13}C NMR (126 MHz, MeOD) δ 157.6, 139.5, 137.9, 129.6, 122.5, 61.8, 45.4, 45.0, 42.2, 36.3, 33.1, 32.8,

30.7, 30.7, 30.6, 30.5, 30.5, 30.3, 23.7, 18.9, 18.6, 14.5. HRMS: (ESI) $[M+H]^+$ calc. for $C_{24}H_{42}N_3O^+$ 388.3322, observed, 388.3323.

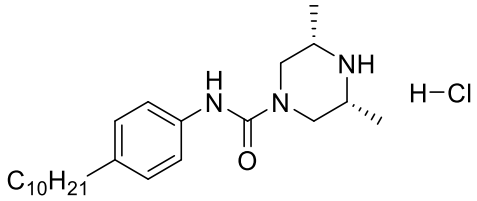

(3R,5S)-N-(4-decylphenyl)-3,5-dimethylpiperazine-1-carboxamide hydrochloride (3.16n): Synthesized according to General Procedure 4.4. Purified *via* trituration with diethyl ether. White solid (75%, 43 mg). ^{1}H NMR (500 MHz, MeOD) δ 7.31 – 7.23 (m, 2H), 7.12 – 7.06 (m, 2H), 4.38 – 4.31 (m, 2H), 3.42 – 3.33 (m, 2H), 2.97 – 2.88 (m, 2H), 2.55 (t, *J* = 7.6 Hz, 2H), 1.62 – 1.52 (m, 2H), 1.41 – 1.23 (m, 23H), 0.94 – 0.86 (m, 3H). ^{13}C NMR (126 MHz, MeOD) δ 157.2, 139.4, 138.0, 129.6, 122.4, 53.2, 48.0, 36.3, 33.1, 32.8, 30.7, 30.7, 30.6, 30.4, 30.3, 23.7, 16.0, 16.0, 14.5. HRMS: (ESI) $[M+H]^+$ calc. for $C_{22}H_{38}N_3O^+$ 360.3009, observed, 360.3015.

5.4 Procedures and Characterization For Chapter 4

General Procedure 4.1: Boc Protection: To a solution of 4-bromo-1,2-phenyldiamine (1.0 equiv.) in a round bottom flask was added DCM (0.2 M), di-tert-butyl dicarbonate (4.0 equiv.), and 2.5 M $NaOH_{(aq)}$ (5.0 equiv.). It was allowed to stir for 16 hours at room temperature. Once complete, it was diluted with ethyl acetate and washed with aqueous $NaHCO_3$ three times. The organic layer was then dried down and hexanes was added. The resulting precipitate and filtered and washed with hexane to afford pure final product.

General Procedure 4.2: One-Pot Hydroboration-Suzuki-Miyaura Cross-coupling: To a flame-dried pressure vial with stir bar under argon was added alkene (1.2 equiv.) followed by 9-BBN (1.5 equiv., 0.5 M in THF). The reaction was allowed to stir under reflux for 60 minutes. After, the reaction mixture was allowed to cool to room temperature. Aryl halide (1.0 equiv.) was added, followed by $PdCl_2(dppf)\cdot CH_2Cl_2$ (0.05 equiv.), followed by dropwise addition of a 3 M $KOH_{(aq)}$ solution (3.0 equiv.). This was then heated back up to reflux for an additional 2-16 hours at which reaction progress was tracked by consumption of the aryl halide *via* TLC. The mixture was cooled, filtered over celite, and concentrated under reduced pressure to afford the crude product. The resulting mixture was then purified by silica gel chromatography with an appropriate ethyl acetate/hexanes solvent system to afford the pure product.

General Procedure 4.3: HCl Boc Deprotection: To a 6-dram vial containing an *N*-Boc-protected amine (1.0 equiv.) was added CH_2Cl_2 (0.2 M), followed by HCl (10 equiv, 4 M in dioxane). The resulting mixture was allowed to stir until complete consumption of starting material was observed *via* TLC (1-4 hours). The reaction mixture was concentrated

in vacuo and the residue was rinsed with diethyl ether until a precipitate formed. The precipitate was subjected to trituration with an appropriate solvent system to afford pure product as the hydrochloride salt.

General Procedure 4.4: Ring closure: To a flame-dried vial with stir bar was added phenyldiamine (1.0 equiv.) followed by acetic acid (0.2 M). This was allowed to cool to 0 °C for 15 minutes. Next, methyl 2,2,2-trichloromethylacetimidate (1.1 equiv.) was added dropwise. The reaction was allowed to warm to room temperature and react for 3 hours or until complete. Once complete, the reaction mixture was diluted with cold water and allowed to stir for 10 minutes. The resulting precipitate was then filtered and washed with cold water to afford the desired pure product.

General Procedure 4.5: Amide Formation To a solution of 6-bromo-2-(trichloromethyl)-1H-benzo[d]imidazole (1.0 equiv) in a 2:1 mixture of water:THF (0.2 M) was added *N*-Boc-piperazine (1.1 equiv), followed according to sodium bicarbonate (10.0 equiv). The reaction was allowed to stir at room temperature for one hour and 50 °C for 16 hours. Once complete, the reaction was allowed to cool, and the reaction was concentrated down. DCM was added and the organic layer was washed 3x with water. After, the organic layer was dried over anhydrous sodium sulfate, filtered, and purified *via* silica chromatography with an appropriate ethyl acetate/hexanes solvent system to afford the desired compound.

General Procedure 4.6: SEM Protection To a flame-dried vial purged with argon was added benzimidazole (1.0 equiv.) followed by dry THF (0.2 M). This was cooled to 0 °C and allowed to stir for 10 minutes. Sodium hydride (1.1 equiv.) was added and the reaction mixture was allowed to stir for an additional 10 minutes. After, SEM-Cl (1.1

equiv.) was added dropwise and the reaction was allowed to warm to room temperature for 2 h. Once complete, the reaction mixture was concentrated down and water was added. This was allowed to stir for 10 minutes to quench any remaining SEM-Cl. Ethyl acetate was then added and the organic layer was collected, dried over anhydrous sodium sulfate, and concentrated down to afford pure final product.

General Procedure 4.7: TBAF SEM Deprotection To a vial containing SEM-protected benzimidazole (1.0 equiv.) was added THF (0.2 M) followed by TBAF (3.0 equiv.). This was allowed to reflux for 16 hours until complete. Once complete, saturated ammonium chloride and ethyl acetate were added to the reaction mixture. The organic layer was washed with water additionally twice, dried over anhydrous sodium sulfate, and concentrated down. The resulting mixture was then purified by silica gel chromatography with an appropriate ethyl acetate/hexanes solvent system to afford the pure product.

General Procedure 4.8: TFA Boc Deprotection To a solution of *N*-Boc-amine in DCM (0.2 M) was added TFA (10.0 equiv.). The resulting mixture was stirred at room temperature for 16 hours or until complete. The reaction mixture was then triturated with diethyl ether to afford pure product.

General Procedure 4.9: Sn2 for Tails To a solution of phenol in acetonitrile (0.2 M) was added appropriate alkene (1.2 equiv.) followed by potassium carbonate (2.0 equiv.) This was heated to reflux and allowed to stir for 16 hours. Once complete, it was diluted with ethyl acetate. It was washed 3 times with water and the organic layer was collected, dried over anhydrous sodium sulfate, and concentrated down. The resulting mixture was then purified via silica gel chromatography with an appropriate ethyl acetate/hexanes solvent system to afford the pure product.

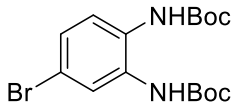

di-tert-butyl (4-bromo-1,2-phenylene)dicarbamate (4.2): Synthesized according to General Procedure 4.1. Purified *via* column chromatography (10% ethyl acetate/hexanes). Off-white solid (77%, 3.20 g). ^{1}H NMR (400 MHz, cdcl$_3$) δ 7.75 (s, 1H), 7.32 (s, 1H), 7.24 – 7.17 (m, 1H), 6.77 (s, 1H), 6.59 (s, 1H), 1.51 (d, *J* = 3.4 Hz, 18Hz). ^{13}C NMR (126 MHz, CDCl$_3$) δ 153.7, 153.3, 131.9, 127.9, 126.4, 125.7, 118.2, 81.3, 28.2. HRMS: (ESI) [M+H]$^+$ calc. for $C_{16}H_{24}BrN_2O_4^+$ 387.0914, observed, 387.0912.

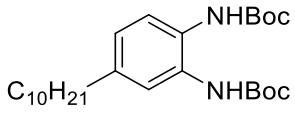

di-tert-butyl (4-decyl-1,2-phenylene)dicarbamate (4.3): Synthesized according to General Procedure 4.2. Purified *via* column chromatography (5-10% ethyl acetate/hexanes). Brown solid (70%, 2.61 g). ^{1}H NMR (400 MHz, cdcl$_3$) δ 7.30 (d, *J* = 17.0 Hz, 2H), 6.88 (dd, *J* = 8.2, 2.0 Hz, 1H), 6.78 (s, 1H), 6.64 (s, 1H), 2.56 – 2.48 (m, 2H), 1.49 (d, *J* = 3.3 Hz, 19H), 1.25 (d, *J* = 10.8 Hz, 17H), 0.90 – 0.82 (m, 4H). ^{13}C NMR (101 MHz, cdcl$_3$) δ 218.3, 154.1, 153.7, 80.5, 41.9, 35.5, 32.2, 31.9, 31.4, 29.6, 29.6, 29.5, 29.3, 28.3, 28.2, 27.1, 26.5, 25.8, 25.6, 22.7, 22.1, 14.1. HRMS: (ESI) [M+H]$^+$ calc. for $C_{26}H_{45}N_2O_4^+$ 449.3374 , observed, 449.2543.

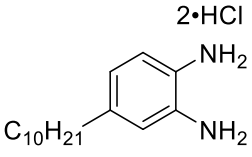

4-decylbenzene-1,2-diamine dihydrochloride (4.4): Synthesized according to General Procedure 4.3. Brown solid (88%, 1.64 g). Product pushed forward crude without isolation.

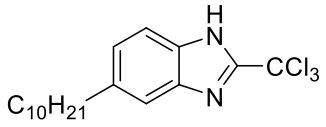

5-decyl-2-(trichloromethyl)-1H-benzo[d]imidazole (4.5): Synthesized according to General Procedure 4.4. Purified *via* column chromatography (10-20% ethyl acetate/hexanes). Yellow solid (73%, 1.70 g). ^{1}H NMR (400 MHz, cdcl$_3$) δ 7.60 (d, *J* = 8.4 Hz, 1H), 7.45 (s, 1H), 7.18 (dd, *J* = 8.4, 1.6 Hz, 1H), 2.74 – 2.67 (m, 2H), 1.67 – 1.58 (m, 2H), 1.32 – 1.22 (m, 14H), 0.87 (t, *J* = 6.8 Hz, 3H). ^{13}C NMR (101 MHz, cdcl$_3$) δ 176.7, 150.5, 140.1, 125.7, 88.6, 36.2, 31.9, 29.6, 29.6, 29.5, 29.3, 29.2, 22.7, 14.1. HRMS: (ESI) [M+H]$^+$ calc. for $C_{18}H_{26}Cl_3N_2^+$ 375.1156, observed, 375.1174.

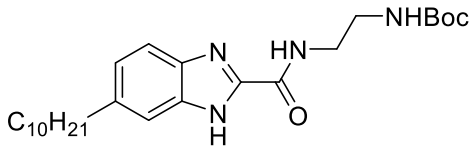

tert-butyl (2-(5-decyl-1H-benzo[d]imidazole-2-carboxamido)ethyl)carbamate (4.6a): Synthesized according to General Procedure 4.5. Purified *via* column chromatography (30-40% ethyl acetate/hexanes). Brown solid (43%, 28 mg). ^{1}H NMR (500 MHz, CDCl$_3$) δ 12.80 – 12.53 (m, 1H), 8.73 – 8.56 (m, 0.5H), 7.67 (d, *J* = 8.3 Hz, 0.5H), 7.56 (s, 0.5H), 7.39 (d, *J* = 8.3 Hz, 0.5H), 7.22 – 7.13 (m, 0.5H), 5.49 (s, 0.5H), 3.80 – 3.64 (m, 2H), 3.53 – 3.44 (m, 2H), 2.71 (t, *J* = 7.6 Hz, 2H), 1.64 (p, *J* = 7.5 Hz, 2H), 1.43 (s, 9H), 1.33 – 1.25 (m, 14H), 0.89 (t, *J* = 6.8 Hz, 3H). ^{13}C NMR (126 MHz, CDCl$_3$) δ 160.3*, 156.3, 145.0*, 144.7*, 143.0*, 141.0*, 140.4*, 138.5*, 134.5*, 132.5*, 126.3*, 124.7*, 119.9*, 119.2*, 112.2*, 111.6*, 79.5, 40.2, 40.0, 36.3, 36.1, 31.9, 31.9, 29.6, 29.6, 29.6, 29.4, 28.4, 22.7, 14.1.Material isolated as an approximately 1:1 ratio of rotamers. HRMS: (ESI) [M+H]$^+$ calc. for $C_{25}H_{41}N_4O_3^+$ 445.3173, observed, 445.3182.

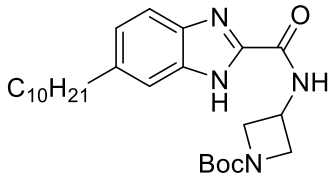

tert-butyl 3-(6-decyl-1H-benzo[d]imidazole-2-carboxamido)azetidine-1-carboxylate (4.6b): Synthesized according to General Procedure 4.5. Purified *via* column chromatography (40-60% ethyl acetate/hexanes). Yellow oil (66%, 60 mg). ^{1}H NMR (500 MHz, $CDCl_3$) δ 12.66 – 12.43 (m, 1H), 8.81 – 8.66 (m, 0.5H), 7.66 (d, *J* = 8.4 Hz, 0.5H), 7.55 (s, 0.5H), 7.36 (d, *J* = 8.3 Hz, 0.5H), 7.23 (s, 0.5H), 7.22 – 7.14 (m, 0.5H), 5.01 – 4.92 (m, 1H), 4.39 – 4.31 (m, 2H), 4.08 – 4.00 (m, 2H), 2.70 (t, *J* = 7.7 Hz, 2H), 1.62 (p, *J* = 7.5 Hz, 2H), 1.45 (s, 9H), 1.32 – 1.23 (m, 14H), 0.90 – 0.83 (m, 3H). ^{13}C NMR (126 MHz, $CDCl_3$) δ 159.5*, 156.1, 144.4*, 144.1*, 143.0*, 141.0*, 140.8*, 138.8*, 134.5*, 132.5*, 126.6*, 125.0*, 120.0*, 119.3*, 112.2*, 111.6*, 79.9, 39.6, 39.6, 36.4, 36.1, 31.9, 31.9, 29.6, 29.6, 29.6, 29.3, 29.3, 28.4, 22.7, 14.1. Material isolated as an approximately 1:1 ratio of rotamers. HRMS: (ESI) $[M+H]^+$ calc. for $C_{27}H_{43}N_4O_3^+$ 471.3330, observed, 471.3348.

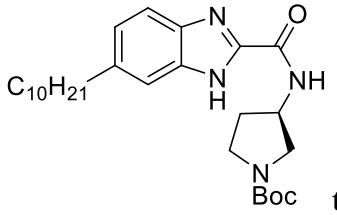

tert-butyl (R)-3-(6-decyl-1H-benzo[d]imidazole-2-carboxamido)pyrrolidine-1-carboxylate ((*R*)-4.6c): Synthesized according to General Procedure 4.5. Purified *via* column chromatography (40-60% ethyl acetate/hexanes). Yellow oil (73%, 70 mg). ^{1}H NMR (500 MHz, $CDCl_3$) δ 12.22 – 11.95 (m, 1H), 8.06 – 7.94 (m, 1H), 7.65 (d, *J* = 8.4 Hz, 0.5H), 7.54 (s, 0.5H), 7.42 (d, *J* = 8.3 Hz, 0.5H), 7.29 (s, 0.5H), 7.18 (dd, *J* = 17.2, 8.4 Hz, 1H), 4.76 – 4.66 (m, 1H), 3.84 – 3.72 (m, 1H), 3.61 – 3.35 (m, 4H), 2.71 (t, *J* = 7.7 Hz, 2H), 2.30 – 2.20 (m, 1H), 2.10 – 1.97 (m, 1H), 1.68 –

1.59 (m, 2H), 1.47 (s, 9H), 1.29 – 1.19 (m, 14H), 0.86 (t, *J* = 6.8 Hz, 3H). ^{13}C NMR (126 MHz, $CDCl_3$) δ 159.6*, 159.6*, 154.5, 144.6*, 144.3*, 143.1*, 141.1*, 140.8*, 138.8*, 134.6*, 132.6*, 126.6*, 125.0*, 120.0*, 119.4*, 112.1*, 111.5*, 79.9, 49.9, 49.3, 44.2, 43.9, 36.5, 36.2, 32.0, 31.9, 29.7, 29.7, 29.7, 29.5, 28.6, 22.8, 14.2. Material isolated as an approximately 1:1 ratio of rotamers. HRMS: (ESI) $[M+H]^+$ calc. for $C_{27}H_{43}N_4O_3^+$ 471.3330, observed, 471.3350.

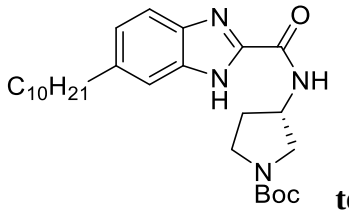

tert-butyl (S)-3-(6-decyl-1H-benzo[d]imidazole-2-carboxamido)pyrrolidine-1-carboxylate ((*S*)-4.6d): Synthesized according to General Procedure 4.5. Purified *via* column chromatography (40-60% ethyl acetate/hexanes). Yellow oil (46%, 51 mg). ^{1}H NMR (500 MHz, $CDCl_3$) δ 12.22 – 11.83 (m, 1H), 8.06 – 7.93 (m, 0.5H), 7.68 (dd, *J* = 8.5, 2.2 Hz, 0.5H), 7.57 (s, 0.5H), 7.45 (dd, *J* = 8.3, 2.3 Hz, 0.5H), 7.32 (s, 0.5H), 7.25 – 7.16 (m, 0.5H), 4.76 (s, 1H), 3.80 (s, 1H), 3.66 – 3.37 (m, 3H), 2.74 (t, *J* = 7.9 Hz, 2H), 2.37 – 2.25 (m, 1H), 2.16 – 2.02 (m, 2H), 1.65 (q, *J* = 7.8 Hz, 2H), 1.50 (s, 9H), 1.34 – 1.24 (m, 14H), 0.92 – 0.85 (m, 3H). ^{13}C NMR (126 MHz, $CDCl_3$) δ 159.5*, 159.5*, 154.4, 143.0*, 141.1*, 134.4*, 132.5*, 126.5*, 124.9*, 119.9*, 119.3*, 112.0*, 111.4*, 79.8, 51.4, 50.8, 49.8, 49.2, 44.1, 43.8, 36.4, 36.1, 31.9, 31.8, 31.0, 29.6, 29.6, 29.5, 29.3, 29.2, 28.5, 22.7, 14.1. Material isolated as an approximately 1:1 ratio of rotamers. HRMS: (ESI) $[M+H]^+$ calc. for $C_{27}H_{43}N_4O_3^+$ 471.3330, observed, 471.3332.

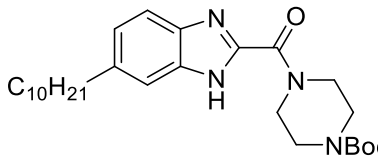

tert-butyl 4-(6-decyl-1H-benzo[d]imidazole-2-carbonyl)piperazine-1-carboxylate (4.6e): Synthesized according to General Procedure 4.5. Purified *via* column chromatography (30-50% ethyl acetate/hexanes). White solid (47%, 21 mg). ^{1}H NMR (500 MHz, $CDCl_3$) δ 11.49 – 11.04 (m, 1H), 7.69 (s, 1H), 7.60 (s, 0H), 7.41 (s, 0H), 7.29 (s, 0H), 7.16 (d, *J* = 10.1 Hz, 1H), 4.77 (t, *J* = 5.1 Hz, 2H), 3.90 – 3.84 (m, 2H), 3.63 – 3.57 (m, 4H), 2.73 (t, *J* = 7.7 Hz, 2H), 1.69 – 1.61 (m, 2H), 1.50 (s, 9H), 1.34 – 1.23 (m, 14H), 0.87 (t, *J* = 6.9 Hz, 3H). ^{13}C NMR (126 MHz, $CDCl_3$) δ 158.9*, 154.7, 144.7*, 143.6*, 141.6*, 140.8*, 138.4*, 133.1*, 131.1*, 126.6*, 124.7*, 120.7*, 120.0*, 111.4*, 110.9*, 80.5, 46.8, 43.3, 32.0, 29.7, 29.7, 29.7, 29.5, 29.4, 28.5, 22.8, 14.3. Material isolated as an approximately 1:1 ratio of isomers. HRMS: (ESI) $[M+H]^+$ calc. for $C_{27}H_{43}BrN_4O_3^+$ 471.3330, observed, 471.3316.

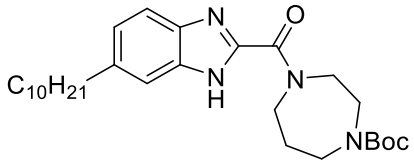

tert-butyl 4-(6-decyl-1H-benzo[d]imidazole-2-carbonyl)-1,4-diazepane-1-carboxylate (4.6f): Synthesized according to General Procedure 4.5. Purified *via* column chromatography (25-50% ethyl acetate/hexanes). White solid (48%, 31 mg). ^{1}H NMR (500 MHz, $CDCl_3$) δ 11.80 – 11.29 (m, 1H), 7.74 – 7.67 (m, 0.5H), 7.63 – 7.57 (m, 0.5H), 7.45 – 7.40 (m, 0.5H), 7.33 – 7.29 (m, 0.5H), 7.21 – 7.11 (m, 0.5H), 4.75 – 4.63 (m, 0.5H), 4.54 (dt, *J* = 12.8, 6.3 Hz, 1H), 3.93 (dt, *J* = 16.1, 5.4 Hz, 1H), 3.83 (d, *J* = 6.4 Hz, 1H), 3.79 – 3.62 (m, 2H), 3.54 – 3.39 (m, 2H), 2.73 (t, *J* = 7.7 Hz, 2H), 2.20 – 2.06 (m, 2H), 1.73 – 1.61 (m, 2H), 1.51 – 1.44 (m, 6H), 1.39 – 1.20 (m, 17H), 0.87 (t, *J* = 6.8 Hz, 3H). ^{13}C NMR (126 MHz, $CDCl_3$) δ 160.0*, 155.5, 155.1*,

144.7*, 143.8*, 142.0*, 141.8*, 140.5*, 138.1*, 133.4*, 131.4*, 126.4*, 124.4*, 120.8*, 120.1*, 111.5*, 110.9*, 79.9, 51.3, 50.7, 49.8, 49.7, 48.7, 47.9, 47.6, 47.2, 46.3, 46.2, 45.8, 36.5, 36.2, 32.0, 29.7, 29.7, 29.7, 29.5, 28.5, 22.8, 14.2. Material isolated as an approximately 1:1 ratio of rotamers. HRMS: (ESI) $[M+H]^+$ calc. for $C_{28}H_{45}N_4O_3^+$ 485.3486, observed, 485.3484.

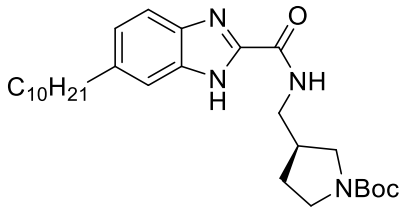

tert-butyl (S)-3-((6-decyl-1H-benzo[d]imidazole-2-carboxamido)methyl)pyrrolidine-1-carboxylate ((*S*)-4.6g): Synthesized according to General Procedure 4.5. Purified *via* column chromatography (20-40% ethyl acetate/hexanes). Yellow oil (53%, 51 mg). ^{1}H NMR (500 MHz, $CDCl_3$) δ 12.45 – 12.06 (m, 1H), 8.28 – 8.14 (m, 0.5H), 7.66 (d, *J* = 8.4 Hz, 0.5H), 7.55 (s, 0.5H), 7.41 (d, *J* = 8.3 Hz, 0.5H), 7.28 (d, *J* = 8.1 Hz, 0.5H), 7.18 (dd, *J* = 17.3, 8.4 Hz, 0.5H), 3.65 – 3.50 (m, 3H), 3.40 – 3.27 (m, 1H), 3.24 – 3.07 (m, 1H), 2.75 – 2.69 (m, 2H), 2.66 – 2.53 (m, 1H), 2.09 – 2.03 (m, 1H), 1.80 – 1.69 (m, 1H), 1.67 – 1.60 (m, 2H), 1.50 – 1.41 (m, 9H), 1.37 – 1.18 (m, 14H), 0.91 – 0.82 (m, 3H). 13C NMR (126 MHz, CDCl3) δ 159.5*, 154.5, 144.6*, 144.3*, 143.1*, 141.1*, 140.7*, 134.2*, 132.2*, 126.5*, 124.9*, 120.0*, 119.4*, 111.8*, 111.2*, 79.4, 49.5, 49.1, 45.2, 45.0, 39.2, 38.3, 36.3, 36.1, 31.9, 31.8, 29.6, 29.6, 29.5, 29.3, 28.5, 22.7, 14.1. Material isolated as an approximately 1:1 ratio of rotamers. HRMS: (ESI) $[M+H]^+$ calc. for $C_{28}H_{45}N_4O_3^+$ 485.3486, observed, 485.3476.

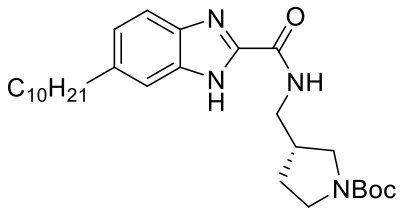

tert-butyl (R)-3-((6-decyl-1H-benzo[d]imidazole-2-carboxamido)methyl)pyrrolidine-1-carboxylate ((*R*)-4.6h): Synthesized according to General Procedure 4.5. Purified *via* column chromatography (30-50% ethyl acetate/hexanes). Yellow oil (67%, 65 mg). ^{1}H NMR (500 MHz, $CDCl_3$) δ 11.39 – 11.09 (m, 1H), 7.94 – 7.81 (m, 0.5H), 7.69 (d, *J* = 8.4 Hz, 0.5H), 7.58 (s, 0.5H), 7.45 (d, *J* = 8.3 Hz, 0.5H), 7.33 (s, 0.5H), 7.21 (dd, *J* = 17.8, 8.5 Hz, 0.5H), 3.67 – 3.49 (m, 4H), 3.37 (p, *J* = 9.1 Hz, 1H), 3.24 – 3.07 (m, 1H), 2.75 (t, *J* = 7.7 Hz, 2H), 2.65 – 2.52 (m, 1H), 2.13 – 2.03 (m, 1H), 1.67 (p, *J* = 7.5 Hz, 2H), 1.48 (d, *J* = 4.8 Hz, 9H), 1.36 – 1.24 (m, 17H), 0.89 (t, *J* = 6.8 Hz, 4H). ^{13}C NMR (126 MHz, $CDCl_3$) δ 160.0*, 154.6, 144.9*, 144.6*, 143.1*, 141.1*, 140.6*, 138.7*, 134.7*, 132.7*, 126.5*, 124.9*, 120.0*, 119.4*, 112.2*, 111.6*, 79.5, 49.7, 49.3, 45.4, 45.1, 39.3, 38.4, 36.5, 36.2, 32.0, 32.0, 29.7, 29.7, 29.7, 29.5, 28.6, 22.8, 14.2. Material isolated as an approximately 1:1 ratio of rotamers. HRMS: (ESI) $[M+H]^+$ calc. for $C_{28}H_{45}N_4O_3^+$ 485.3486, observed, 485.3470.

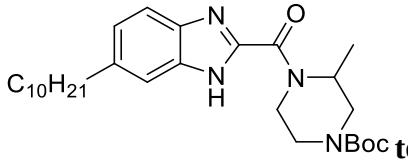

tert-butyl 4-(6-decyl-1H-benzo[d]imidazole-2-carbonyl)-3-methylpiperazine-1-carboxylate ((±)-4.6i): Synthesized according to General Procedure 4.2. Purified *via* column chromatography (30-40% ethyl acetate/hexanes). Yellow oil (34%, 39 mg). ^{1}H NMR (500 MHz, $CDCl_3$) δ 11.70 – 11.28 (m, 1H), 10.09 – 9.35 (m, 0.5H), 7.70 (d, *J* = 8.3 Hz, 0.5H), 7.61 (s, 0.5H), 7.41 (d, *J* = 8.3 Hz, 0.5H), 7.29 (s, 0.5H), 7.22 – 7.12 (m, 0.5H), 6.45 (s, 0.5H), 6.00 (d, *J* = 13.9 Hz, 0.5H),

5.02 (s, 0.5H), 4.60 (d, *J* = 13.5 Hz, 0.5H), 4.51 (t, *J* = 6.3 Hz, 0.5H), 4.37 – 3.92 (m, 2H), 3.64 (t, *J* = 13.3 Hz, 1H), 3.34 – 3.17 (m, 1H), 2.73 (t, *J* = 7.7 Hz, 2H), 1.70 – 1.60 (m, 2H), 1.50 (s, 8H), 1.43 – 1.39 (m, 1H), 1.37 – 1.22 (m, 9H), 0.87 (t, *J* = 6.9 Hz, 3H). ^{13}C NMR (126 MHz, $CDCl_3$) δ 160.4*, 158.9*, 155.1, 140.5*, 133.1*, 131.1*, 126.4*, 124.5*, 111.3*, 110.8*, 80.2*, 65.6, 44.4, 41.3, 37.4, 36.4, 36.1, 31.9, 31.8, 29.6, 29.6, 29.5, 29.3, 29.0, 28.4, 26.0, 22.7, 14.1. Material isolated as an approximately 1:1 ratio of rotamers. HRMS: (ESI) $[M+H]^+$ calc. for $C_{28}H_{45}N_4O_3^+$ 485.3486, observed, 485.3470.

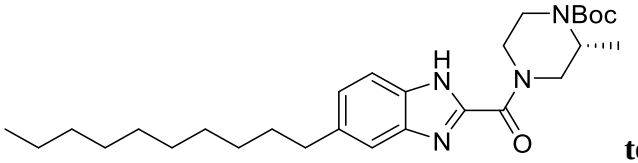

tert-butyl (R)-4-(5-decyl-1H-benzo[d]imidazole-2-carbonyl)-2-methylpiperazine-1-carboxylate ((*R*)-4.6j): Synthesized according to General Procedure 4.5. Purified *via* column chromatography (30-50% ethyl acetate/hexanes). Clear oil (26%, 63mg). ^{1}H NMR (500 MHz, $CDCl_3$) δ 11.04 – 10.81 (m, 1H), 7.70 (t, *J* = 8.8 Hz, 0H), 7.60 (d, *J* = 9.2 Hz, 0H), 7.42 (d, *J* = 8.3 Hz, 0H), 7.29 (d, *J* = 1.5 Hz, 0H), 7.21 (dt, *J* = 8.4, 1.7 Hz, 0H), 7.17 – 7.14 (m, 0H), 6.17 – 5.97 (m, 1H), 4.71 – 4.53 (m, 1H), 4.52 – 4.35 (m, 1H), 4.01 (t, *J* = 12.3 Hz, 1H), 3.69 – 3.03 (m, 3H), 2.76 – 2.69 (m, 2H), 1.64 (s, 2H), 1.49 (t, *J* = 1.3 Hz, 9H), 1.37 – 1.23 (m, 14H), 1.22 – 1.15 (m, 3H), 0.87 (t, *J* = 6.9 Hz, 3H). ^{13}C NMR (126 MHz, $CDCl_3$) δ 159.2*, 159.1*, 154.5, 144.9*, 144.5*, 143.6*, 141.6*, 140.7*, 138.3*, 132.9*, 130.9*, 126.5*, 124.6*, 120.7*, 120.0*, 111.2*, 110.7*, 80.2, 50.2, 47.3, 46.6, 43.3, 43.3, 36.4, 36.1, 31.9, 29.6, 29.5, 29.3, 28.4, 22.7, 15.3, 15.0, 14.1. Material isolated as an approximately 1:1 ratio of rotamers. HRMS: (ESI) $[M+H]^+$ calc. for $C_{28}H_{45}N_4O_3^+$ 485.3486, observed, 485.3458.

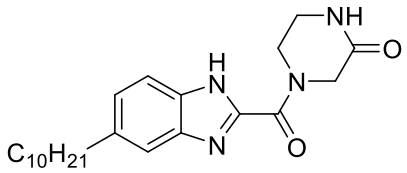

(3*R*,5*S*)-*N*-(4-decylphenyl)-3,5-dimethylpiperazine-1-carboxamide (4.6k): Synthesized according to General Procedure 4.5. Purified *via* column chromatography (50-60% ethyl acetate/hexanes). Light brown solid (70%, 17 mg). ^{1}H NMR (500 MHz, DMSO) δ 13.15 – 13.00 (m, 1H), 8.24 – 8.14 (m, 1H), 7.66 (dd, *J* = 16.6, 8.4 Hz, 0.5H), 7.58 – 7.51 (m, 0.5H), 7.44 (d, *J* = 8.3 Hz, 0.5H), 7.31 (s, 0.5H), 7.18 (d, *J* = 8.3 Hz, 0.5H), 7.12 (ddd, *J* = 8.6, 3.5, 1.6 Hz, 0.5H), 4.69 (q, *J* = 4.6 Hz, 1H), 3.87 (t, *J* = 5.4 Hz, 1H), 2.69 (q, *J* = 7.0 Hz, 2H), 1.65 – 1.57 (m, 2H), 1.30 – 1.22 (m, 14H), 0.85 (t, *J* = 6.7 Hz, 3H). ^{13}C NMR (126 MHz, DMSO) δ 166.3*, 165.9*, 158.0*, 157.8*, 144.7*, 140.8*, 139.1*, 136.9*, 133.6*, 131.6*, 125.5*, 123.8*, 119.9*, 119.1*, 111.9*, 111.2*, 49.8, 46.6, 43.0, 40.5, 35.5, 35.3, 31.5, 31.3, 29.0, 29.0, 28.9, 28.7, 28.7, 22.1, 14.0. Material isolated as an approximately 1:1 ratio of rotamers. HRMS: (ESI) $[M+H]^+$ calc. for $C_{22}H_{38}N_3O^+$ 360.3009, observed, 360.3015.

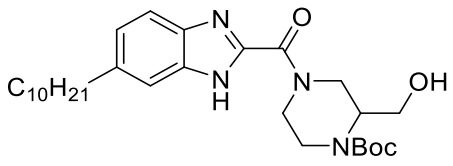

tert-butyl 4-(6-decyl-1H-benzo[d]imidazole-2-carbonyl)-2-(hydroxymethyl)piperazine-1-carboxylate ((±)-4.6l): Synthesized according to General Procedure 4.2. Purified *via* column chromatography (70-80% ethyl acetate/hexanes). Yellow oil (69%, 46 mg). ^{1}H NMR (500 MHz, $CDCl_3$) δ 11.84 – 11.55 (m, 1H), 7.65 (d, *J* = 8.8 Hz, 0.5H), 7.44 (d, *J* = 8.3 Hz, 0.5H), 7.31 (s, 0.5H), 7.24 – 7.14 (m, 0.5H), 7.03 – 6.60 (m, 0.5H), 5.61 (d, *J* = 13.6 Hz, 0.5H), 4.75 (d, *J* = 13.5 Hz, 1H), 4.32 – 4.12 (m, 1H), 4.06 – 3.92 (m, 1H), 3.69 – 3.54 (m, 1H), 3.30 (d, *J* = 13.8 Hz, 1H), 3.17 – 3.00 (m, 1H), 2.96 (d, *J* = 13.0 Hz, 1H), 2.71 (q, *J* = 7.8 Hz, 2H), 1.64 (dd, *J* = 14.1,

6.9 Hz, 2H), 1.51 (s, 9H), 1.32 – 1.22 (m, 16H), 0.89 – 0.83 (m, 4H). ^{13}C NMR (126 MHz, $CDCl_3$) δ 159.4*, 154.8, 143.8*, 143.6*, 142.1*, 141.2*, 140.1*, 139.1*, 133.0*, 131.0*, 127.0*, 125.2*, 119.8*, 119.1*, 111.6*, 111.0*, 80.8, 57.1, 53.4, 43.4, 39.5, 36.3, 36.1, 31.9, 31.8, 29.6, 29.6, 29.5, 29.3, 29.3, 29.2, 28.4, 22.7, 14.1. Material isolated as an approximately 1:1 ratio of rotamers. HRMS: (ESI) $[M+H]^+$ calc. for $C_{28}H_{45}N_4O_4^+$ 501.3435, observed, 501.3421.

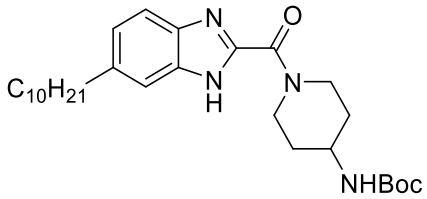

tert-butyl (1-(6-decyl-1H-benzo[d]imidazole-2-carbonyl)piperidin-4-yl)carbamate (4.6m): Synthesized according to General Procedure 4.2. Purified *via* column chromatography (40-60% ethyl acetate/hexanes). White solid (73%, 83 mg). ^{1}H NMR (500 MHz, $CDCl_3$) δ 12.08 – 11.87 (m, 1H), 7.81 – 7.55 (m, 0.5H), 7.41 (s, 0.5H), 7.20 – 7.11 (m, 0.5H), 5.89 (s, 0.5H), 4.82 – 4.58 (m, 2H), 3.82 (s, 1H), 3.51 (t, *J* = 12.6 Hz, 1H), 3.06 (t, *J* = 12.5 Hz, 1H), 2.77 – 2.68 (m, 2H), 2.11 (d, *J* = 13.1 Hz, 2H), 1.71 – 1.60 (m, 2H), 1.54 (s, 9H), 1.46 (s, 9H), 1.36 – 1.19 (m, 14H), 0.87 (t, *J* = 7.1 Hz, 3H). ^{13}C NMR (126 MHz, $CDCl_3$) δ 160.0*, 155.5, 155.1*, 144.7*, 143.8*, 142.0*, 141.8*, 140.5*, 138.1*, 133.4*, 131.4*, 126.4*, 124.4*, 120.8*, 120.1*, 111.5*, 110.9*, 79.9, 49.7, 48.7, 47.9, 46.3, 46.2, 36.5, 36.2, 32.0, 29.7, 29.7, 29.7, 29.5, 28.5, 22.8, 14.2. Material isolated as an approximately 1:1 ratio of rotamers. HRMS: (ESI) $[M+H]^+$ calc. for $C_{28}H_{45}N_4O_3^+$ 485.3486, observed, 485.3513.

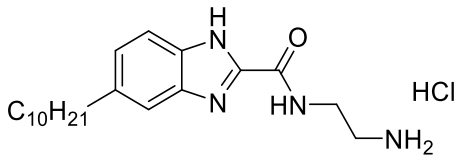

N-(2-aminoethyl)-5-decyl-1H-benzo[d]imidazole-2-carboxamide hydrochloride (4.7a): Synthesized according to General Procedure 4.3. Purified *via* trituration with diethyl ether. White solid (92%, 22 mg). ^{1}H NMR (500 MHz, CD_3OD) δ 7.81 (d, *J* = 8.6 Hz, 1H), 7.70 (s, 1H), 7.57 (dd, *J* = 8.6, 1.4 Hz, 1H), 3.84 (t, *J* = 5.9 Hz, 2H), 3.32 – 3.29 (m, 2H), 2.89 – 2.83 (m, 2H), 1.77 – 1.68 (m, 2H), 1.41 – 1.29 (m, 14H), 0.91 (t, *J* = 6.9 Hz, 3H). ^{13}C NMR (126 MHz, CD_3OD) δ 155.0, 143.6, 141.3, 131.9, 130.1, 128.8, 114.4, 113.3, 38.9, 37.3, 35.6, 31.7, 31.4, 29.3, 29.2, 29.0, 28.8, 22.3, 13.0. HRMS: (ESI) $[M+H]^+$ calc. for $C_{20}H_{33}N_4O^+$ 345.2649, observed, 345.2656.

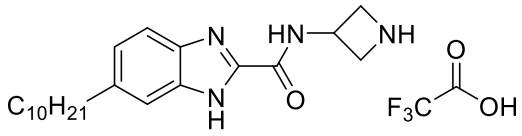

N-(azetidin-3-yl)-6-decyl-1H-benzo[d]imidazole-2-carboxamide 2,2,2-trifluoroacetate (4.7b): Synthesized according to General Procedure 4.8. Purified *via* trituration with diethyl ether. Light brown solid (93%. 43 mg). ^{1}H NMR (500 MHz, CD_3OD) δ 7.59 (d, *J* = 8.4 Hz, 1H), 7.45 (s, 1H), 7.22 (dd, *J* = 8.4, 1.5 Hz, 1H), 5.01 – 4.97 (m, 1H), 4.42 (d, *J* = 7.8 Hz, 4H), 2.73 (t, *J* = 7.6 Hz, 2H), 1.71 – 1.61 (m, 2H), 1.35 – 1.25 (m, 15H), 0.89 (t, *J* = 6.9 Hz, 4H). ^{13}C NMR (126 MHz, CD_3OD) δ 158.7, 143.6, 140.0, 137.1, 136.2, 125.6, 115.9, 114.2, 52.2, 42.1, 35.8, 31.7, 31.6, 29.3, 29.3, 29.2, 29.1, 28.9, 22.3, 13.1. HRMS: (ESI) $[M+H]^+$ calc. for $C_{21}H_{33}N_4O^+$ 357.2649, observed, 357.2636.

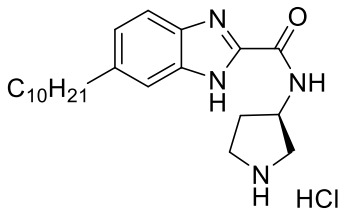

(R)-6-decyl-N-(pyrrolidin-3-yl)-1H-benzo[d]imidazole-2-carboxamide hydrochloride ((*R*)-**4.7c):** Synthesized according to General Procedure 4.3. Purified *via* trituration with diethyl ether. Brown solid (61%, 18 mg). ^{1}H NMR (500 MHz, CD_3OD) δ 7.79 – 7.76 (m, 1H), 7.66 (s, 1H), 7.55 – 7.52 (m, 1H), 4.75 (tt, *J* = 6.9, 4.4 Hz, 1H), 3.70 – 3.63 (m, 2H), 3.56 – 3.46 (m, 2H), 2.86 – 2.81 (m, 2H), 2.51 – 2.43 (m, 1H), 2.38 – 2.29 (m, 1H), 1.74 – 1.67 (m, 2H), 1.39 – 1.25 (m, 14H), 0.91 – 0.87 (m, 3H). ^{13}C NMR (126 MHz, CD_3OD) δ 155.7, 144.9, 142.7, 133.4, 131.6, 130.1, 115.8, 114.7, 51.3, 50.9, 45.8, 37.0, 33.1, 32.8, 30.9, 30.7, 30.6, 30.4, 30.2, 23.7, 14.4. HRMS: (ESI) $[M+H]^+$ calc. for $C_{22}H_{35}N_4O^+$ 371.2805, observed, 371.2806.

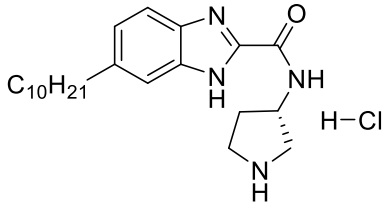

(S)-6-decyl-N-(pyrrolidin-3-yl)-1H-benzo[d]imidazole-2-carboxamide hydrochloride ((S)-**4.7d):** Synthesized according to General Procedure 4.3. Purified *via* trituration with diethyl ether. White solid (61%, 18 mg). ^{1}H NMR (400 MHz, cd_3od) δ 7.79 (d, *J* = 8.6 Hz, 1H), 7.68 (s, 1H), 7.56 (dd, *J* = 8.6, 1.5 Hz, 1H), 4.76 (td, *J* = 6.8, 3.4 Hz, 1H), 3.73 – 3.64 (m, 2H), 3.58 – 3.44 (m, 2H), 2.84 (t, *J* = 7.7 Hz, 2H), 2.54 – 2.41 (m, 1H), 2.41 – 2.29 (m, 1H), 1.74 – 1.64 (m, 2H), 1.39 – 1.23 (m, 14H), 0.89 (t, *J* = 6.5 Hz, 3H). ^{13}C NMR (126 MHz, MeOD) δ 155.7, 145.0, 142.6, 133.4, 131.5, 130.1, 115.8, 114.7, 66.9, 51.3, 50.9, 45.8, 37.0, 33.1, 32.8, 30.9, 30.7, 30.6, 30.4, 30.2, 23.7, 14.4. HRMS: (ESI) $[M+H]^+$ calc. for $C_{22}H_{35}N_4O^+$ 371.2805, observed, 371.2802.

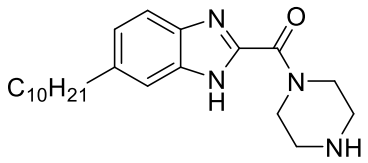

HCl **(6-decyl-1H-benzo[d]imidazol-2-yl)(piperazin-1-yl)methanone hydrochloride (4.7e):** Synthesized according to General Procedure 3. Purified *via* trituration with diethyl ether. White solid (99%, 18 mg). ^{1}H NMR (600 MHz, MeOD) δ 7.78 (d, *J* = 8.4 Hz, 1H), 7.67 (s, 1H), 7.54 (dd, *J* = 8.6, 1.5 Hz, 1H), 4.12 (t, *J* = 5.3 Hz, 4H), 3.44 (t, *J* = 5.4 Hz, 4H), 2.84 (t, *J* = 7.7 Hz, 2H), 1.70 (q, *J* = 7.1 Hz, 2H), 1.37 – 1.24 (m, 14H), 0.89 (t, *J* = 7.0 Hz, 3H). ^{13}C NMR (151 MHz, MeOD) δ 156.7, 144.7, 142.0, 133.4, 131.6, 129.8, 115.8, 114.7, 41.4, 37.0, 33.1, 32.8, 30.7, 30.7, 30.6, 30.4, 30.2, 23.7, 14.4. HRMS: (ESI) $[M+H]^+$ calc. for $C_{22}H_{35}N_4O^+$ 371.2805, observed, 371.2807.

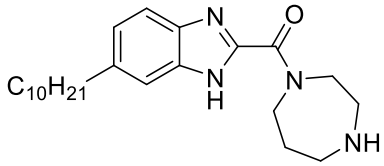

HCl **(6-decyl-1H-benzo[d]imidazol-2-yl)(1,4-diazepan-1-yl)methanone hydrochloride (4.7f):** Synthesized according to General Procedure 3. Purified *via* trituration with diethyl ether. White solid (97%, 26 mg). ^{1}H NMR (500 MHz, CD_3OD) δ 7.82 – 7.73 (m, 1H), 7.71 – 7.62 (m, 1H), 7.57 – 7.46 (m, 1H), 4.28 – 4.05 (m, 2H), 3.97 (t, *J* = 6.0 Hz, 2H), 3.64 – 3.49 (m, 2H), 3.47 – 3.40 (m, 2H), 2.84 (t, *J* = 7.7 Hz, 2H), 2.31 (d, *J* = 10.0 Hz, 2H), 1.71 (p, *J* = 7.2 Hz, 2H), 1.37 – 1.23 (m, 14H), 0.89 (t, *J* = 6.9 Hz, 3H). ^{13}C NMR (126 MHz, CD_3OD) δ 156.4, 143.4, 141.2, 131.7, 129.8, 128.5, 128.0, 114.3, 113.3, 45.1, 44.5, 42.1, 35.6, 31.7, 31.4, 29.3, 29.2, 29.0, 28.8, 24.9, 22.3, 13.0. HRMS: (ESI) $[M+H]^+$ calc. for $C_{23}H_{37}N_4O^+$ 385.2962, observed, 385.2957.

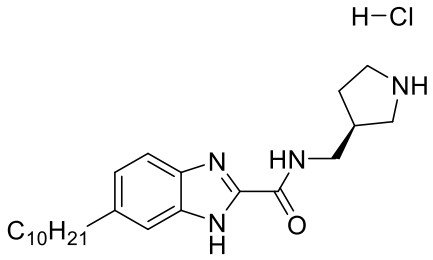

(S)-6-decyl-N-(pyrrolidin-3-ylmethyl)-1H-benzo[d]imidazole-2-carboxamide hydrochloride ((S)-**4.7g):** Synthesized according to General Procedure 4.3. Purified *via* trituration with diethyl ether. Off-white solid (71%, 40 mg). ^{1}H NMR (500 MHz, CD_3OD) δ 7.77 (d, *J* = 8.5 Hz, 1H), 7.65 (s, 1H), 7.50 (dd, *J* = 8.6, 1.4 Hz, 1H), 3.70 – 3.60 (m, 2H), 3.57 (dd, *J* = 11.9, 7.9 Hz, 1H), 3.51 – 3.45 (m, 1H), 3.17 (dd, *J* = 12.0, 8.2 Hz, 1H), 2.88 – 2.79 (m, 3H), 2.35 – 2.27 (m, 1H), 1.93 (dq, *J* = 13.3, 8.5 Hz, 1H), 1.71 (p, *J* = 7.2 Hz, 2H), 1.41 – 1.22 (m, 16H), 0.90 (t, *J* = 6.9 Hz, 3H). ^{13}C NMR (126 MHz, CD_3OD) δ 155.1, 142.9, 141.9, 132.7, 130.9, 129.2, 128.2, 114.6, 113.4, 45.0, 41.0, 38.0, 35.6, 31.7, 31.4, 29.3, 29.2, 29.0, 28.9, 27.8, 22.3, 13.1. HRMS: (ESI) $[M+H]^+$ calc. for $C_{23}H_{37}N_4O^+$ 385.2962, observed, 385.2958.

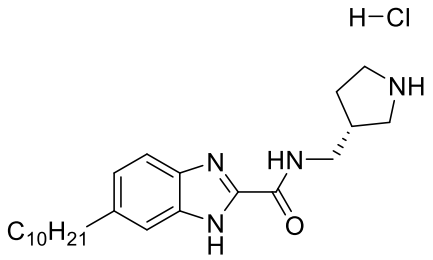

(R)-6-decyl-N-(pyrrolidin-3-ylmethyl)-1H-benzo[d]imidazole-2-carboxamide hydrochloride ((*R*)-**4.7h):** Synthesized according to General Procedure 4.3. Purified *via* trituration with diethyl ether. Brown oil (45%, 20 mg). ^{1}H NMR (500 MHz, CD_3OD) δ 7.73 (d, *J* = 8.5 Hz, 1H), 7.62 (s, 1H), 7.47 (dd, *J* = 8.5, 1.5 Hz, 1H), 3.62 (dd, *J* = 6.8, 5.4 Hz, 2H), 3.53 (dd, *J* = 11.9, 7.9 Hz, 1H), 3.48 – 3.43 (m, 1H), 3.14 (dd, *J* = 11.9, 8.2 Hz, 1H), 2.84 – 2.78 (m, 3H), 2.33 – 2.23 (m, 1H), 1.95 – 1.84 (m, 1H), 1.69 (p, *J* = 7.2 Hz, 2H), 1.40 – 1.22 (m, 16H), 0.89 (t, *J* = 6.8 Hz, 3H). ^{13}C NMR

(126 MHz, CD_3OD) δ 155.5, 142.7, 142.2, 133.1, 131.4, 127.9, 114.7, 113.5, 48.1, 45.0, 40.9, 38.0, 35.7, 31.7, 31.4, 29.3, 29.2, 29.0, 28.9, 27.7, 22.3, 13.0. HRMS: (ESI) $[M+H]^+$ calc. for $C_{23}H_{37}N_4O^+$ 385.2962, observed, 385.2979.

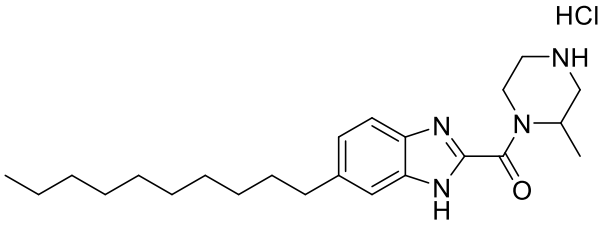

(6-decyl-1H-benzo[d]imidazol-2-yl)(2-methylpiperazin-1-yl)methanone hydrochloride ((±**)-4.7i):** Synthesized according to General Procedure 4.3. Purified *via* trituration with diethyl ether. Off-white solid (56%, 19 mg). ^1H NMR (500 MHz, CD_3OD) δ 7.75 (d, *J* = 8.5 Hz, 1H), 7.64 – 7.62 (m, 1H), 7.48 (dd, *J* = 8.5, 1.5 Hz, 1H), 5.14 – 5.04 (m, 1H), 4.58 – 4.51 (m, 1H), 3.75 (t, *J* = 13.5 Hz, 1H), 3.54 – 3.42 (m, 3H), 3.38 – 3.32 (m, 1H), 2.89 – 2.79 (m, 2H), 1.75 – 1.64 (m, 2H), 1.54 (d, *J* = 7.2 Hz, 3H), 1.38 – 1.27 (m, 14H), 0.89 (t, *J* = 6.9 Hz, 3H). ^{13}C NMR (126 MHz, CD_3OD) δ 157.4, 144.0, 142.8, 134.3, 132.7, 129.2, 116.1, 115.7, 114.9, 114.6, 47.8, 44.2, 37.0, 33.1, 32.9, 30.7, 30.7, 30.6, 30.4, 30.2, 23.7, 15.5, 14.4. HRMS: (ESI) $[M+H]^+$ calc. for $C_{23}H_{37}N_4O^+$ 385.2962 , observed, 385.2978.

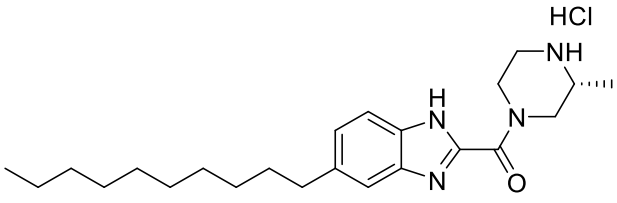

(R)-(5-decyl-1H-benzo[d]imidazol-2-yl)(3-methylpiperazin-1-yl)methanone hydrochloride ((*R***)-4.7j):** Synthesized according to General Procedure 4.3. Purified *via* trituration with diethyl ether. White solid (74%, 41mg). ^1H NMR (500 MHz, CD_3OD) δ 7.81 (d, *J* = 8.6 Hz, 1H), 7.71 – 7.67 (m, 1H), 7.69 (s, 1H), 7.54 (dd, *J* = 8.5, 1.5 Hz, 1H), 4.54 (br s, 2H), 3.72 – 3.51 (m, 3H), 3.42

(s, 1H), 2.89 – 2.81 (m, 2H), 1.72 (p, *J* = 7.2 Hz, 2H), 1.52 – 1.41 (m, 3H), 1.40 – 1.26 (m, 14H), 0.91 (t, *J* = 6.9 Hz, 3H). ^{13}C NMR (126 MHz, MeOD) δ 156.5, 144.6, 141.9, 133.2, 131.4, 129.8, 115.8, 114.7, 52.4, 46.6, 43.9, 41.0, 37.0, 33.0, 32.8, 30.7, 30.7, 30.6, 30.4, 30.2, 23.7, 15.9, 14.4. HRMS: (ESI) $[M+H]^+$ calc. for $C_{23}H_{37}N_4O^+$ 385.2962, observed, 385.2949.

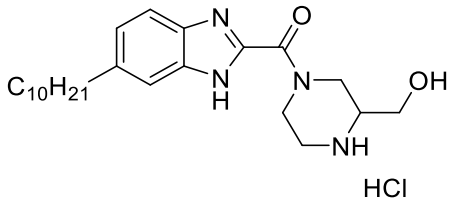

(6-decyl-1H-benzo[d]imidazol-2-yl)(3-(hydroxymethyl)piperazin-1-yl)methanone hydrochloride ((±)-4.7l): Synthesized according to General Procedure 4.3. Purified *via* trituration with diethyl ether. White solid (90%, 36 mg). ^{1}H NMR (500 MHz, CD_3OD) δ 7.81 (d, *J* = 8.5 Hz, 1H), 7.69 (s, 1H), 7.55 (d, *J* = 8.4 Hz, 1H), 4.67 – 4.45 (m, 1H), 3.95 – 3.87 (m, 1H), 3.82 – 3.75 (m, 1H), 3.68 – 3.50 (m, 3H), 3.50 – 3.38 (m, 1H), 2.86 (t, *J* = 7.6 Hz, 2H), 1.72 (p, *J* = 7.2 Hz, 2H), 1.39 – 1.26 (m, 14H), 0.91 (t, *J* = 6.9 Hz, 3H). ^{13}C NMR (126 MHz, CD_3OD) δ 155.4, 143.2, 140.7, 132.2, 130.3, 128.4, 114.5, 113.4, 58.7, 55.9, 42.5, 35.6, 31.7, 31.4, 29.3, 29.3, 29.2, 29.0, 28.8, 22.3, 13.0. HRMS: (ESI) $[M+H]^+$ calc. for $C_{23}H_{37}N_4O_2^+$ 401.2911, observed, 401.2909.

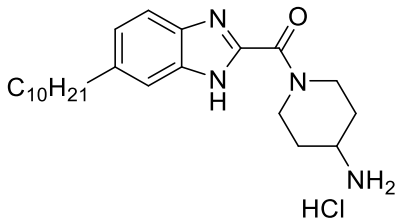

(4-aminopiperidin-1-yl)(6-decyl-1H-benzo[d]imidazol-2-yl)methanone hydrochloride (4.7m): Synthesized according to General Procedure 4.3. Purified *via* trituration with diethyl ether. Off-white solid (94%, 68 mg). ^{1}H NMR (500

MHz, CD_3OD) δ 7.79 (d, *J* = 8.5 Hz, 1H), 7.68 (s, 1H), 7.53 (dd, *J* = 8.5, 1.5 Hz, 1H), 4.70 (s, 1H), 4.21 (s, 1H), 3.62 – 3.51 (m, 2H), 3.18 (s, 1H), 2.85 (t, *J* = 7.7 Hz, 2H), 2.30 – 2.10 (m, 2H), 1.83 (s, 2H), 1.72 (p, *J* = 7.2 Hz, 2H), 1.40 – 1.25 (m, 15H), 0.90 (t, *J* = 6.9 Hz, 3H). ^{13}C NMR (126 MHz, CD_3OD) δ 155.0, 143.1, 141.5, 131.8, 129.9, 128.3, 114.3, 113.3, 47.7, 45.0, 41.0, 35.6, 31.7, 31.4, 29.9, 29.3, 29.2, 29.1, 28.9, 22.3, 13.1. HRMS: (ESI) $[M+H]^+$ calc. for $C_{23}H_{37}N_4O^+$ 385.2962, observed, 385.2975.

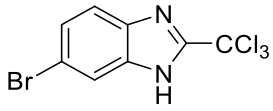

6-bromo-2-(trichloromethyl)-1H-benzo[d]imidazole (4.8): Synthesized according to General Procedure 4.4. Purified *via* precipitation. White solid (92%, 15.49 g). ^1H NMR (400 MHz, $cdcl_3$) δ 9.95 (s, 1H), 8.01 (d, *J* = 1.6 Hz, 1H), 7.73 (d, *J* = 8.7 Hz, 1H), 7.68 (d, *J* = 1.8 Hz, 1H), 7.53 – 7.45 (m, 1H), 7.40 (d, *J* = 8.7 Hz, 1H). ^{13}C NMR (126 MHz, DMSO) δ 151.7, 139.6, 137.1, 127.0, 119.2, 118.2, 116.0 88.4. HRMS: (ESI) $[M+H]^+$ calc. for $C_8H_5BrCl_3N_2^+$ 312.8696, observed, 312.8667.

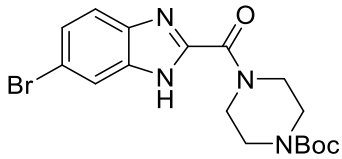

tert-butyl 4-(6-bromo-1H-benzo[d]imidazole-2-carbonyl)piperazine-1-carboxylate (4.9): Synthesized according to General Procedure 4.5. Purified *via* column chromatography (30-50% ethyl acetate/hexanes). White solid (79%, 410 mg). ^1H NMR (500 MHz, $CDCl_3$) δ 11.77 (s, 1H), 7.72 – 7.67 (m, 1H), 7.51 – 7.37 (m, 2H), 4.80 – 4.72 (m, 2H), 3.91 (t, *J* = 5.2 Hz, 2H), 3.68 – 3.59 (m, 5H), 1.52 (s, 9H). ^{13}C NMR (126 MHz, $CDCl_3$) δ 158.6*, 158.5*, 154.7, 145.9*, 145.6*, 144.5*, 142.2*, 134.0*, 131.9*, 128.4*, 126.9*, 124.0*, 122.5*, 118.7*, 116.2*, 115.0*, 113.2*, 80.6, 46.8, 43.5, 28.50. Material isolated as an approximately 1:1 ratio of isomers. HRMS: (ESI) $[M+H]^+$ calc. for $C_{17}H_{22}BrN_4O_3^+$ 409.0870, observed, 409.0884.

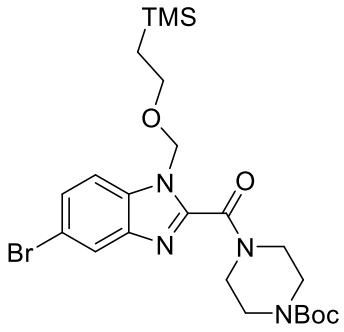

tert-butyl 4-(5-bromo-1-((2-(trimethylsilyl)ethoxy)methyl)-1H-benzo[d]imidazole-2-carbonyl)piperazine-1-carboxylate (4.10): Synthesized according to General Procedure 4.6. Purified *via* extraction. Yellow oil (98%, 1280 mg). ^{1}H NMR (400 MHz, cdcl$_3$) δ 7.94 (d, *J* = 1.8 Hz, 0.5H), 7.77 – 7.71 (m, 0.5H), 7.65 (dd, *J* = 8.7, 1.3 Hz, 1H), 7.51 – 7.43 (m, 2H), 5.75 (dd, *J* = 6.6, 1.3 Hz, 2H), 3.90 – 3.77 (m, 4H), 3.62 – 3.51 (m, 6H), 1.48 (d, *J* = 1.4 Hz, 9H), 0.91 – 0.83 (m, 2H), -0.06 (d, *J* = 1.3 Hz, 9H). HRMS: (ESI) $[M+H]^+$ calc. for $C_{23}H_{36}BrN_4O_4Si^+$ 539.1684, observed, 539.1686.

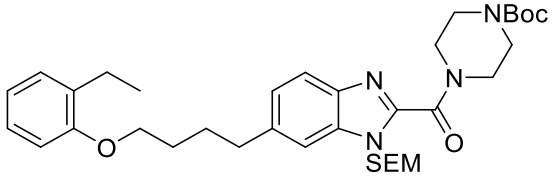

tert-butyl 4-(6-(4-(2-ethylphenoxy)butyl)-1-((2-(trimethylsilyl)ethoxy)methyl)-1H-benzo[d]imidazole-2-carbonyl)piperazine-1-carboxylate (4.11a): Synthesized according to General Procedure 4.2. Purified *via* column chromatography (40-50% ethyl acetate/hexanes). Yellow oil (61%, 145 mg). ^{1}H NMR (500 MHz, CDCl$_3$) δ 7.74 (d, *J* = 8.3 Hz, 0.5H), 7.65 (s, 0.5H), 7.51 (d, *J* = 8.3 Hz, 0.5H), 7.41 (d, *J* = 1.6 Hz, 0.5H), 7.28 (dd, *J* = 8.4, 1.6 Hz, 0.5H), 7.24 (dd, *J* = 8.4, 1.6 Hz, 0.5H), 7.20 – 7.12 (m, 3H), 6.94 – 6.86 (m, 1H), 6.84 (d, *J* = 8.1 Hz, 1H), 5.80 (s, 2H), 4.05 – 3.97 (m, 3H), 3.96 – 3.88 (m, 2H), 3.83 (t, *J* = 5.1 Hz, 2H), 3.63 – 3.53 (m, 6H), 2.88 (q, *J* = 7.5 Hz, 2H), 2.71 – 2.63 (m, 3H), 1.97 – 1.86 (m, 5H), 1.51 (s, 9H), 1.25 – 1.18 (m, 4H), 0.95 – 0.85 (m, 2H), -0.03 (d, *J* = 1.5 Hz, 9H). ^{13}C NMR (126 MHz, CDCl$_3$) δ 160.3, 156.8, 156.8,

156.7, 154.7, 144.6, 144.2, 141.9, 140.0, 139.7, 138.0, 135.2, 133.3, 132.8, 132.8, 132.8, 129.0, 129.0, 128.9, 126.8, 126.8, 125.9, 124.7 (d, J = 271 Hz), 120.5, 120.5, 120.4, 120.4, 120.0, 111.1, 111.1, 111.0, 111.0, 110.8, 110.3, 80.5, 73.7, 73.6, 67.6, 67.5, 66.6, 66.6, 47.3, 42.4, 36.1, 35.7, 29.1, 29.0, 28.5, 28.5, 23.4, 17.9, 14.3, 14.3, -1.3. Material isolated as an approximately 1:1 ratio of regioisomers. HRMS: (ESI) $[M+H]^+$ calc. for $C_{35}H_{53}N_4O_5Si^+$ 637.3780, observed,

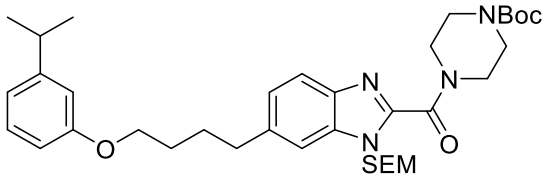

tert-butyl 4-(6-(4-(3-isopropylphenoxy)butyl)-1-((2-(trimethylsilyl)ethoxy)methyl)-1H-benzo[d]imidazole-2-carbonyl)piperazine-1-carboxylate (4.11b): Synthesized according to General Procedure 4.2. Purified *via* column chromatography (20-30% ethyl acetate/hexanes). Yellow oil (82%, 198 mg). ^{1}H NMR (500 MHz, $CDCl_3$) δ 7.72 (d, J = 8.2 Hz, 0H), 7.64 (s, 0H), 7.50 (d, J = 8.4 Hz, 0H), 7.41 (d, J = 1.5 Hz, 0H), 7.27 – 7.19 (m, 2H), 6.86 – 6.82 (m, 1H), 6.79 (p, J = 1.3 Hz, 1H), 6.73 (dd, J = 7.9, 2.4 Hz, 1H), 5.79 (d, J = 1.8 Hz, 2H), 4.03 – 3.97 (m, 2H), 3.94 – 3.89 (m, 2H), 3.86 – 3.79 (m, 2H), 3.60 – 3.53 (m, 6H), 2.87 (p, J = 7.0 Hz, 3H), 1.91 – 1.83 (m, 4H), 1.50 (s, 9H), 1.26 (d, J = 6.9 Hz, 6H), 0.94 – 0.88 (m, 2H), -0.04 (d, J = 1.5 Hz, 9H). ^{13}C NMR (126 MHz, $CDCl_3$) δ 160.3, 159.2, 159.2, 154.7, 150.8, 144.6, 144.3, 141.9, 140.0, 139.7, 138.0, 135.2, 133.3, 129.3, 126.0, 124.8, 120.6, 120.0, 118.9, 113.1, 111.3, 110.8, 110.4, 80.5, 73.7, 73.6, 67.7, 67.6, 66.6, 47.4, 42.5, 36.2, 35.8, 34.3, 32.2, 29.1, 28.5, 26.3, 24.1, 18.0, -1.3. Material isolated as an approximately 1:1 mixture of regioisomers. Material isolated

as an approximately 1:1 ratio of regioisomers. HRMS: (ESI) $[M+H]^+$ calc. for $C_{36}H_{55}N_4O_5Si^+$ 651.3936, observed, 651.3916.

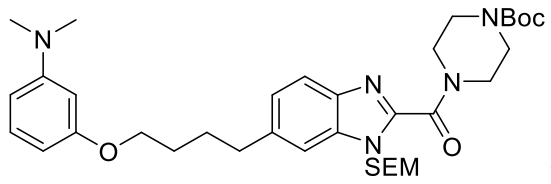

tert-butyl 4-(6-(4-(3-(dimethylamino)phenoxy)butyl)-1-((2-(trimethylsilyl)ethoxy)methyl)-1H-benzo[d]imidazole-2-carbonyl)piperazine-1-carboxylate (4.11c): Synthesized according to General Procedure 4.2. Purified *via* column chromatography (20-40% ethyl acetate/hexanes). Yellow oil (86%, 187 mg). ^{1}H NMR (500 MHz, $CDCl_3$) δ 7.72 (d, *J* = 8.3 Hz, 0.5H), 7.63 (s, 0.5H), 7.50 (d, *J* = 8.3 Hz, 0.5H), 7.40 (d, *J* = 1.5 Hz, 0.5H), 7.29 – 7.21 (m, 0.5H), 7.15 (dd, *J* = 9.4, 7.1 Hz, 1H), 6.40 – 6.35 (m, 1H), 6.32 – 6.28 (m, 2H), 5.82 – 5.77 (m, 2H), 4.04 – 3.97 (m, 2H), 3.94 – 3.89 (m, 2H), 3.86 – 3.80 (m, 2H), 3.63 – 3.53 (m, 6H), 2.94 (s, 6H), 2.86 (q, *J* = 7.4 Hz, 2H), 1.93 – 1.81 (m, 4H), 1.50 (s, 9H), 1.28 (t, *J* = 7.1 Hz, 2H), 0.90 (ddd, *J* = 9.6, 7.5, 2.3 Hz, 2H), -0.04 (d, *J* = 1.1 Hz, 9H). ^{13}C NMR (126 MHz, $CDCl_3$) δ 160.2, 160.2, 154.7, 152.1, 144.6, 144.2, 141.9, 140.0, 139.8, 138.0, 135.2, 133.3, 129.8, 126.0, 124.8, 120.5, 120.0, 110.8, 110.3, 105.8, 105.8, 102.1, 99.8, 99.8, 80.5, 73.7, 73.6, 67.6, 67.6, 66.6, 47.4, 42.4, 40.7, 36.2, 35.8, 29.1, 29.0, 28.5, 17.9, -1.3. Material isolated as an approximately 1:1 ratio of regioisomers. Material isolated as an approximately 1:1 ratio of rotamers. HRMS: (ESI) $[M+H]^+$ calc. for C35H54N5O5Si+ 652.3889, observed, 652.3871.

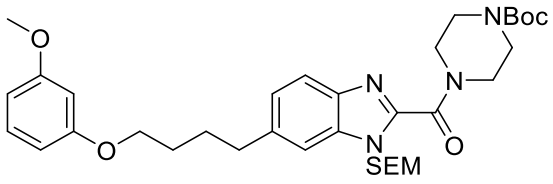

tert-butyl 4-(6-(4-(3-methoxyphenoxy)butyl)-1-((2-(trimethylsilyl)ethoxy)methyl)-1H-benzo[d]imidazole-2-carbonyl)piperazine-1-carboxylate (4.11d): Synthesized according to General Procedure 4.2. Purified *via* column chromatography (20-30% ethyl acetate/hexanes). Yellow oil (86%, 213 mg). ^{1}H NMR (500 MHz, $CDCl_3$) δ 7.74 (d, *J* = 8.3 Hz, 1H), 7.65 (s, 1H), 7.52 (d, *J* = 8.3 Hz, 1H), 7.41 (d, *J* = 1.4 Hz, 1H), 7.29 – 7.17 (m, 2H), 6.55 – 6.51 (m, 2H), 6.49 (d, *J* = 2.4 Hz, 1H), 5.86 – 5.78 (m, 2H), 4.02 – 3.98 (m, 2H), 3.95 – 3.91 (m, 2H), 3.86 – 3.83 (m, 2H), 3.82 (s, 3H), 3.63 – 3.53 (m, 6H), 2.87 (q, *J* = 7.3 Hz, 2H), 1.93 – 1.85 (m, 5H), 1.52 (s, 9H), 0.91 (ddd, *J* = 9.5, 7.5, 2.3 Hz, 2H), -0.02 (d, *J* = 1.5 Hz, 9H). ^{13}C NMR (126 MHz, $CDCl_3$) δ 171.2, 160.8, 160.3, 160.3, 154.6, 144.5, 144.2, 141.8, 139.9, 139.5, 137.8, 135.1, 133.2, 129.8, 125.9, 124.6, 120.5, 119.9, 110.7, 110.2, 106.7, 106.6, 106.2, 106.1, 100.9, 100.9, 80.4, 73.6, 73.5, 67.7, 67.7, 66.5, 60.4, 55.3, 47.2, 42.3, 36.1, 35.6, 32.1, 28.9, 28.8, 28.4, 28.3, 26.2, 22.0, 21.1, 17.8, 14.2, -1.4. Material isolated as an approximately 1:1 ratio of regioisomers. HRMS: (ESI) $[M+H]^+$ calc. for $C_{34}H_{51}N_4O_6Si^+$ 639.3572, observed, 639.3560.

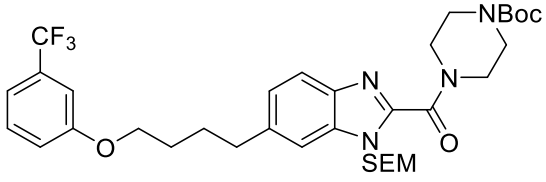

tert-butyl 4-(6-(4-(3-(trifluoromethyl)phenoxy)butyl)-1-((2-(trimethylsilyl)ethoxy)methyl)-1H-benzo[d]imidazole-2-carbonyl)piperazine-1-carboxylate (4.11e): Synthesized according to General Procedure 4.2. Purified *via* column chromatography (10-30% ethyl

acetate/hexanes). Yellow oil (70%, 158 mg). ^{1}H NMR (500 MHz, $CDCl_3$) δ 7.70 (d, *J* = 8.3 Hz, 1H), 7.61 (s, 0H), 7.48 (d, *J* = 8.4 Hz, 0H), 7.40 – 7.33 (m, 2H), 7.26 – 7.15 (m, 2H), 7.10 (q, *J* = 2.4 Hz, 1H), 7.04 (dd, *J* = 8.3, 2.5 Hz, 1H), 5.77 (d, *J* = 3.6 Hz, 2H), 4.01 (dt, *J* = 5.9, 2.9 Hz, 2H), 3.89 (dt, *J* = 7.7, 3.0 Hz, 2H), 3.80 (t, *J* = 5.1 Hz, 2H), 3.62 – 3.50 (m, 6H), 2.85 (q, *J* = 7.3 Hz, 2H), 1.86 (dt, *J* = 11.9, 6.0 Hz, 5H), 1.48 (s, 10H), 0.87 (ddd, *J* = 9.1, 7.3, 1.8 Hz, 2H), -0.07 (d, *J* = 2.8 Hz, 9H). ^{13}C NMR (126 MHz, $CDCl_3$) δ 160.3, 159.3, 159.3, 154.7, 144.7, 144.3, 141.9, 140.1, 139.5, 137.8, 135.2, 133.4, 130.0, 126.0, 124.7, 120.6, 120.0, 118.1, 117.4, 117.4, 117.3, 80.5, 73.7, 73.7, 71.0, 68.1, 68.1, 66.7, 47.4, 42.5, 36.1, 35.7, 32.2, 28.9, 28.7, 28.5, 28.4, 28.3, 26.3, 22.1, 18.0, -1.3. Material isolated as an approximately 1:1 ratio of regioisomers. HRMS: (ESI) $[M+H]^+$ calc. for $C_{34}H_{48}F_3N_4O_5Si^+$ 677.3341, observed, 677.3320.

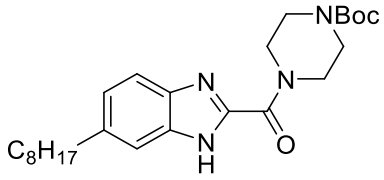

tert-butyl 4-(6-octyl-1H-benzo[d]imidazole-2-carbonyl)piperazine-1-carboxylate (4.12a): Synthesized according to General Procedure 4.2. Purified *via* column chromatography (35-50% ethyl acetate/hexanes). Clear oil (74%, 160 mg). ^{1}H NMR (500 MHz, $CDCl_3$) δ 10.88 (s, 1H), 7.70 (d, *J* = 8.4 Hz, 0.5H), 7.60 (s, 0.5H), 7.42 (d, *J* = 8.3 Hz, 0.5H), 7.29 (d, *J* = 1.5 Hz, 0.5H), 7.23 – 7.13 (m, 0.5H), 4.76 (q, *J* = 5.3 Hz, 2H), 3.85 (td, *J* = 6.0, 3.3 Hz, 2H), 3.64 – 3.53 (m, 4H), 2.73 (t, *J* = 7.7 Hz, 2H), 1.66 (p, *J* = 7.0 Hz, 2H), 1.50 (s, 8H), 1.33 – 1.24 (m, 9H), 0.87 (q, *J* = 4.2 Hz, 3H). ^{13}C NMR (126 MHz, $CDCl_3$) δ 158.8*, 154.8, 145.1*, 144.7*, 143.7*, 141.7*, 140.9*, 138.4*, 133.0*, 131.0*, 126.7*, 124.7*, 120.7*, 120.1*, 111.4*, 110.8*, 80.5, 46.7, 43.3,

36.5, 36.2, 32.0, 32.0, 29.6, 29.4, 29.4, 28.5, 22.8, 14.3. Material isolated as an approximately 1:1 ratio of rotamers. HRMS: (ESI) $[M+H]^+$ calc. for $C_{25}H_{39}N_4O_3^+$ 443.3017, observed, 443.2784.

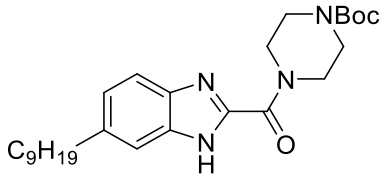

tert-butyl 4-(6-nonyl-1H-benzo[d]imidazole-2-carbonyl)piperazine-1-carboxylate (4.12b): Synthesized according to General Procedure 4.2. Purified *via* column chromatography (20-35% ethyl acetate/hexanes). Clear oil (62%, 70 mg). ^{1}H NMR (500 MHz, $CDCl_3$) δ 11.51 – 11.24 (m, 1H), 7.69 (d, *J* = 8.4 Hz, 0.5H), 7.60 (s, 0.5H), 7.40 (d, *J* = 8.2 Hz, 0.5H), 7.27 (s, 0.5H), 7.21 – 7.12 (m, 0.5H), 4.75 (q, *J* = 5.1 Hz, 2H), 4.40 (tt, *J* = 5.8, 3.1 Hz, 1H), 3.85 (dt, *J* = 7.2, 4.1 Hz, 2H), 3.63 – 3.53 (m, 4H), 2.72 (t, *J* = 7.7 Hz, 2H), 1.65 (d, *J* = 2.8 Hz, 2H), 1.49 (s, 9H), 1.33 – 1.20 (m, 12H), 0.86 (t, *J* = 6.9 Hz, 3H). ^{13}C NMR (126 MHz, $CDCl_3$) δ 159.0*, 154.7, 145.0*, 144.6*, 143.6*, 141.6*, 140.7*, 138.3*, 133.1*, 131.2*, 126.6*, 124.6*, 120.6*, 120.0*, 111.4*, 110.9*, 80.5, 46.8, 43.3, 42.0, 36.5, 36.2, 32.2, 32.0, 29.7, 28.5, 26.3, 22.8, 22.1, 14.2. Material isolated as an approximately 1:1 ratio of rotamers. HRMS: (ESI) $[M+H]^+$ calc. for $C_{26}H_{41}N_4O_3^+$ 457.3173, observed, 457.3226.

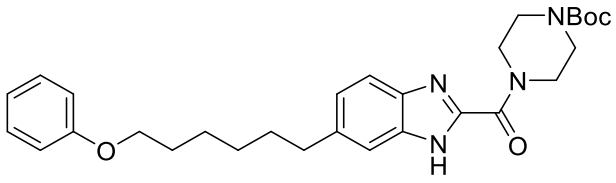

tert-butyl 4-(6-(6-phenoxyhexyl)-1H-benzo[d]imidazole-2-carbonyl)piperazine-1-carboxylate (4.12d): Synthesized according to General Procedure 4.2. Purified *via* column chromatography (30-40% ethyl acetate/hexanes). Clear oil (60%, 60 mg). ^{1}H NMR (500 MHz, MeOD) δ 7.76 (d, *J* = 8.6

Hz, 1H), 7.67 (d, *J* = 1.3 Hz, 1H), 7.52 (dd, *J* = 8.6, 1.5 Hz, 1H), 7.26 – 7.20 (m, 2H), 6.90 – 6.83 (m, 3H), 4.12 (t, *J* = 5.3 Hz, 4H), 3.93 (t, *J* = 6.3 Hz, 2H), 3.44 (t, *J* = 5.3 Hz, 4H), 2.85 (t, *J* = 7.6 Hz, 2H), 1.74 (dq, *J* = 8.5, 6.4 Hz, 4H), 1.55 – 1.49 (m, 2H), 1.48 – 1.41 (m, 2H). ^{13}C NMR (126 MHz, MeOD) δ 160.5*, 156.7*, 144.5*, 142.1*, 130.4*, 129.8*, 121.5*, 115.9*, 115.5*, 114.8*, 68.7, 44.2, 41.7, 36.9, 32.7, 30.3, 29.9, 27.0. HRMS: (ESI) $[M+H]^+$ calc. for $C_{34}H_{47}N_4O_6^+$ 607.3490 observed, 607.3486.

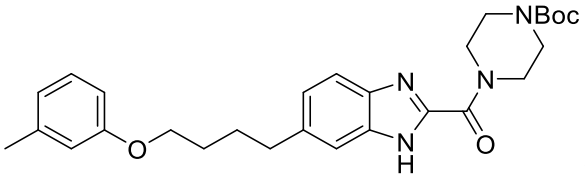

tert-butyl 4-(6-(4-(m-tolyloxy)butyl)-1H-benzo[d]imidazole-2-carbonyl)piperazine-1-carboxylate (4.12e): Synthesized according to General Procedure 4.2. Purified *via* column chromatography (35-50% ethyl acetate/hexanes). Clear oil (93%, 287 mg). ^{1}H NMR (400 MHz, cdcl$_3$) δ 11.21 – 10.83 (m, 1H), 7.71 (d, *J* = 8.4 Hz, 0.5H), 7.30 (s, 0.5H), 7.17 – 7.12 (m, 0.5H), 6.76 – 6.68 (m, 0.5H), 3.94 – 3.91 (m, 2H), 3.86 (h, *J* = 3.6 Hz, 2H), 3.59 (q, *J* = 5.9 Hz, 4H), 2.78 (t, *J* = 7.6 Hz, 2H), 2.31 (s, 4H), 1.86 – 1.70 (m, 5H), 1.50 (s, 9H). ^{13}C NMR (151 MHz, CDCl$_3$) δ 159.2*, 159.1*, 154.7, 141.7*, 139.6*, 129.3*, 126.6*, 124.7*, 121.5*, 121.5*, 121.4*, 120.6*, 115.4*, 111.4*, 80.5, 67.8, 67.7, 46.7, 43.2, 36.4, 36.1, 31.8, 31.7, 29.3, 29.3, 29.2, 28.5, 25.9, 25.8, 21.7. Material isolated as an approximately 1:1 ratio of rotamers. HRMS: (ESI) $[M+H]^+$ calc. for $C_{28}H_{37}N_4O_4^+$ 493.2809, observed, 493.2824.

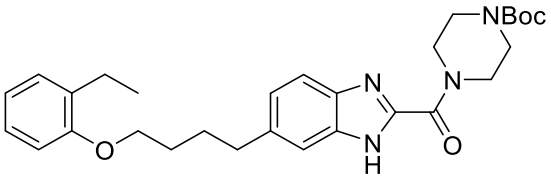

tert-butyl 4-(6-(4-(2-ethylphenoxy)butyl)-1H-benzo[d]imidazole-2-carbonyl)piperazine-1-carboxylate (4.12f): Synthesized

according to General Procedure 4.7. Purified *via* column chromatography (40-50% ethyl acetate/hexanes). White solid (72%, 83 mg). ^{1}H NMR (500 MHz, $CDCl_3$) δ 12.01 – 11.62 (m, 1H), 7.74 (d, *J* = 8.4 Hz, 0.5H), 7.66 (s, 0.5H), 7.45 (d, *J* = 8.3 Hz, 0.5H), 7.32 (s, 0.5H), 7.27 – 7.22 (m, 0.5H), 7.19 (dd, *J* = 8.4, 1.6 Hz, 0.5H), 7.14 (t, *J* = 7.2 Hz, 2H), 6.88 (t, *J* = 7.4 Hz, 1H), 6.81 (d, *J* = 8.1 Hz, 1H), 4.83 – 4.73 (m, 2H), 3.99 (t, *J* = 5.7 Hz, 2H), 3.91 (s, 2H), 3.63 (s, 4H), 2.84 (q, *J* = 6.6 Hz, 2H), 2.66 (qd, *J* = 7.5, 3.7 Hz, 2H), 1.96 – 1.81 (m, 4H), 1.52 (s, 9H), 1.23 – 1.16 (m, 3H). ^{13}C NMR (126 MHz, $CDCl_3$) δ 159.1*, 156.8*, 154.7, 145.0*, 144.7*, 143.5*, 141.7*, 139.9*, 137.5*, 133.3*, 132.7*, 131.5*, 129.0*, 129.0*, 126.8*, 126.4*, 124.5*, 120.7*, 120.4*, 120.0*, 111.7*, 111.0*, 80.4, 67.5, 46.8, 43.3, 36.0, 35.7, 29.0, 28.5, 28.3, 23.4, 14.3. Material isolated as an approximately 1:1 ratio of rotamers. HRMS: (ESI) $[M+H]^+$ calc. for $C_{29}H_{39}N_4O_4^+$ 507.2966, observed,

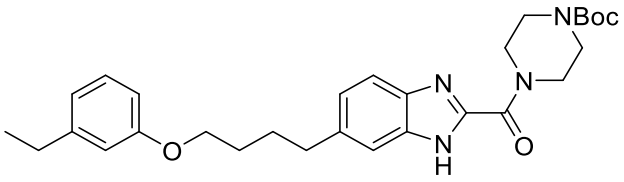

tert-butyl 4-(6-(4-(3-ethylphenoxy)butyl)-1H-benzo[d]imidazole-2-carbonyl)piperazine-1-carboxylate (4.12g): Synthesized according to General Procedure 4.7. Purified *via* column chromatography (40-50% ethyl acetate/hexanes). Clear oil (93%, 258 mg). ^{1}H NMR (600 MHz, $CDCl_3$) δ 10.74 – 10.51 (m, 1H), 7.71 (d, *J* = 8.4 Hz, 1H), 7.62 (s, 1H), 7.43 (d, *J* = 8.3 Hz, 0H), 7.31 (s, 1H), 7.23 – 7.15 (m, 2H), 6.78 (d, *J* = 7.5 Hz, 1H), 6.76 – 6.73 (m, 1H), 6.70 (dt, *J* = 8.1, 4.2 Hz, 1H), 4.76 (q, *J* = 6.0 Hz, 2H), 3.97 – 3.92 (m, 2H), 3.83 (q, *J* = 4.5 Hz, 2H), 3.63 – 3.55 (m, 4H), 2.78 (t, *J* = 7.7 Hz, 2H), 2.63 – 2.57 (m, 2H), 1.85 – 1.79 (m, 2H), 1.75 (q, *J* = 7.7 Hz, 2H), 1.51 (s, 0H), 1.58 – 1.47 (m, 9H), 1.22

(td, *J* = 7.6, 1.3 Hz, 3H). ^{13}C NMR (151 MHz, $CDCl_3$) δ 159.2*, 146.0*, 143.7*, 141.7*, 140.5*, 132.8*, 129.3*, 126.7*, 124.7*, 120.6*, 120.3*, 120.3*, 114.4*, 111.5*, 110.9*, 80.5, 67.8, 67.7, 46.7, 43.2, 36.4, 36.1, 31.8, 31.7, 29.4, 29.3, 29.1, 28.5, 25.9, 25.8, 22.1, 15.7. Material isolated as an approximately 1:1 ratio of rotamers. HRMS: (ESI) $[M+H]^+$ calc. for $C_{29}H_{39}N_4O_4^+$ 507.2966, observed, 507.2960.

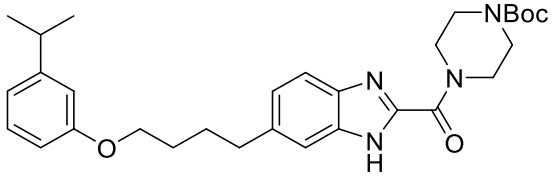

tert-butyl 4-(6-(4-(3-isopropylphenoxy)butyl)-1H-benzo[d]imidazole-2-carbonyl)piperazine-1-carboxylate (4.12h): Synthesized according to General Procedure 4.7. Purified *via* column chromatography (40-50% ethyl acetate/hexanes). White solid (98%, 155 mg). ^{1}H NMR (600 MHz, MeOD) δ 7.66 – 7.35 (m, 2H), 7.18 (d, *J* = 7.5 Hz, 1H), 7.13 (td, *J* = 7.9, 1.5 Hz, 1H), 6.76 (d, *J* = 7.6 Hz, 1H), 6.72 (t, *J* = 2.1 Hz, 1H), 6.66 (dd, *J* = 8.1, 2.6 Hz, 1H), 4.44 – 4.31 (m, 2H), 3.95 (t, *J* = 5.9 Hz, 2H), 3.77 (t, *J* = 5.3 Hz, 2H), 3.55 (t, *J* = 5.4 Hz, 4H), 2.81 (h, *J* = 7.0 Hz, 3H), 1.89 – 1.76 (m, 4H), 1.46 (dt, *J* = 6.1, 3.4 Hz, 9H), 1.19 (dd, *J* = 6.8, 2.8 Hz, 6H). ^{13}C NMR (151 MHz, MeOD) δ 160.5*, 159.8*, 155.7, 151.4*, 145.3*, 129.9*, 119.5*, 113.6*, 112.1*, 81.6, 68.4, 47.5, 43.6, 36.6, 36.5, 34.9, 29.6, 29.1, 28.8, 24.4. Material isolated as an approximately 1:1 ratio of rotamers. HRMS: (ESI) $[M+H]^+$ calc. for $C_{30}H_{41}N_4O_4^+$ 521.3122, observed, 521.3111.

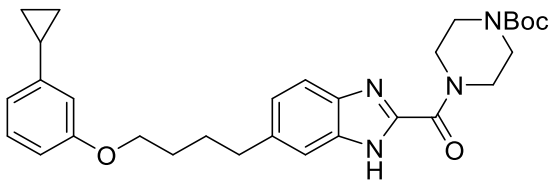

tert-butyl 4-(6-(4-(3-cyclopropylphenoxy)butyl)-1H-benzo[d]imidazole-2-carbonyl)piperazine-1-

carboxylate (4.12i): Synthesized according to General Procedure 4.2. Purified *via* column chromatography (20-40% ethyl acetate/hexanes). White solid (64%, 52 mg). ^{1}H NMR (400 MHz, cdcl$_3$) δ 10.61 – 10.38 (m, 1H), 7.72 (d, *J* = 8.4 Hz, 0H), 7.63 (s, 0H), 7.45 – 7.41 (m, 0H), 7.32 (dd, *J* = 1.6, 0.8 Hz, 0H), 7.23 (dd, *J* = 8.3, 1.6 Hz, 0H), 7.18 (dd, *J* = 8.4, 1.6 Hz, 0H), 7.14 (t, *J* = 7.9 Hz, 1H), 6.70 – 6.64 (m, 2H), 6.59 (t, *J* = 2.2 Hz, 1H), 4.76 (dt, *J* = 7.4, 4.2 Hz, 2H), 3.96 (td, *J* = 6.0, 2.8 Hz, 2H), 3.83 (s, 2H), 3.59 (dt, *J* = 10.6, 5.5 Hz, 4H), 2.82 (t, *J* = 7.0 Hz, 2H), 1.88 – 1.81 (m, 4H), 1.50 (d, *J* = 0.6 Hz, 9H), 0.97 – 0.90 (m, 2H), 0.71 – 0.64 (m, 2H). ^{13}C NMR (126 MHz, CDCl$_3$) δ 159.3*, 159.2*, 154.7, 145.8*, 145.0*, 144.7*, 143.6*, 141.7*, 140.0*, 137.6*, 129.3*, 126.5*, 124.6*, 120.7*, 120.1*, 118.1*, 112.2*, 111.2*, 80.5, 71.0, 67.6, 46.8, 43.3, 36.1, 35.8, 29.0, 28.9, 28.5, 28.4, 28.3, 26.3, 15.5, 9.3. Material isolated as an approximately 1:1 ratio of rotamers. HRMS: (ESI) [M+H]$^+$ calc. for $C_{30}H_{39}N_4O_4^+$ 519.2966, observed, 519.2987.

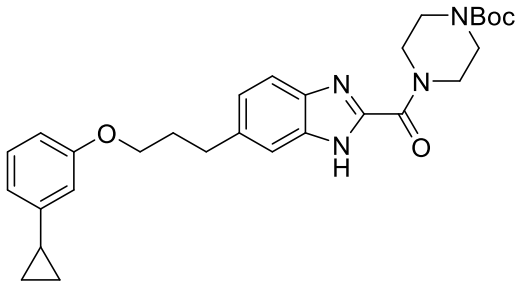

tert-butyl 4-(6-(3-(3-cyclopropylphenoxy)propyl)-1H-benzo[d]imidazole-2-carbonyl)piperazine-1-carboxylate (4.12j): Synthesized according to General Procedure 4.2. Purified *via* column chromatography (30-50% ethyl acetate/hexanes). Orange oil (53%, 224 mg). 1H NMR (500 MHz, CDCl$_3$) δ 11.86 – 11.56 (m, 1H), 7.72 (d, *J* = 8.4 Hz, 0.5H), 7.65 (s, 0.5H), 7.43 (d, *J* = 8.2 Hz, 0.5H), 7.32 (d, *J* = 1.5 Hz, 0.5H), 7.24 – 7.11 (m, 2H), 6.70 – 6.59 (m, 3H), 4.76 (q, *J* = 5.2 Hz, 2H), 3.95 (td, *J* = 6.2, 3.7 Hz, 2H), 3.88 (q, *J* = 5.3 Hz,

2H), 3.61 (dq, *J* = 10.8, 3.5 Hz, 4H), 2.94 (td, *J* = 7.6, 3.1 Hz, 2H), 2.19 – 2.09 (m, 2H), 1.85 (ttd, *J* = 8.0, 5.0, 2.3 Hz, 1H), 1.51 (s, 9H), 1.26 (d, *J* = 7.1 Hz, 1H), 0.93 (tdd, *J* = 6.2, 4.4, 1.4 Hz, 2H), 0.68 (ddd, *J* = 6.9, 3.1, 1.5 Hz, 2H). ^{13}C NMR (126 MHz, $CDCl_3$) δ 159.2*, 159.1*, 154.7, 145.8*, 145.1*, 144.8*, 143.6*, 141.7*, 139.1*, 136.8*, 133.3*, 131.5*, 129.3*, 126.5*, 124.5*, 120.8*, 120.1*, 118.1*, 118.1*, 112.2*, 112.2*, 111.3*, 111.2*, 80.4, 66.6, 46.8, 43.2, 32.6, 32.4, 31.2, 28.5, 15.5, 9.3. Material isolated as an approximately 1:1 ratio of rotamers. HRMS: (ESI) $[M+H]^+$ calc. for $C_{29}H_{37}N_4O_4^+$ 505.2809, observed, 505.2819.

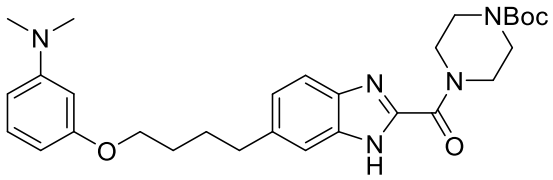

tert-butyl 4-(6-(4-(3-(dimethylamino)phenoxy)butyl)-1H-benzo[d]imidazole-2-carbonyl)piperazine-1-carboxylate (4.12k): Synthesized according to General Procedure 4.7. Purified *via* column chromatography (40-60% ethyl acetate/hexanes). White solid (89%, 113 mg). ^{1}H NMR (500 MHz, $CDCl_3$) δ 11.88 – 11.28 (m, 1H), 7.76 – 7.59 (m, 1H), 7.46 – 7.28 (m, 0.5H), 7.25 – 7.15 (m, 0.5H), 7.12 (t, *J* = 8.1 Hz, 1H), 6.38 – 6.32 (m, 1H), 6.30 – 6.23 (m, 2H), 4.77 (q, *J* = 5.2 Hz, 2H), 4.04 – 3.96 (m, 2H), 3.93 – 3.85 (m, 2H), 3.67 – 3.56 (m, 4H), 2.91 (s, 6H), 2.85 – 2.77 (m, 2H), 1.90 – 1.78 (m, 4H), 1.50 (s, 9H). ^{13}C NMR (126 MHz, $CDCl_3$) δ 160.2*, 159.0*, 154.7, 152.1*, 144.7*, 143.5*, 141.7*, 139.9*, 137.5*, 133.2*, 131.4*, 129.8*, 129.8*, 126.5*, 124.5*, 120.7*, 120.0*, 111.6*, 111.1*, 105.8*, 102.1*, 99.8*, 80.4, 80.4, 67.6, 67.6, 46.7, 43.3, 40.7, 29.0, 28.5, 28.3. Material isolated as an approximately 1:1 ratio of rotamers. HRMS: (ESI) $[M+H]^+$ calc. for $C_{29}H_{40}N_5O_4^+$ 522.3075, observed, 522.3098.

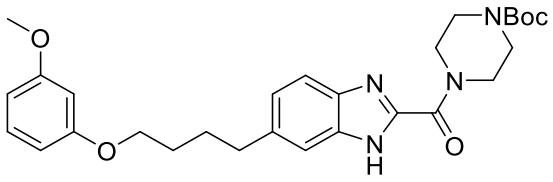

tert-butyl 4-(6-(4-(3-methoxyphenoxy)butyl)-1H-benzo[d]imidazole-2-carbonyl)piperazine-1-carboxylate (4.12l): Synthesized according to General Procedure 4.7. Purified *via* column chromatography (30-50% ethyl acetate/hexanes). White solid (93%, 132 mg). ^{1}H NMR (500 MHz, $CDCl_3$) δ 11.95 – 11.51 (m, 1H), 7.71 (d, *J* = 8.4 Hz, 0.5H), 7.63 (s, 0.5H), 7.42 (d, *J* = 8.3 Hz, 0.5H), 7.30 (s, 0.5H), 7.21 (d, *J* = 8.3 Hz, 0.5H), 7.19 – 7.13 (m, 2H), 6.50 – 6.43 (m, 3H), 4.81 – 4.72 (m, 2H), 3.97 – 3.91 (m, 2H), 3.92 – 3.87 (m, 2H), 3.77 (s, 3H), 3.66 – 3.55 (m, 4H), 2.85 – 2.78 (m, 2H), 1.88 – 1.78 (m, 4H), 1.50 (s, 9H). ^{13}C NMR (126 MHz, $CDCl_3$) δ 160.9*, 160.4*, 159.0*, 154.7, 145.0*, 144.7*, 143.5*, 141.7*, 139.8*, 137.5*, 133.3*, 131.4*, 129.9*, 129.9*, 126.4*, 124.5*, 120.7*, 120.0*, 111.6*, 111.1*, 106.7*, 106.2*, 101.0*, 80.4, 67.8, 55.3, 46.8, 43.3, 36.0, 35.8, 28.9, 28.8, 28.5, 28.3, 28.3. Material isolated as an approximately 1:1 ratio of rotamers. HRMS: (ESI) $[M+H]^+$ calc. for $C_{28}H_{37}N_4O_5^+$ 509.2758, observed, 509.2784.

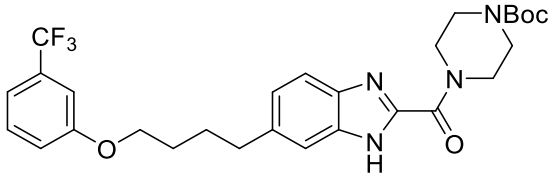

tert-butyl 4-(6-(4-(3-(trifluoromethyl)phenoxy)butyl)-1H-benzo[d]imidazole-2-carbonyl)piperazine-1-carboxylate (4.12m): Synthesized according to General Procedure 4.7. Purified *via* column chromatography (30-50% ethyl acetate/hexanes). White solid (70%, 158 mg). ^{1}H NMR (500 MHz, $CDCl_3$) δ 12.02 – 11.65 (m, 1H), 7.72 (d, *J* = 8.4 Hz, 0.5H), 7.63 (s, 0.5H), 7.43 (d, *J* = 8.3 Hz, 0.5H), 7.34 (dd, *J* = 16.8, 8.8 Hz, 1.5H), 7.24 – 7.19 (m,

0.5H), 7.17 (d, *J* = 7.9 Hz, 1.5H), 7.09 (t, *J* = 2.1 Hz, 1H), 7.02 (dd, *J* = 8.4, 2.5 Hz, 1H), 4.79 – 4.73 (m, 2H), 4.01 – 3.96 (m, 2H), 3.94 – 3.87 (m, 2H), 3.64 – 3.57 (m, 4H), 2.85 – 2.78 (m, 2H), 1.90 – 1.79 (m, 4H), 1.50 (s, 9H). ^{13}C NMR (126 MHz, $CDCl_3$) δ 159.2*, 159.1*, 154.7, 145.1*, 144.7*, 143.6*, 141.7*, 139.7*, 137.3*, 133.3*, 132.2*, 131.8 (q, *J* = 32 Hz), 130.0*, 126.4*, 124.4*, 124.1 (d, *J* = 271 Hz), 120.8*, 120.0*, 118.0*, 117.2 (q, *J* = 3.7 Hz), 111.7*, 111.2 (q, *J* = 3.7 Hz), 111.1*, 80.5, 68.1, 46.8, 43.3, 36.0, 35.7, 28.5, 28.2. HRMS: (ESI) $[M+H]^+$ calc. for $C_{28}H_{34}F_3N_4O_4^+$ 547.2527, observed, 547.2521.

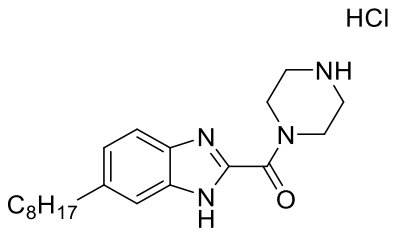

(6-octyl-1H-benzo[d]imidazol-2-yl)(piperazin-1-yl)methanone hydrochloride (4.13a): Synthesized according to General Procedure 4.3. Purified *via* trituration with diethyl ether. White solid (90%, 54 mg). ^{1}H NMR (500 MHz, CD_3OD) δ 7.78 (d, *J* = 8.5 Hz, 1H), 7.67 (s, 1H), 7.54 (dd, *J* = 8.6, 1.4 Hz, 1H), 4.12 (t, *J* = 5.3 Hz, 4H), 3.44 (t, *J* = 5.2 Hz, 4H), 2.84 (t, *J* = 7.6 Hz, 2H), 1.71 (t, *J* = 7.4 Hz, 2H), 1.39 – 1.23 (m, 9H), 0.89 (t, *J* = 6.9 Hz, 3H). ^{13}C NMR (126 MHz, CD_3OD) δ 156.6, 144.7, 142.0, 133.3, 131.6, 129.9, 115.8, 114.7, 44.2, 37.0, 33.0, 32.8, 30.5, 30.4, 30.2, 23.7, 14.4. HRMS: (ESI) $[M+H]^+$ calc. for $C_{20}H_{31}N_4O^+$ 343.2492, observed, 343.2495.

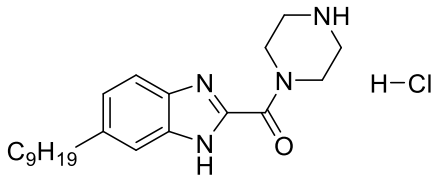

(6-nonyl-1H-benzo[d]imidazol-2-yl)(piperazin-1-yl)methanone hydrochloride (4.13b): Synthesized according to General Procedure 4.3. Purified *via* trituration with diethyl ether. White solid (57%, 34 mg). ^{1}H NMR (500 MHz, CD_3OD) δ 7.82 (d, *J* = 8.6 Hz, 1H), 7.70 (s, 1H), 7.57 (dd, *J* = 8.6, 1.4 Hz, 1H), 4.12 (t, *J*

= 5.2 Hz, 4H), 3.47 (t, *J* = 5.2 Hz, 4H), 3.33 (p, *J* = 1.6 Hz, 1H), 2.86 (t, *J* = 7.6 Hz, 2H), 1.76 – 1.69 (m, 2H), 1.42 – 1.25 (m, 12H), 0.91 (t, *J* = 6.8 Hz, 3H). ^{13}C NMR (126 MHz, CD_3OD) δ 155.0, 143.5, 140.4, 131.6, 129.7, 128.7, 114.3, 113.3, 42.8, 35.6, 31.6, 31.4, 29.3, 29.2, 29.0, 28.8, 22.3, 13.0. HRMS: (ESI) $[M+H]^+$ calc. for $C_{21}H_{32}N_4O^+$ 357.2654, observed, 357.2643.

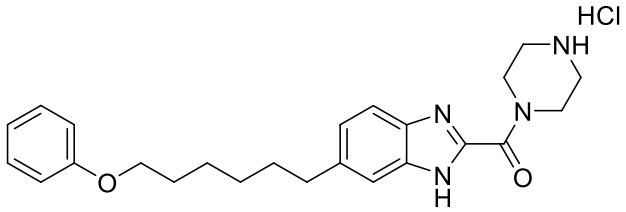

(6-(6-phenoxyhexyl)-1H-benzo[d]imidazol-2-yl)(piperazin-1-yl)methanone hydrochloride (4.13d): Synthesized according to General Procedure 4.3. Purified *via* trituration with diethyl ether. White solid (89%, 39 mg). ^{1}H NMR (500 MHz, CD_3OD) δ 7.76 (d, *J* = 8.6 Hz, 1H), 7.67 (d, *J* = 1.3 Hz, 1H), 7.52 (dd, *J* = 8.6, 1.5 Hz, 1H), 7.26 – 7.20 (m, 2H), 6.90 – 6.83 (m, 3H), 4.12 (t, *J* = 5.3 Hz, 4H), 3.93 (t, *J* = 6.3 Hz, 2H), 3.44 (t, *J* = 5.3 Hz, 5H), 2.85 (t, *J* = 7.6 Hz, 2H), 1.75 (dtd, *J* = 15.1, 7.5, 5.3 Hz, 4H), 1.55 – 1.49 (m, 2H), 1.48 – 1.41 (m, 2H). ^{13}C NMR (126 MHz, CD_3OD) δ 160.5, 156.7, 144.5, 142.1, 130.4, 129.8, 121.5, 115.9, 115.5, 114.8, 68.7, 44.2, 41.7, 36.9, 32.7, 30.3, 29.9, 27.0. HRMS: (ESI) $[M+H]^+$ calc. for $C_{24}H_{31}N_4O_2^+$ 407.2442 observed, 407.2452.

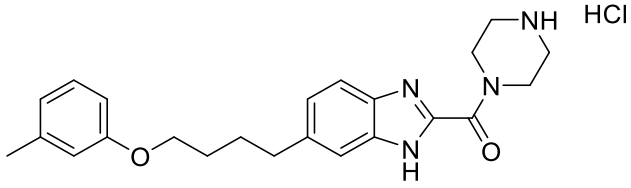

piperazin-1-yl(6-(4-(m-tolyloxy)butyl)-1H-benzo[d]imidazol-2-yl)methanone hydrochloride (4.13e): Synthesized according to General Procedure 4.3. Purified *via* trituration with diethyl ether. White solid (89%, 222 mg). ^{1}H NMR (600 MHz, CD_3OD) δ 7.80 (d, *J* = 8.5 Hz, 1H), 7.70

(s, 1H), 7.55 (dd, *J* = 8.6, 1.4 Hz, 1H), 7.09 (t, *J* = 7.8 Hz, 1H), 6.71 – 6.61 (m, 3H), 4.10 (t, *J* = 5.2 Hz, 4H), 3.91 (t, *J* = 6.3 Hz, 2H), 3.46 (t, *J* = 5.3 Hz, 4H), 2.86 (t, *J* = 7.6 Hz, 2H), 2.27 (s, 3H), 1.83 – 1.73 (m, 4H), 1.57 – 1.49 (m, 2H). ^{13}C NMR (151 MHz, CD_3OD) δ 160.4, 156.2, 144.7, 141.6, 140.4, 132.7, 130.8, 130.1, 122.3, 116.1, 115.6, 114.7, 112.3, 68.5, 44.1, 41.6, 36.9, 32.5, 30.2, 26.7, 21.6. HRMS: (ESI) $[M+H]^+$ calc. for $C_{23}H_{29}N_4O_2^+$ 393.2285, observed, 393.2153.

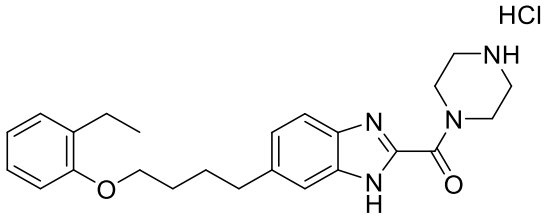

(6-(4-(2-ethylphenoxy)butyl)-1H-benzo[d]imidazol-2-yl)(piperazin-1-yl)methanone hydrochloride (4.13f): Synthesized according to General Procedure 4.3. Purified *via* trituration with diethyl ether. White solid (72%, 52 mg). ^{1}H NMR (500 MHz, CD_3OD) δ 7.79 (d, *J* = 8.6 Hz, 1H), 7.70 (s, 1H), 7.58 (dd, *J* = 8.6, 1.5 Hz, 1H), 7.12 – 7.07 (m, 2H), 6.87 – 6.79 (m, 2H), 4.11 (t, *J* = 5.4 Hz, 4H), 4.01 (t, *J* = 6.0 Hz, 2H), 3.46 – 3.41 (m, 4H), 2.95 (t, *J* = 7.5 Hz, 2H), 2.60 (q, *J* = 7.5 Hz, 2H), 1.99 – 1.84 (m, 4H), 1.14 (t, *J* = 7.5 Hz, 3H). ^{13}C NMR (126 MHz, CD_3OD) δ 156.6, 155.2, 143.0, 140.7, 132.2, 132.0, 130.3, 128.6, 128.4, 126.5, 120.0, 114.5, 113.4, 110.8, 67.0, 42.8, 35.3, 28.6, 28.0, 23.1, 13.6. HRMS: (ESI) $[M+H]^+$ calc. for $C_{24}H_{31}N_4O_2^+$ 407.2442 , observed, 407.2458.

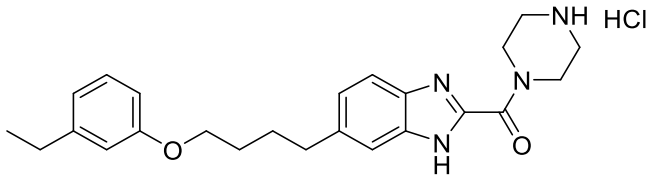

(6-(4-(3-ethylphenoxy)butyl)-1H-benzo[d]imidazol-2-yl)(piperazin-1-yl)methanone hydrochloride (4.13g): Synthesized according to General Procedure 4.3. Purified *via* trituration with diethyl ether. White solid

(85%, 36 mg). ^{1}H NMR (600 MHz, CD_3OD) δ 7.76 (d, *J* = 8.5 Hz, 1H), 7.66 (d, *J* = 1.5 Hz, 1H), 7.53 (dd, *J* = 8.5, 1.5 Hz, 1H), 7.13 (t, *J* = 7.8 Hz, 1H), 6.76 – 6.73 (m, 1H), 6.70 (t, *J* = 2.1 Hz, 1H), 6.69 – 6.65 (m, 1H), 3.94 (t, *J* = 6.3 Hz, 2H), 3.45 – 3.40 (m, 4H), 2.89 (t, *J* = 7.6 Hz, 2H), 2.58 (q, *J* = 7.6 Hz, 2H), 1.85 – 1.76 (m, 4H), 1.58 – 1.51 (m, 2H), 1.20 (t, *J* = 7.6 Hz, 3H). HRMS: (ESI) $[M+H]^+$ calc. for $C_{24}H_{31}N_4O_2^+$ 407.2442, observed, 407.2458.

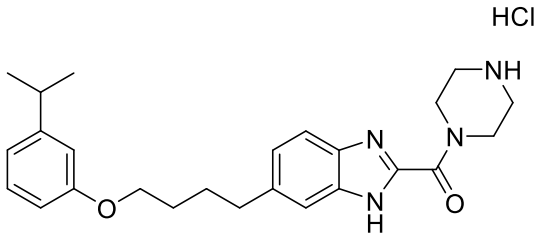

(6-(4-(3-isopropylphenoxy)butyl)-1H-benzo[d]imidazol-2-yl)(piperazin-1-yl)methanone hydrochloride (4.13h): Synthesized according to General Procedure 4.3. Purified *via* trituration with diethyl ether. White solid (79%, 115 mg). ^{1}H NMR (500 MHz, CD_3OD) δ 7.80 (d, *J* = 8.6 Hz, 1H), 7.72 (s, 1H), 7.59 (dd, *J* = 8.6, 1.5 Hz, 1H), 7.14 (t, *J* = 7.9 Hz, 1H), 6.77 (dt, *J* = 7.7, 1.3 Hz, 1H), 6.75 – 6.72 (m, 1H), 6.68 (ddd, *J* = 8.2, 2.6, 0.9 Hz, 1H), 4.10 (t, *J* = 5.4 Hz, 4H), 3.99 (t, *J* = 6.1 Hz, 2H), 3.44 (t, *J* = 5.3 Hz, 4H), 2.93 (t, *J* = 7.5 Hz, 2H), 2.83 (p, *J* = 6.9 Hz, 1H), 1.94 – 1.79 (m, 4H), 1.21 (d, *J* = 6.9 Hz, 6H). ^{13}C NMR (126 MHz, CD_3OD) δ 160.5, 156.4, 151.7, 144.5, 141.9, 133.1, 131.3, 130.3, 130.0, 119.7, 115.8, 114.8, 113.8, 112.6, 68.5, 44.2, 36.7, 35.4, 29.9, 29.3, 24.4. HRMS: (ESI) $[M+H]^+$ calc. for C25H33N4O2+ 421.2598, observed, 421.2591.

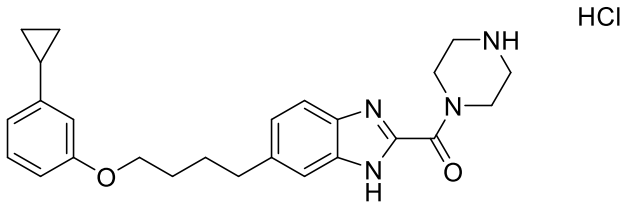

(6-(4-(3-cyclopropylphenoxy)butyl)-1H-benzo[d]imidazol-2-yl)(piperazin-1-yl)methanone hydrochloride (4.13i): Synthesized according to General Procedure 4.3. Purified *via* trituration with diethyl ether. White solid (73%, 51 mg). ^{1}H NMR (500 MHz, CD_3OD) δ 7.78 (d, *J* = 8.5 Hz, 1H), 7.69 (s, 1H), 7.54 (d, *J* = 8.5 Hz, 1H), 7.08 (t, *J* = 8.0 Hz, 1H), 6.66 – 6.55 (m, 3H), 4.13 (t, *J* = 5.1 Hz, 4H), 3.96 (t, *J* = 6.1 Hz, 2H), 3.44 (t, *J* = 5.2 Hz, 4H), 2.91 (t, *J* = 7.5 Hz, 2H), 1.93 – 1.76 (m, 5H), 0.96 – 0.87 (m, 2H), 0.67 – 0.59 (m, 2H). ^{13}C NMR (126 MHz, CD_3OD) δ 160.5, 156.7, 147.0, 144.2, 142.1, 133.5, 131.8, 130.2, 129.8, 118.8, 115.9, 114.9, 112.9, 112.3, 68.4, 44.2, 36.6, 29.9, 29.3, 16.2, 9.6. HRMS: (ESI) $[M+H]^+$ calc. for $C_{25}H_{31}N_4O_2^+$ 419.2442 observed, 419.2448.

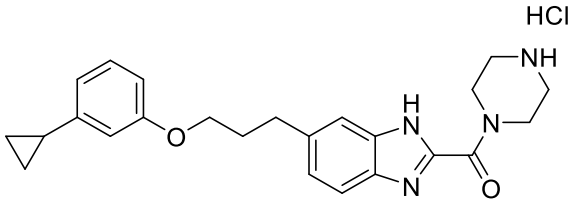

(6-(3-(3-cyclopropylphenoxy)propyl)-1H-benzo[d]imidazol-2-yl)(piperazin-1-yl)methanone (4.13j): Synthesized according to General Procedure 4.3. Purified *via* trituration with diethyl ether. White solid (88%, 100 mg). ^{1}H NMR (400 MHz, CD_3OD) δ 7.79 (dd, *J* = 8.5, 0.7 Hz, 1H), 7.70 (s, 1H), 7.57 (dd, *J* = 8.6, 1.5 Hz, 1H), 7.10 (t, *J* = 7.9 Hz, 1H), 6.68 – 6.57 (m, 3H), 4.11 (t, *J* = 5.4 Hz, 4H), 3.95 (t, *J* = 6.1 Hz, 2H), 3.46 – 3.42 (m, 4H), 3.04 (dd, *J* = 8.3, 6.7 Hz, 2H), 2.21 – 2.11 (m, 2H), 1.84 (tt, *J* = 8.4, 5.1 Hz, 1H), 0.96 – 0.87 (m, 2H), 0.65 – 0.60 (m,

2H). ^{13}C NMR (151 MHz, CD_3OD) δ 160.4, 157.3, 147.0, 142.9, 142.7, 134.3, 132.8, 130.2, 129.3, 118.9, 116.2, 115.2, 112.9, 112.2, 67.4, 44.3, 41.6, 33.3, 32.2, 16.2, 9.7.

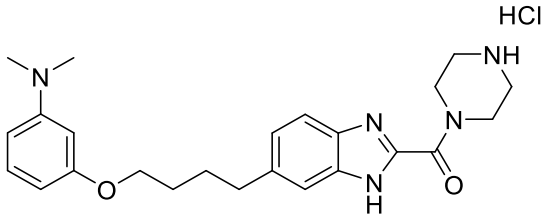

(6-(4-(3-(dimethylamino)phenoxy)butyl)-1H-benzo[d]imidazol-2-yl)(piperazin-1-yl)methanone hydrochloride (4.13k): Synthesized according to General Procedure 4.3. Purified *via* trituration with diethyl ether.). ^{1}H NMR (400 MHz, CD_3OD) δ 7.81 (dd, *J* = 8.5, 2.6 Hz, 1H), 7.73 (d, *J* = 5.3 Hz, 1H), 7.62 – 7.56 (m, 1H), 7.47 (td, *J* = 8.2, 3.0 Hz, 1H), 7.27 (q, *J* = 2.5 Hz, 1H), 7.21 (dt, *J* = 8.2, 2.5 Hz, 1H), 7.08 (dt, *J* = 8.5, 2.5 Hz, 1H), 4.10 – 4.03 (m, 6H), 3.63 – 3.58 (m, 2H), 3.45 – 3.41 (m, 4H), 3.29 – 3.27 (m, 4H), 2.93 (dt, *J* = 7.5, 3.7 Hz, 2H), 1.89 (d, *J* = 14.5 Hz, 4H). ^{13}C NMR (151 MHz, CD_3OD) δ 161.8, 156.2, 145.0, 144.5, 141.7, 132.8, 132.4, 130.9, 130.2, 128.8, 116.0, 115.7, 114.8, 69.4, 68.1, 47.2, 44.1, 36.5, 29.6, 29.1, 15.5. HRMS: (ESI) $[M+H]^+$ calc. for $C_{24}H_{32}N_5O_2^+$ 422.2551, observed, 422.2573.

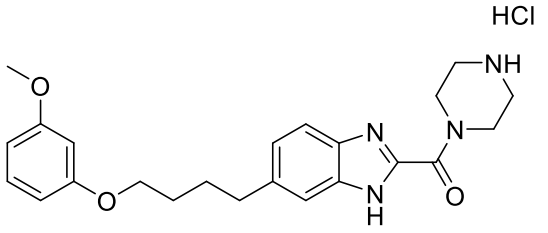

(6-(4-(3-methoxyphenoxy)butyl)-1H-benzo[d]imidazol-2-yl)(piperazin-1-yl)methanone hydrochloride (4.13l): Synthesized according to General Procedure 4.3. Purified *via* trituration with diethyl ether. White solid (98%, 113 mg). ^{1}H NMR (400 MHz, CD_3OD) δ 7.77 (dd, *J* = 8.6, 0.8 Hz, 1H), 7.69 (s, 1H), 7.55 (dd, *J* = 8.6, 1.5 Hz, 1H), 7.09 (t, *J* = 8.2 Hz, 1H), 6.46 – 6.41 (m, 2H), 6.39

(t, *J* = 2.4 Hz, 1H), 4.10 – 4.05 (m, 5H), 3.94 (t, *J* = 6.1 Hz, 2H), 3.71 (s, 3H), 3.47 – 3.38 (m, 5H), 2.90 (t, *J* = 7.4 Hz, 2H), 1.91 – 1.74 (m, 4H). ^{13}C NMR (151 MHz, CD_3OD) δ 162.3, 161.6, 156.4, 144.4, 141.9, 133.1, 131.3, 130.7, 130.6, 130.6, 130.0, 115.8, 114.8, 101.9, 68.5, 55.6, 44.2, 41.6, 36.6, 29.8, 29.2. HRMS: (ESI) $[M+H]^+$ calc. for $C_{23}H_{29}N_4O_3^+$ 409.2234, observed, 409.2222.

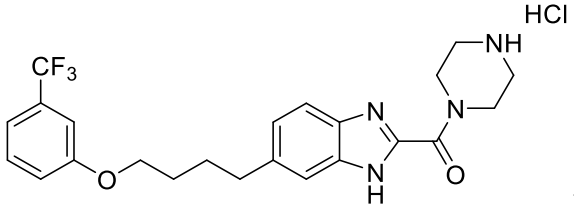

piperazin-1-yl(6-(4-(3-(trifluoromethyl)phenoxy)butyl)-1H-benzo[d]imidazol-2-yl)methanone hydrochloride (4.13m): Synthesized according to General Procedure 4.3. Purified *via* trituration with diethyl ether. White solid (98%, 136 mg). ^{1}H NMR (600 MHz, MeOD) δ 7.81 (d, *J* = 8.6 Hz, 1H), 7.73 (s, 1H), 7.59 (dd, *J* = 8.6, 1.5 Hz, 1H), 7.44 (t, *z* 8.0 Hz, 1H), 7.21 – 7.10 (m, 3H), 4.10 (t, *J* = 5.4 Hz, 4H), 4.06 (t, *J* = 6.0 Hz, 2H), 3.45 (t, *J* = 5.4 Hz, 4H), 2.94 (t, *J* = 7.4 Hz, 2H), 1.94 – 1.83 (m, 4H). ^{13}C NMR (151 MHz, MeOD) δ 160.7, 156.3, 144.4, 141.8, 132.9, 132.7 (q, *J* = 32 Hz) 131.4, 131.1, 130.0, 125.5 (d, *J* = 271 Hz), 119.2, 118.0 (q, *J* = 3.7 Hz), 115.8, 114.8, 112.1 (q, *J* = 3.7 Hz), 69.0, 68.1, 44.1, 36.6, 29.7, 29.1. HRMS: (ESI) $[M+H]^+$ calc. for $C_{23}H_{26}F_3N_4O_2^+$ 447.2002, observed, 447.1979.

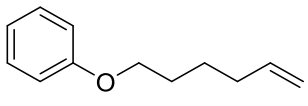

(hex-5-en-1-yloxy)benzene (4.15a): Synthesized according to General Procedure 9. Purified *via* column chromatography (0-5% ethyl acetate/hexanes). Clear oil (63%, 219 mg). ^{1}H NMR (500 MHz, $CDCl_3$) δ 7.32 – 7.27 (m, 2H), 6.97 – 6.88 (m, 3H), 5.85 (ddt, *J* = 16.9, 10.2, 6.6 Hz, 1H), 5.08 – 5.02 (m, 1H), 5.01 – 4.96 (m, 1H),

3.98 (t, *J* = 6.5 Hz, 2H), 2.20 – 2.11 (m, 2H), 1.86 – 1.79 (m, 2H), 1.62 – 1.56 (m, 2H). ^{13}C NMR (126 MHz, $CDCl_3$) δ 159.2, 138.7, 129.5, 120.6, 114.9, 114.6, 67.7, 33.6, 28.9, 25.5. HRMS: (ESI) $[M+H]^+$ calc. for $C_{12}H_{17}O^+$, 177.1274, observed, 177.1282.

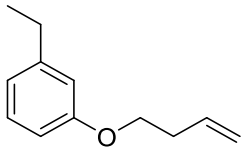

1-(but-3-en-1-yloxy)-3-ethylbenzene (4.15d): Synthesized according to General Procedure 9. Purified *via* column chromatography (0-5% ethyl acetate/hexanes). Clear oil (63%, 219 mg). ^{1}H NMR (500 MHz, $CDCl_3$) δ 7.20 (t, *J* = 7.8 Hz, 1H), 6.82 – 6.76 (m, 2H), 6.73 (ddd, *J* = 8.2, 2.6, 0.9 Hz, 1H), 5.93 (ddt, *J* = 17.1, 10.3, 6.7 Hz, 1H), 5.19 (dq, *J* = 17.2, 1.7 Hz, 1H), 5.12 (dq, *J* = 10.3, 1.3 Hz, 1H), 4.02 (t, *J* = 6.7 Hz, 2H), 2.63 (q, *J* = 7.6 Hz, 2H), 2.56 (qt, *J* = 6.7, 1.4 Hz, 2H), 1.24 (t, *J* = 7.6 Hz, 3H). ^{13}C NMR (126 MHz, $CDCl_3$) δ 159.1, 146.0, 134.7, 129.4, 120.5, 117.1, 114.5, 111.6, 67.2, 33.9, 29.1, 15.6. HRMS: (ESI) $[M+H]^+$ calc. for $C_{12}H_{17}O^+$, 177.1274, observed, 177.1304.

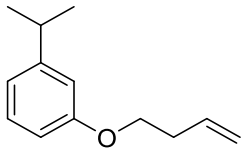

1-(but-3-en-1-yloxy)-3-isopropylbenzene (4.15e): Synthesized according to General Procedure 9. Purified *via* column chromatography (0-5% ethyl acetate/hexanes). Clear oil (48%, 130 mg). ^{1}H NMR (500 MHz, $CDCl_3$) δ 7.21 (t, *J* = 7.9 Hz, 1H), 6.86 – 6.80 (m, 2H), 6.73 (ddd, *J* = 8.2, 2.6, 1.0 Hz, 1H), 5.98 – 5.89 (m, 1H), 5.19 (dq, *J* = 17.2, 1.7 Hz, 1H), 5.12 (dq, *J* = 10.3, 1.4 Hz, 1H), 4.02 (t, *J* = 6.8 Hz, 2H), 2.88 (hept, *J* = 6.9 Hz, 1H), 2.55 (qt, *J* = 6.7, 1.4 Hz, 2H), 1.25 (d, *J* = 6.9 Hz, 6H). ^{13}C NMR (126 MHz, $CDCl_3$) δ 159.1, 150.8, 134.7, 129.4, 119.1, 117.1, 113.3, 111.4, 67.2, 34.3, 33.9, 24.1. HRMS: (ESI) $[M+H]^+$ calc. for $C_{13}H_{19}O^+$ 191.1430, observed, 191.1429.

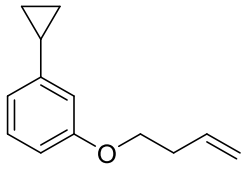

1-(but-3-en-1-yloxy)-3-cyclopropylbenzene (4.15f): Synthesized according to General Procedure 9. Purified *via* column chromatography (0-5% ethyl acetate/hexanes). Clear oil (39%, 145 mg). ^{1}H NMR (600 MHz, $CDCl_3$) δ 7.16 (t, *J* = 7.9 Hz, 1H), 6.71 – 6.66 (m, 2H), 6.62 (t, *J* = 2.1 Hz, 1H), 5.95 – 5.87 (m, 1H), 5.17 (dq, *J* = 17.1, 1.6 Hz, 1H), 5.11 (dq, *J* = 10.3, 1.4 Hz, 1H), 4.00 (t, *J* = 6.7 Hz, 2H), 2.54 (qt, *J* = 6.7, 1.4 Hz, 2H), 1.89 – 1.83 (m, 1H), 0.97 – 0.92 (m, 2H), 0.71 – 0.67 (m, 2H). ^{13}C NMR (151 MHz, $CDCl_3$) δ 159.2, 145.9, 134.7, 129.3, 118.3, 117.1, 112.3, 111.3, 67.2, 33.8, 15.6, 9.4. HRMS: (ESI) $[M+H]^+$ calc. for $C_{13}H_{17}O^+$ 189.1274, observed, 189.1279.

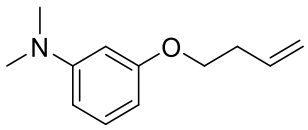

3-(but-3-en-1-yloxy)-N,N-dimethylaniline (4.15g): Synthesized according to General Procedure 9. Purified *via* column chromatography (0-5% ethyl acetate/hexanes). Clear oil (25%, 106 mg). ^{1}H NMR (500 MHz, $CDCl_3$) δ 7.20 – 7.14 (m, 1H), 6.42 – 6.37 (m, 1H), 6.34 – 6.30 (m, 2H), 5.95 (ddt, *J* = 17.0, 10.2, 6.7 Hz, 1H), 5.20 (dq, *J* = 17.3, 1.8 Hz, 1H), 5.13 (dq, *J* = 10.2, 1.4 Hz, 1H), 4.05 (t, *J* = 6.8 Hz, 2H), 2.57 (qt, *J* = 6.8, 1.5 Hz, 2H). ^{13}C NMR (126 MHz, $CDCl_3$) δ 160.1, 152.1, 134.8, 129.8, 117.0, 105.9, 102.1, 99.9, 67.1, 40.8, 33.9.

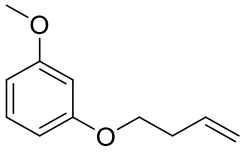

1-(but-3-en-1-yloxy)-3-methoxybenzene (4.15h): Synthesized according to General Procedure 9. Purified *via* column chromatography (0-5% ethyl acetate/hexanes). Clear oil (36%, 160 mg). ^{1}H NMR (600 MHz, $CDCl_3$) δ 7.17 (t, *J* = 8.2 Hz, 1H), 6.51 (dd, *J* = 8.2, 2.4 Hz, 2H), 6.47 (t, *J* = 2.4 Hz, 1H), 5.91 (ddt, *J* = 17.0, 10.3,

6.7 Hz, 1H), 5.17 (dq, *J* = 17.2, 1.7 Hz, 1H), 5.11 (dq, *J* = 10.3, 1.4 Hz, 1H), 4.00 (t, *J* = 6.7 Hz, 2H), 3.79 (s, 3H), 2.54 (qt, *J* = 6.7, 1.4 Hz, 2H). ^{13}C NMR (151 MHz, $CDCl_3$) δ 161.0, 160.3, 134.6, 130.0, 117.2, 106.8, 106.5, 101.1, 67.3, 55.4, 33.8. HRMS: (ESI) $[M+H]^+$ calc. for $C_{11}H_{15}O^+$ 179.1067, observed, 179.1065.

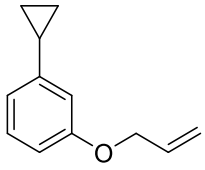

1-(allyloxy)-3-cyclopropylbenzene (4.15j): Synthesized according to General Procedure 9. Purified *via* column chromatography (0-5% ethyl acetate/hexanes). Clear oil (54%, 119 mg). ^{1}H NMR (600 MHz, $CDCl_3$) δ 7.17 (t, *J* = 7.9 Hz, 1H), 6.72 – 6.68 (m, 2H), 6.65 – 6.63 (m, 1H), 6.07 (ddt, *J* = 17.2, 10.6, 5.3 Hz, 1H), 5.42 (dp, *J* = 17.3, 1.7 Hz, 1H), 5.29 (dq, *J* = 10.5, 1.4 Hz, 1H), 4.53 (dt, *J* = 5.3, 1.5 Hz, 2H), 1.87 (tt, *J* = 8.4, 5.1 Hz, 1H), 0.97 – 0.93 (m, 2H), 0.70 (dt, *J* = 6.5, 4.7 Hz, 2H). ^{13}C NMR (126 MHz, $CDCl_3$) δ 158.8, 145.9, 133.6, 129.3, 118.5, 117.7, 112.4, 111.5, 68.8, 15.6, 9.4. HRMS: (ESI) $[M+H]^+$ calc. for $C_{12}H_{15}O^+$ 175.1117, observed, 175.1116.

Appendix A. Spectra for Chapter 2

HMBC of **2.7a**

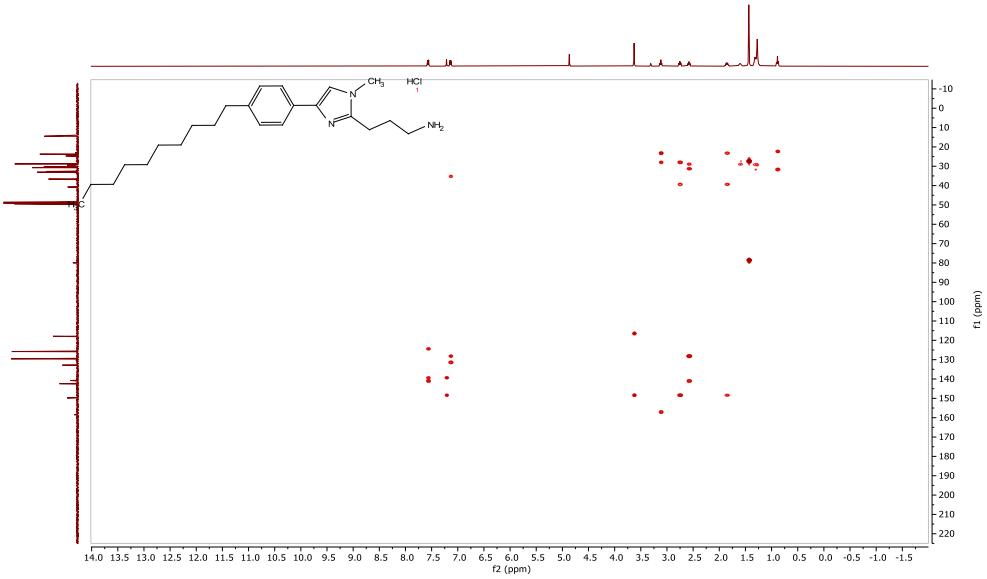

HMBC of **2.7c**

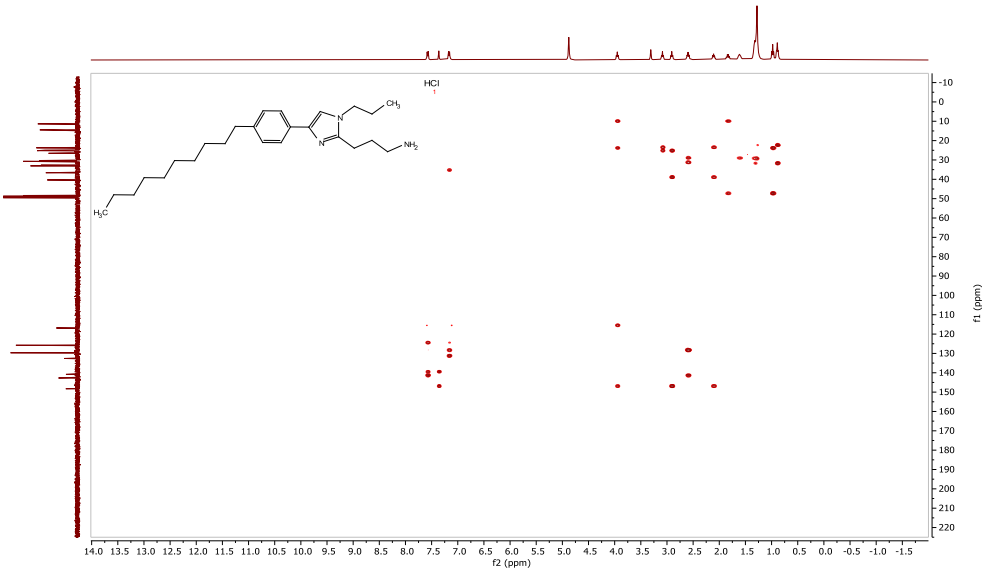

^{1}H NMR of **2.7a**

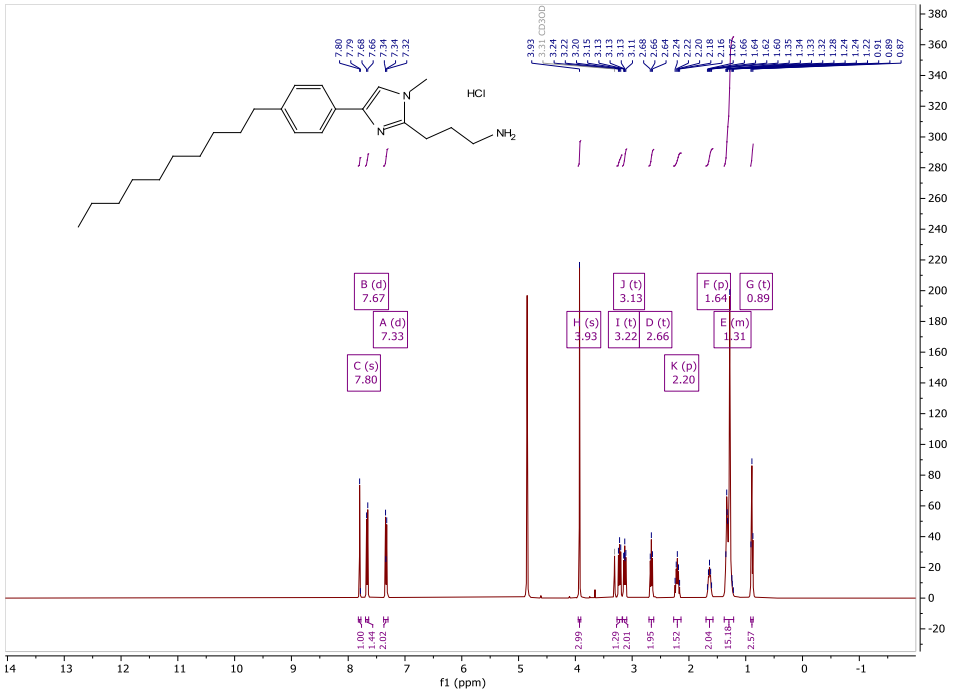

^{13}C NMR of **2.7a**

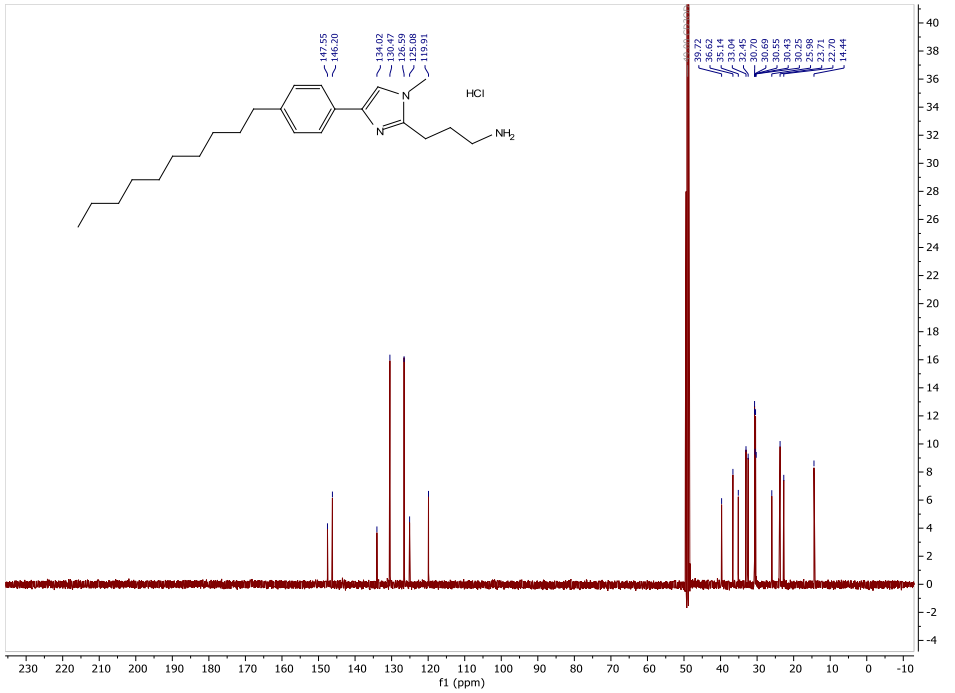

^{1}H NMR of **2.7b**

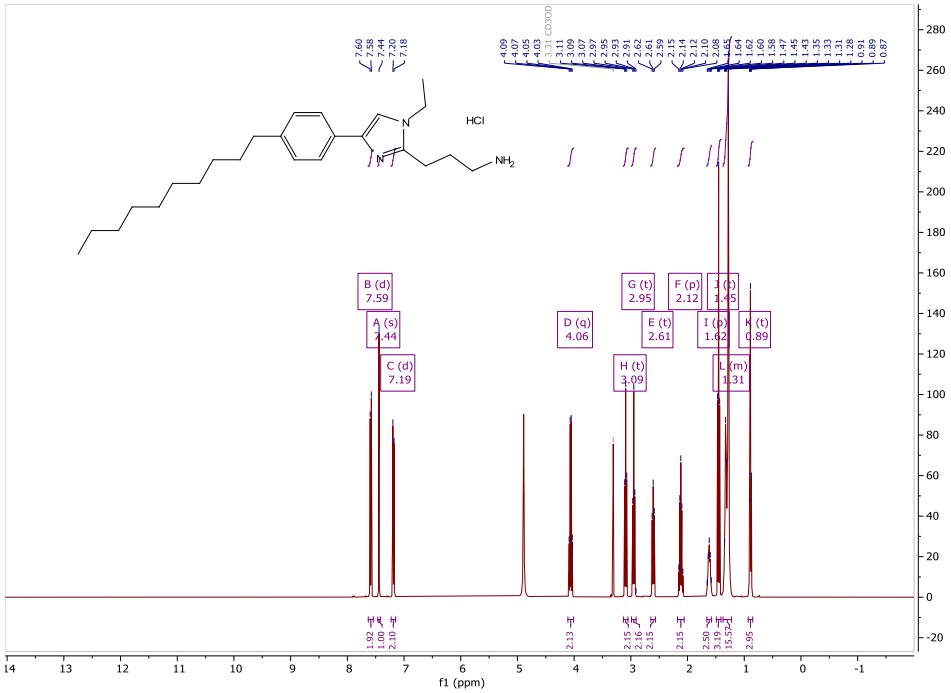

^{13}C NMR of **2.7b**

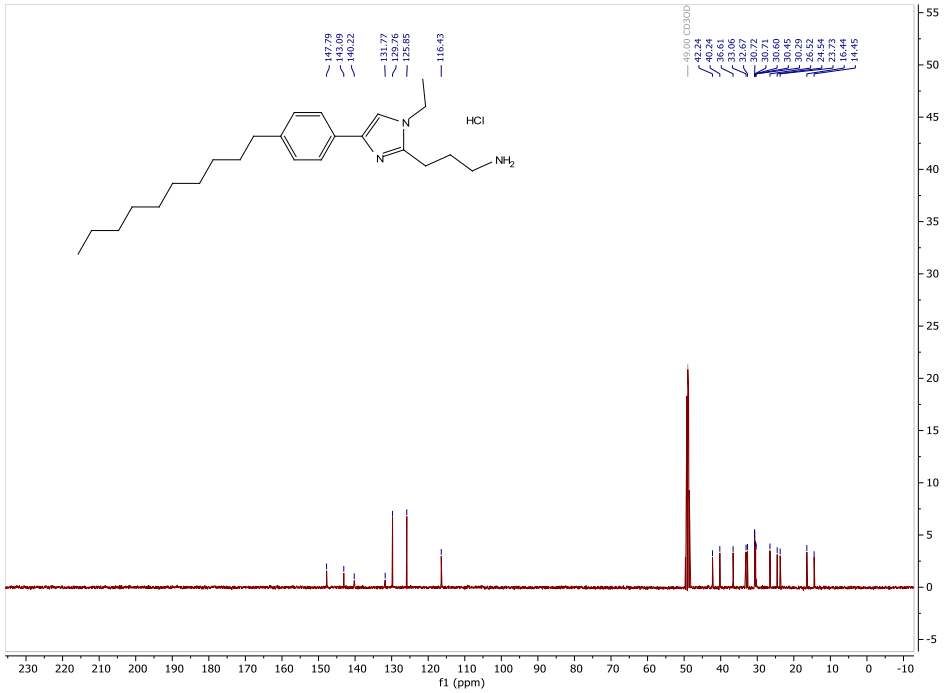

^{1}H NMR of **2.7c**

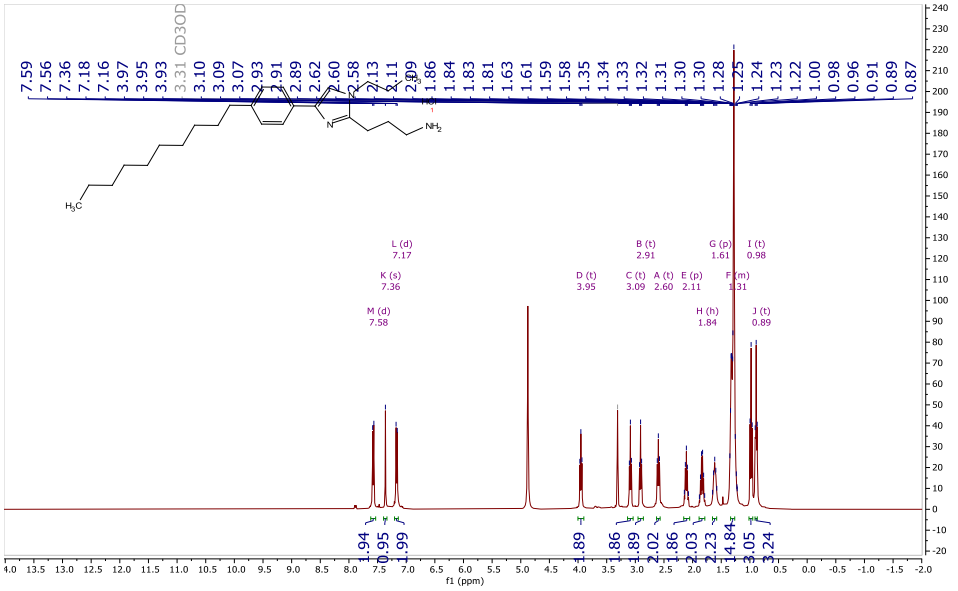

^{13}C NMR of **2.7c**

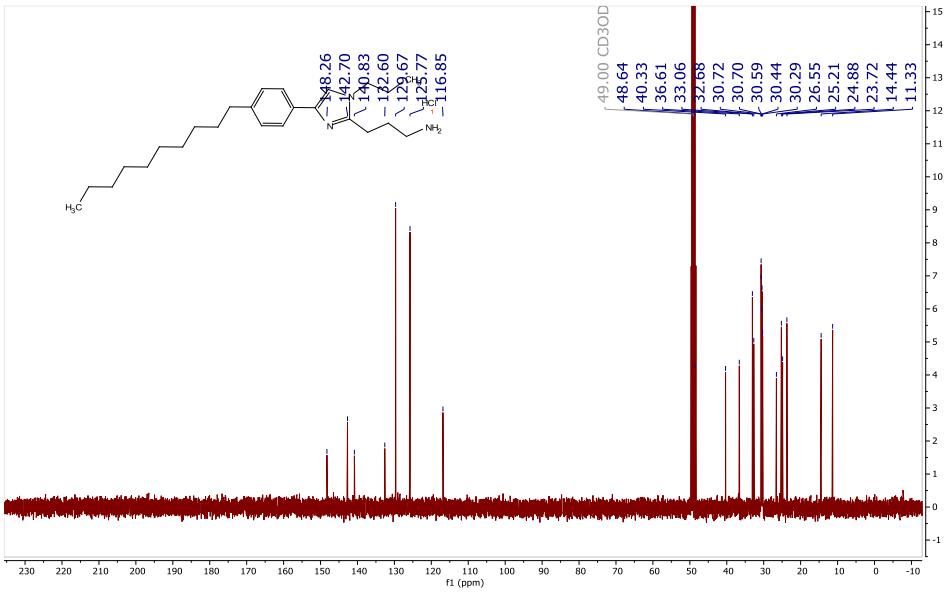

^{1}H NMR of **2.7d**

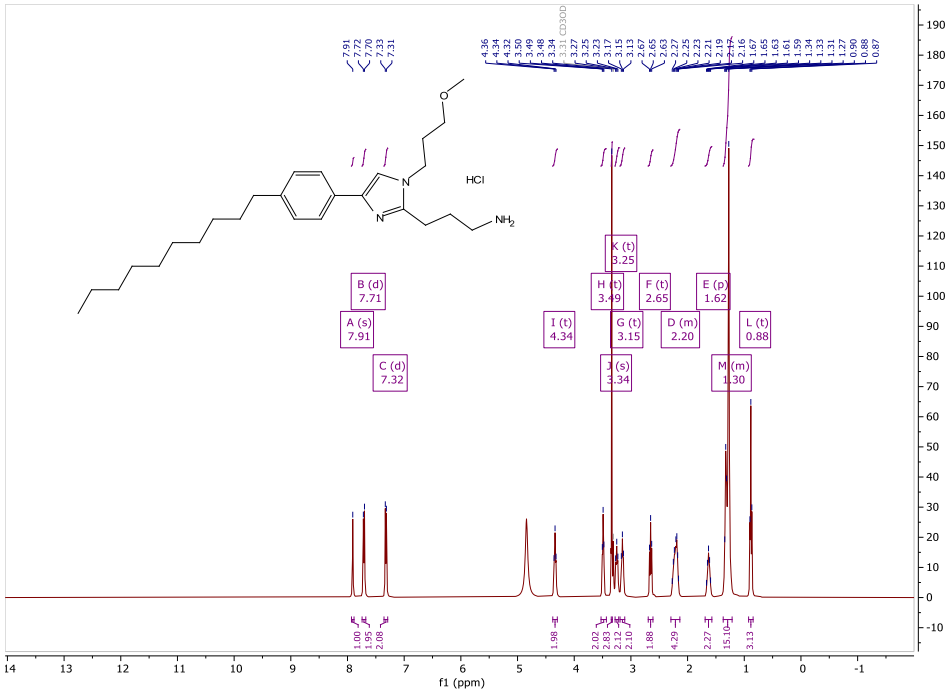

^{13}C NMR of **2.7d**

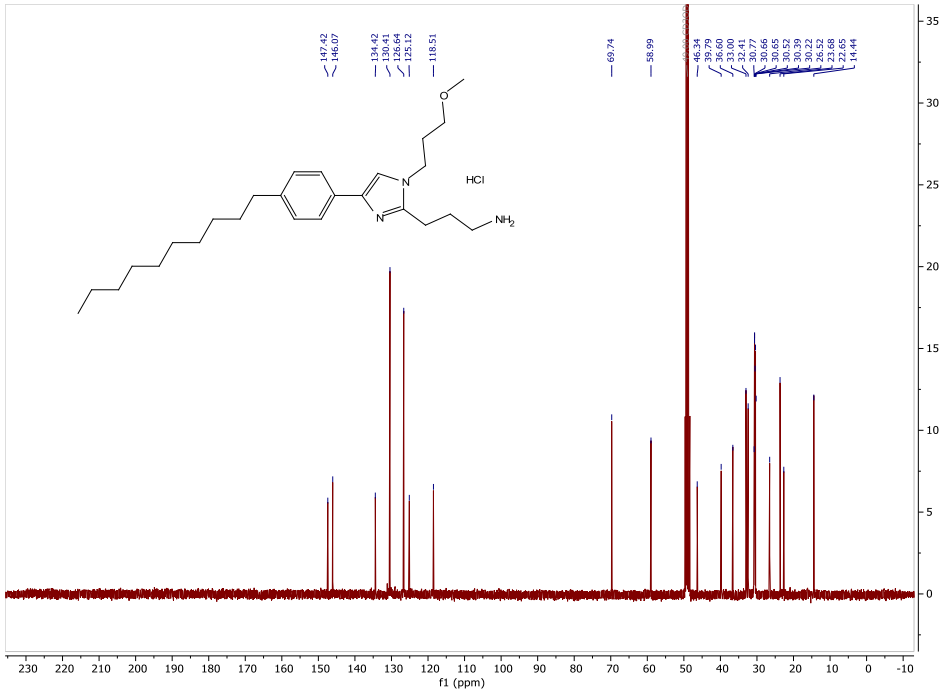

^{1}H NMR of **2.7e**

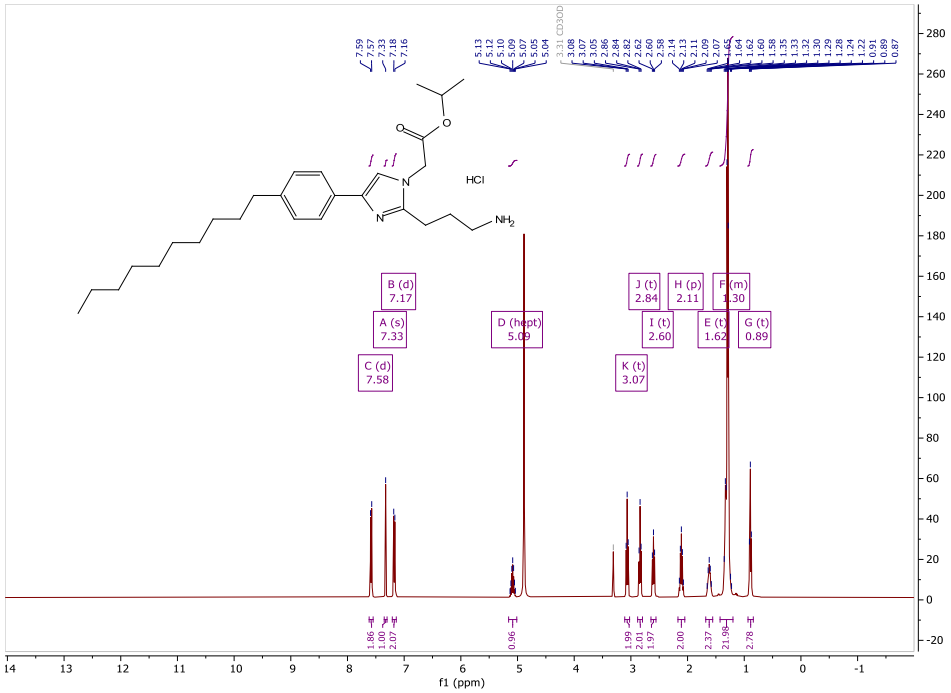

^{13}C NMR of **2.7e**

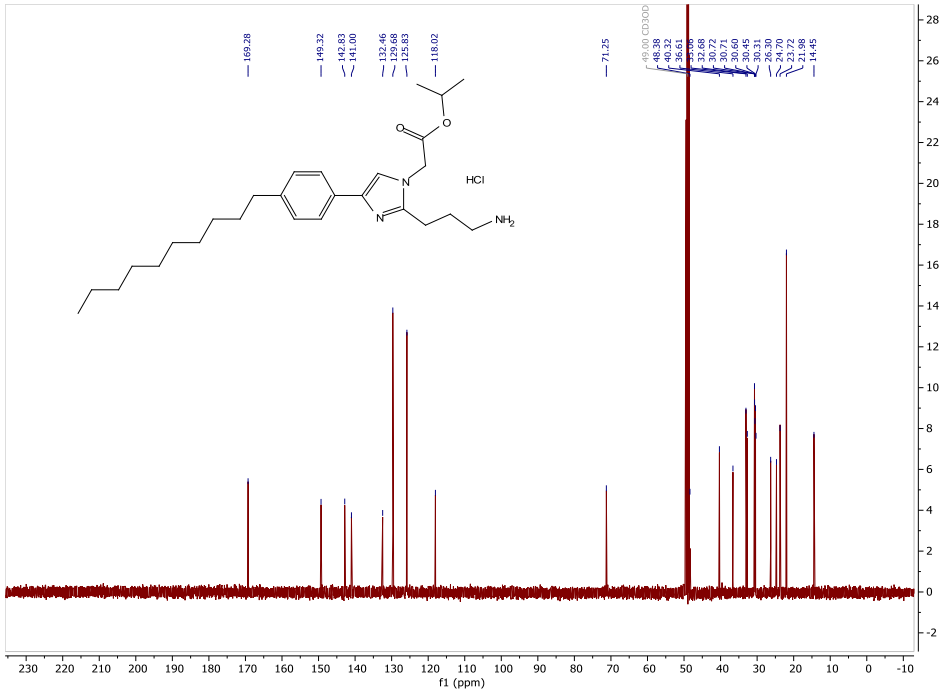

^{1}H NMR of **2.7g**

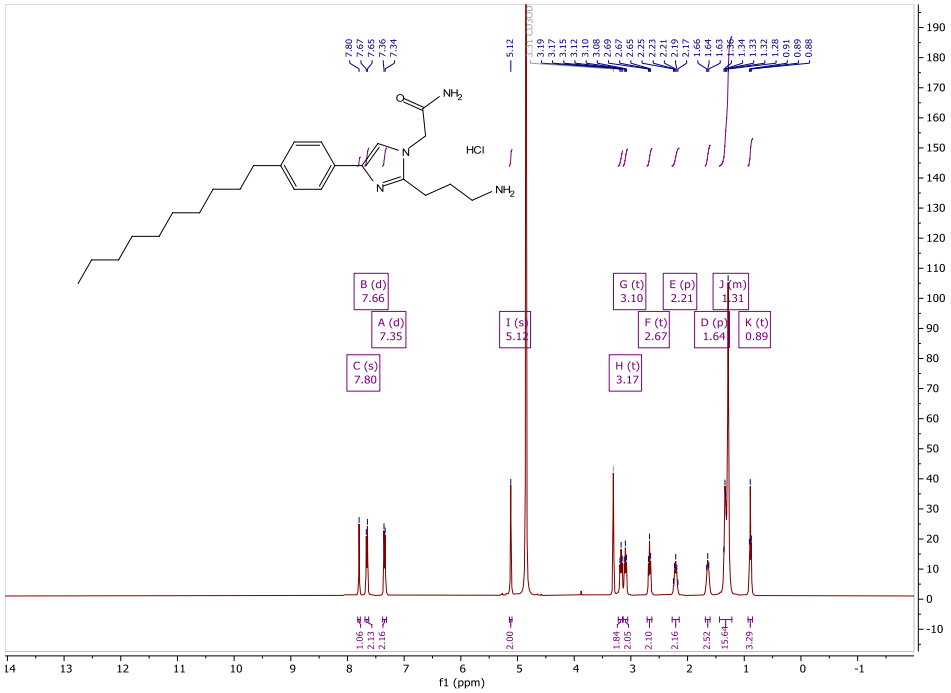

^{13}C NMR of **2.7g**

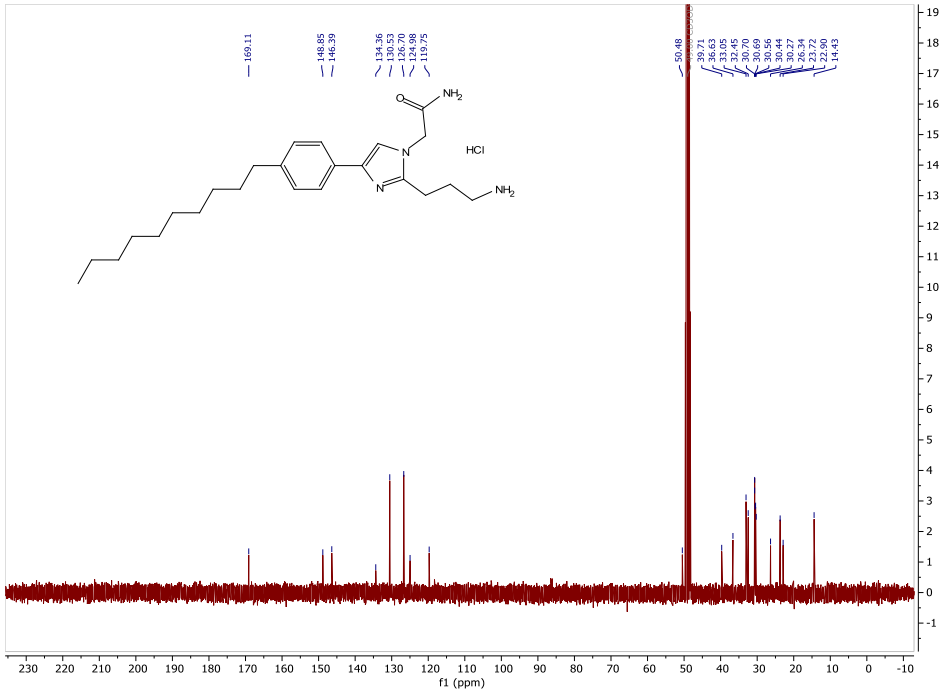

^{1}H NMR of **2.11a**

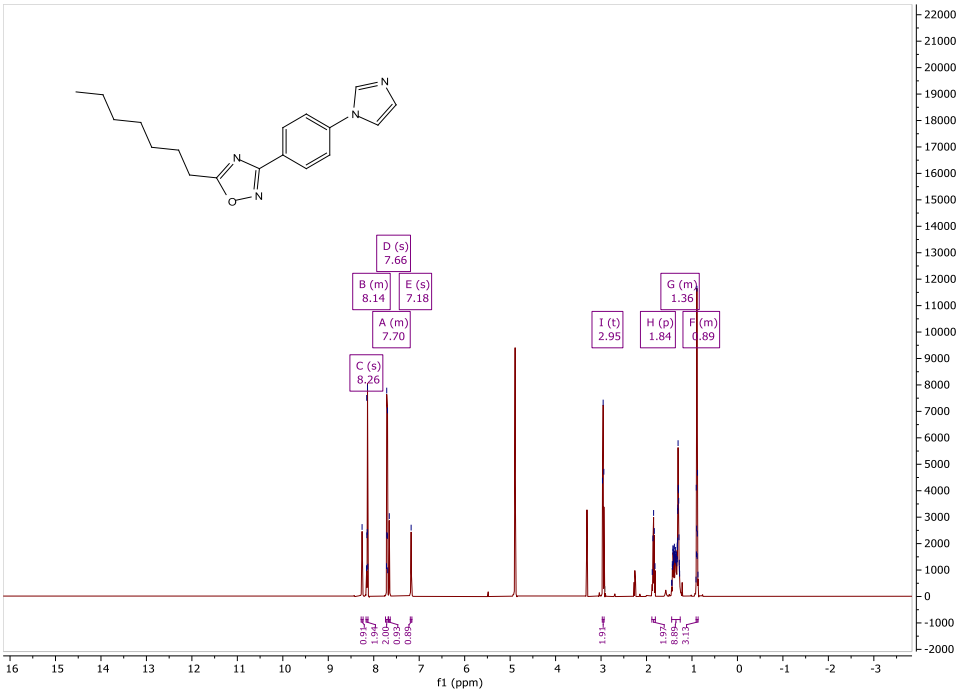

^{13}C NMR of **2.11a**

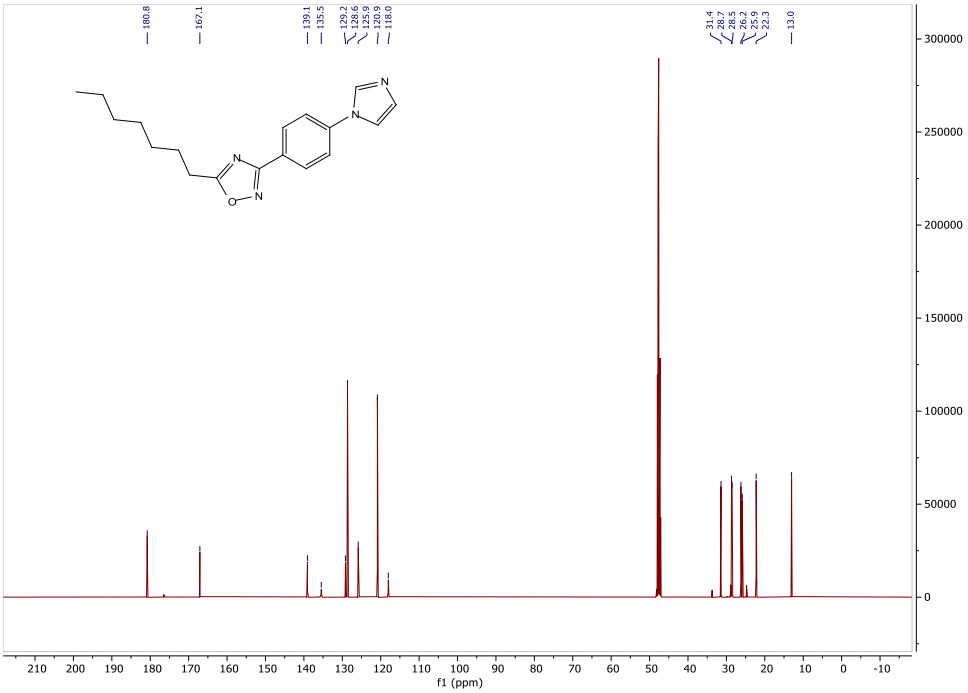

^{1}H NMR of **2.11b**

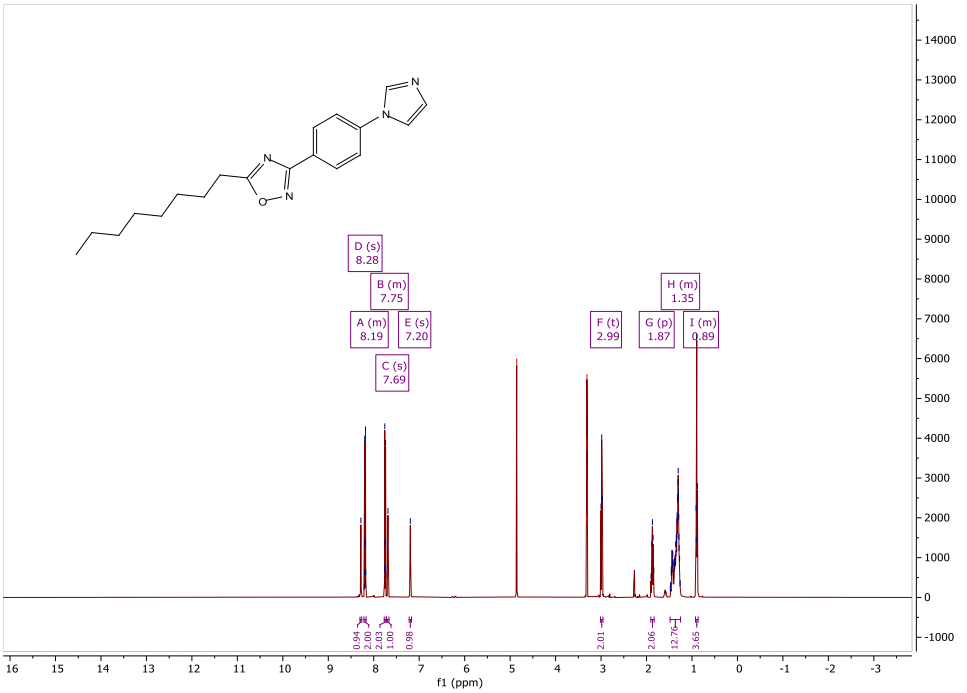

^{13}C NMR of **2.11b**

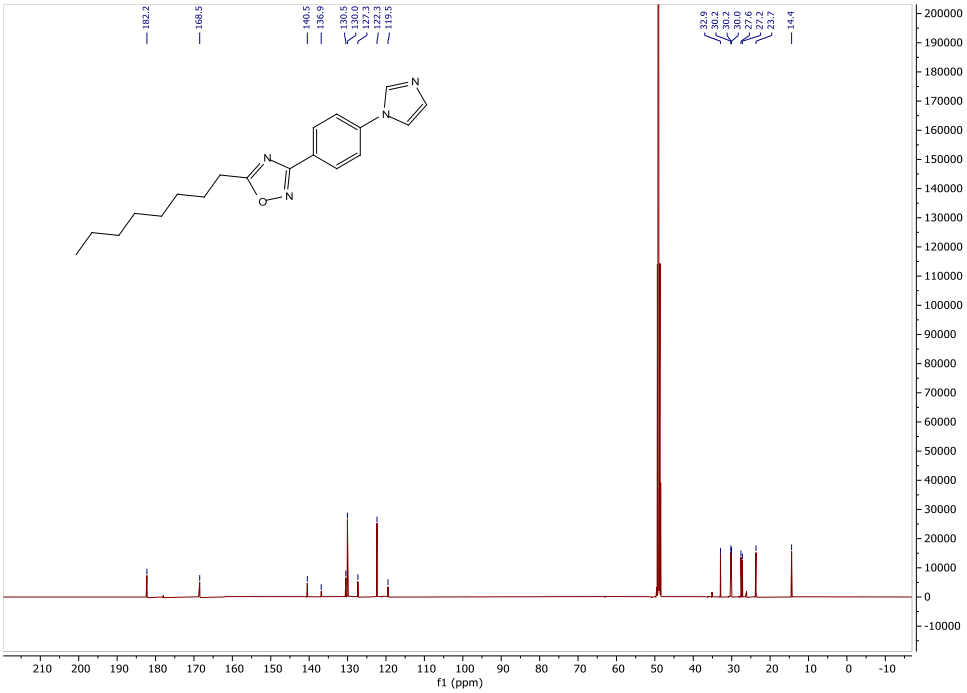

^{1}H NMR of **2.11c**

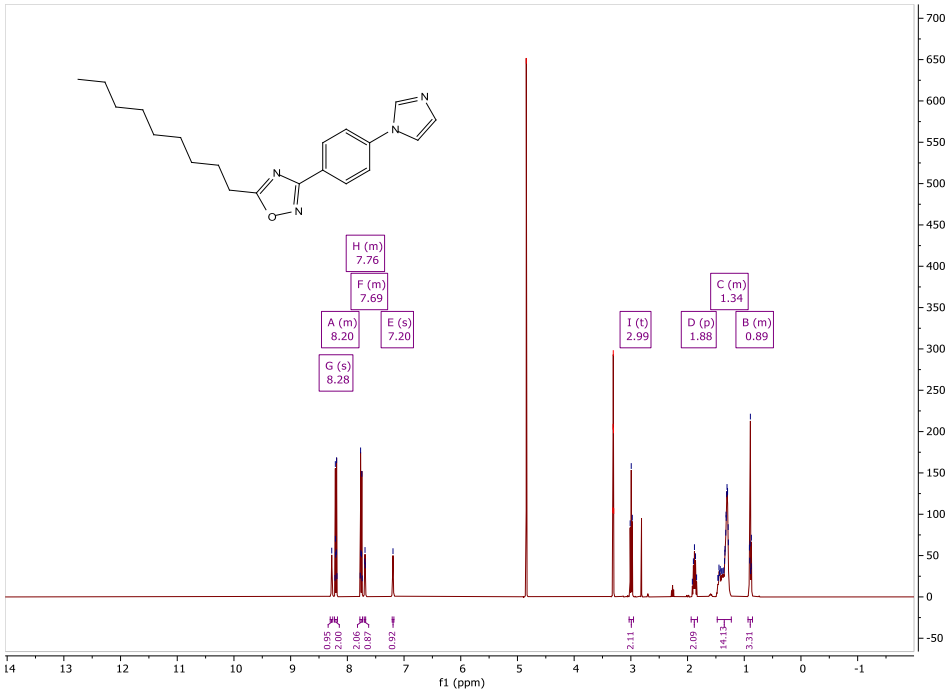

^{13}C NMR of **2.11c**

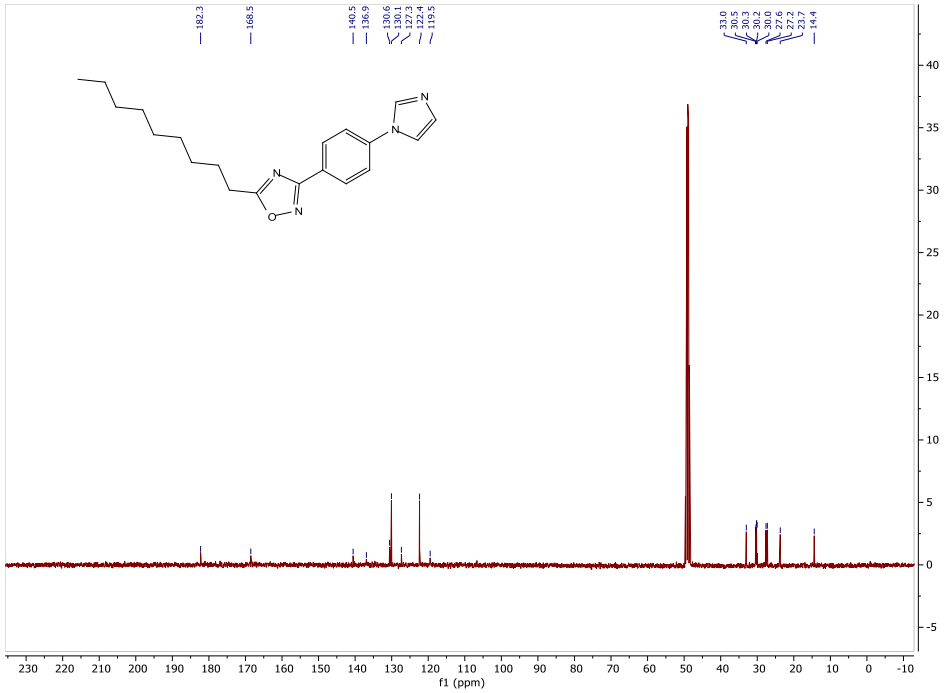

^{1}H NMR of **2.11d**

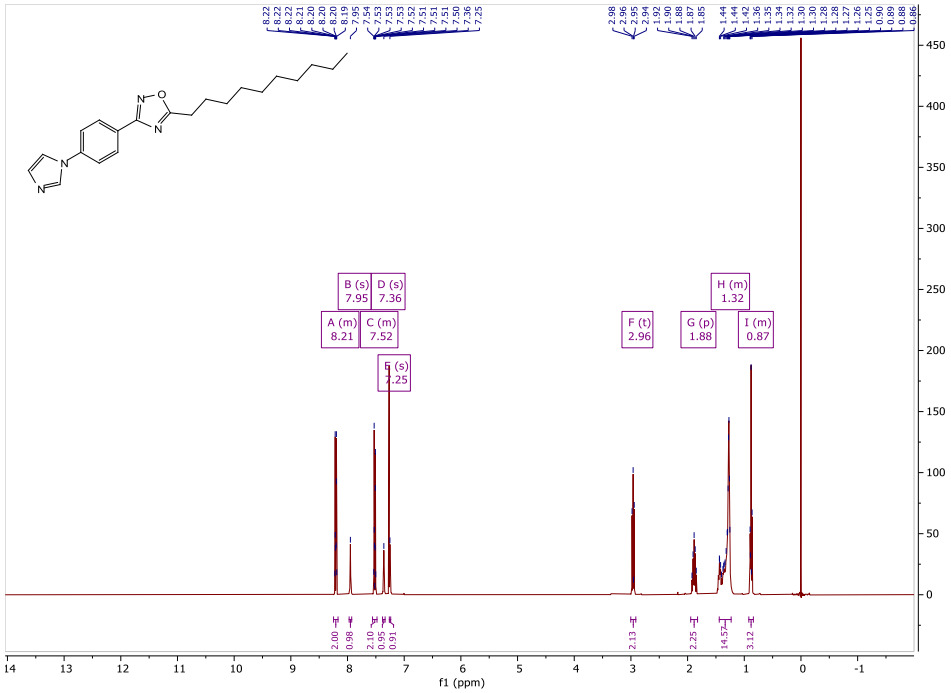

^{13}C NMR of **2.11d**

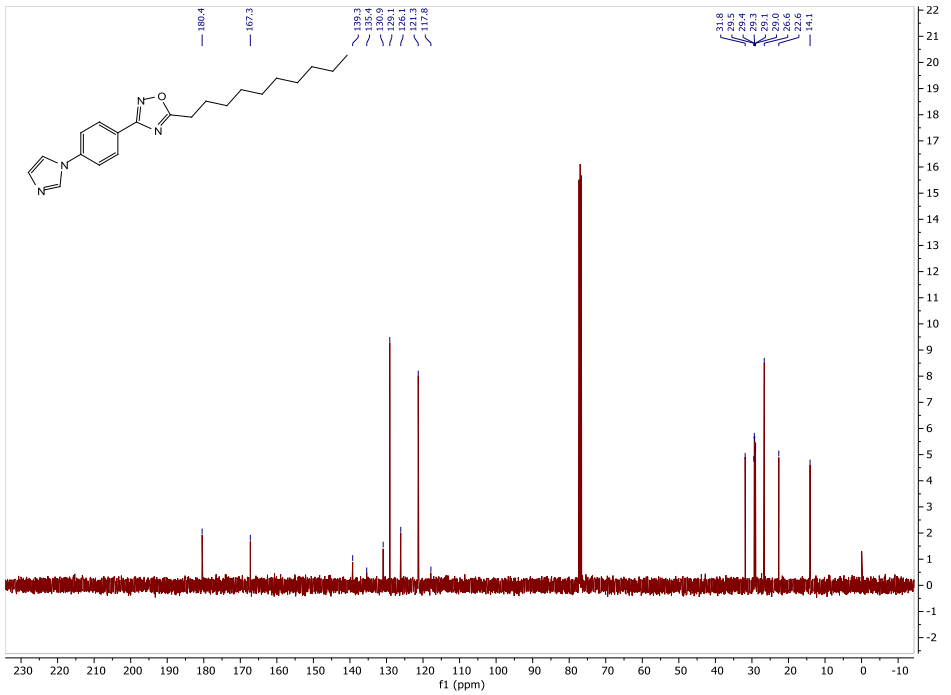

^{1}H NMR of **2.11e**

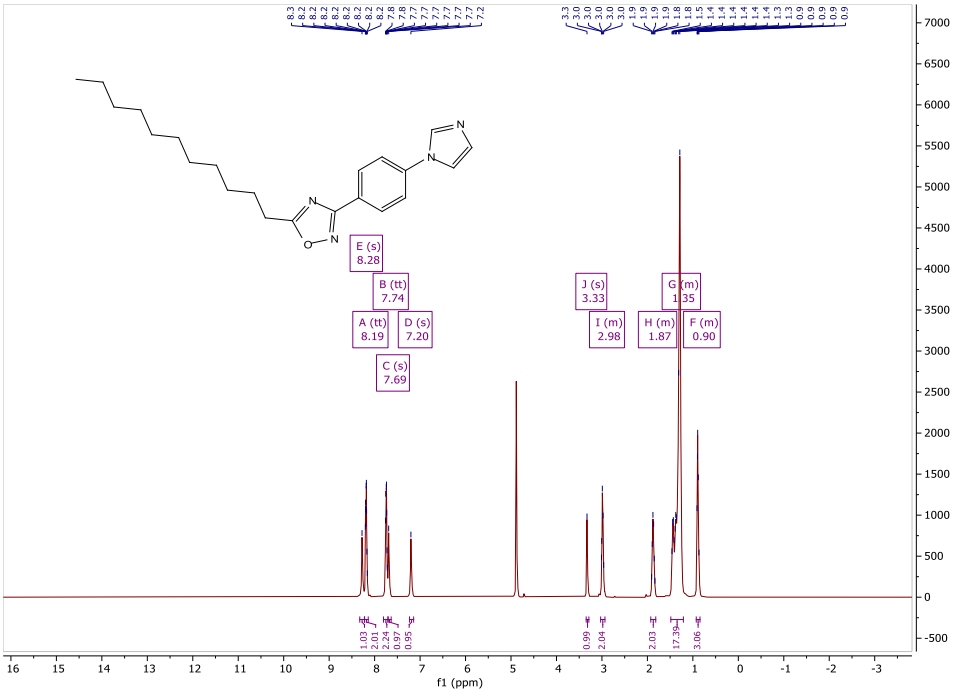

^{13}C NMR of **2.11e**

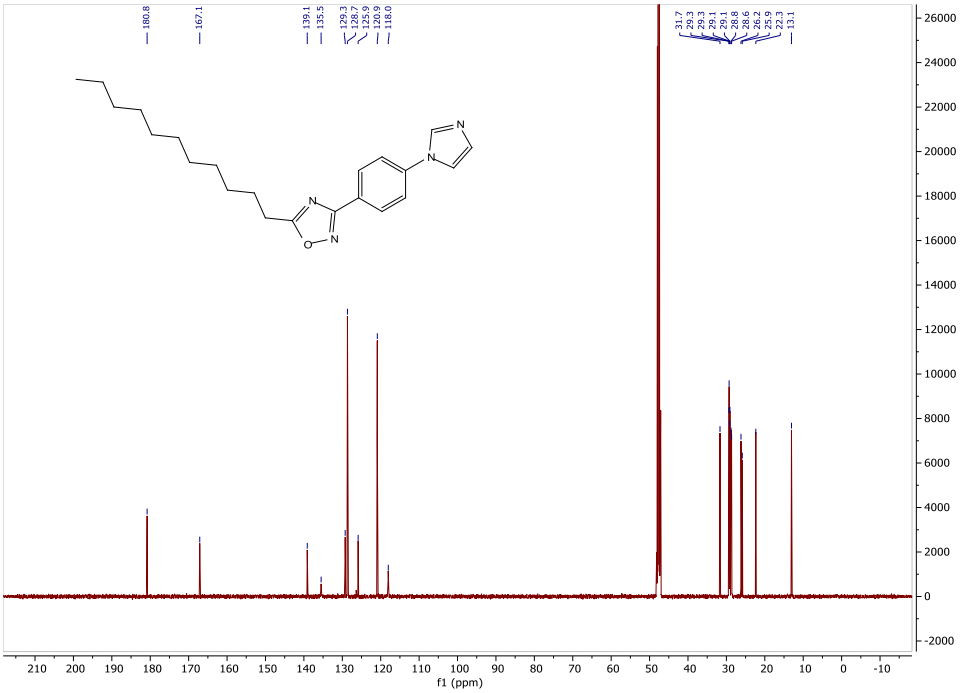

^{1}H NMR of **2.12a**

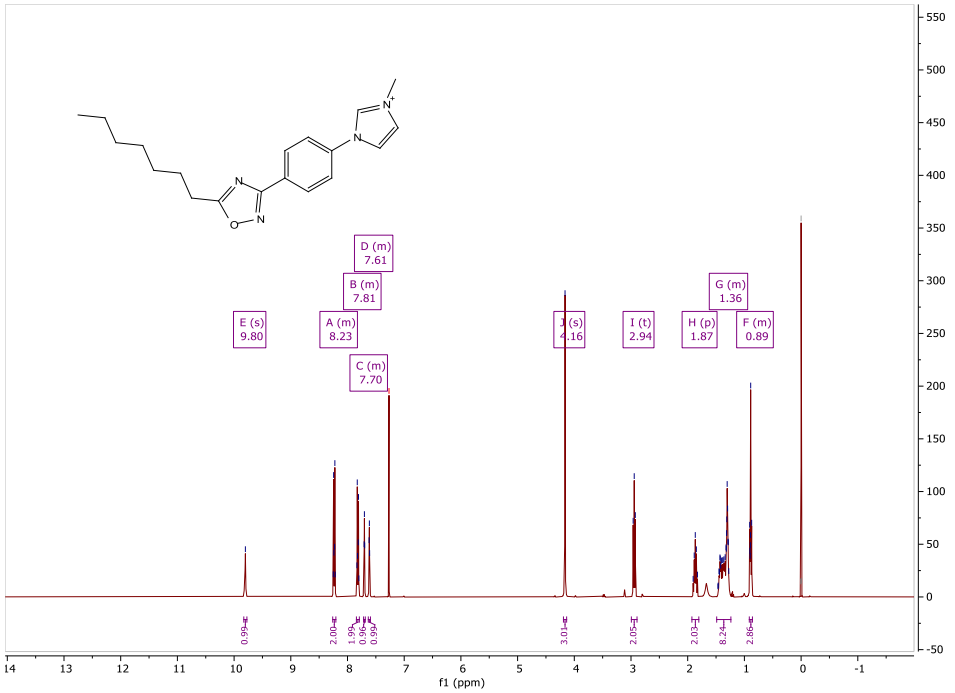

^{13}C NMR of **2.12a**

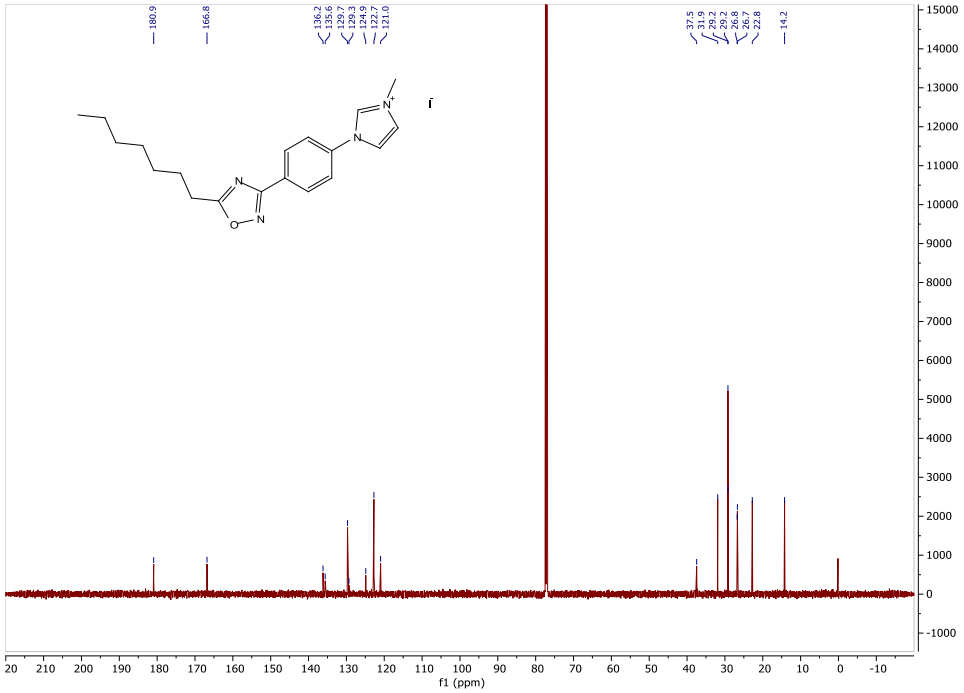

^{1}H NMR of **2.12b**

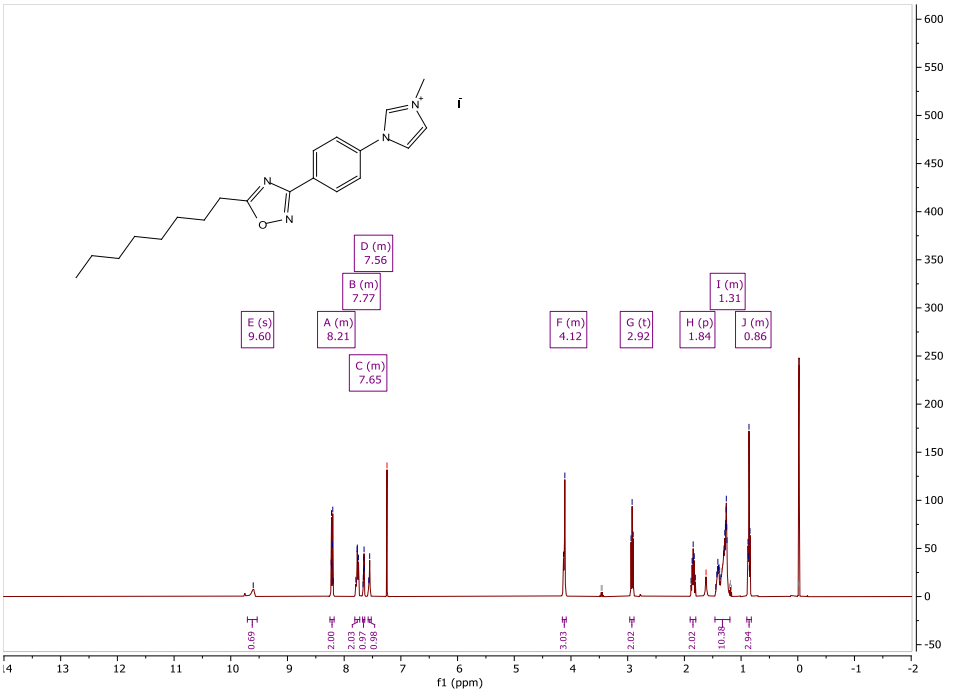

^{13}C NMR of **2.12b**

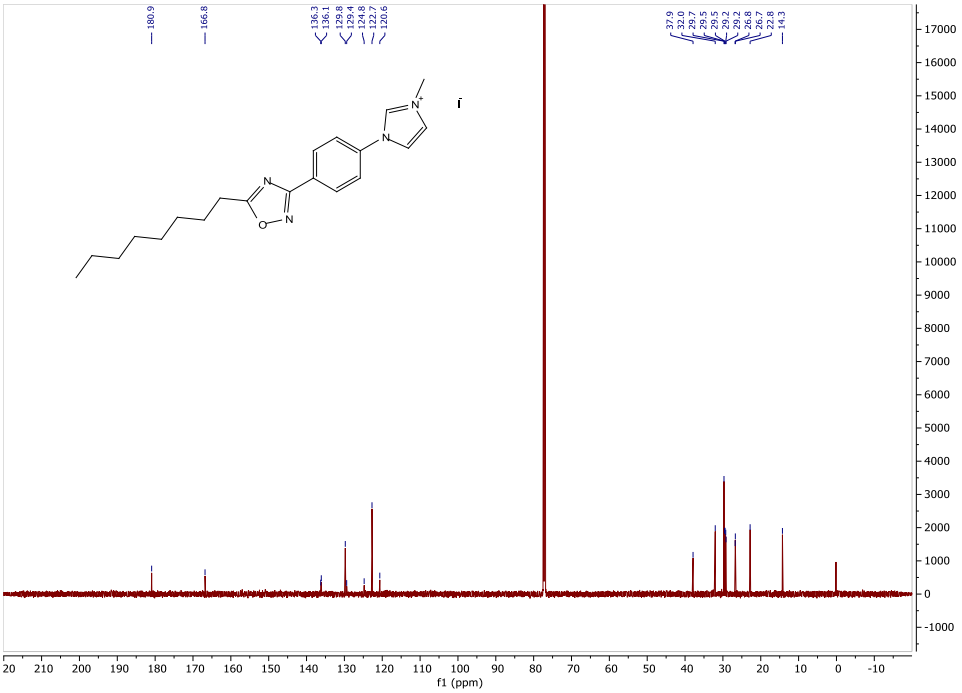

^{1}H NMR of **2.12c**

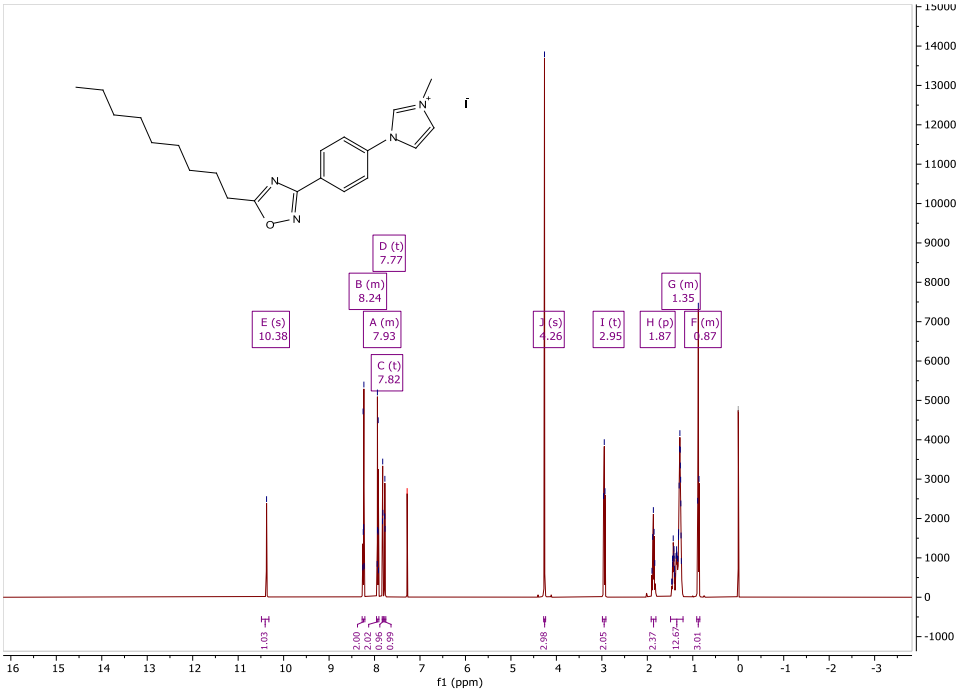

^{13}C NMR of **2.12c**

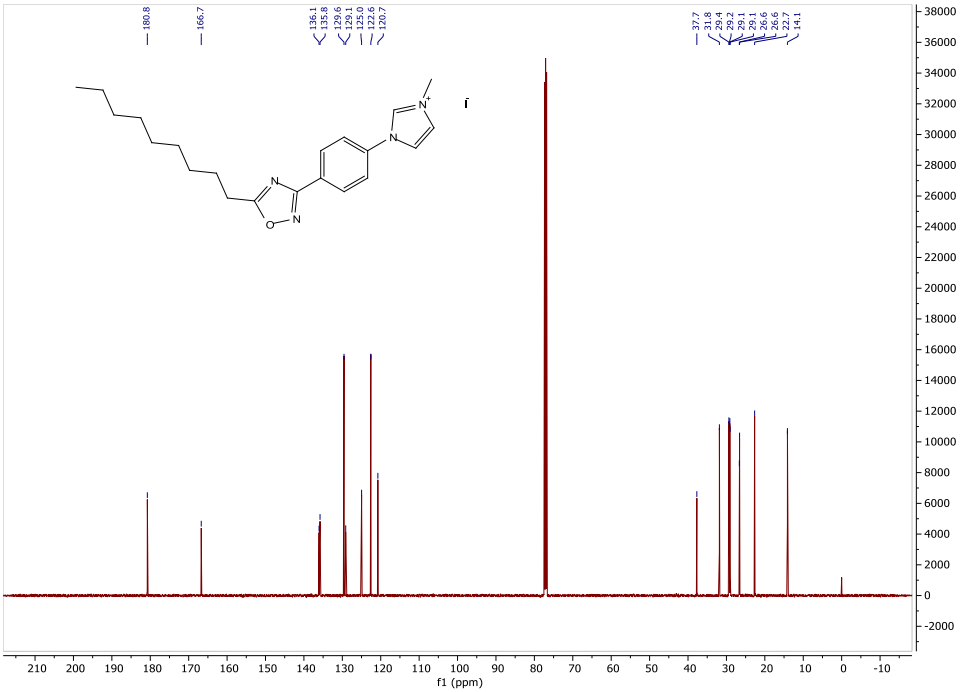

^{1}H NMR of **2.12d**

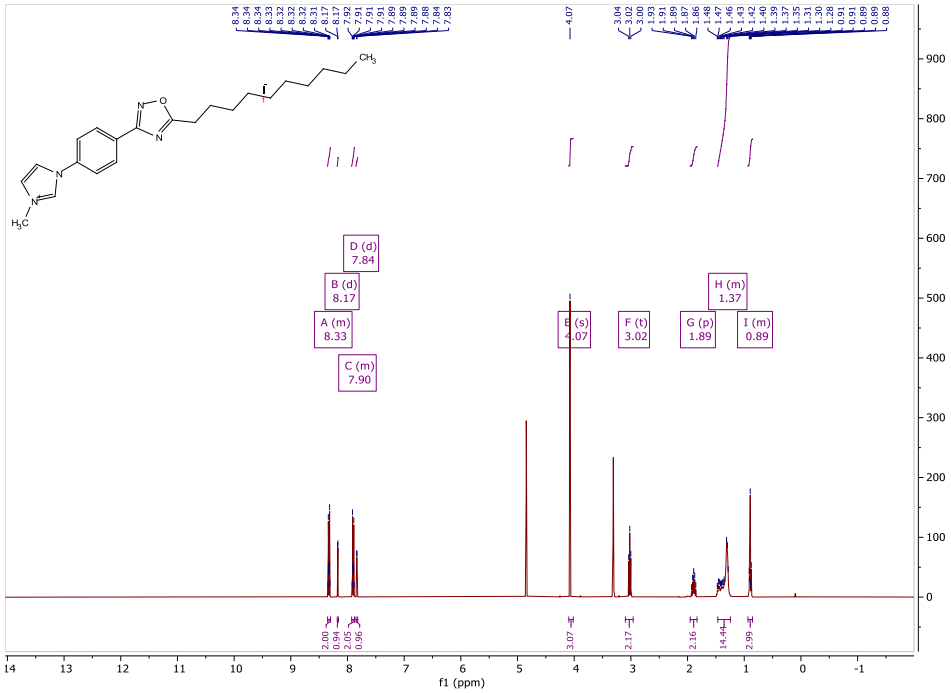

^{13}C NMR of **2.12d**

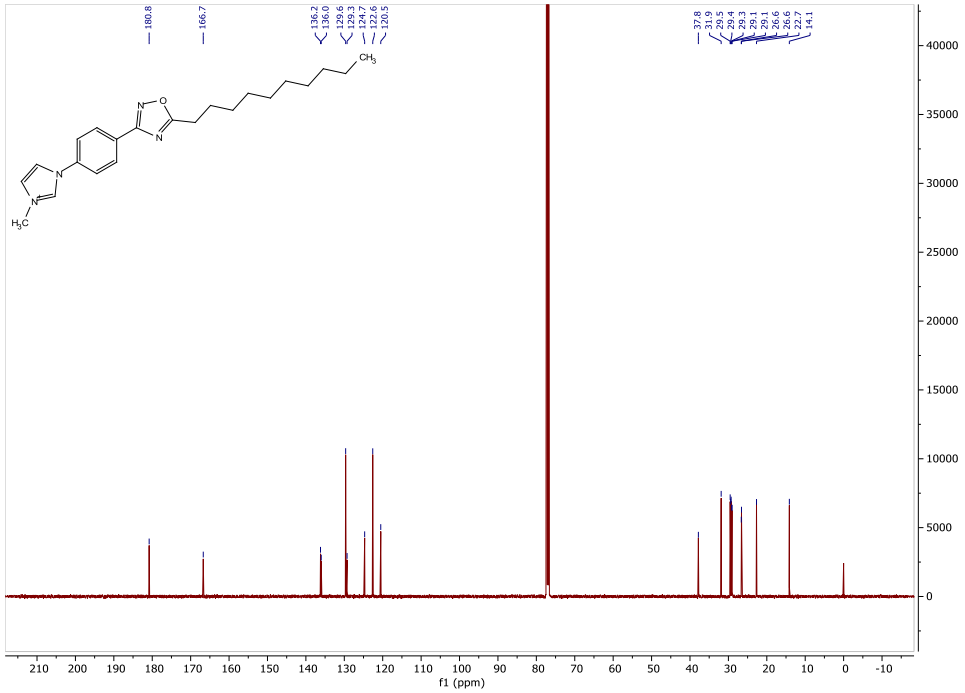

^{1}H NMR of **2.12e**

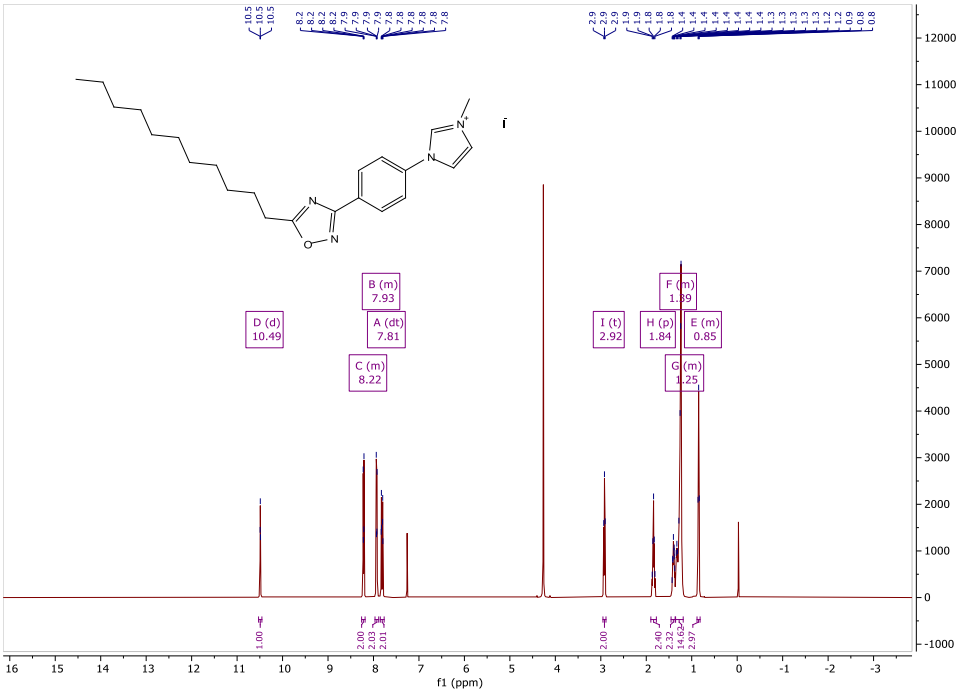

^{13}C NMR of **2.12e**

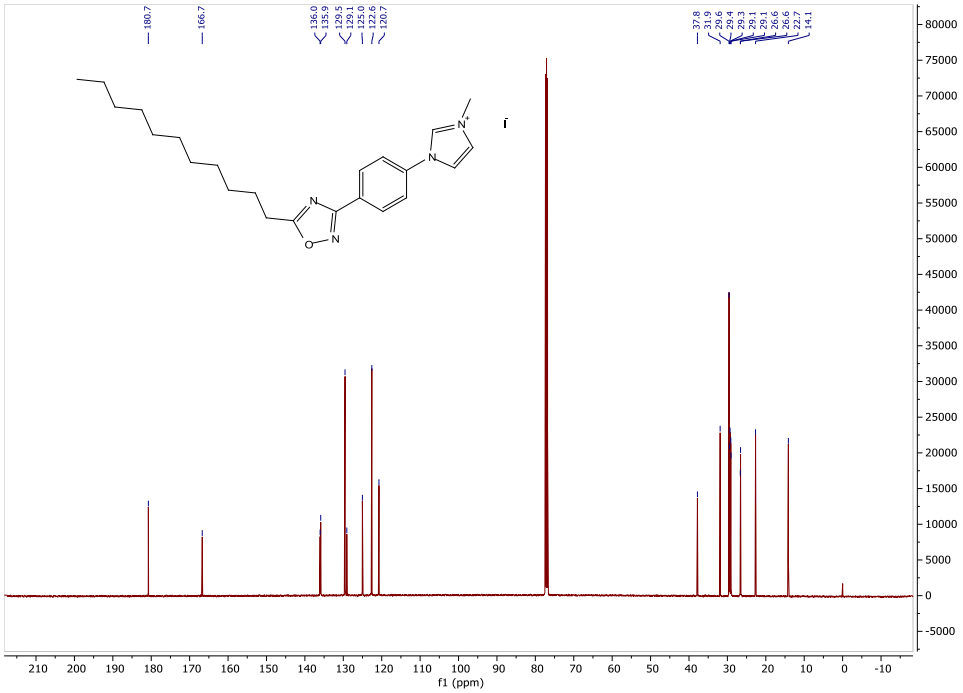

Appendix B. Spectra for Chapter 3

^{1}H NMR of **3.5a**

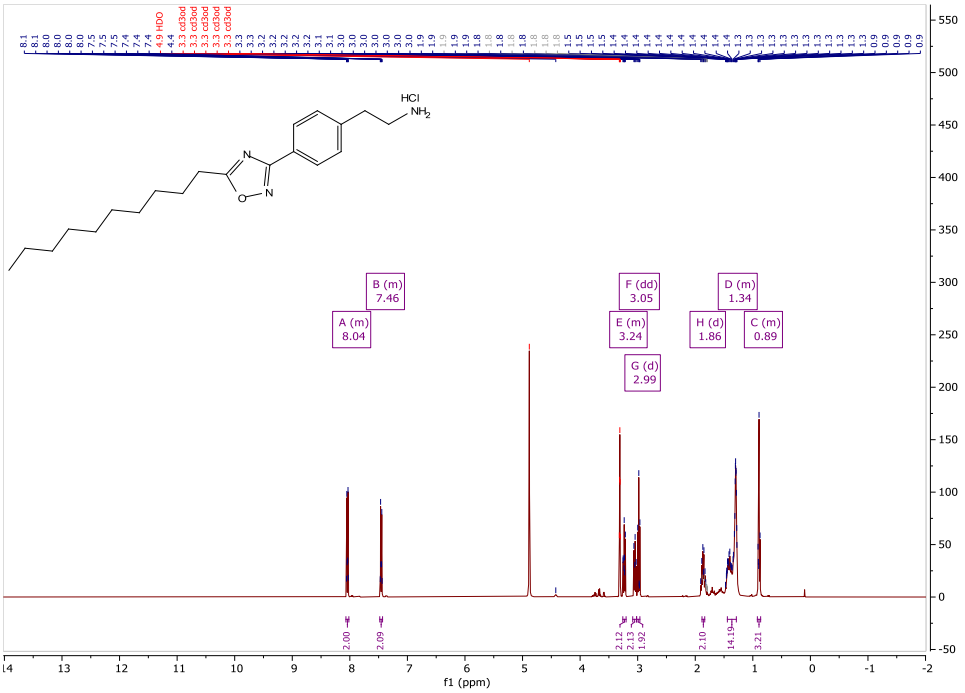

^{13}C NMR of **3.5a**

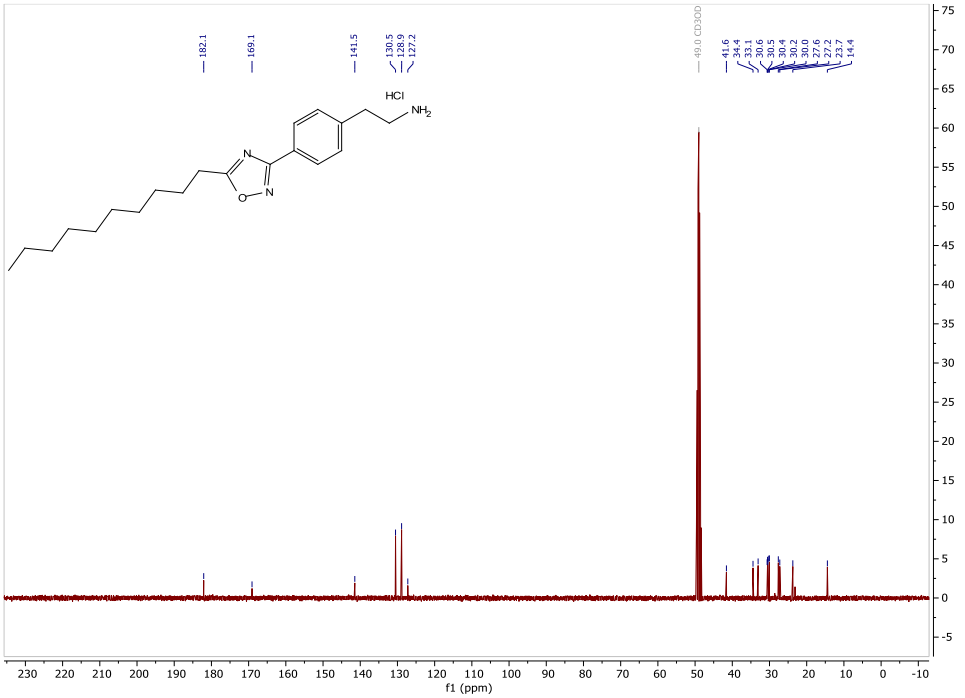

^{1}H NMR of **3.5b**

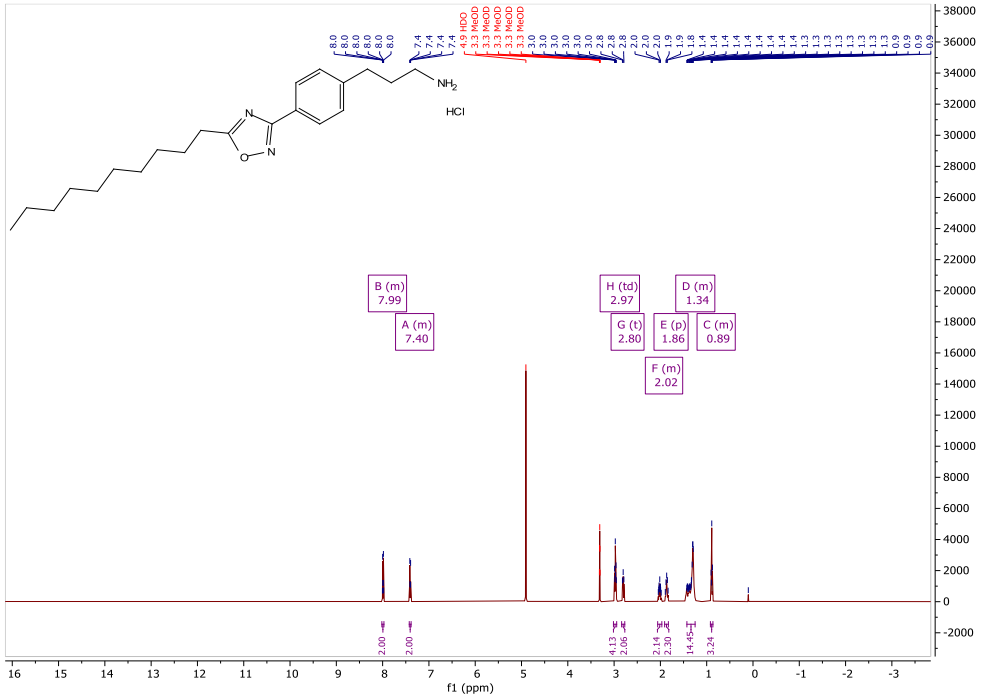

^{13}C NMR of **3.5b**

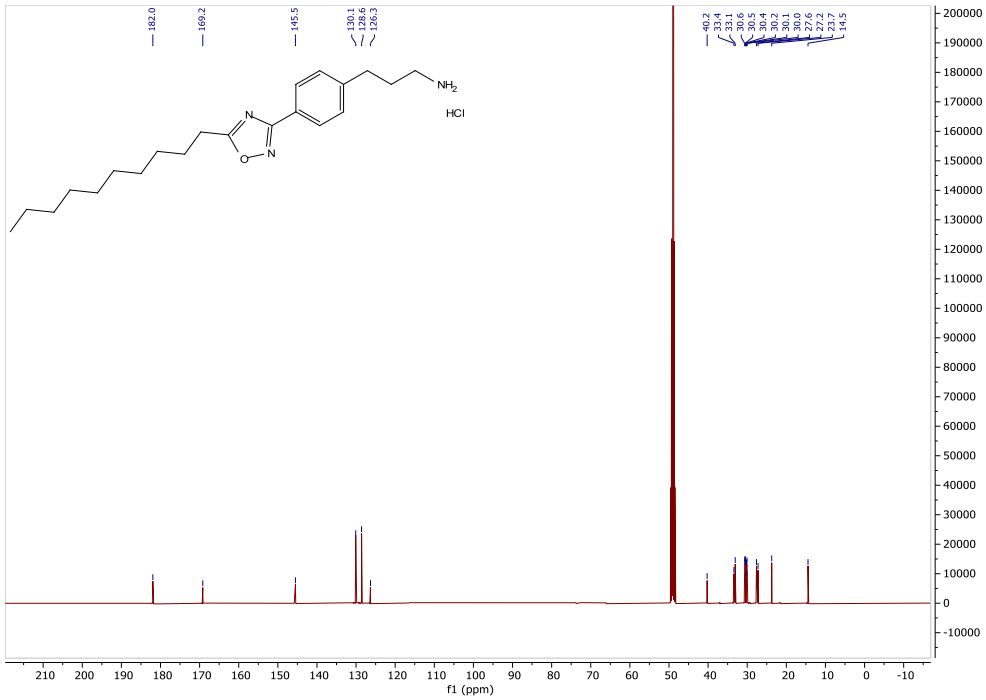

^{1}H NMR of **3.8a**

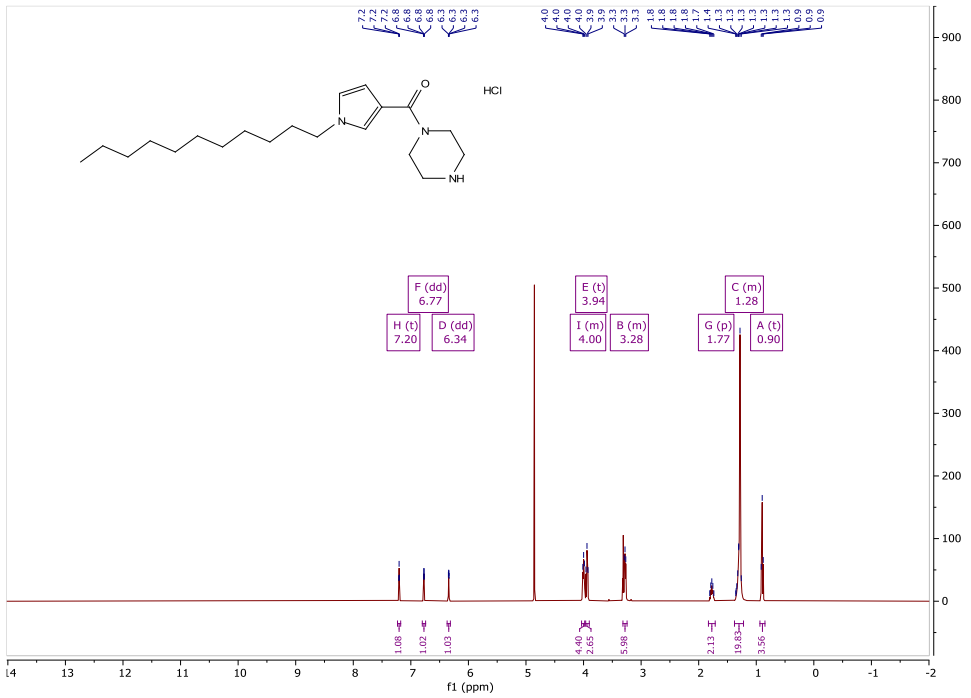

^{13}C NMR of **3.8a**

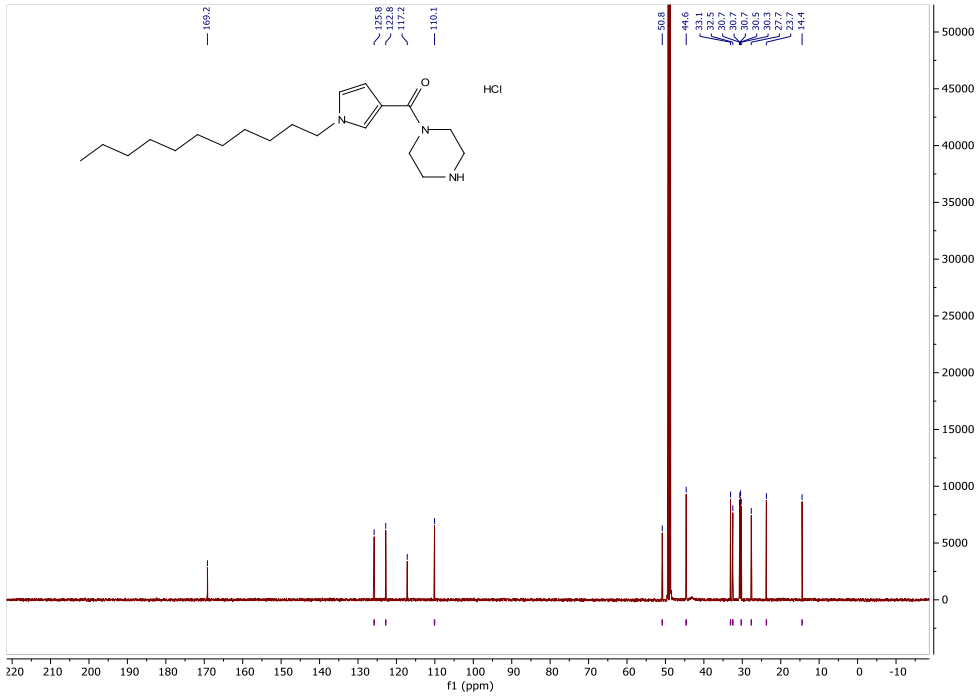

^{1}H NMR of **3.8b**

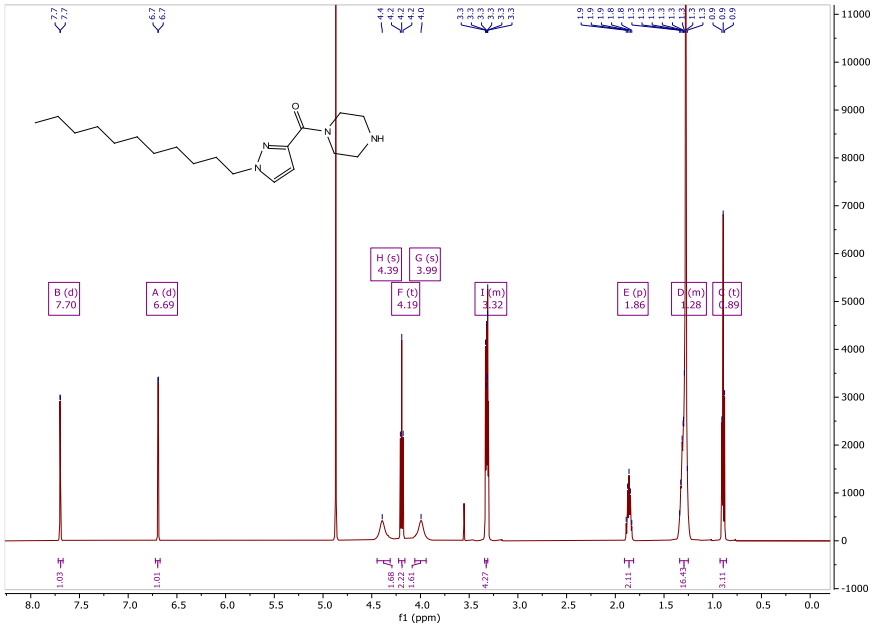

^{13}C NMR of **3.8b**

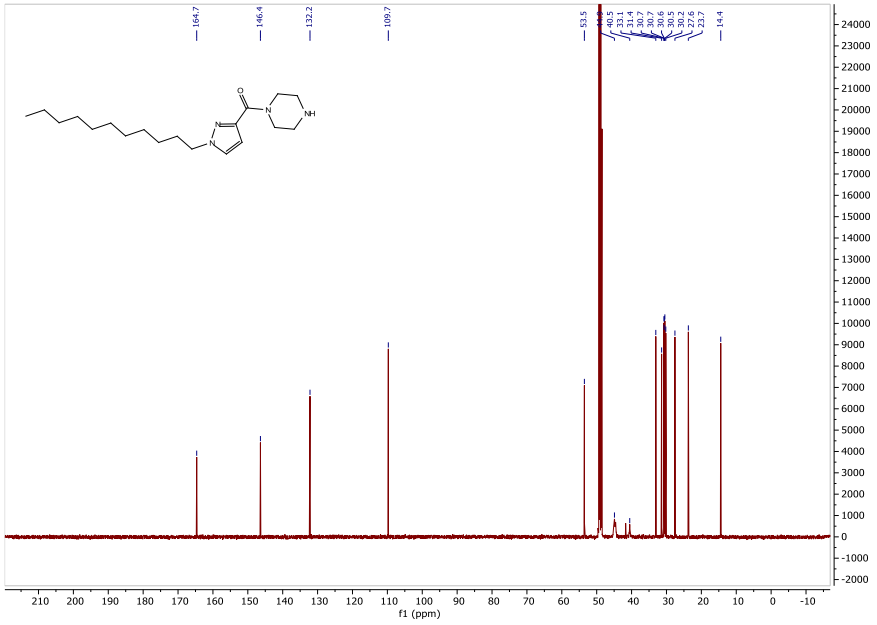

^{1}H NMR of **3.8c**

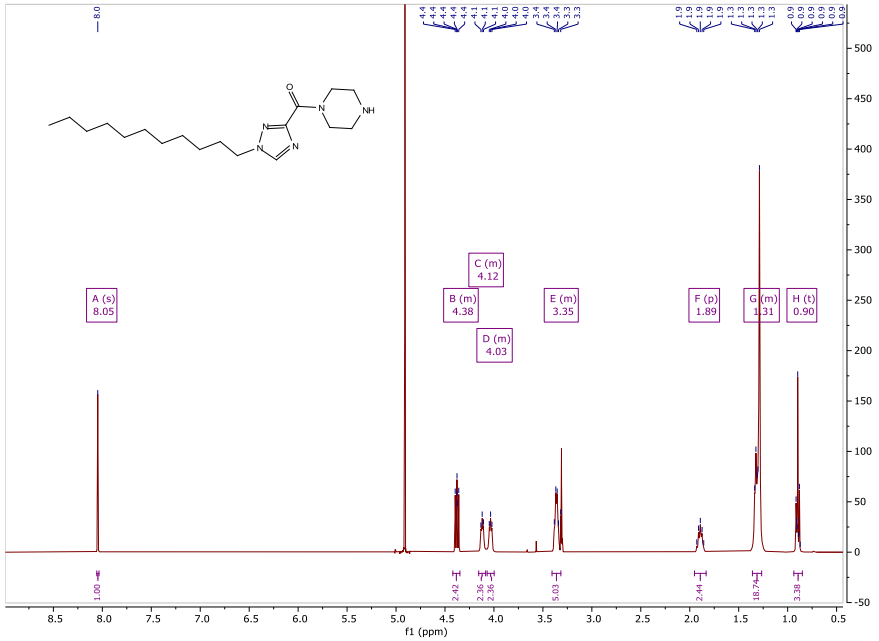

^{13}C NMR of **3.8c**

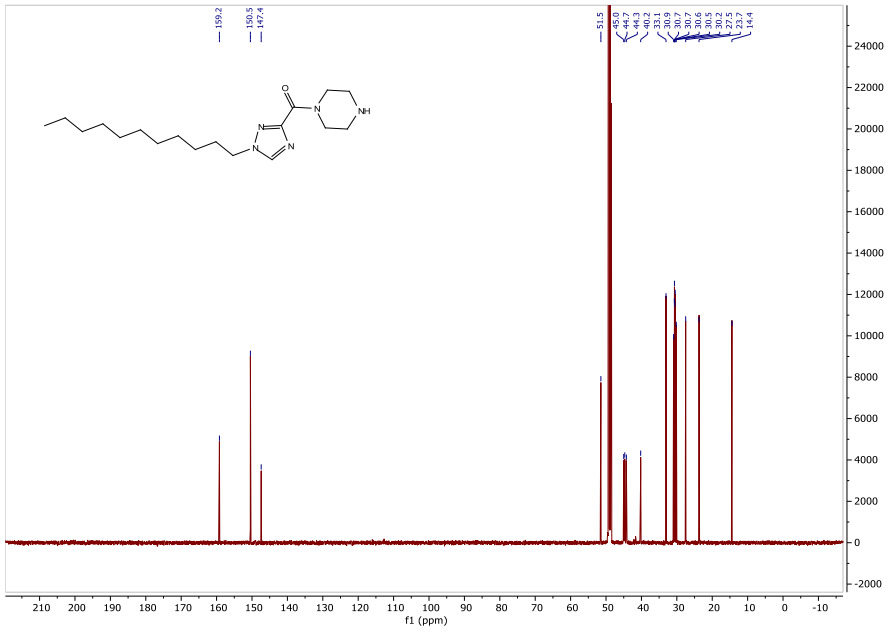

^{1}H NMR of **3.8d**

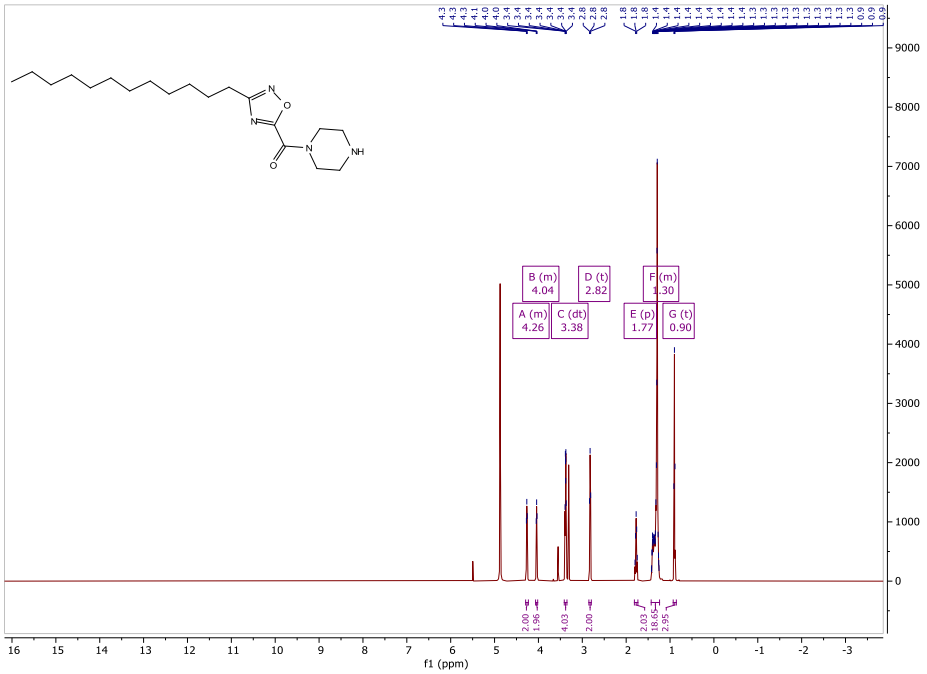

^{13}C NMR of **3.8d**

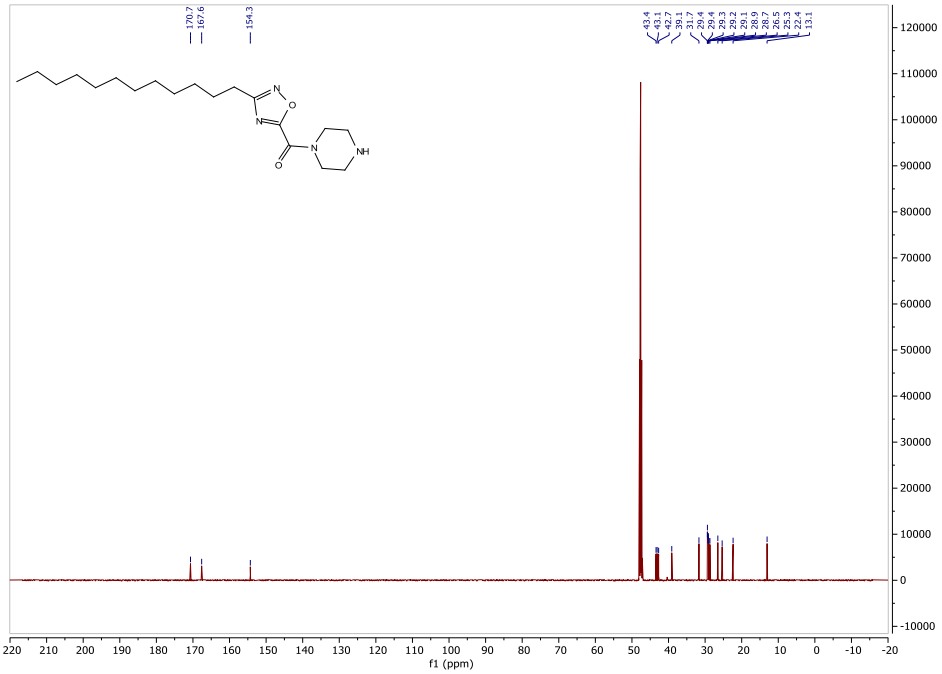

^{1}H NMR of **3.16a**

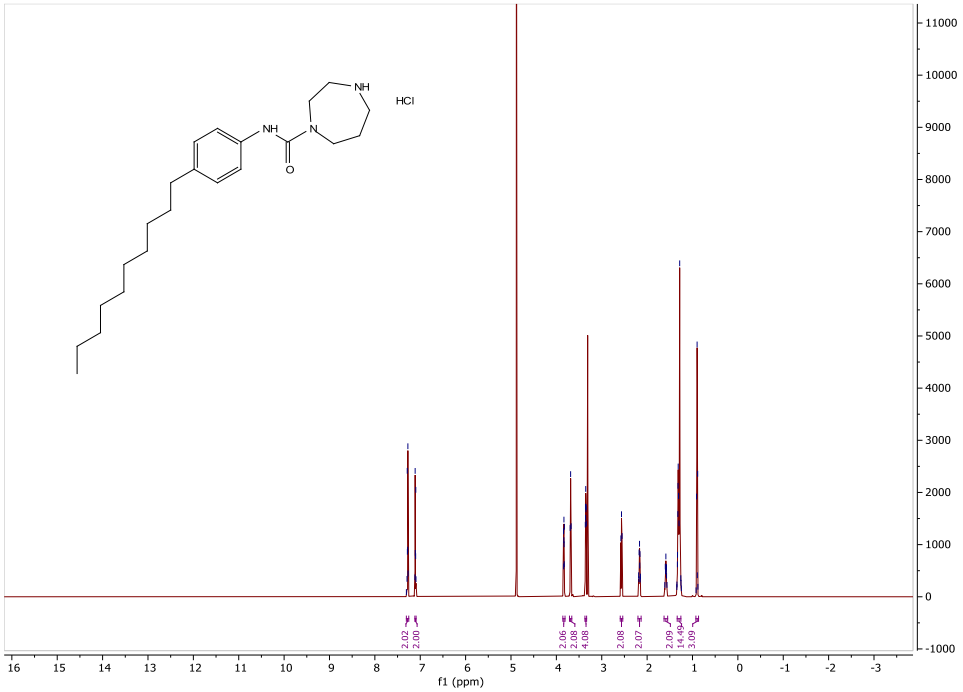

^{13}C NMR of **3.16a**

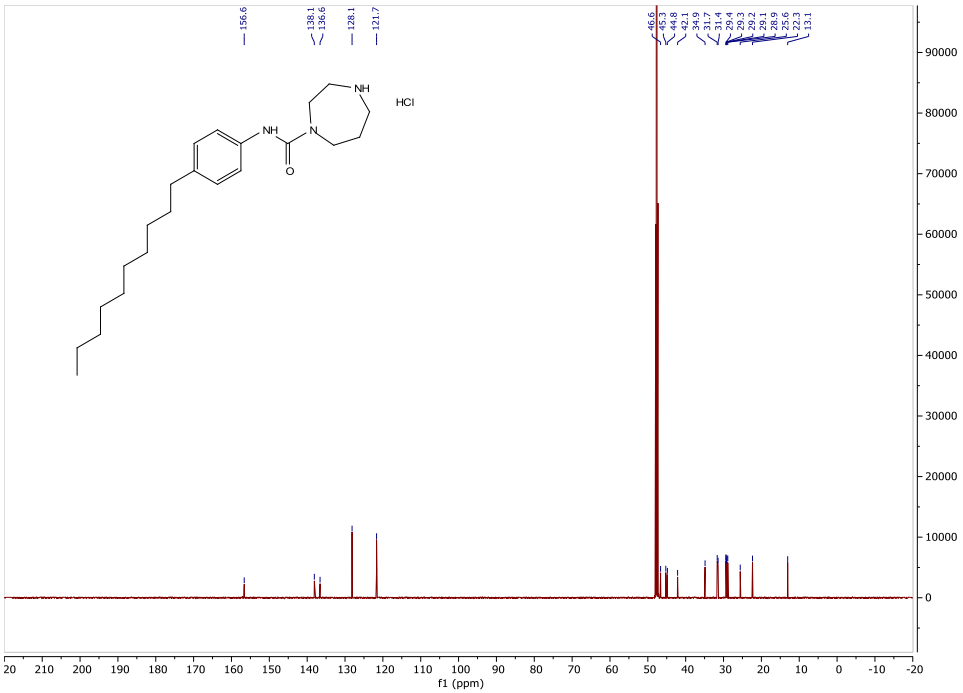

^{1}H NMR of **3.16b**

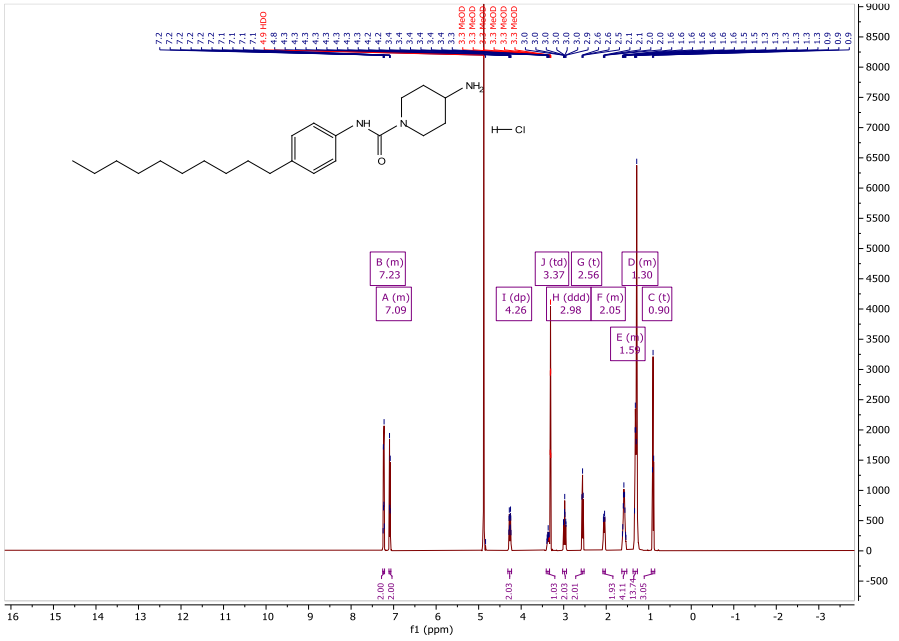

^{13}C NMR of **3.16b**

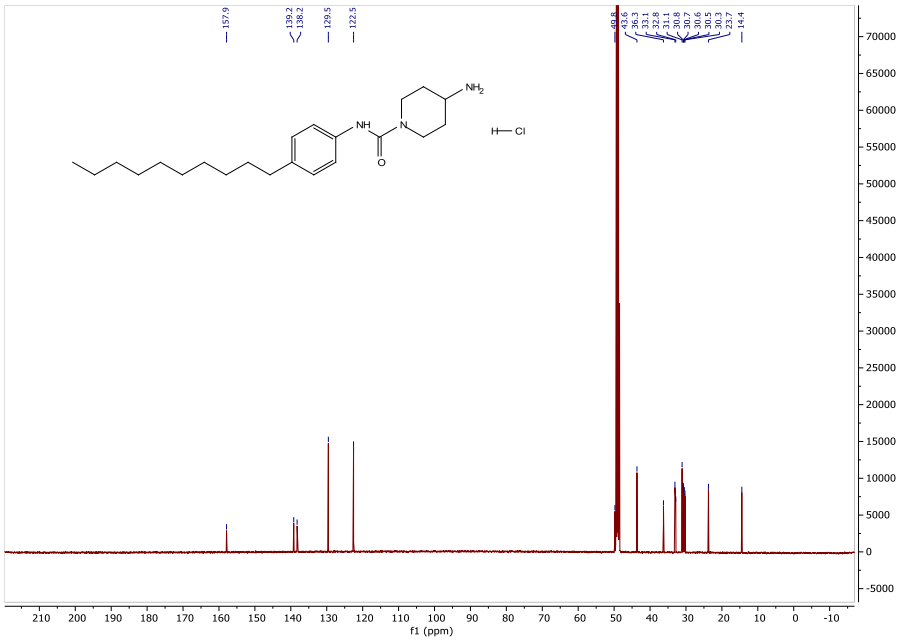

^{1}H NMR of **3.16c**

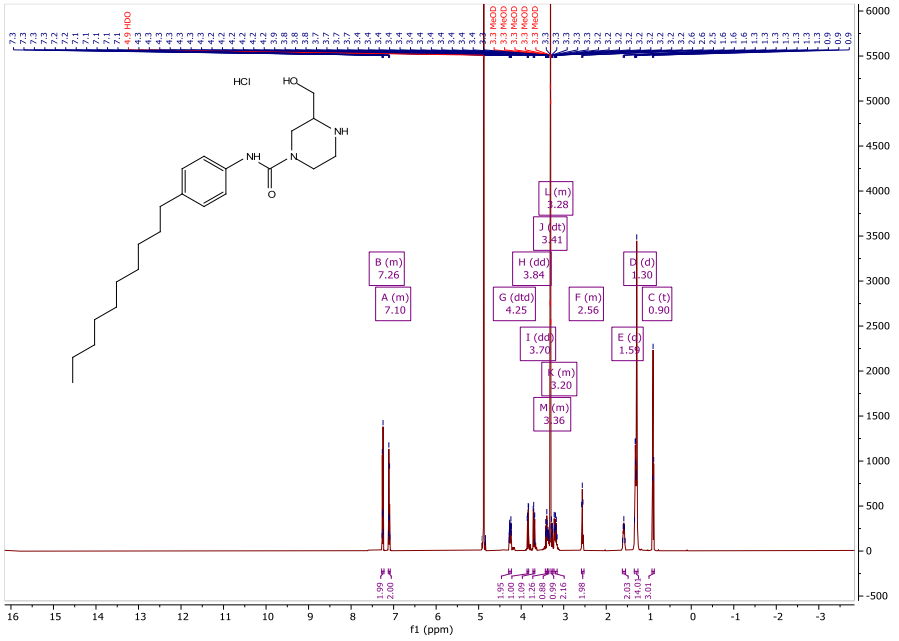

^{13}C NMR of **3.16c**

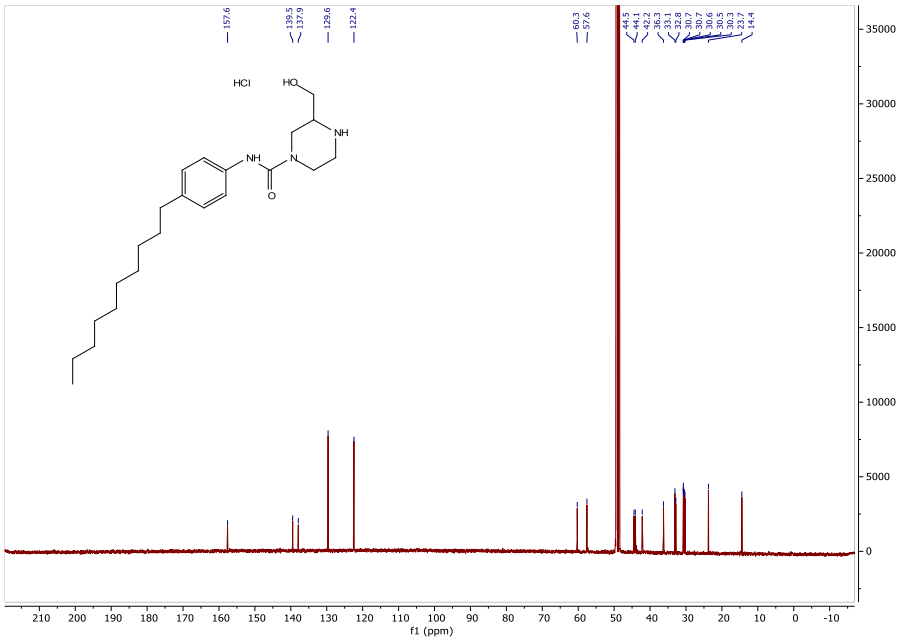

^{1}H NMR of **3.16d**

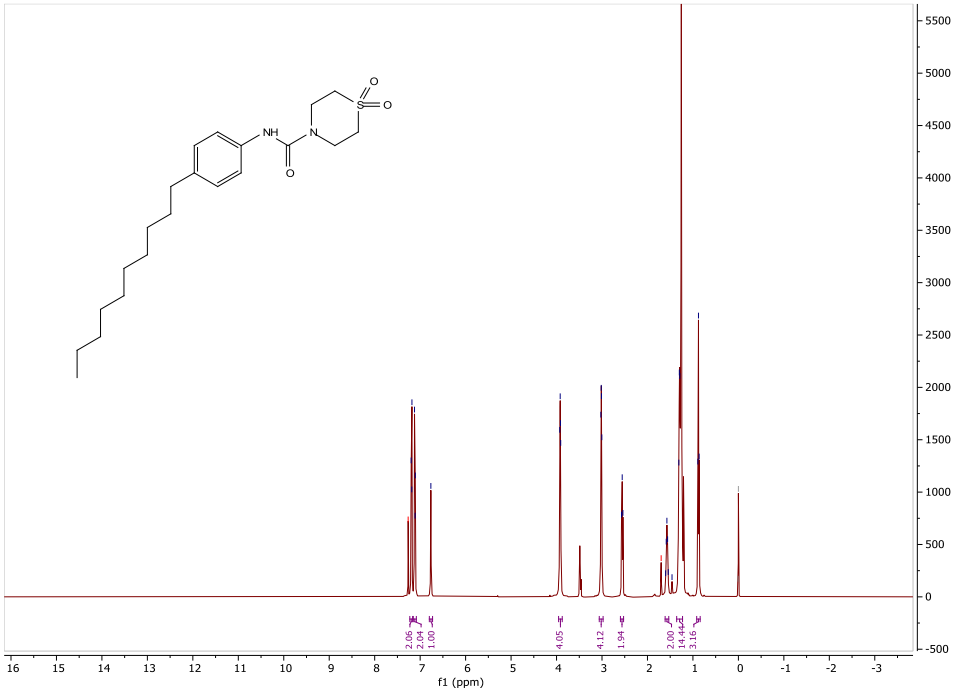

^{13}C NMR of **3.16d**

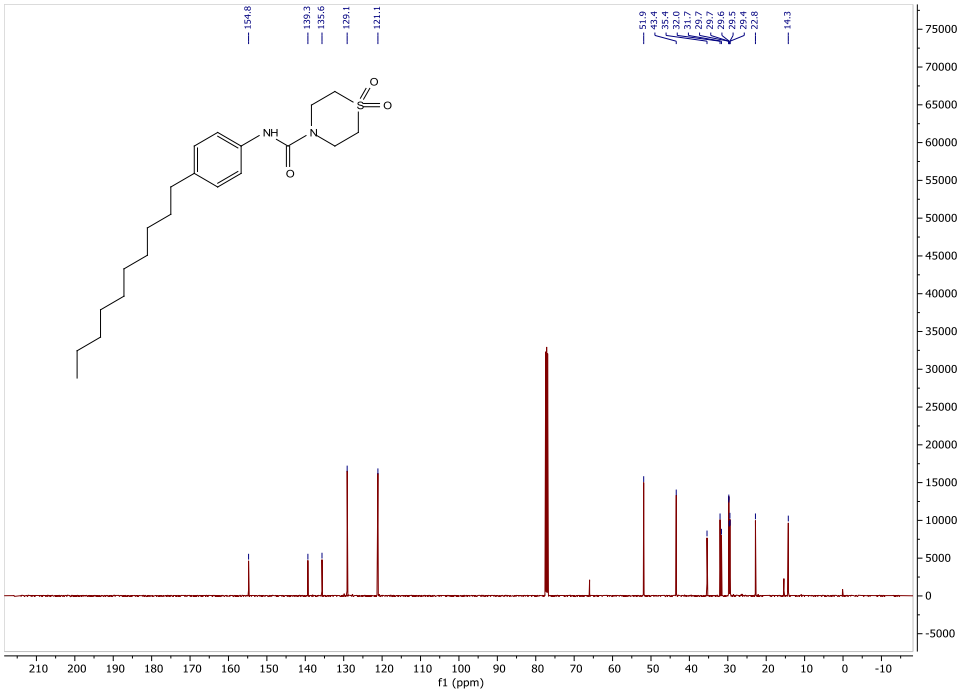

^{1}H NMR of **3.16e**

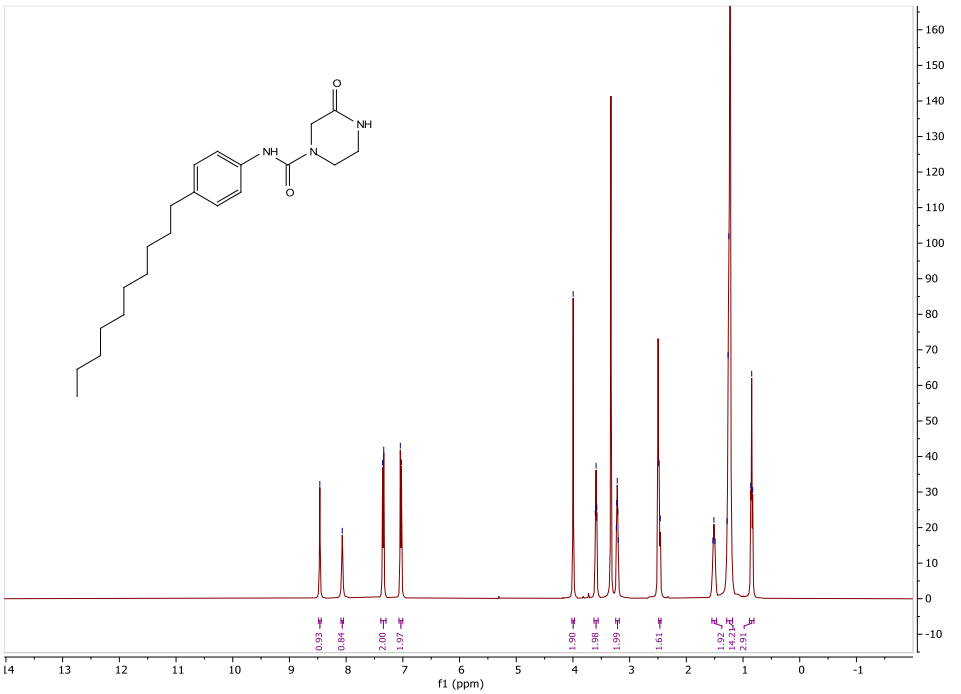

^{13}C NMR of **3.16e**

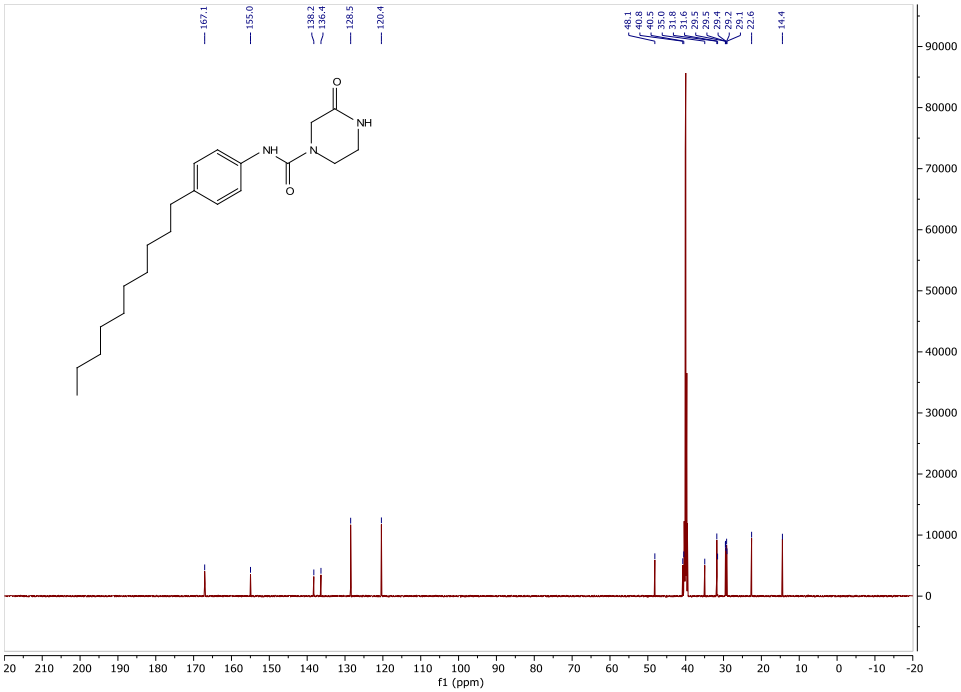

^{1}H NMR of **3.16f**

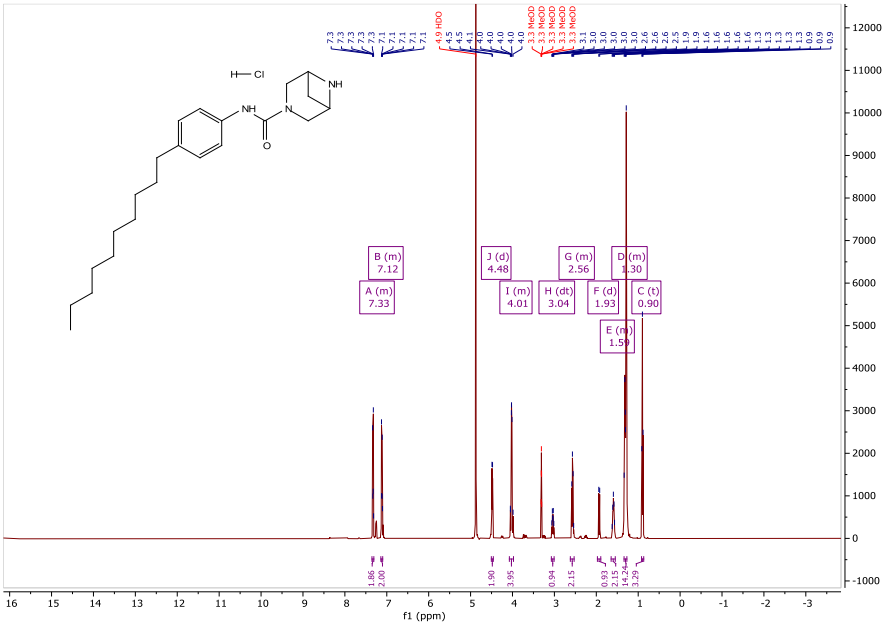

^{13}C NMR of **3.16f**

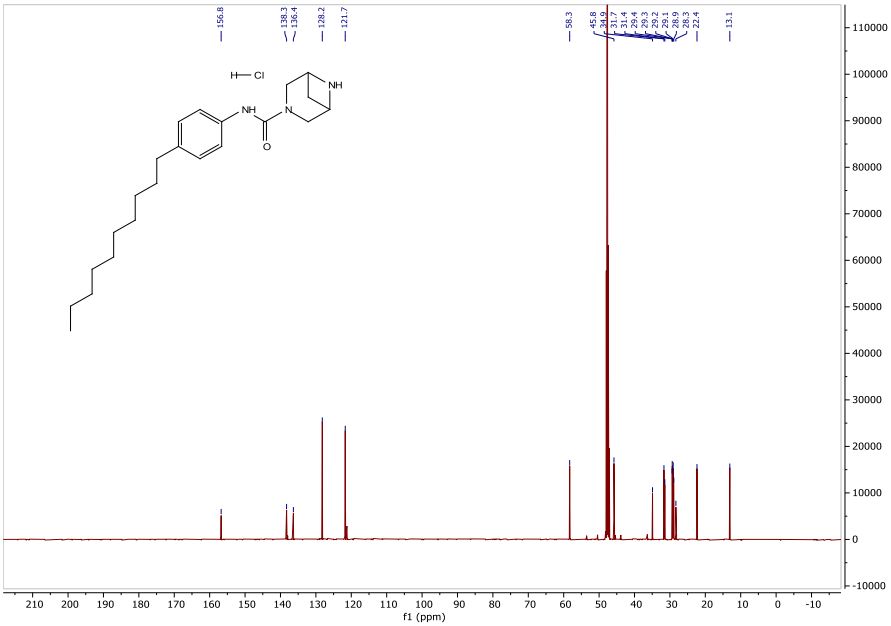

^{1}H NMR of **3.16g**

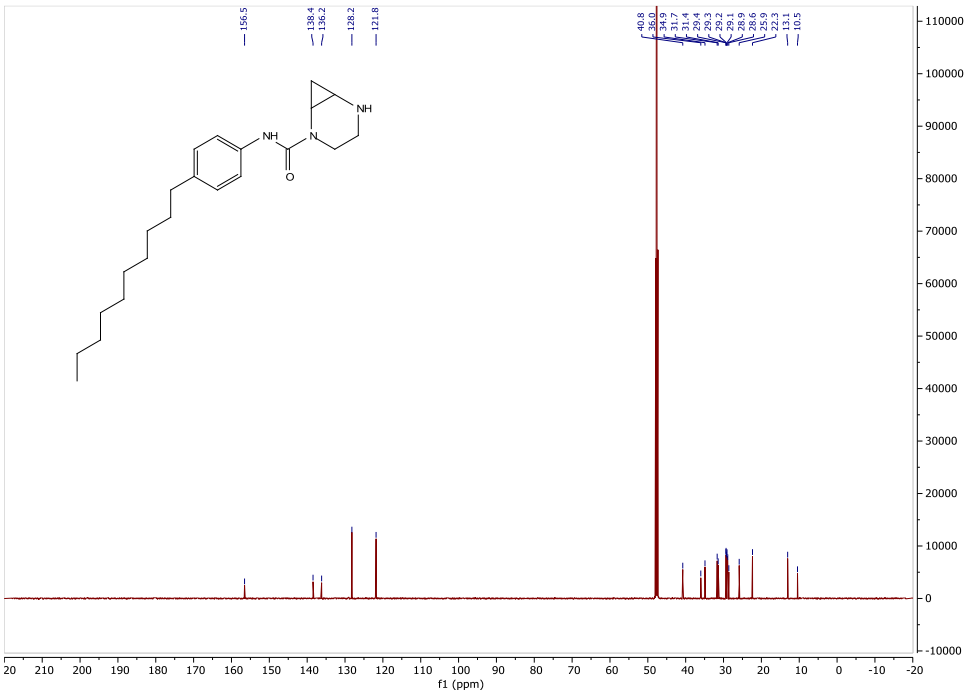

^{13}C NMR of **3.16g**

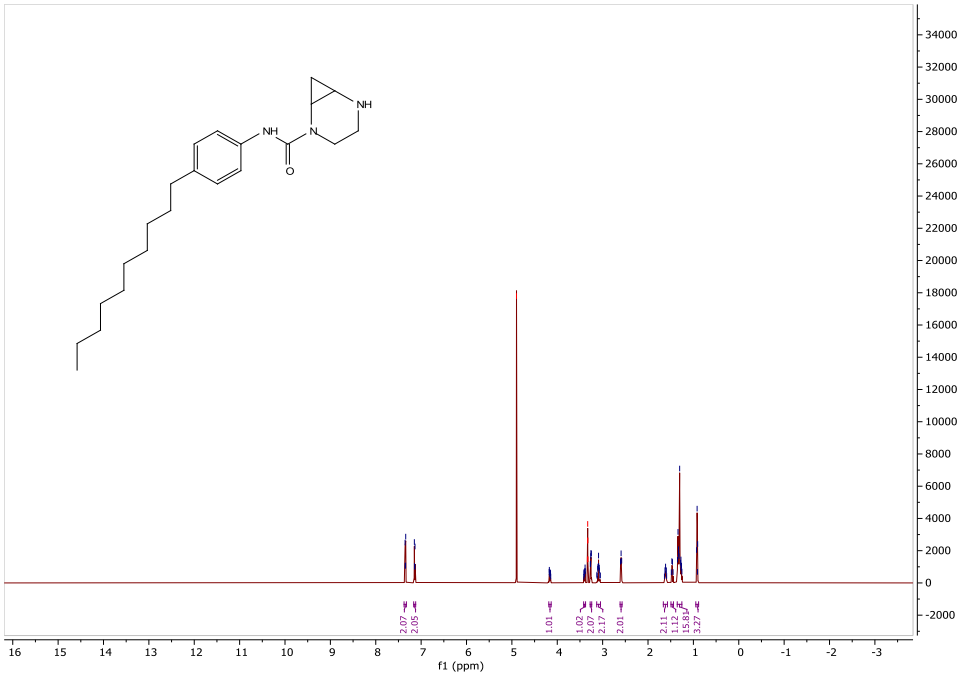

^{1}H NMR of **3.16h**

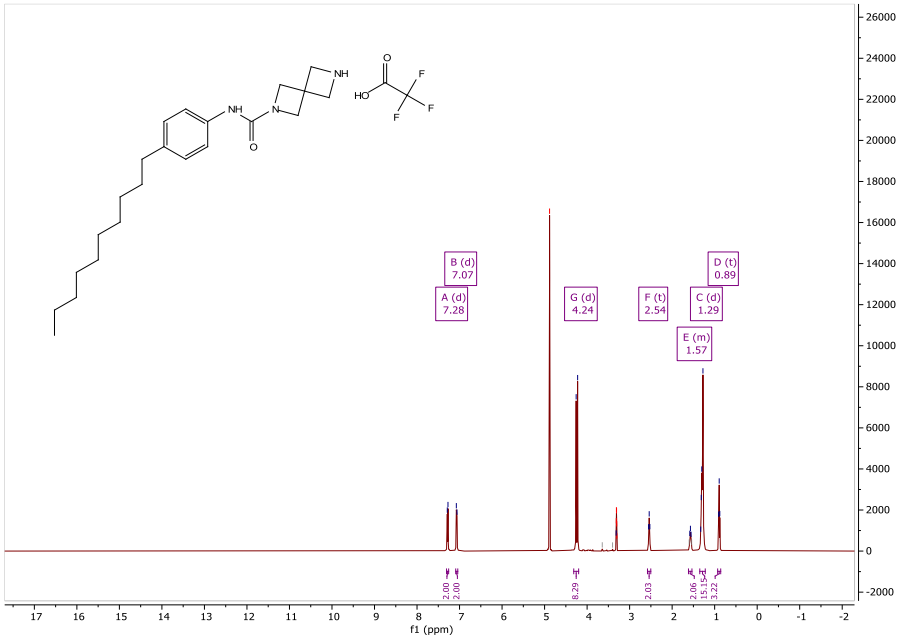

^{13}C NMR of **3.16h**

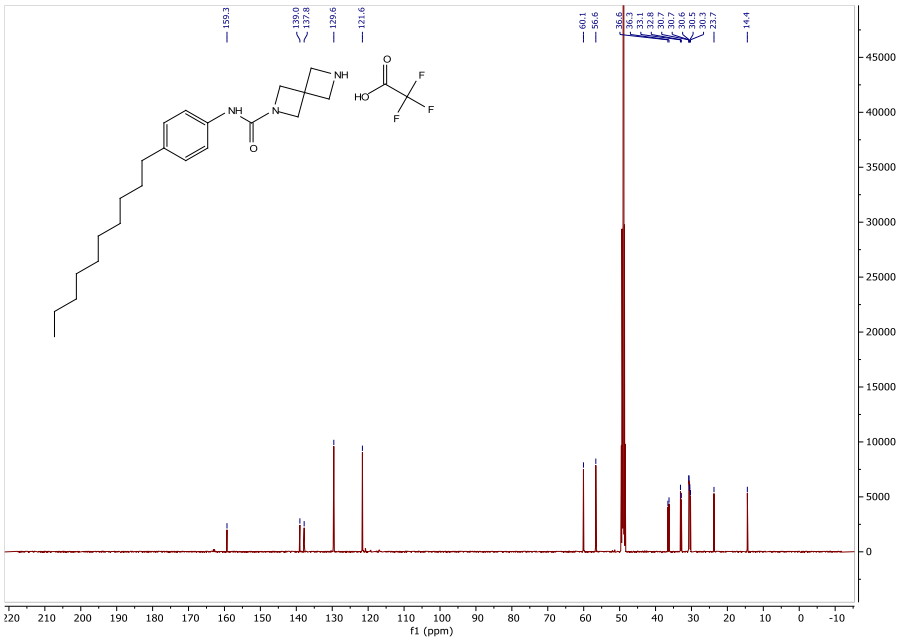

^{1}H NMR of **3.16i**

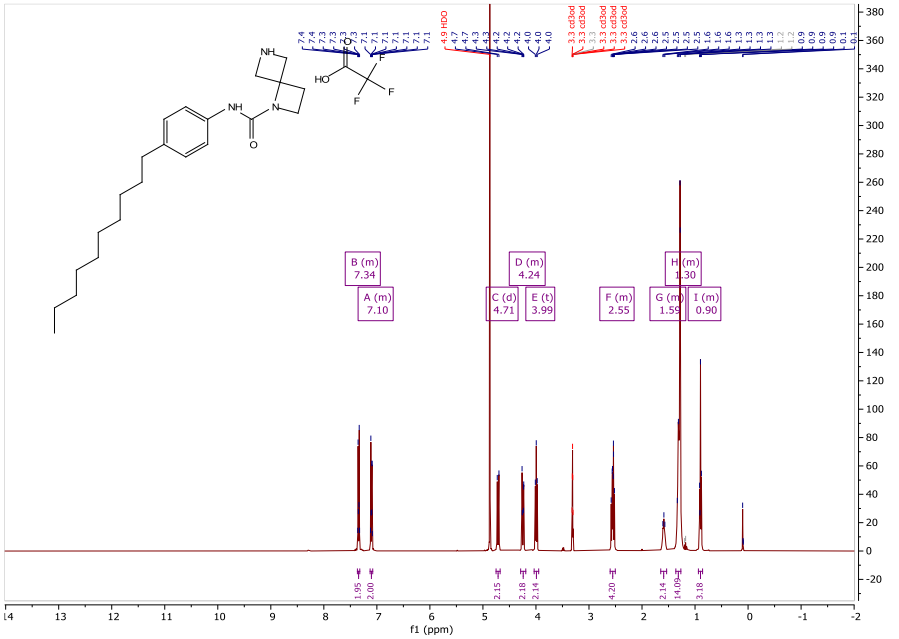

^{13}C NMR of **3.16i**

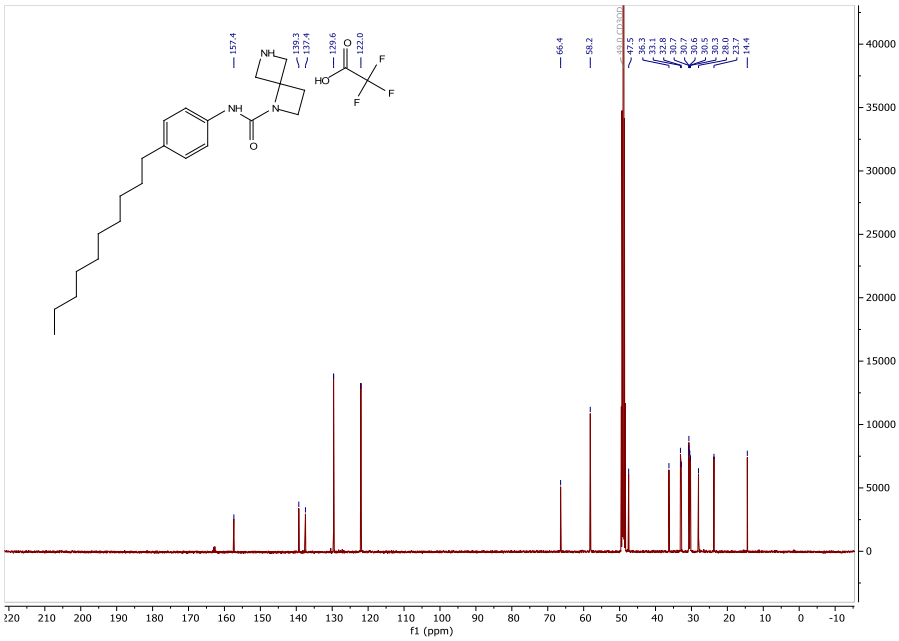

^{1}H NMR of **3.16j**

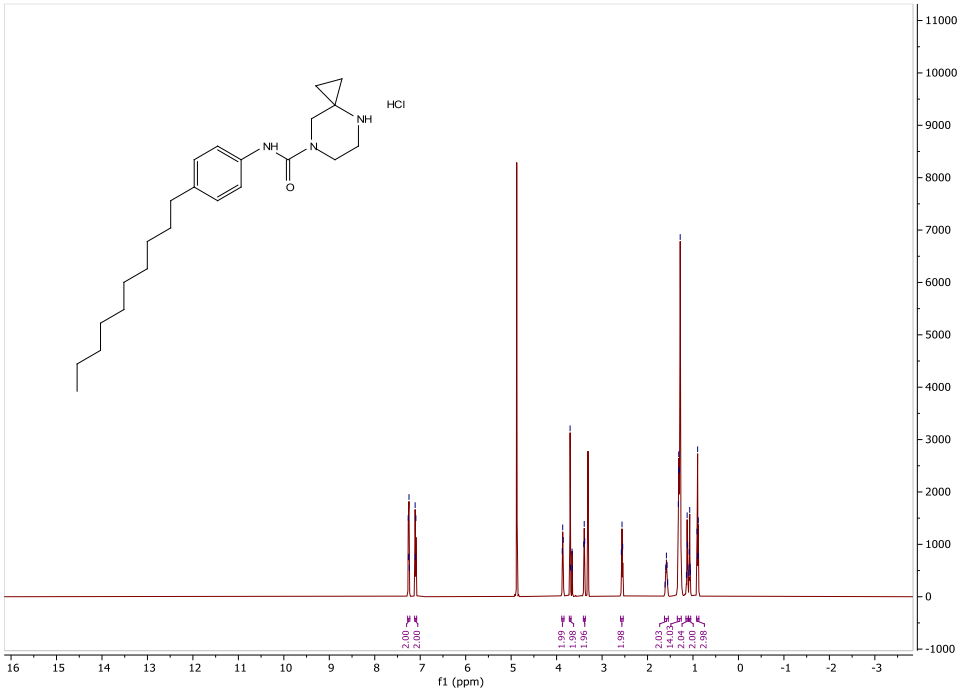

^{13}C NMR of **3.16j**

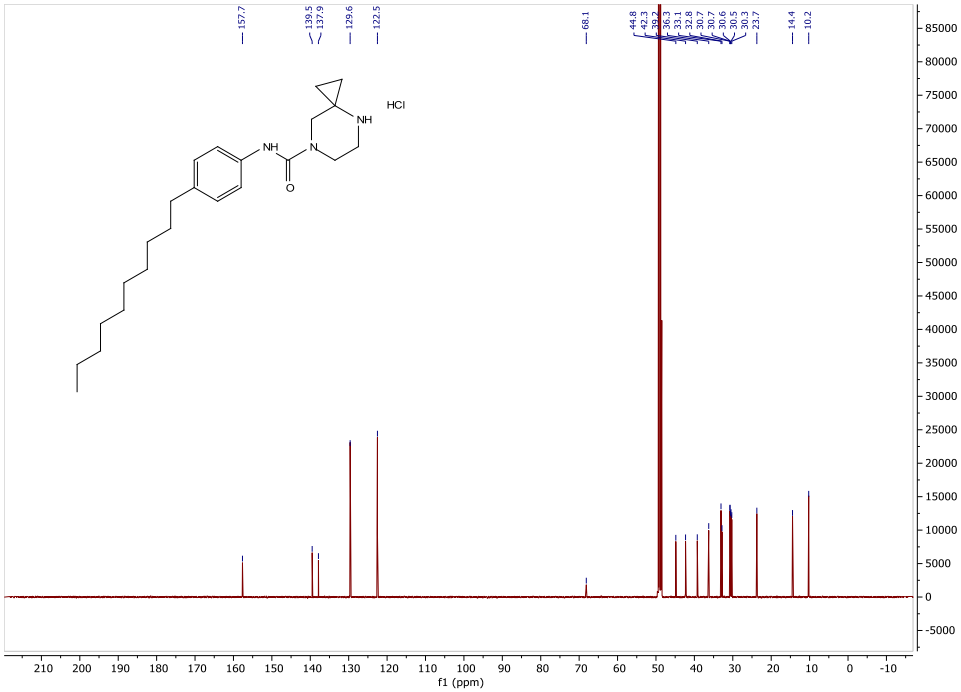

^{1}H NMR of **3.16k**

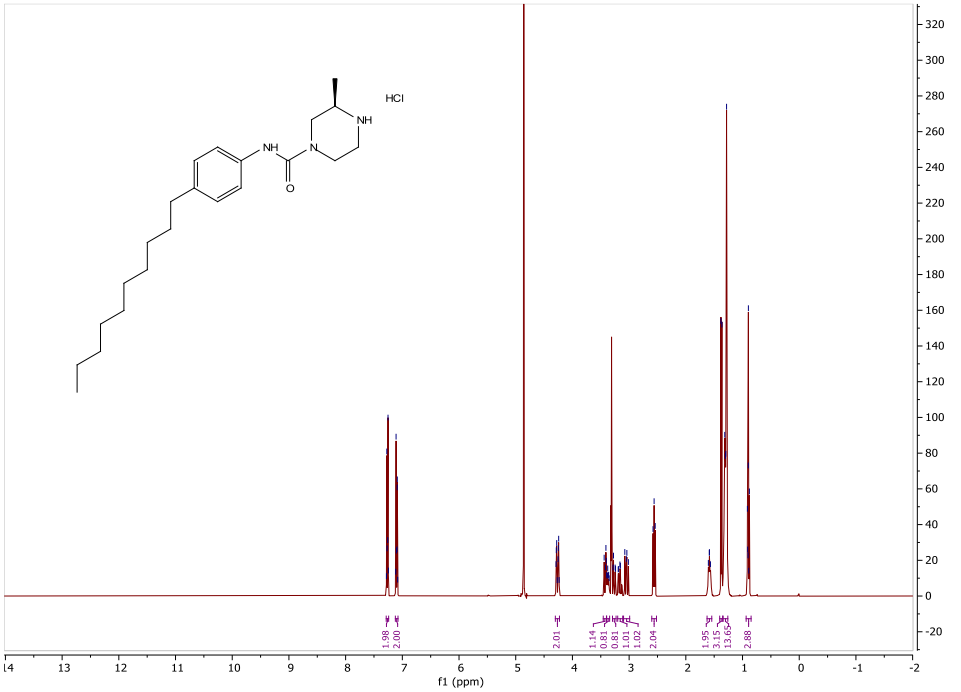

^{13}C NMR of **3.16k**

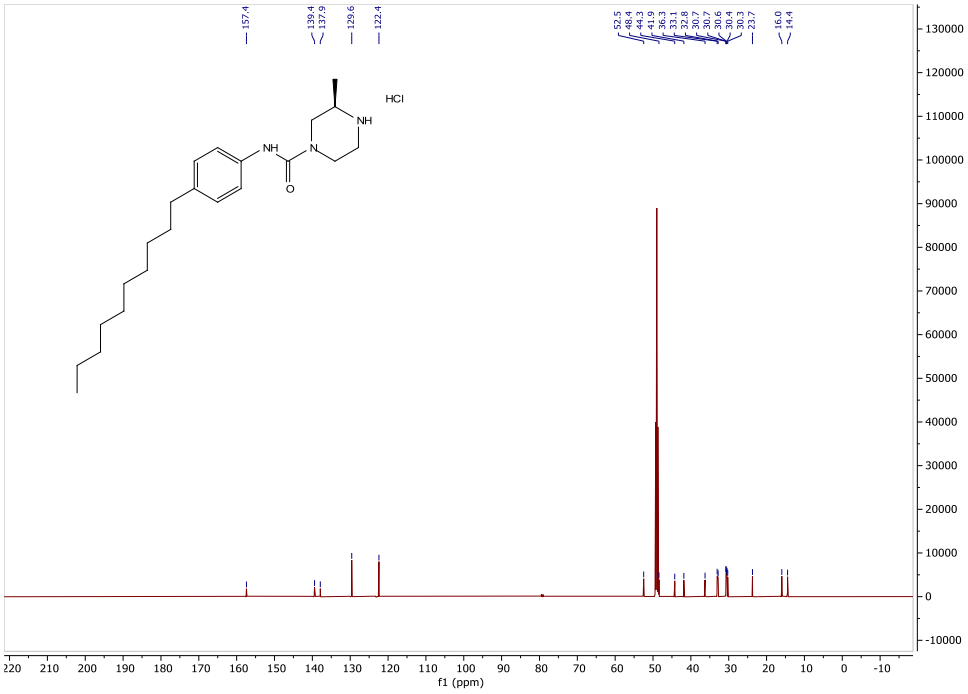

^{1}H NMR of **3.16l**

^{13}C NMR of **3.16l**

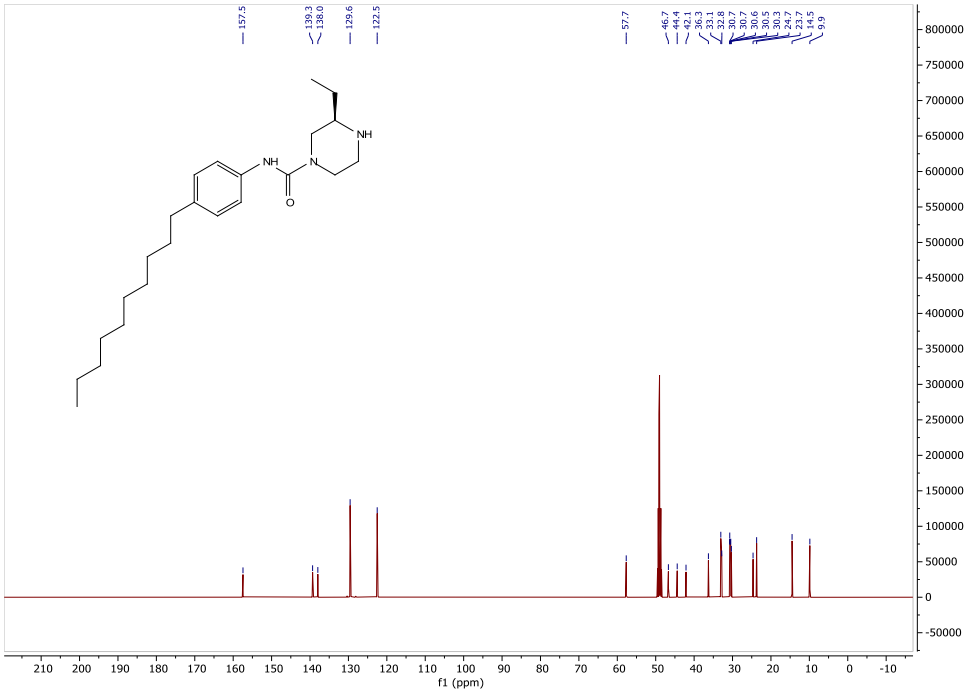

^{1}H NMR of **3.16m**

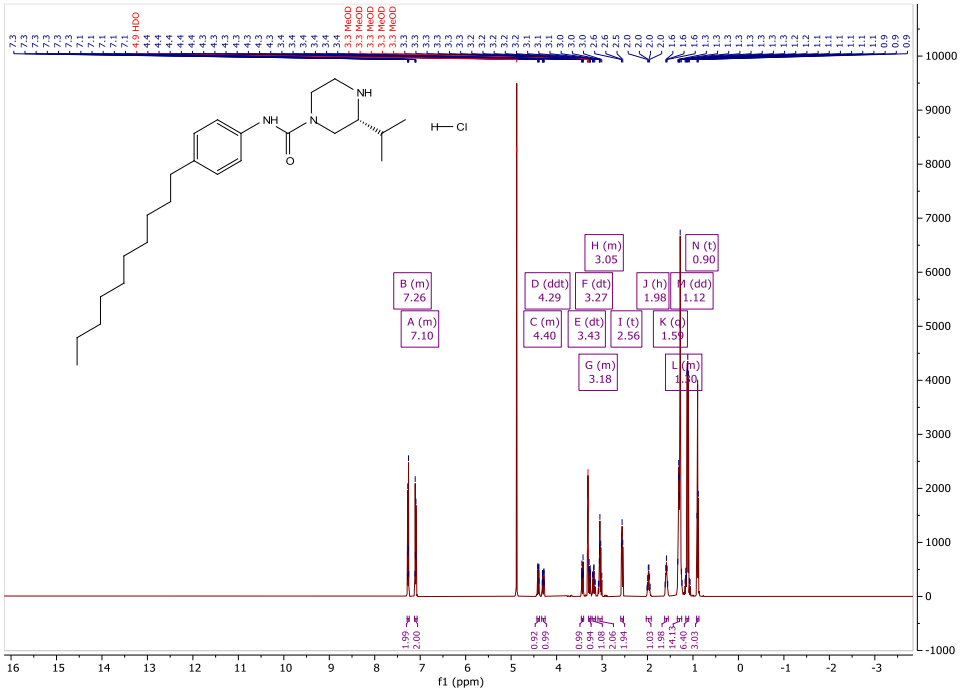

^{13}C NMR of **3.16m**

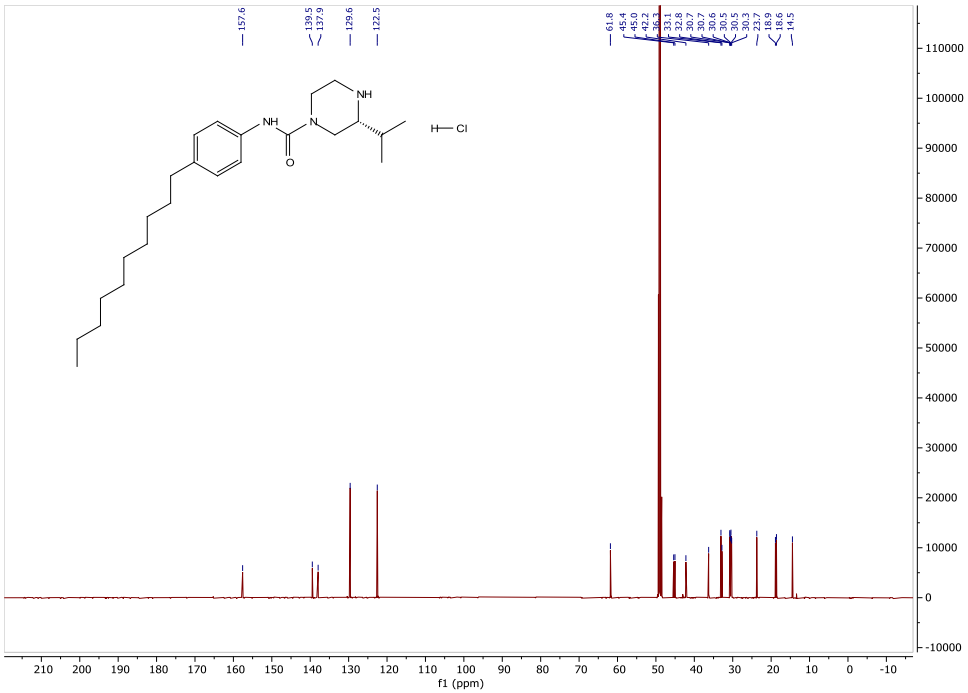

^{1}H NMR of **3.16n**

^{13}C NMR of **3.16n**

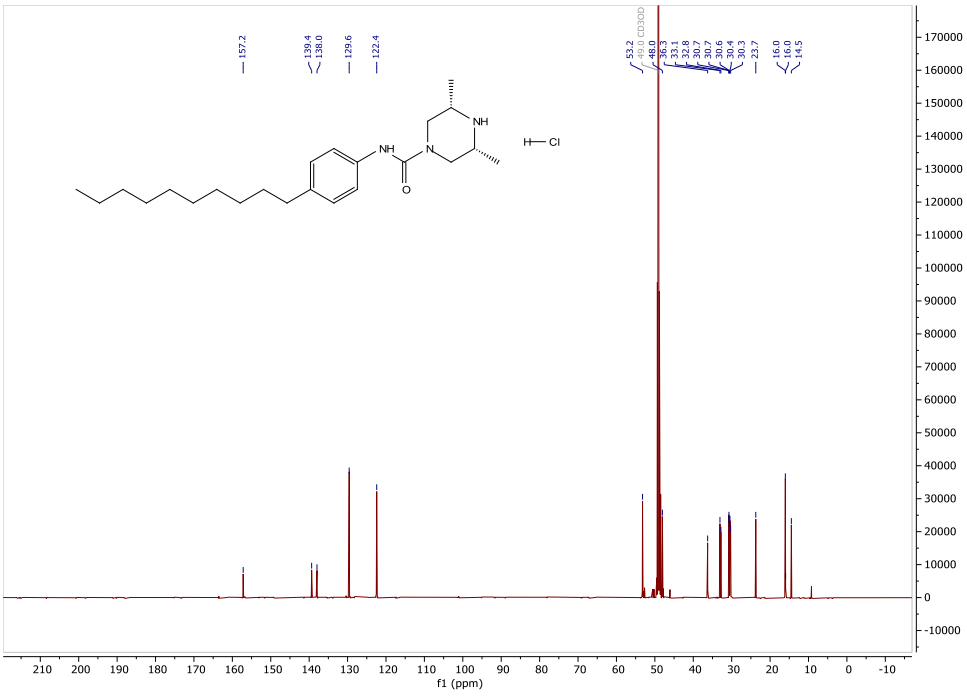

Appendix C. Spectra for Chapter 4

^{1}H NMR of **4.7a**

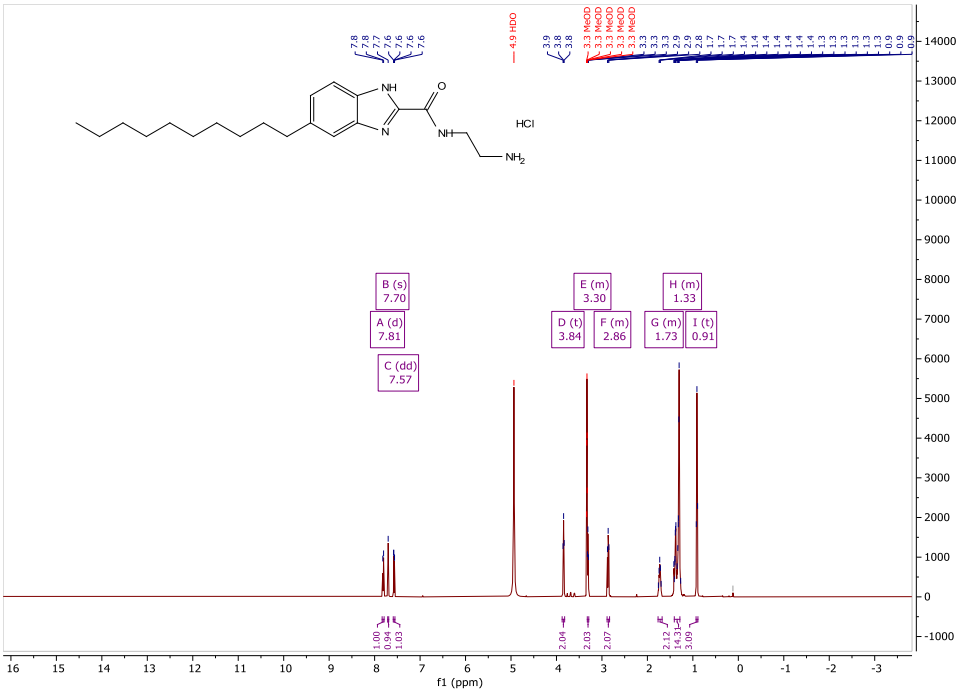

^{13}C NMR of **4.7a**

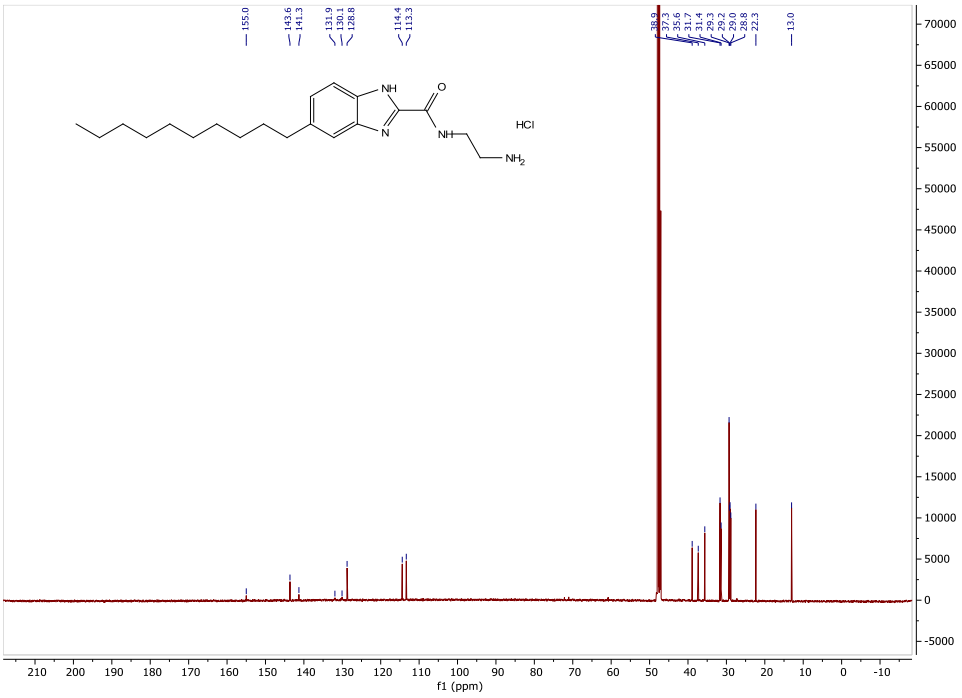

^{1}H NMR of **4.7b**

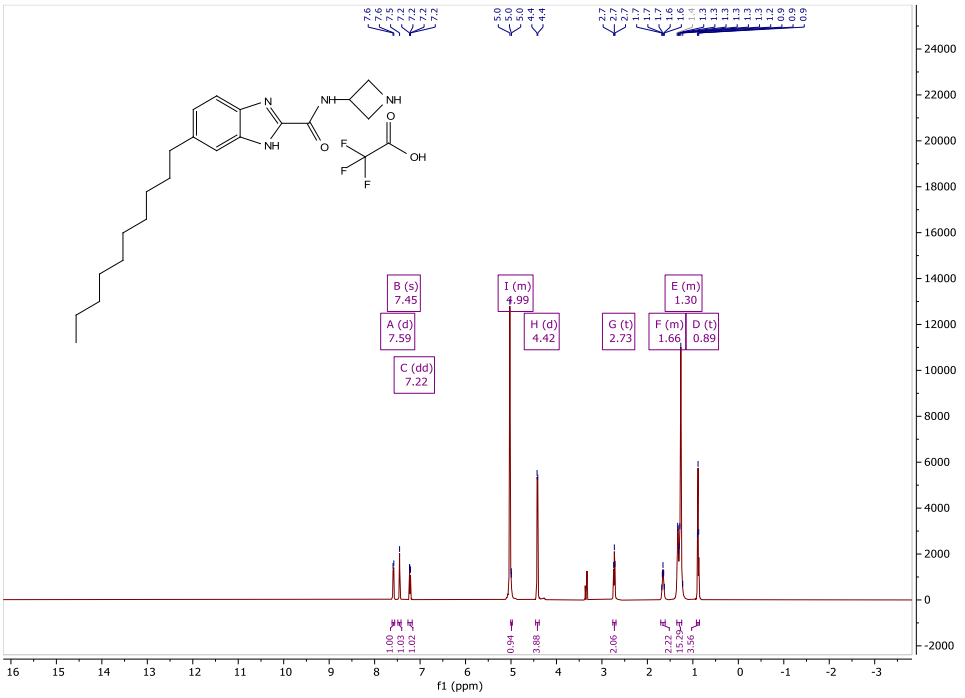

^{13}C NMR of **4.7b**

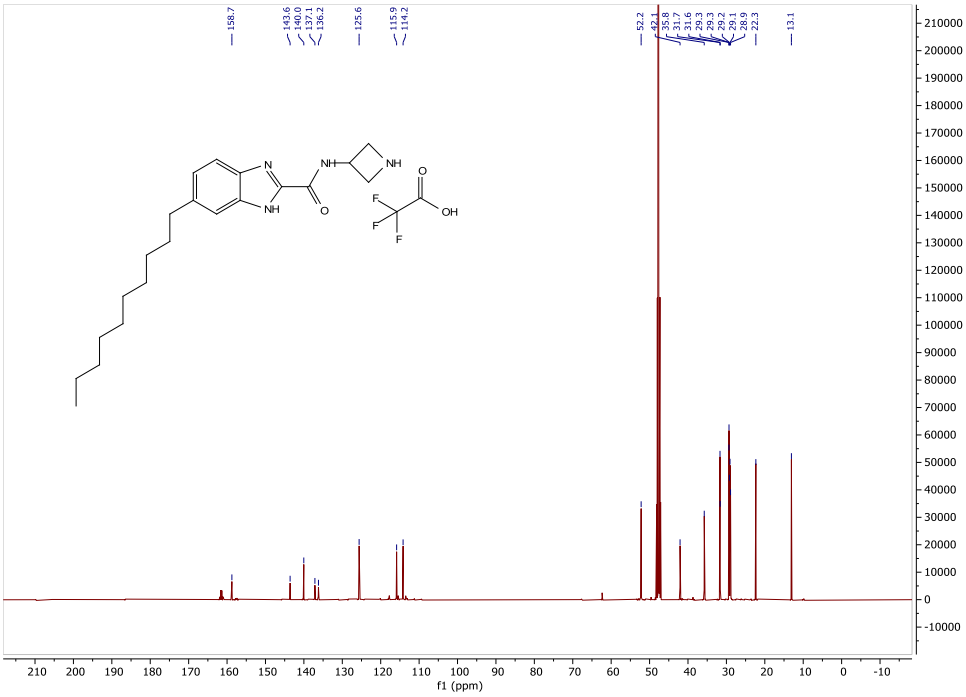

^{1}H NMR of **4.7c**

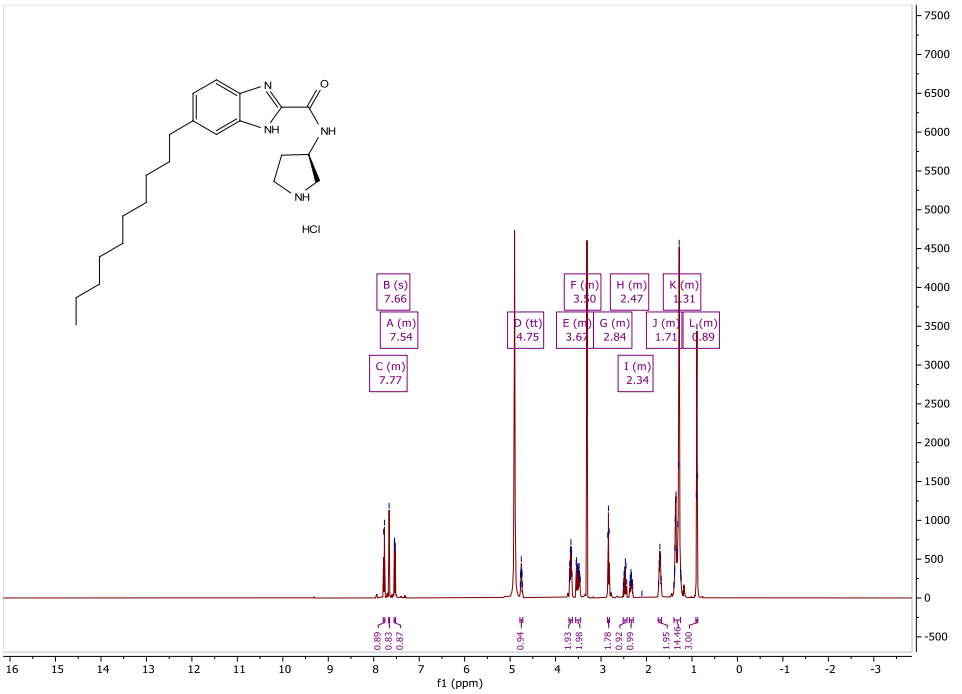

^{13}C NMR of **4.7c**

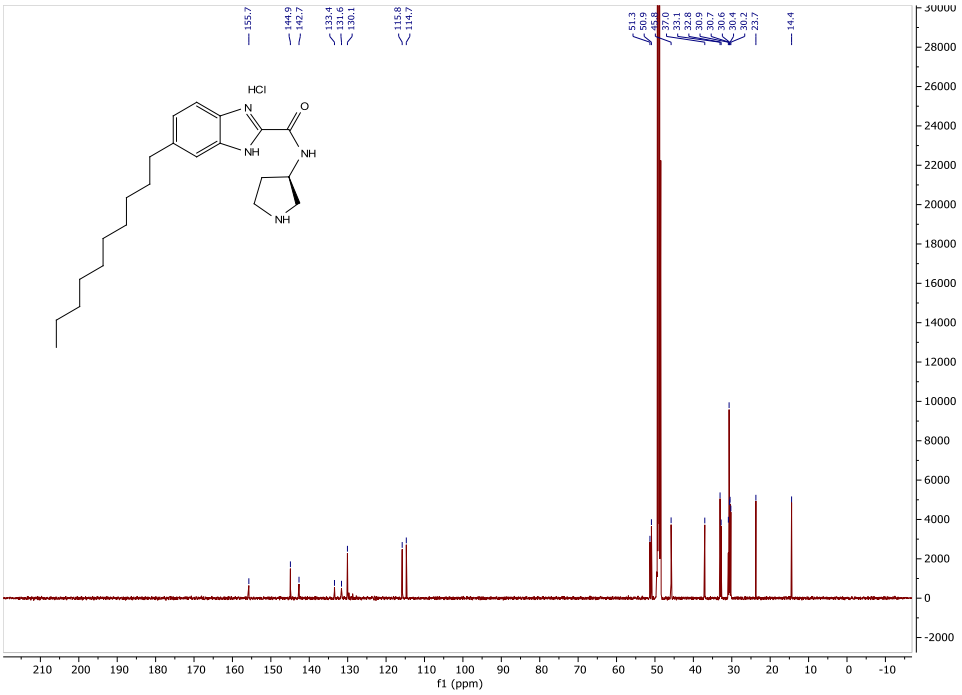

^{1}H NMR of (*R*)-**4.7d**

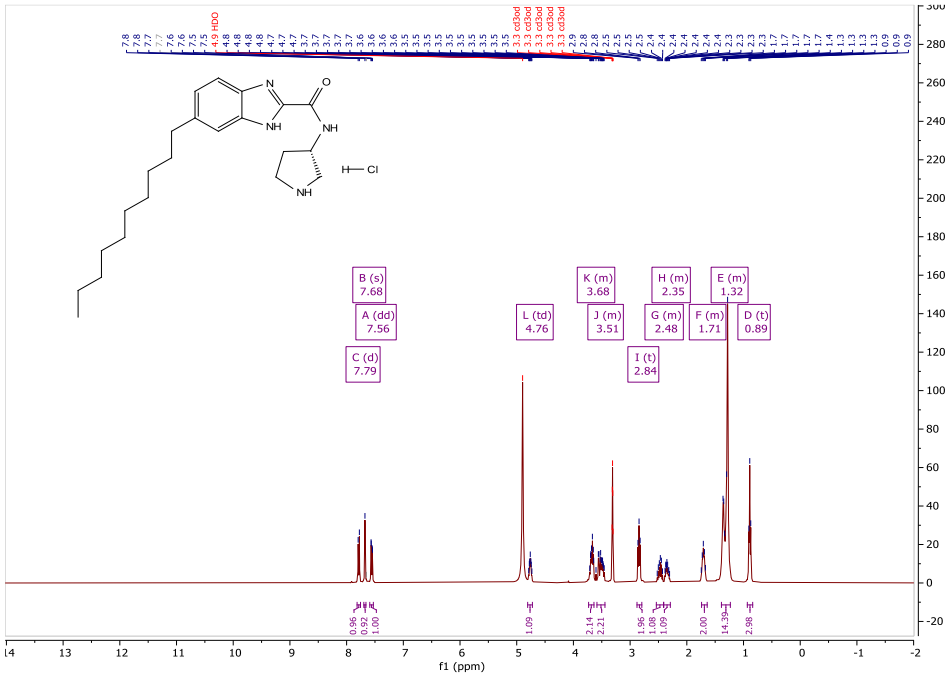

^{13}C NMR of (*R*)-**4.7d**

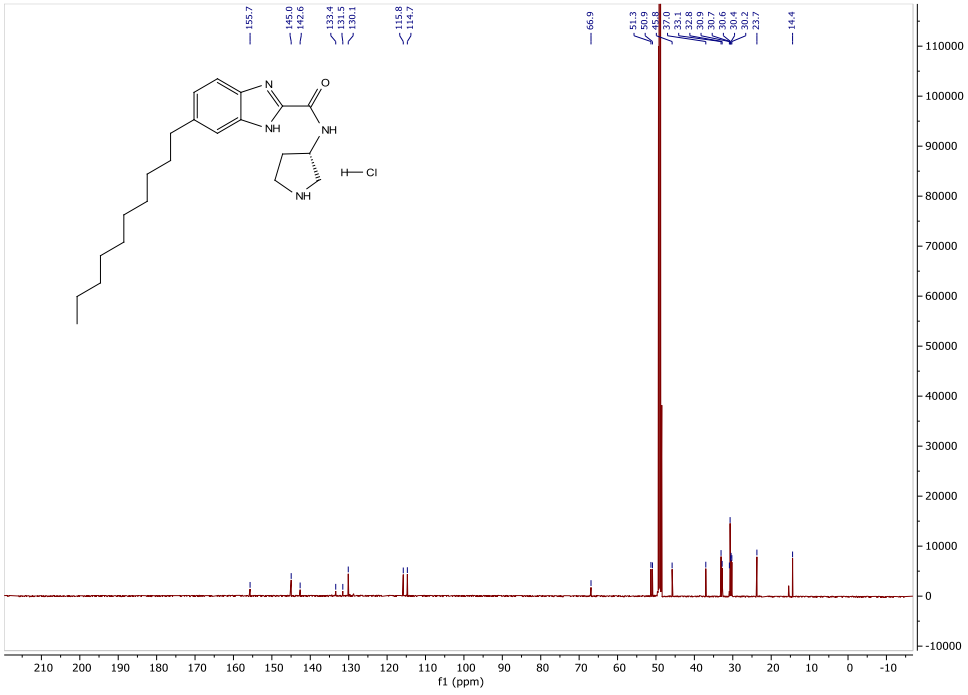

^{1}H NMR of (*S*)-**4.7e**

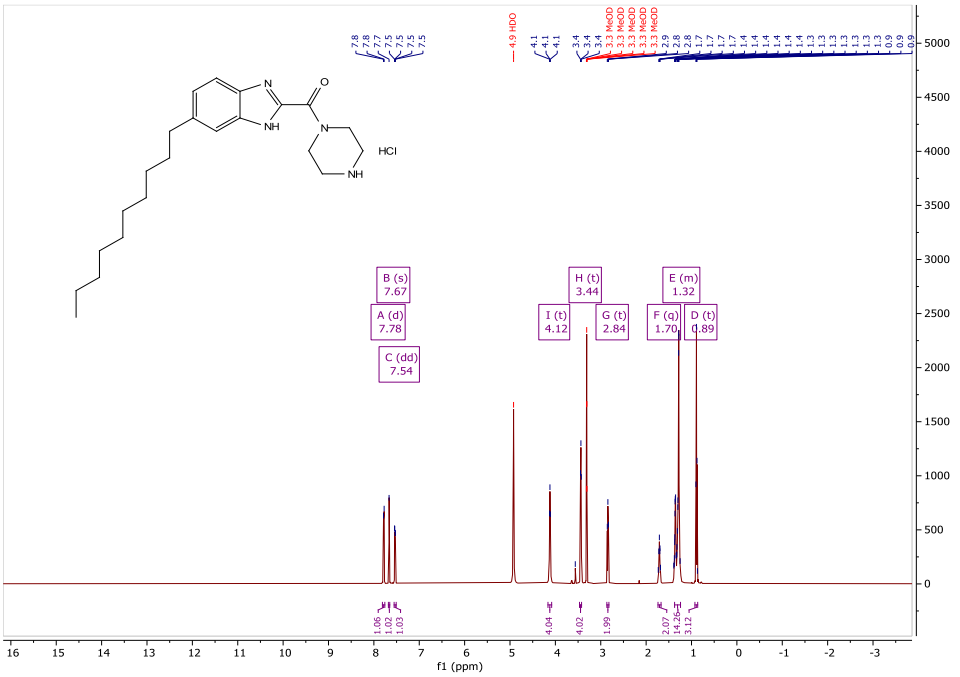

^{13}C NMR of (S)-**4.7e**

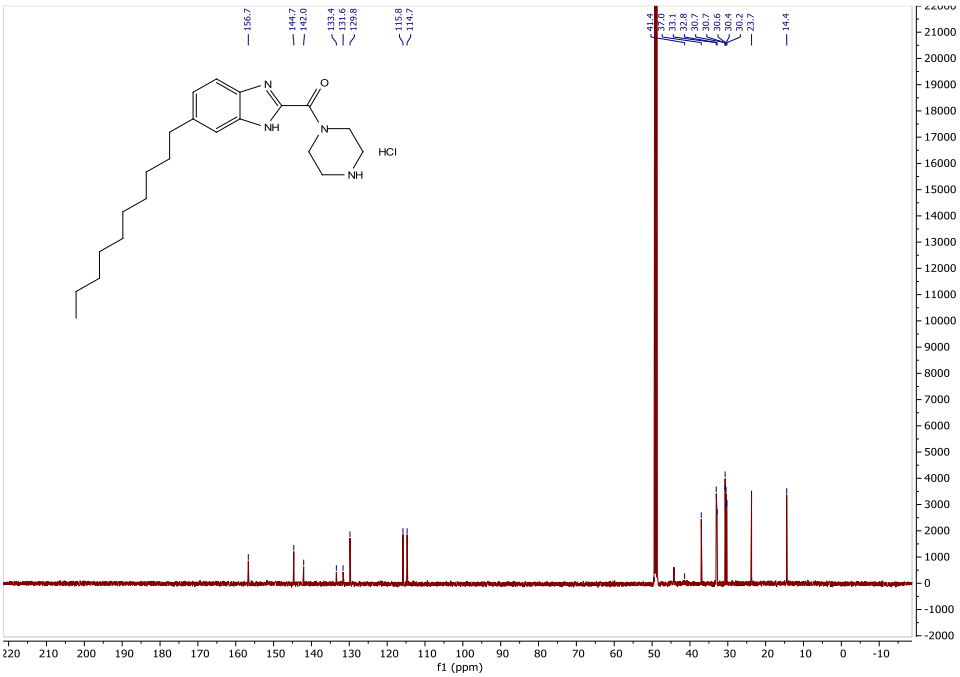

^{1}H NMR of **4.7f**

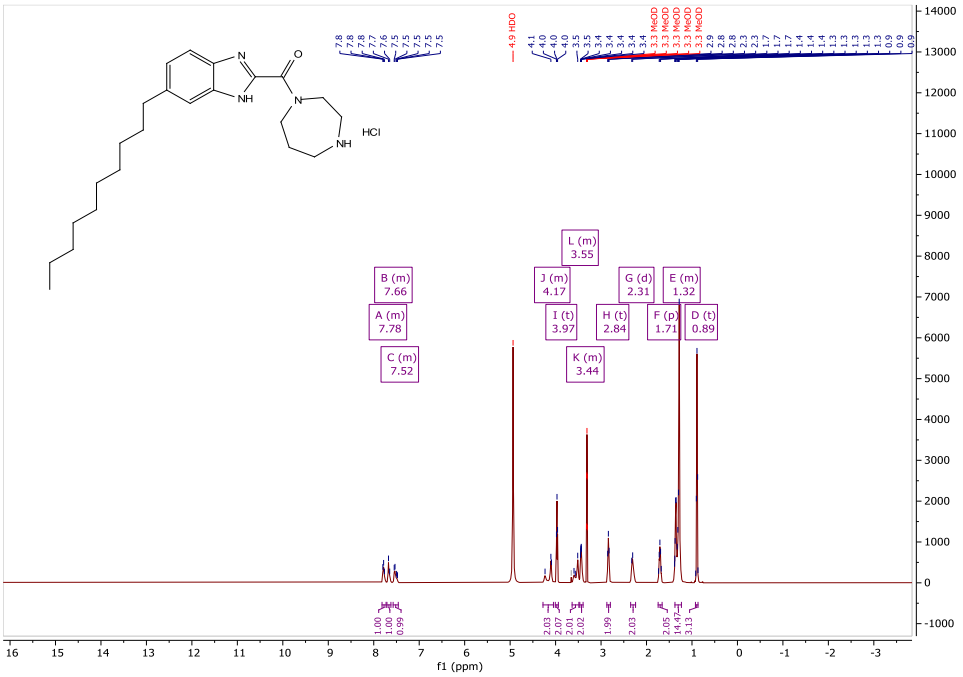

^{13}C NMR of **4.7f**

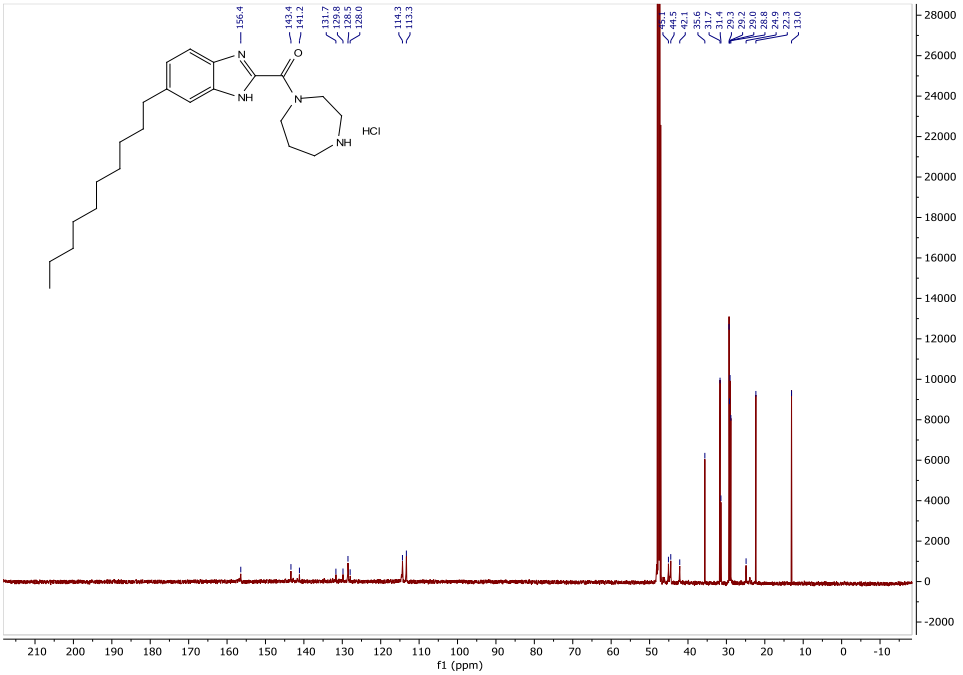

^{1}H NMR of (*S*)-**4.7g**

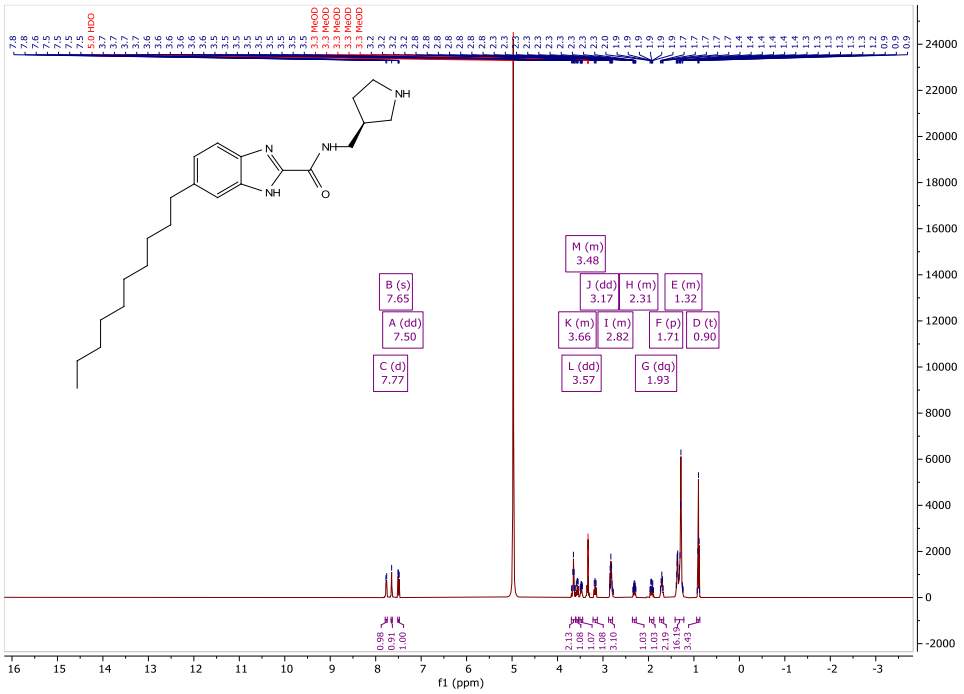

^{13}C NMR of (S)-**4.7g**

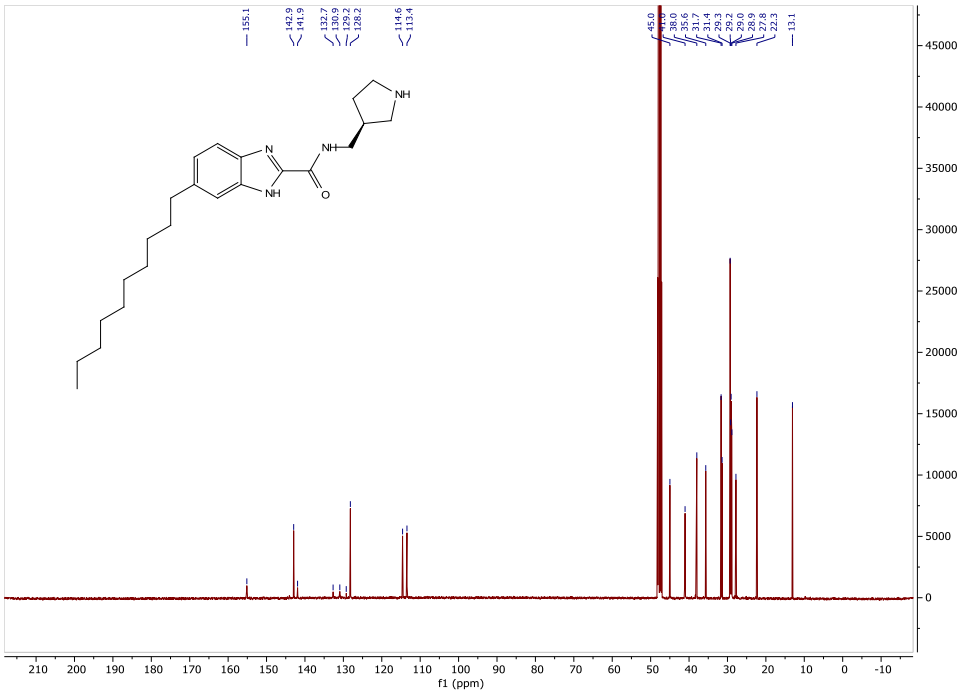

^{1}H NMR of (*R*)-**4.7h**

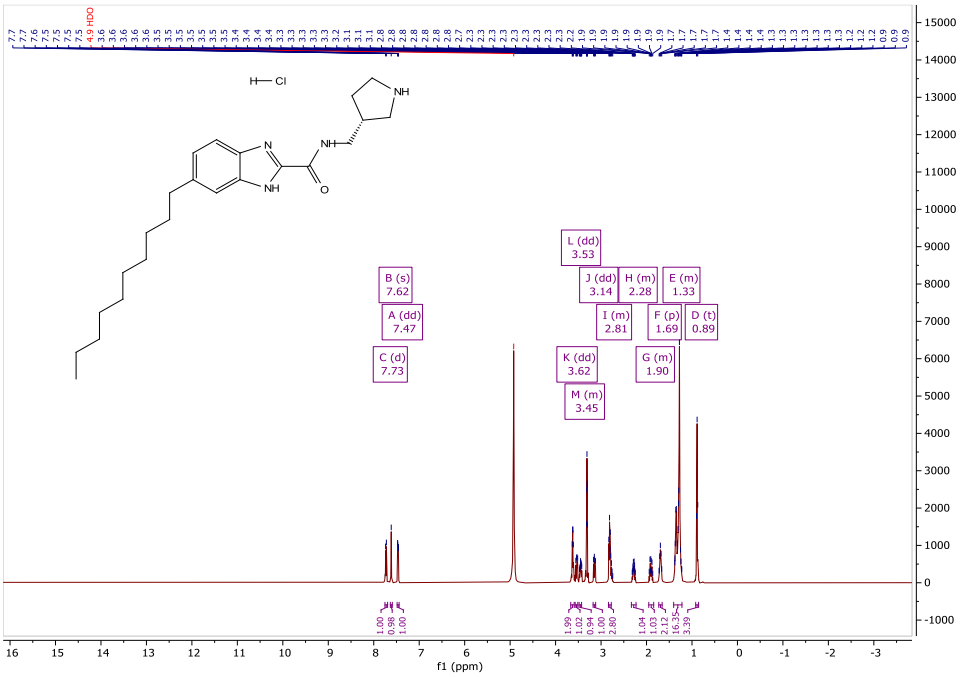

^{13}C NMR of (*R*)-**4.7h**

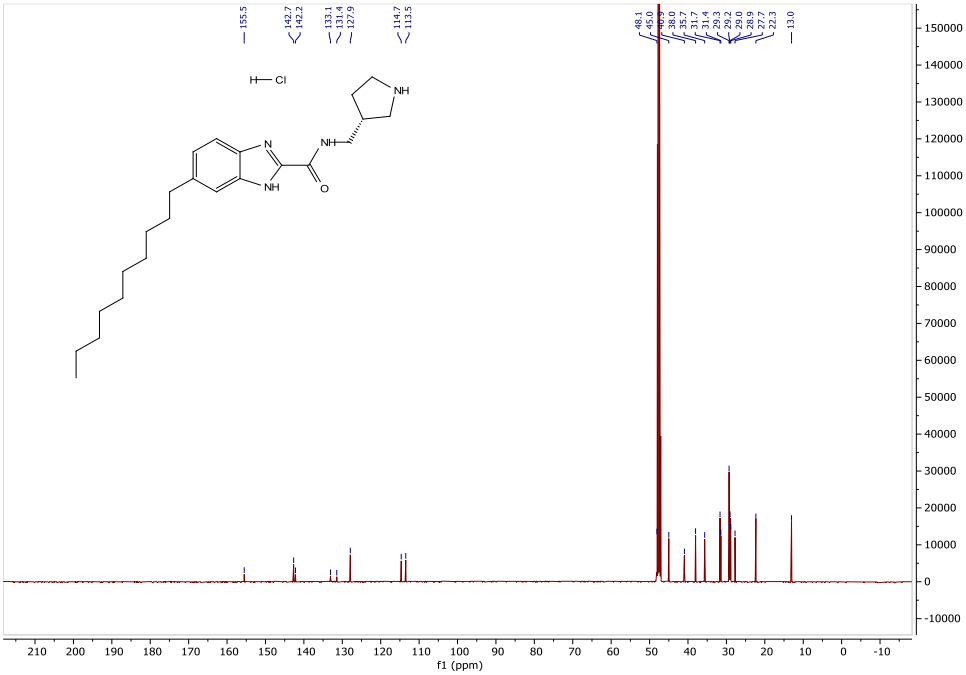

^{1}H NMR of (±)-**4.7i**

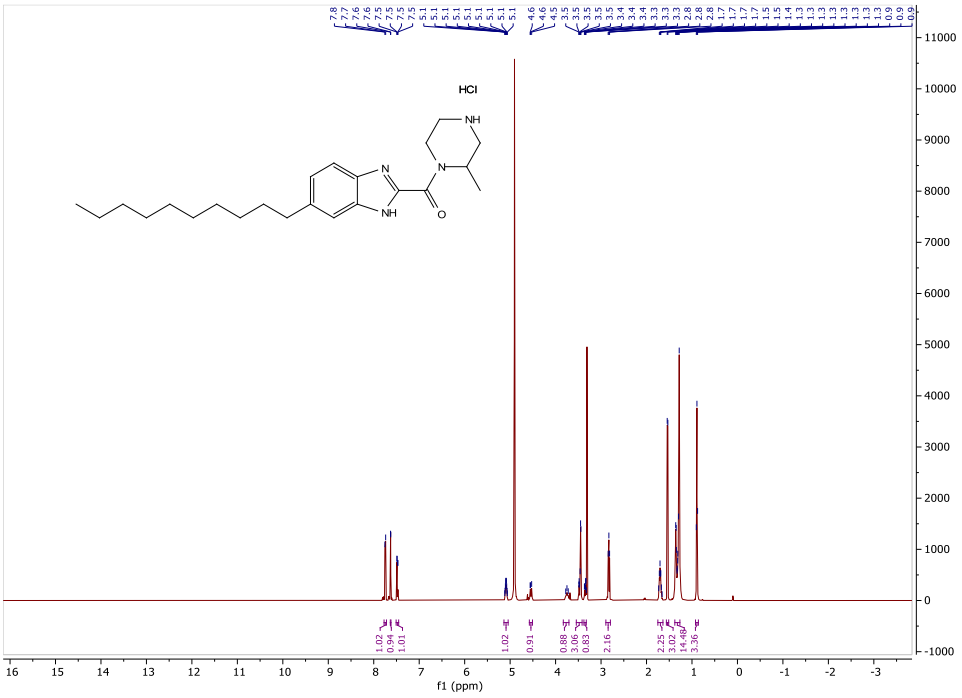

^{13}C NMR of (±)-**4.7i**

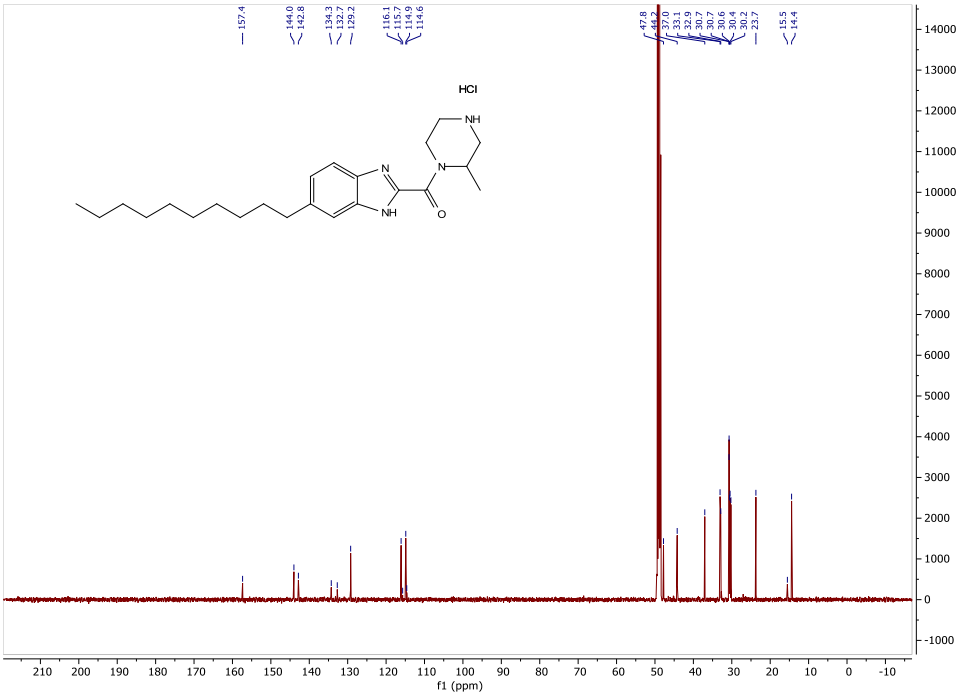

^{1}H NMR of (*R*)-**4.7j**

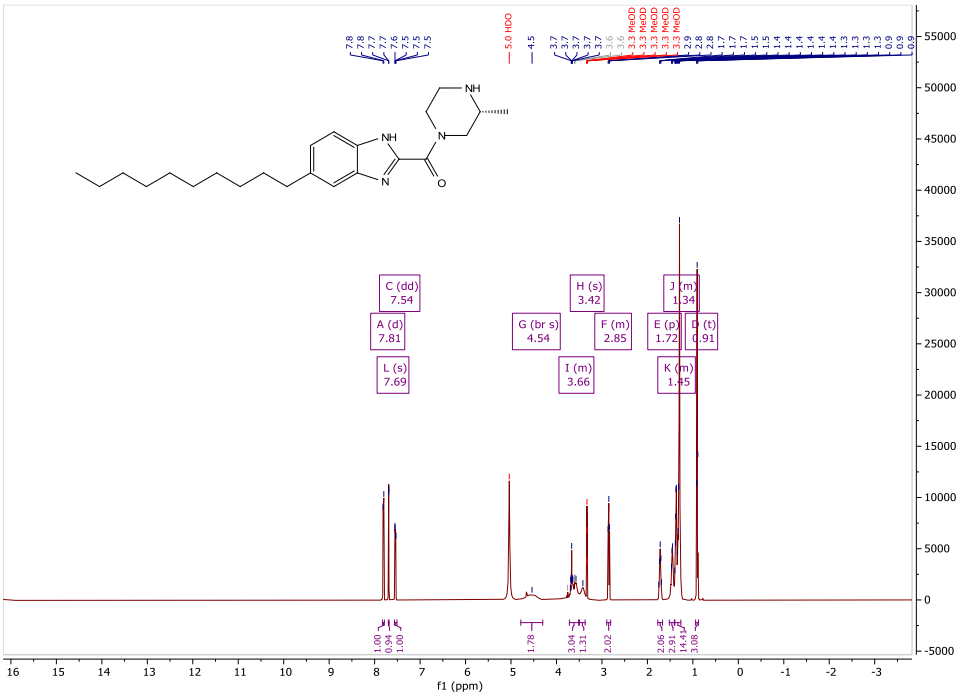

^{13}C NMR of (*R*)-**4.7j**

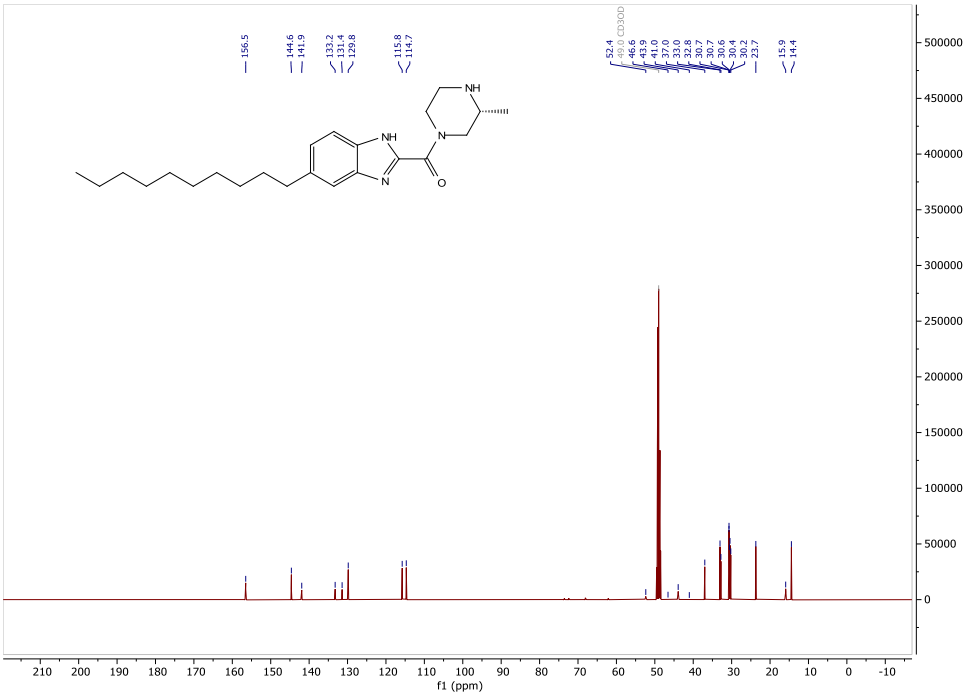

^{1}H NMR of **4.7k**

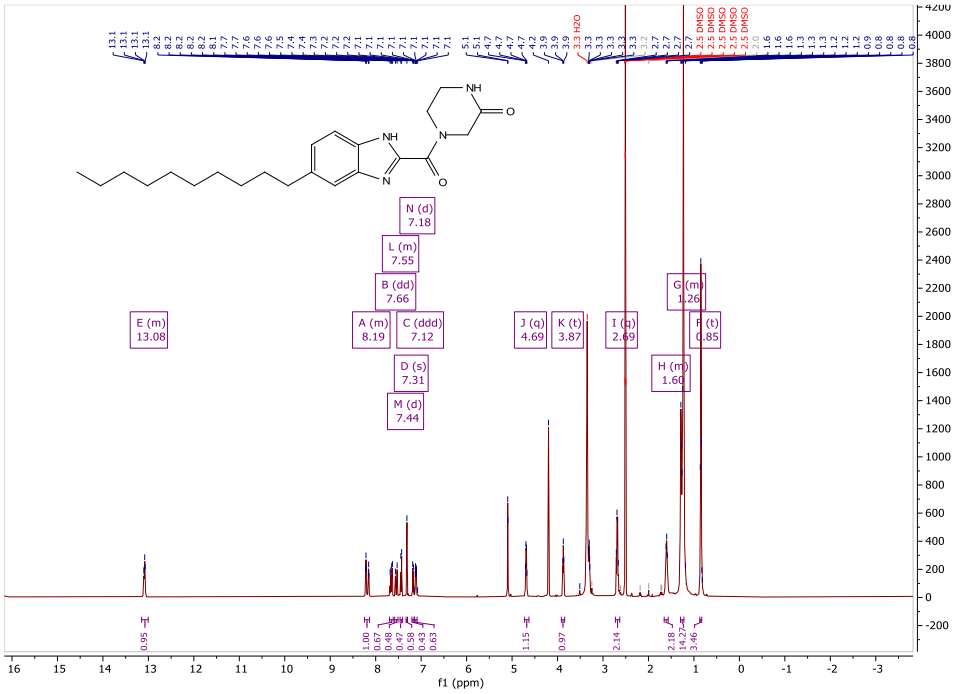

^{13}C NMR of **4.7k**

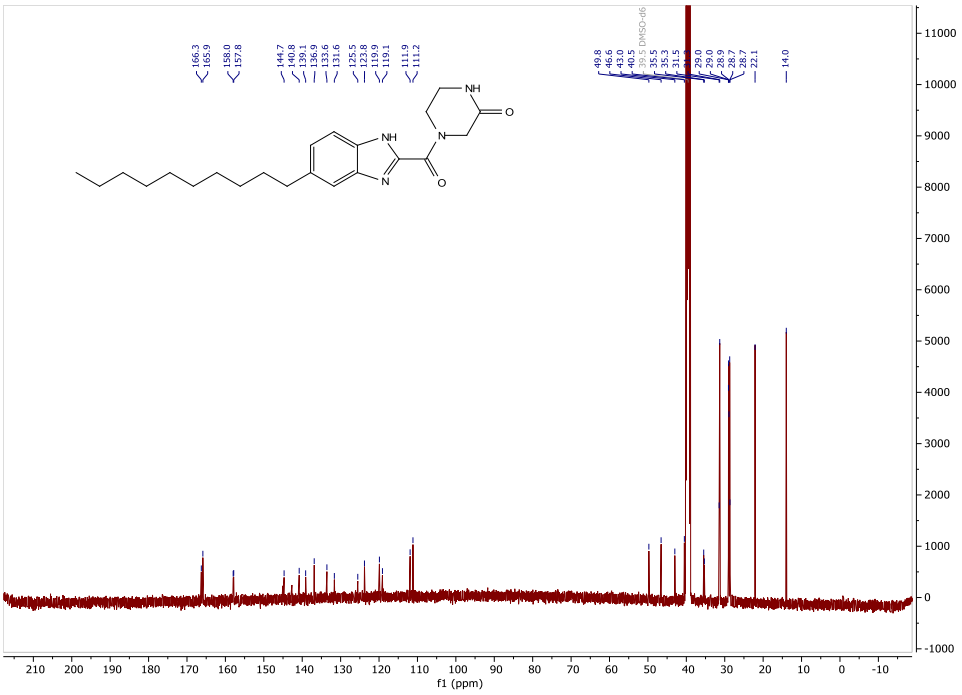

^{1}H NMR of (±)-**4.7l**

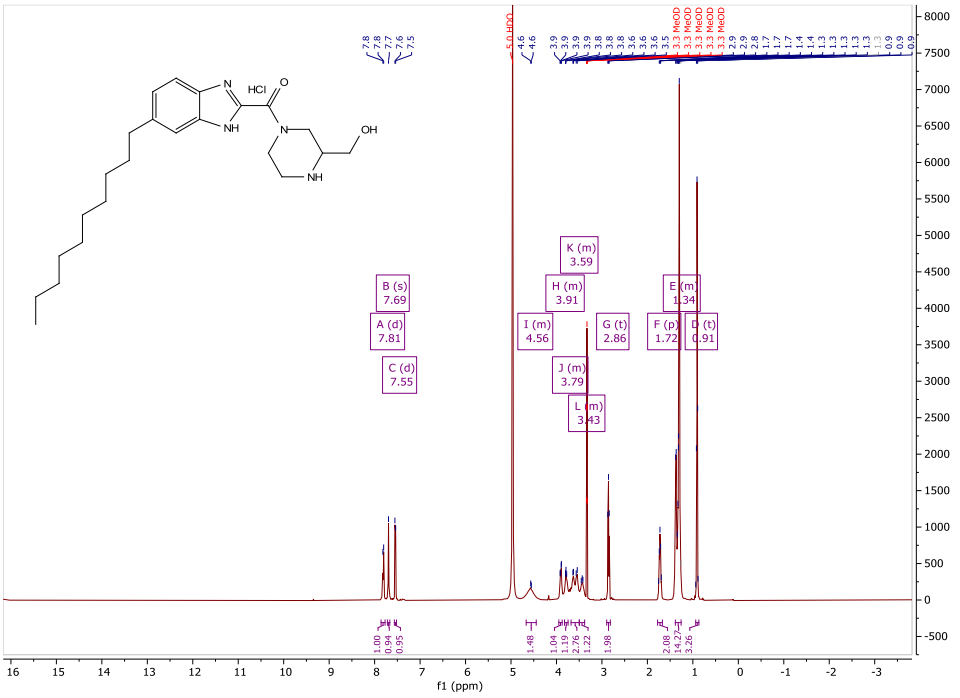

^{13}C NMR of (±)-**4.7l**

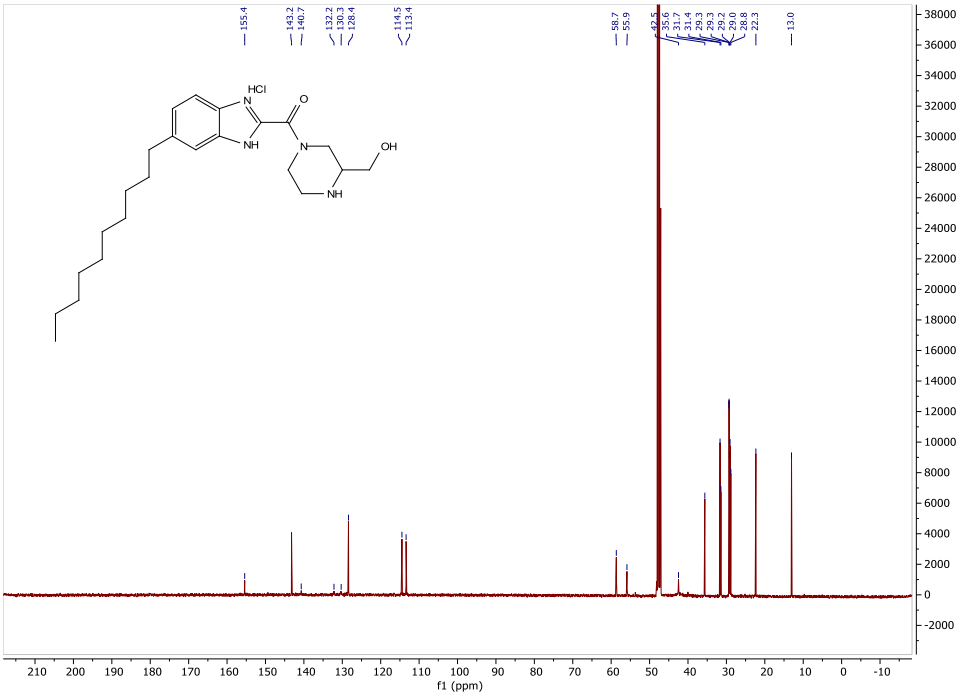

^{1}H NMR of **4.7m**

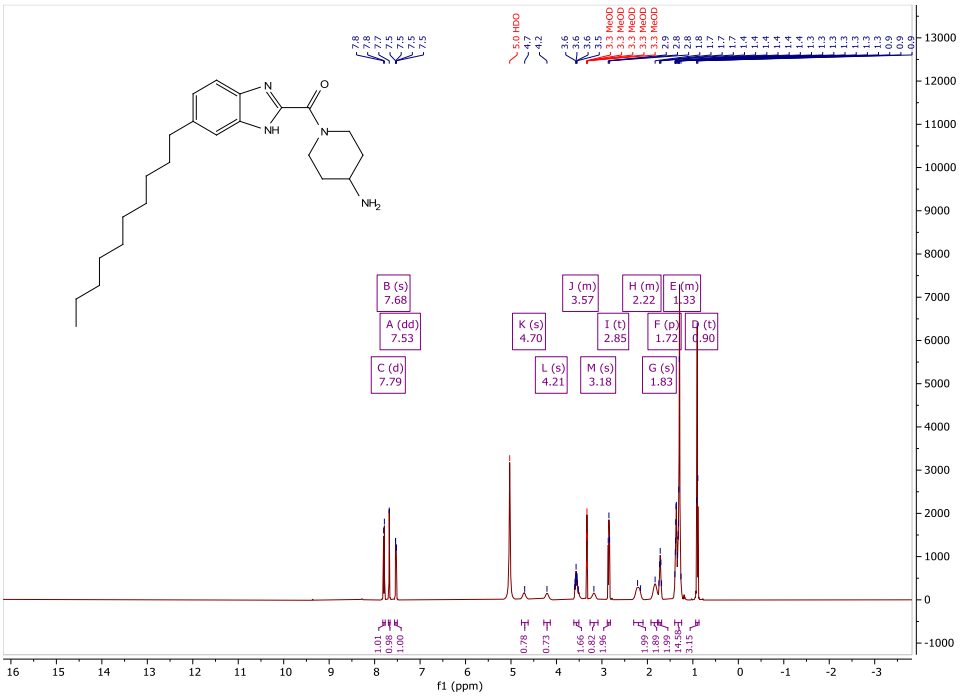

^{13}C NMR of **4.7m**

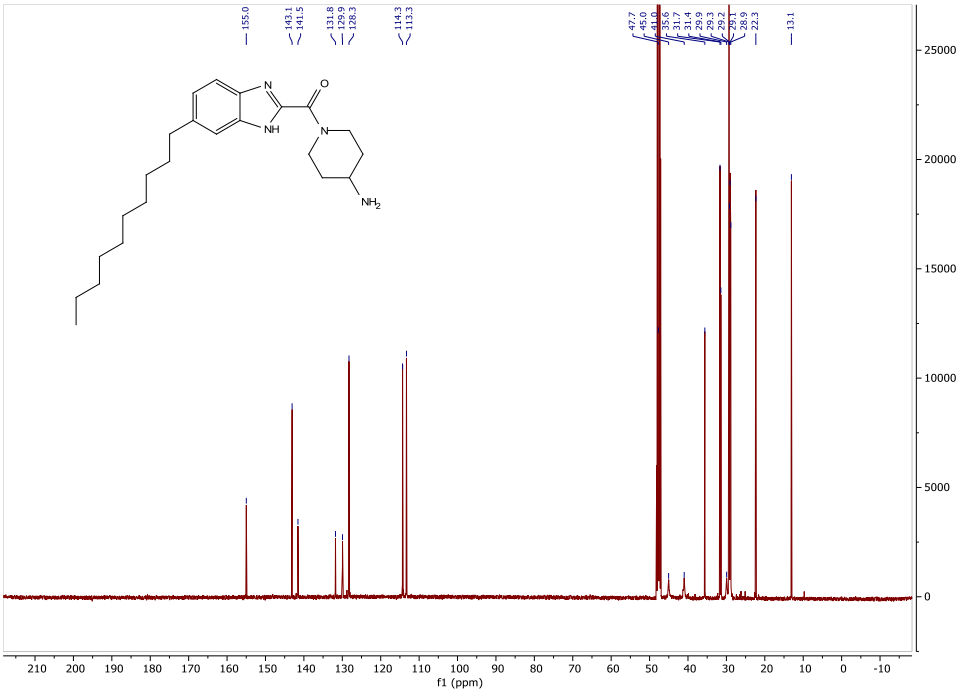

^{1}H NMR of **4.13a**

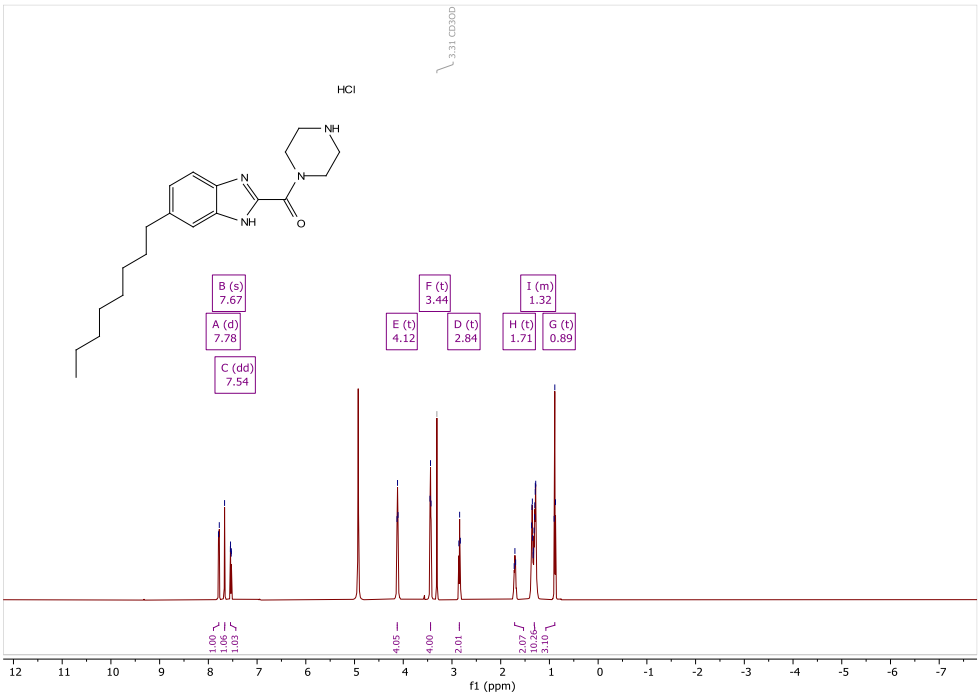

^{13}C NMR of **4.13a**

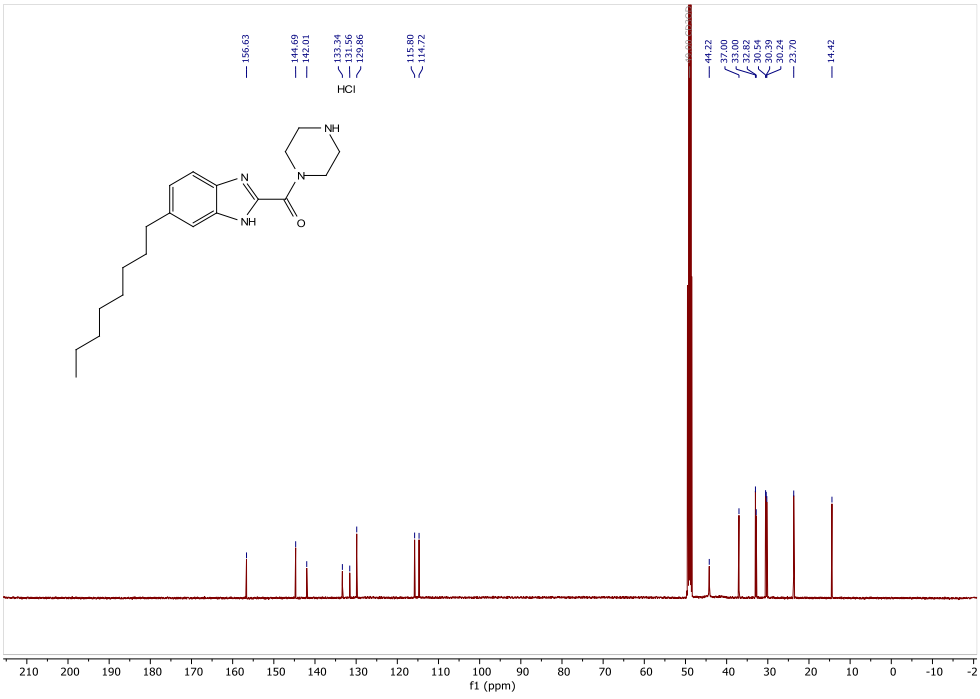

^{1}H NMR of **4.13b**

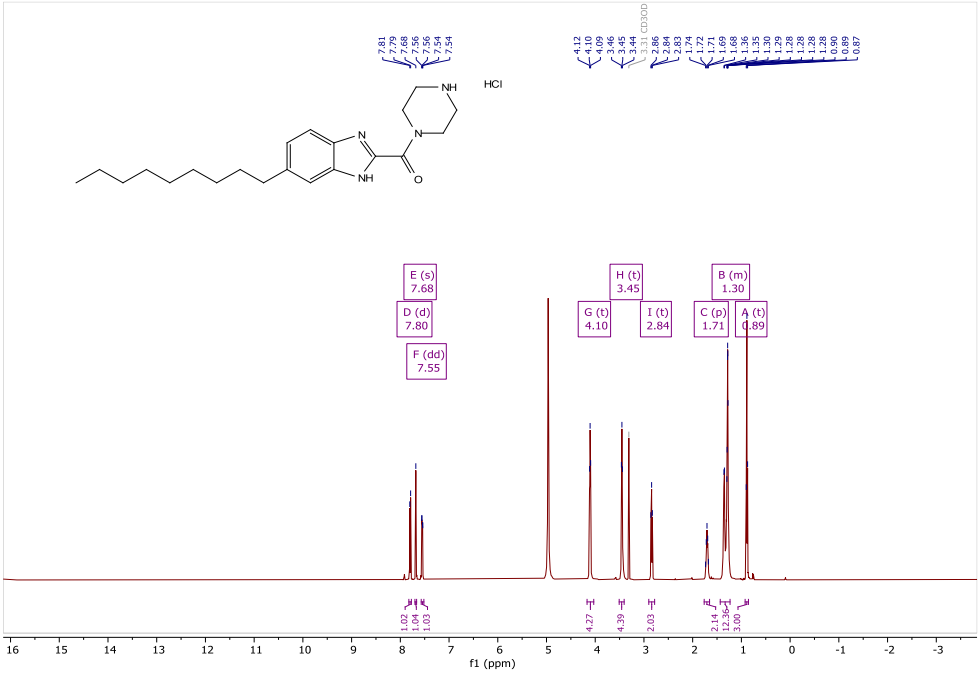

^{13}C NMR of **4.13b**

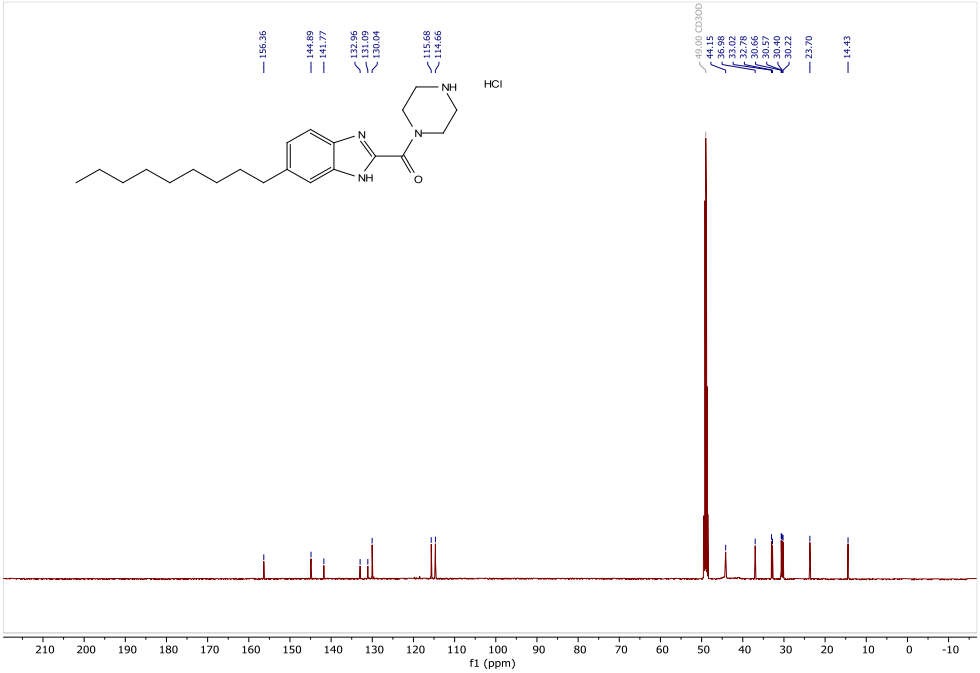

^{1}H NMR of **4.13c**

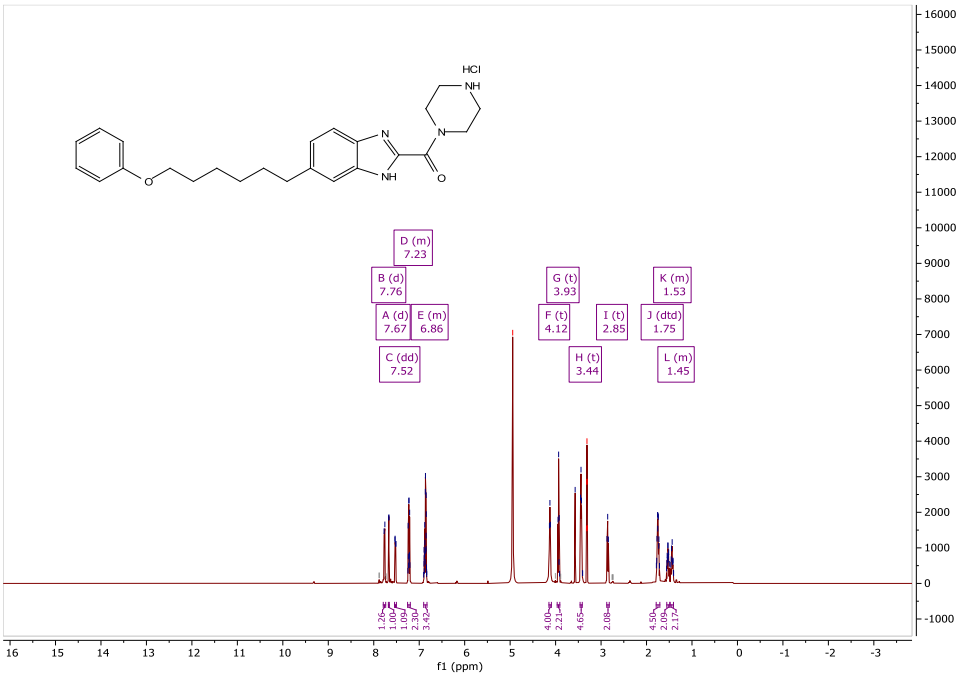

^{13}C NMR of **4.13c**

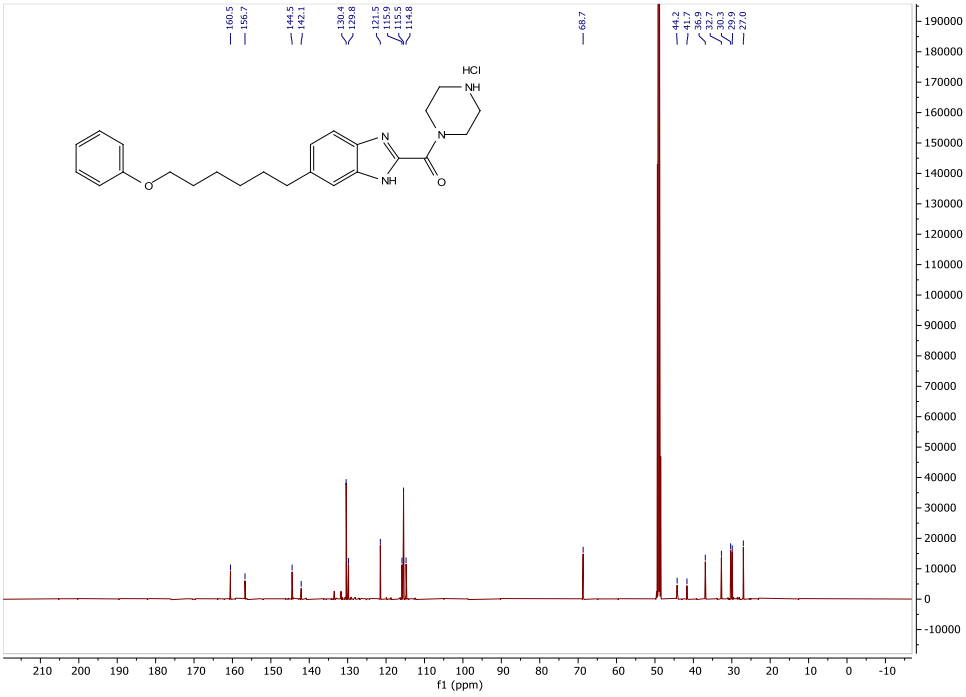

^{1}H NMR of **4.13d**

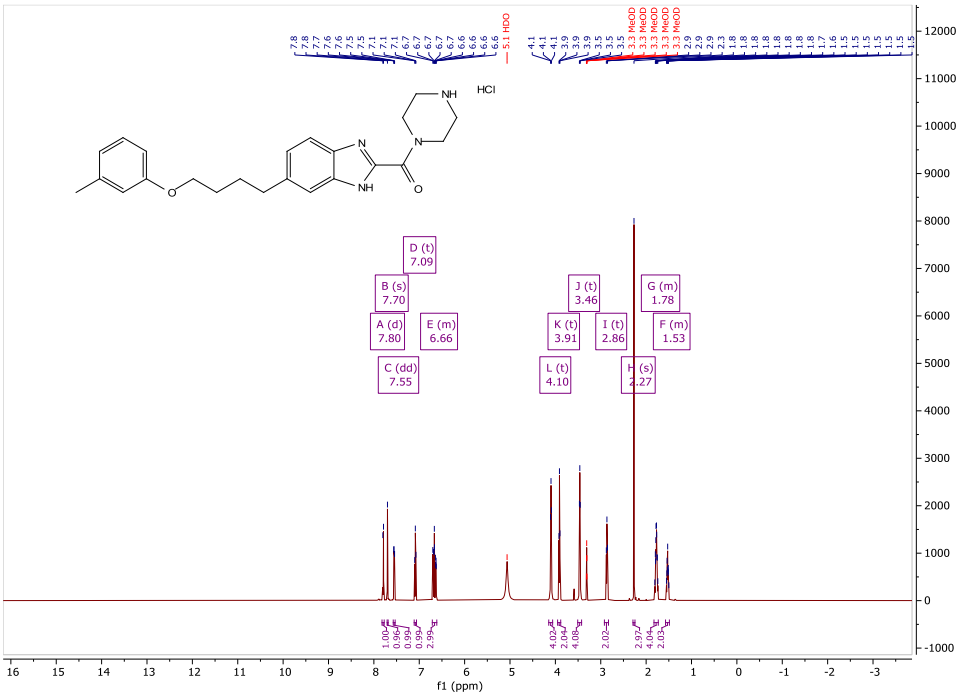

^{13}C NMR of **4.13d**

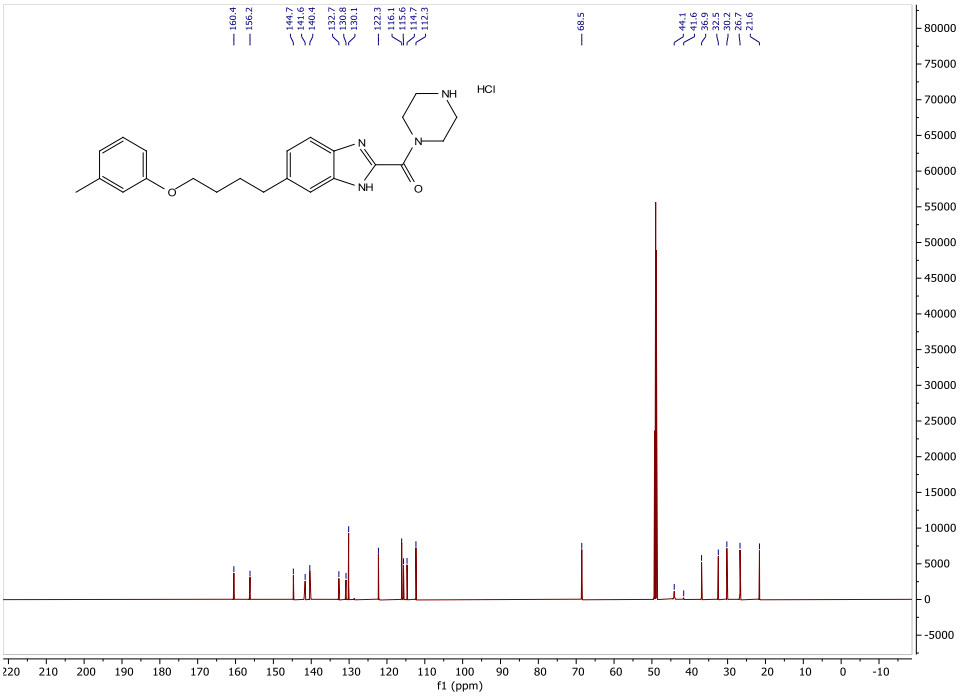

^{1}H NMR of **4.13e**

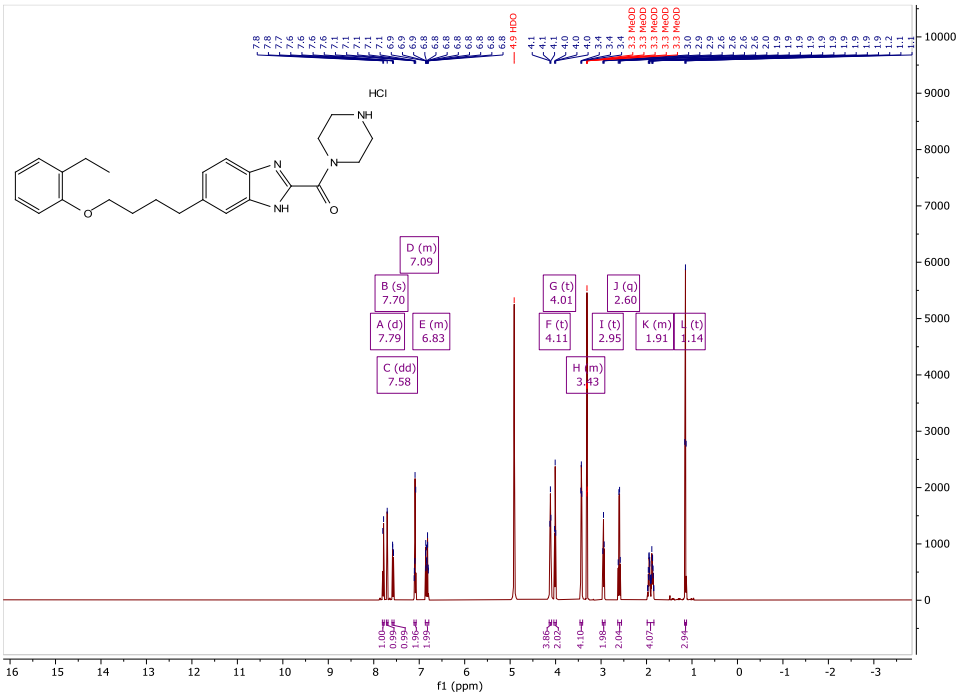

^{13}C NMR of **4.13e**

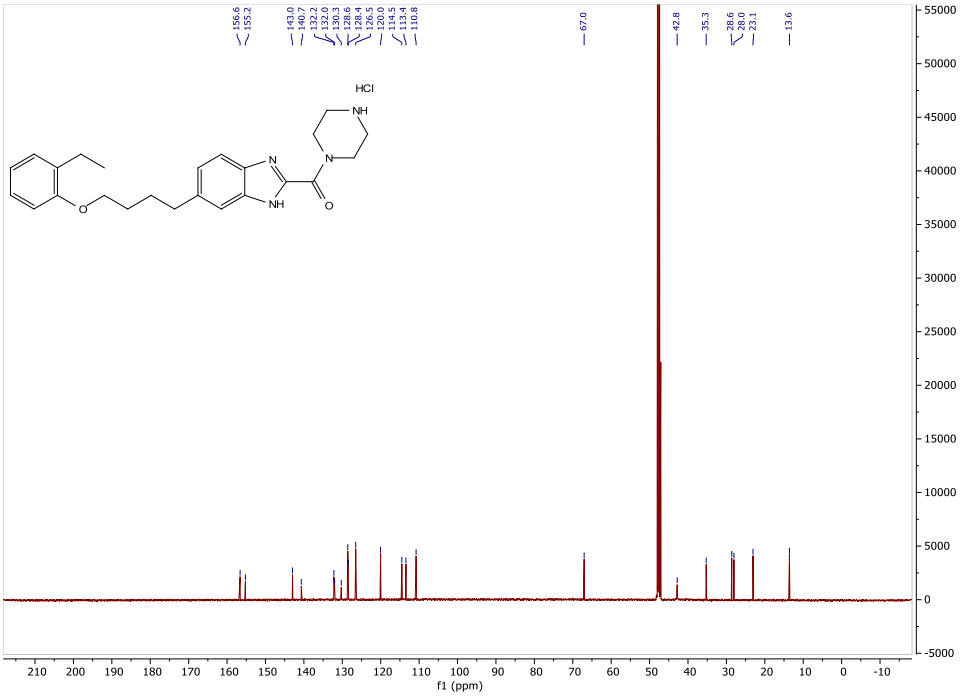

^{1}H NMR of **4.13f**

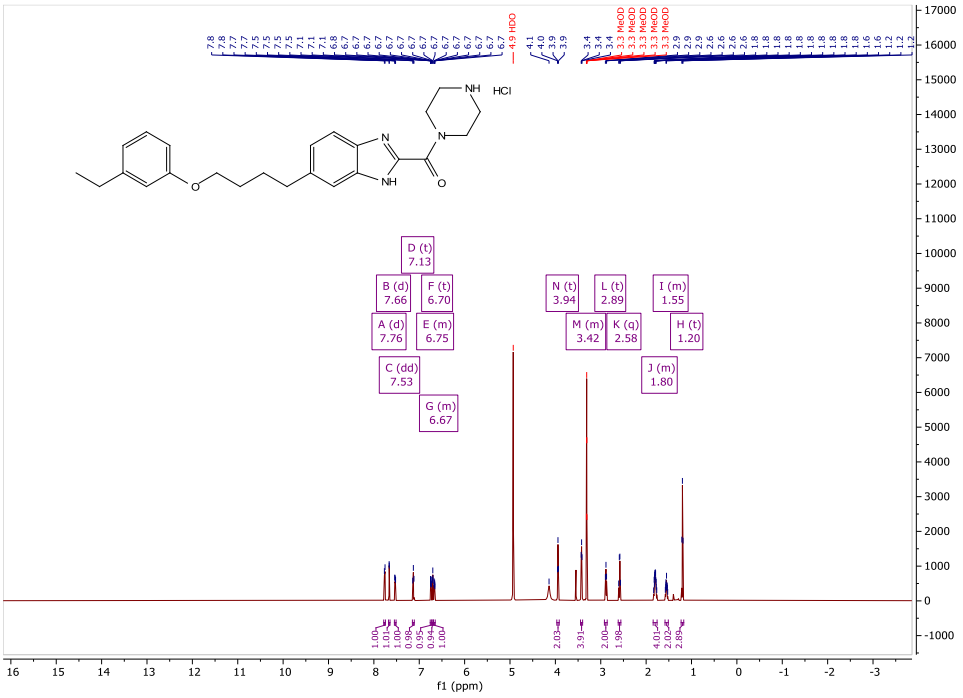

^{13}C NMR of **4.13f**

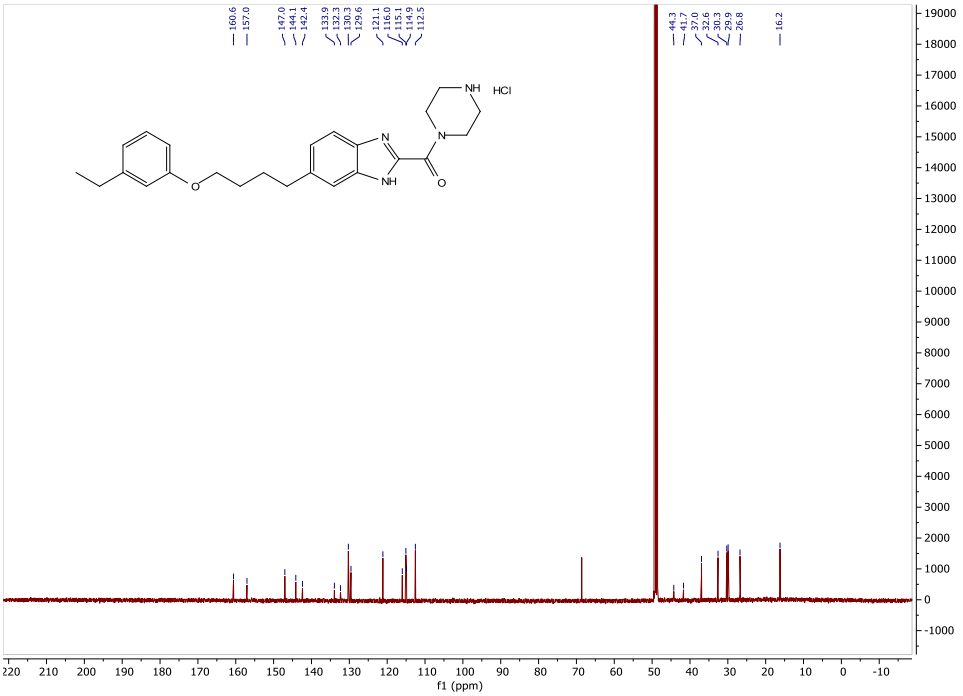

^{1}H NMR of **4.13g**

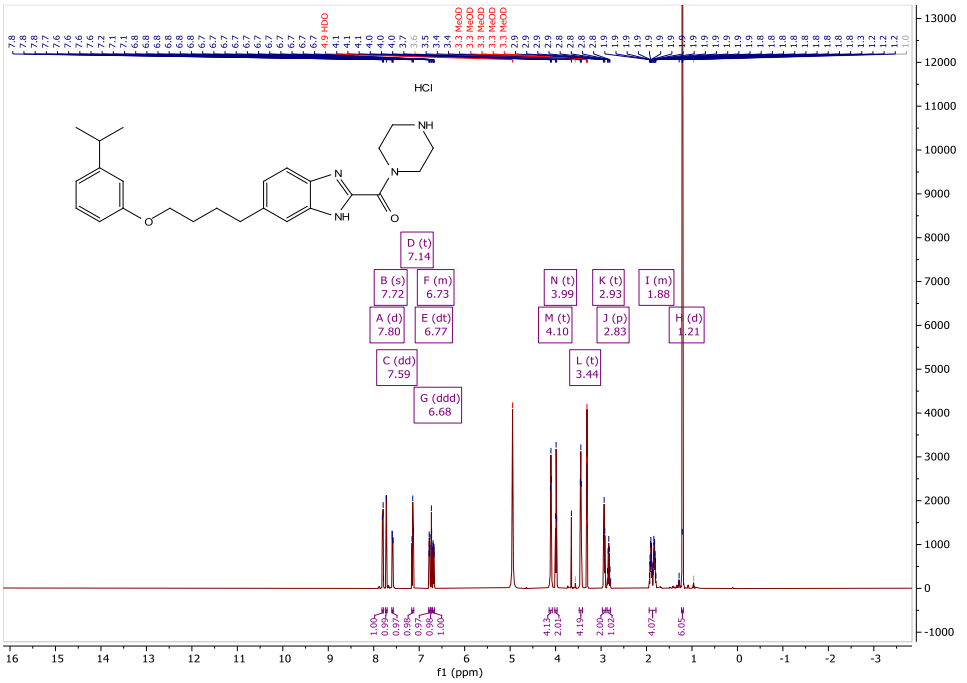

^{13}C NMR of **4.13g**

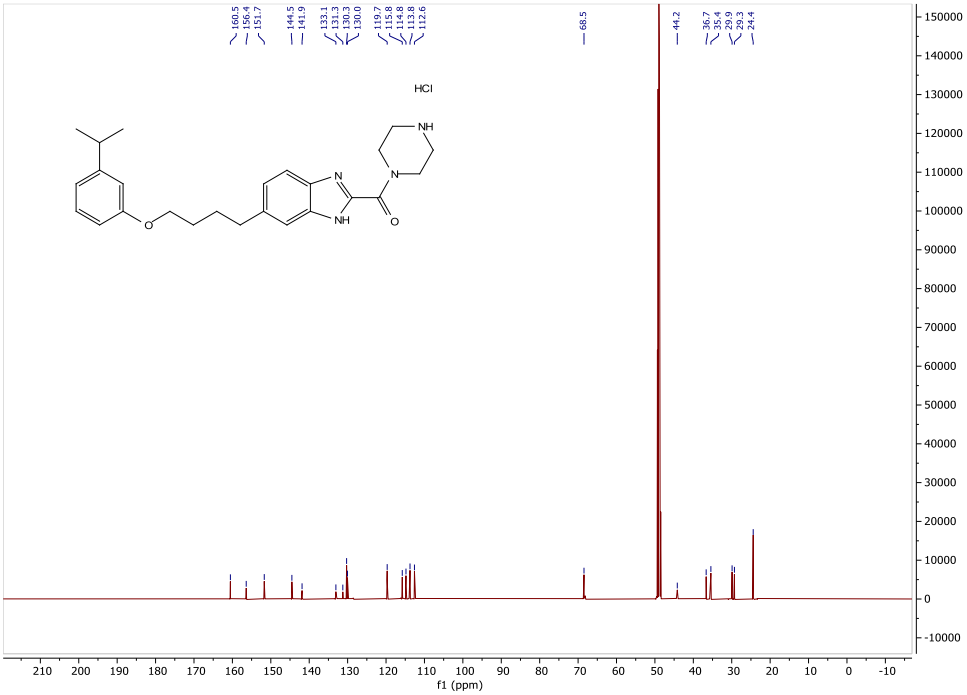

^{1}H NMR of **4.13h**

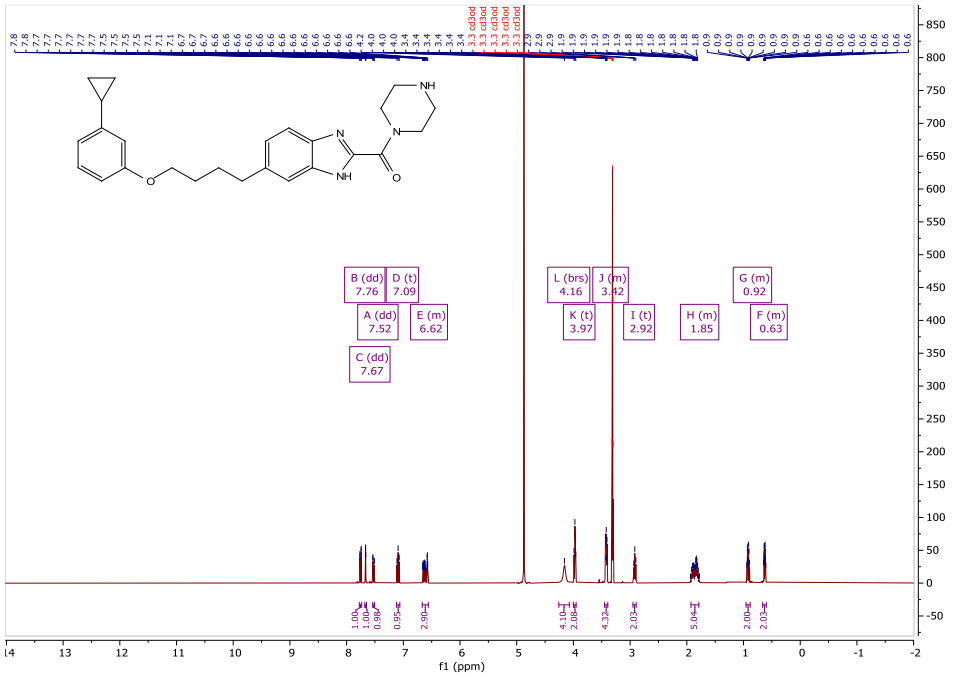

^{13}C NMR of **4.13h**

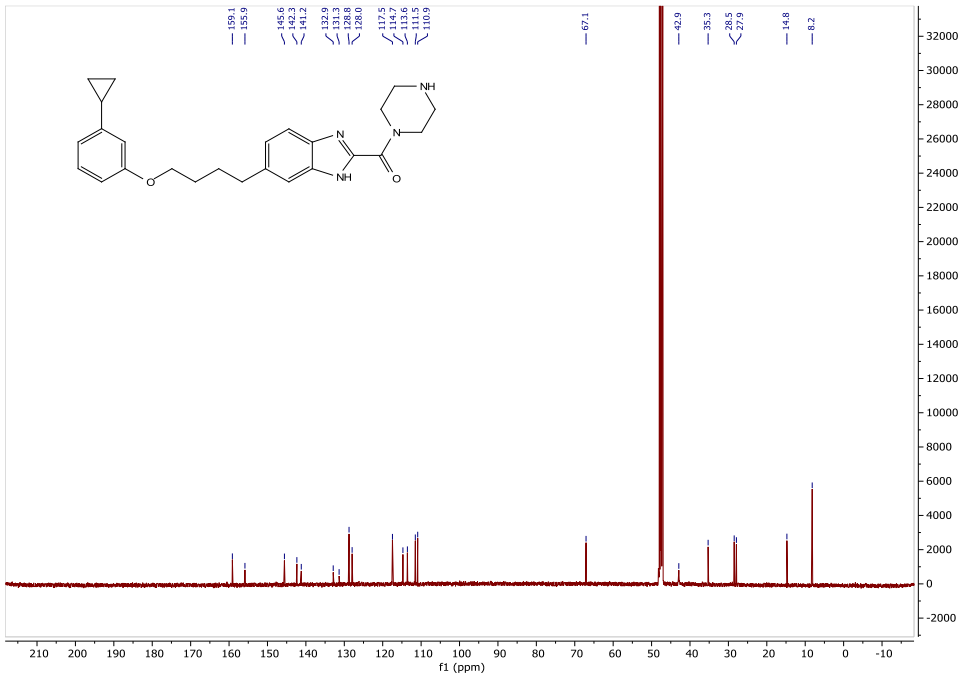

^{1}H NMR of **4.13i**

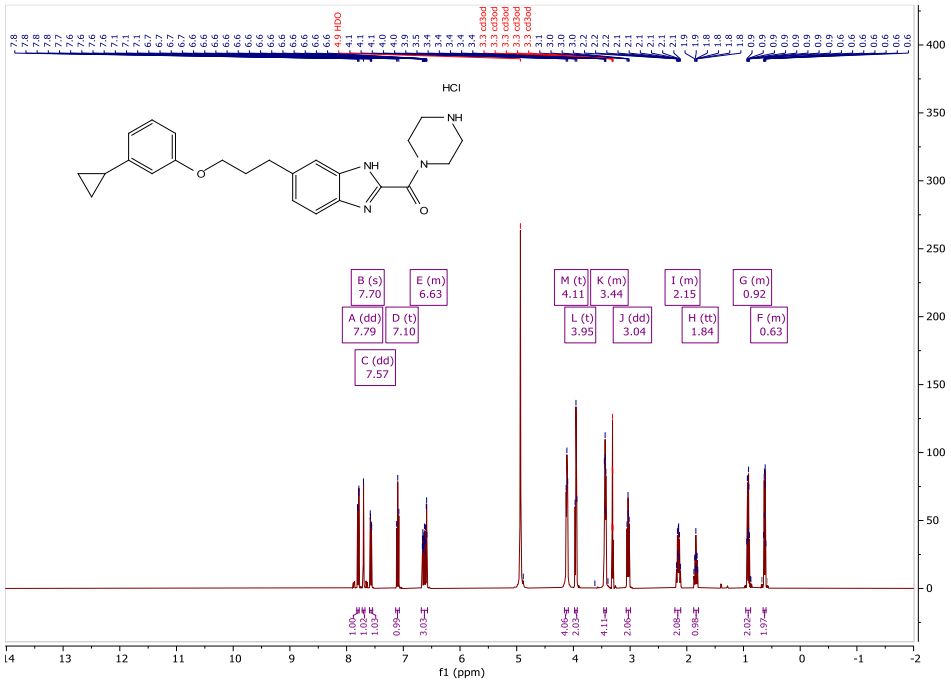

^{13}C NMR of **4.13i**

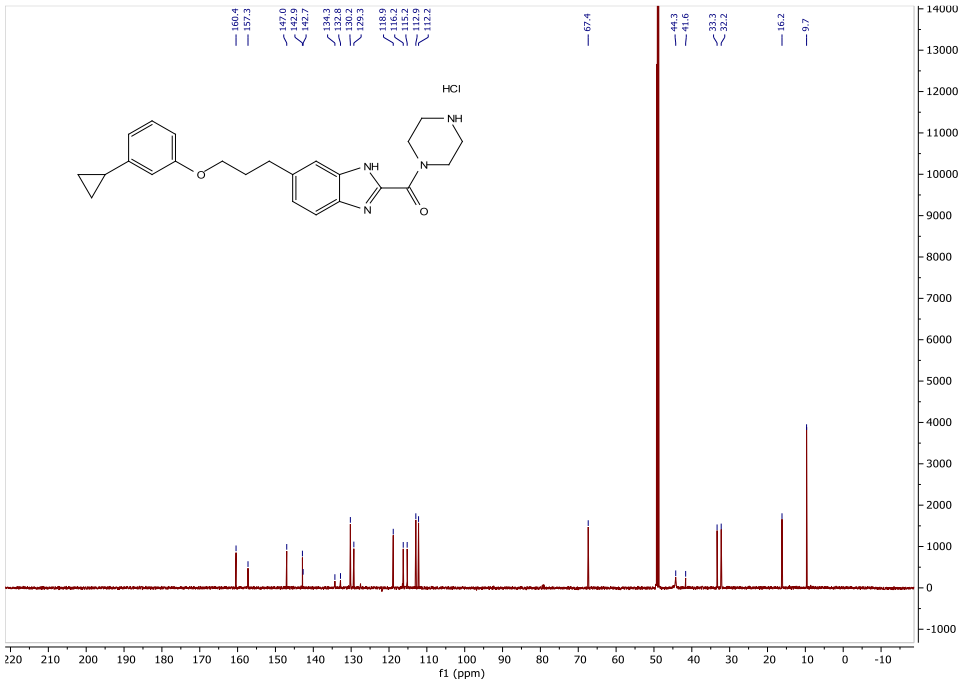

^{1}H NMR of **4.13j**

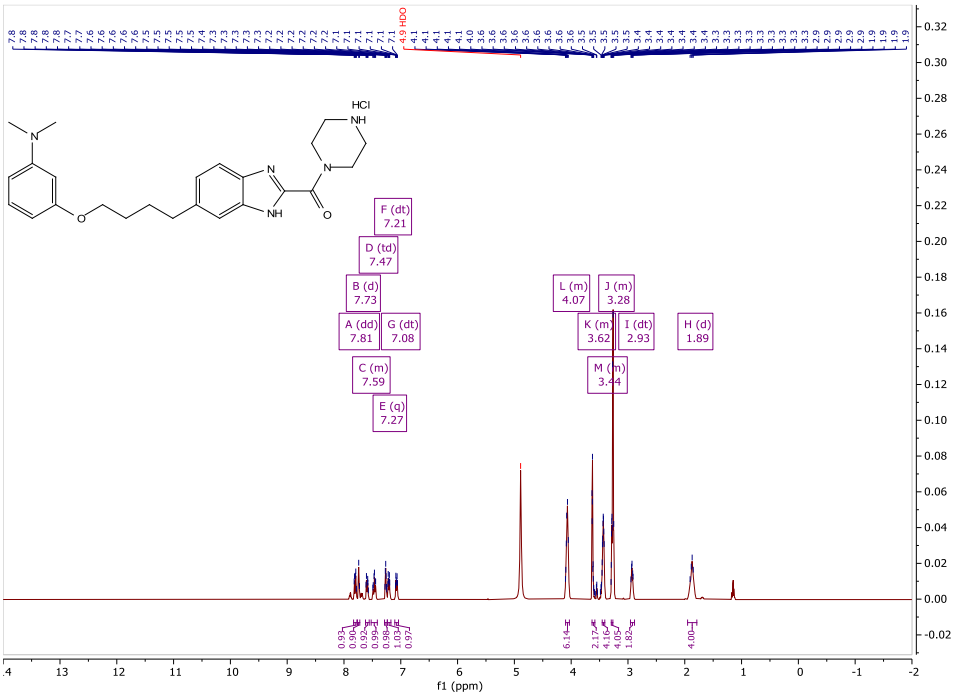

^{13}C NMR of **4.13j**

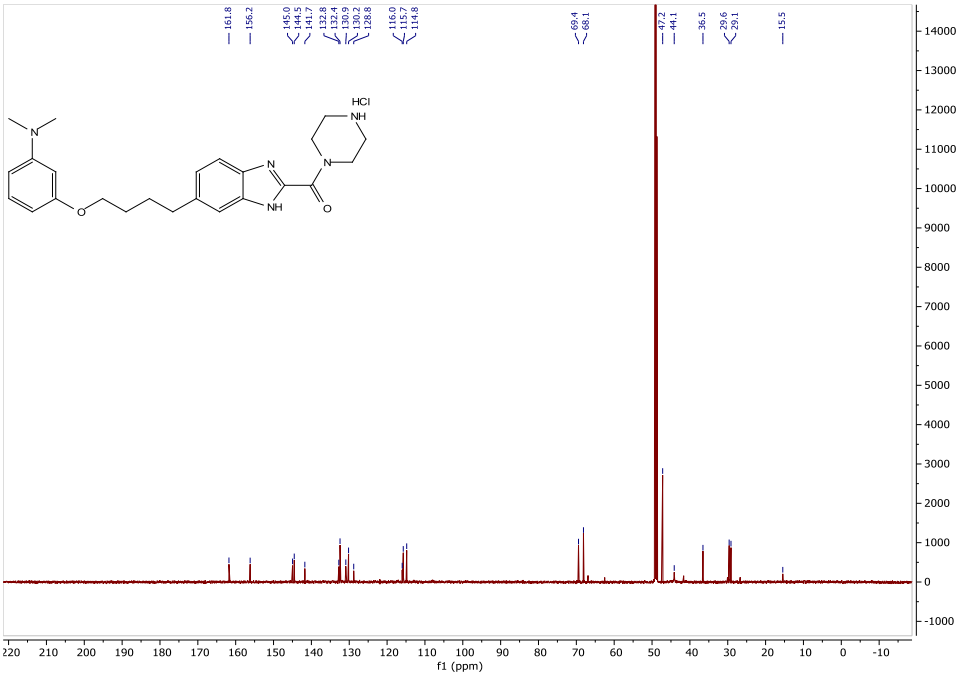

^{1}H NMR of **4.13k**

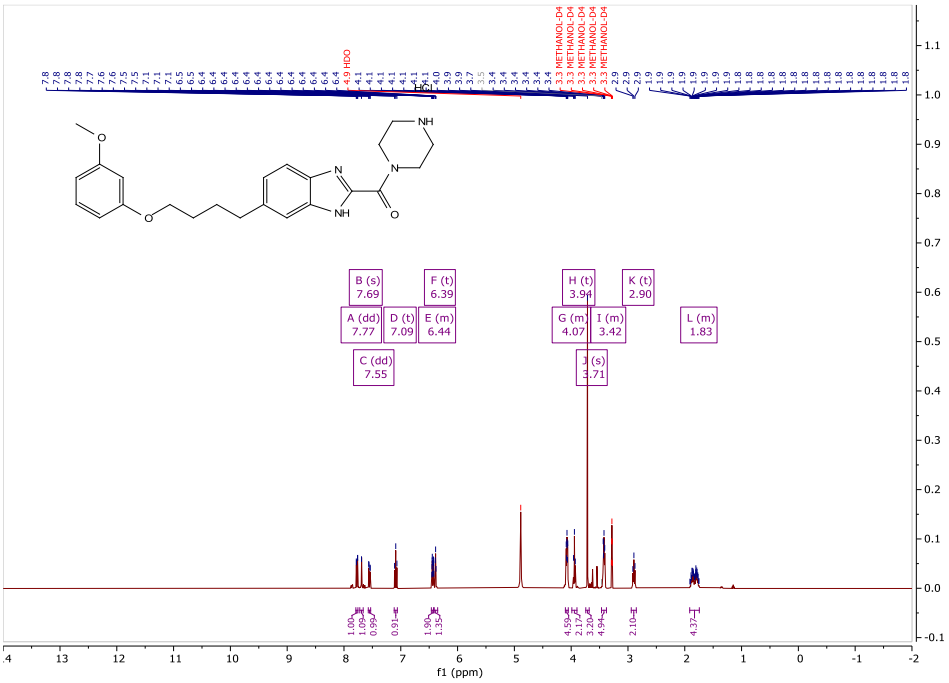

^{13}C NMR of **4.13k**

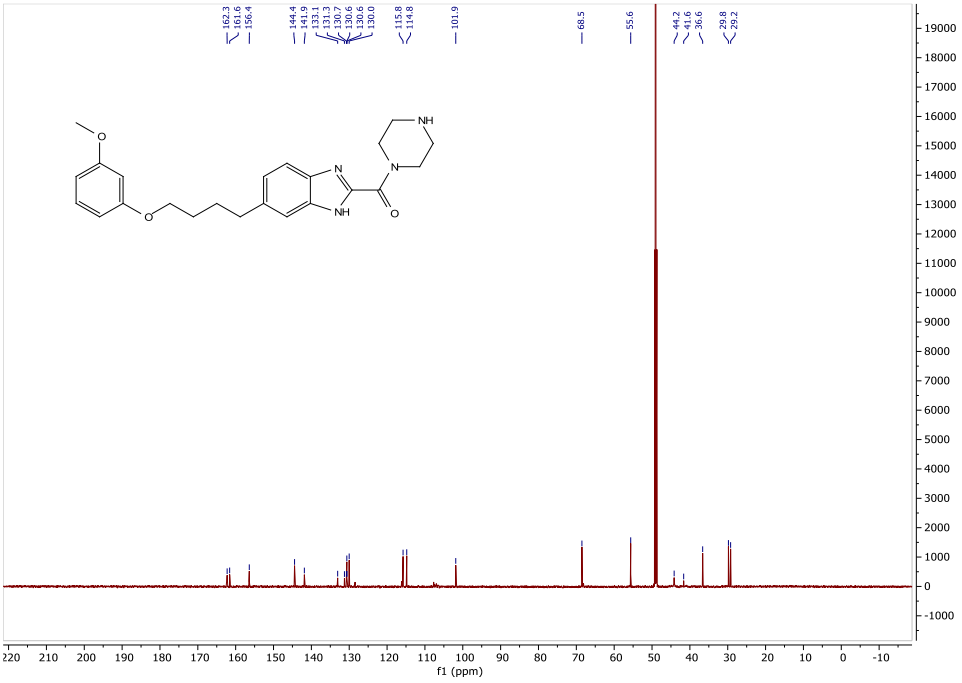

^{1}H NMR of **4.13ll**

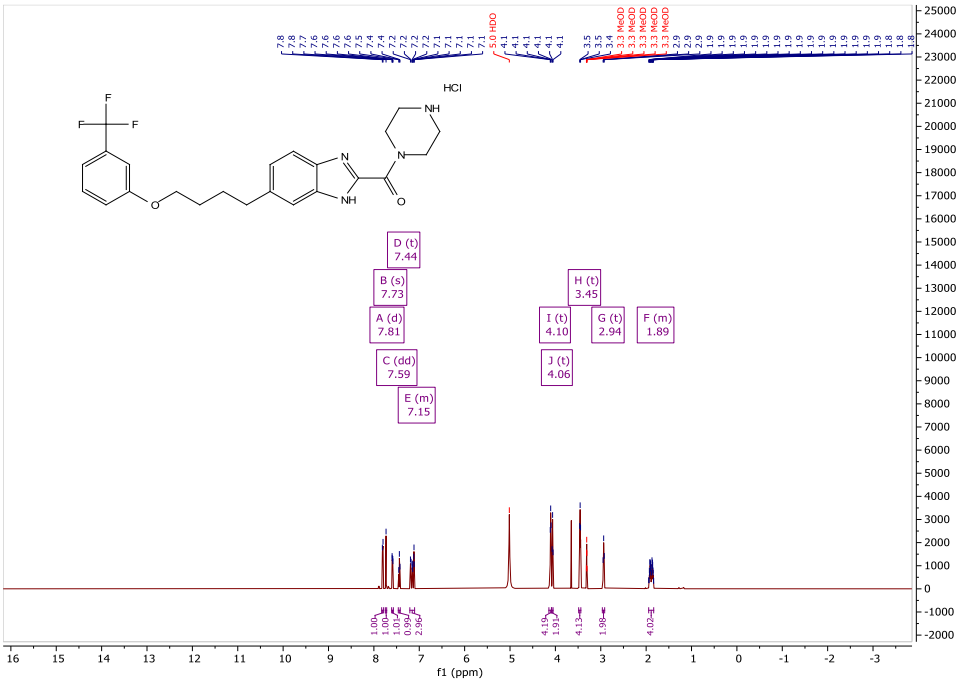

^{13}C NMR of **4.13l**